University of Dundee

University of Dundee

DOCTOR OF PHILOSOPHY

Folate transport and drug resistance in the African Trypanosome

Dewar, Simon

Award date:
2017

Link to publication

General rights
Copyright and moral rights for the publications made accessible in the public portal are retained by the authors and/or other copyright owners and it is a condition of accessing publications that users recognise and abide by the legal requirements associated with these rights.

- Users may download and print one copy of any publication from the public portal for the purpose of private study or research.
- You may not further distribute the material or use it for any profit-making activity or commercial gain
- You may freely distribute the URL identifying the publication in the public portal

Take down policy
If you believe that this document breaches copyright please contact us providing details, and we will remove access to the work immediately and investigate your claim.

Download date: 05. May. 2023

Division of Biological Chemistry and Drug Discovery

Folate transport and drug resistance in the African Trypanosome

Dr Simon Dewar

Ph.D. Thesis

Supervisors: Professor Alan H. Fairlamb

Professor David Horn

This Ph.D. was funded by the Wellcome Trust Clinical Ph.D Programme

Contents

List of figures

List of tables

Abstract

The aim of this thesis was to expand upon the knowledge of the mechanism of action and resistance of antifolate drugs in African trypanosomes with a specific focus on transport mechanisms. A media deficient in folate and thymidine was established which enabled the assessment of their modulation on antifolate *in vitro* potencies and also screen a small set of antifolate compounds. The phenomenon of 'thymineless-death' was found to account for methotrexate toxicity, as well as the primary mechanism of raltitrexed toxicity. This was confirmed by cell cycle studies demonstrating cell cycle arrest in S phase which could be rescued with thymidine. Transport kinetics of folate and methotrexate were characterised and found to be competitive substrates for uptake in *T. brucei.* Transport of these substrates was inhibited by classical antifolates, but not by non-classical antifolates. Genome-wide RNAi library screens with methotrexate and raltitrexed identified the putative folate transporter genes to be involved in drug resistance. RNAi knockdown of the folate transport genes resulted in a substantial reduction in folate transport was seen. RNAi knockdown also led to cross-resistance to classical antifolates, whereas these parasites became hypersensitive to non-classical antifolates. Methotrexate-resistant trypanosomes were generated in which transport of methotrexate and folate was substantially reduced. Amino acid changes were evident in the putative folate transporter genes but no change in transcription or copy number was evident. Cross resistance to classical antifolates was demonstrated in these resistant parasites and cells become hypersensitivity to non-classical antifolates (a similar phenotype to folate transporter RNAi knockdown). Proteomic studies were performed in drug-resistant trypanosomes; however, no conclusive findings were evident due to

limitations of these experiments. In conclusion, these studies demonstrate good evidence of both transport-mediated drug action and drug resistance.

Acknowledgments

I would like to thank my supervisors Professor Alan Fairlamb and Professor David Horn for guidance and support throughout my studies.

A would also like to thank Dr Natasha Sienkiewicz and Dr Han Ong for their many hours of training and mentoring. I would also like to thank Dr Natasha Sienkiewicz for reading and commenting on this manuscript.

A thankyou to all those in the AHF and DH research groups with a special mention to Dr Richard Wall, Dr Stephen Paterson, Dr Adam Roberts, Dr Susan Wyllie, Dr Deuan Jones, Dr Lucy Glover, Sebastian Hutchinson and Dr Catarina Marquez.

I would like to acknowledge the FingerPrints Proteomics facility, DNA Sequencing and services, and the Flow Cytometry and Cell Sorting facility of the College of Life Sciences. Also, much gratitude and appreciation to all of the support staff and services of the University; they do a great job.

I would also like to thank my friends and family, especially my partner Lisa, for all the support, prayers and encouragement.

Thank you to the Wellcome Trust for funding this research.

Declaration

I certify that I am the author of this thesis and the work in which this thesis is a record has been my own, under the supervision of Professor Alan H. Fairlamb and Professor David Horn. Work that is not of my own has been specifically stated by referencing the said researchers and/or citing the relevant publication. This thesis, or any part of it, has not been previously submitted or accepted for a higher degree.

Dr Simon Dewar

I certify that Dr Simon Dewar has completed and performed the work in which this thesis is a record, under my supervision. The conditions of the relevant ordinance and regulations of the University of Dundee have been fulfilled and he is qualified to submit this thesis for the degree of Doctor of Philosophy.

Professor Alan Fairlamb

Wellcome Trust Principal Research Fellow

List of abbreviations

ABC	ATP-binding cassette
AdoMet	S-adenosylmethionine
AICART	Aminoimidazole-4-carboxamide ribonucleotide transformylase
AQP	Aquaglyceroporin
*p*ABA	*p*–aminobenzoic acid
BLAST	Basic local alignment search tool
BSF	Blood-stream form
BT	Biopterin transporter
CATT	Card-agglutination trypanosomiasis test
CNS	Central nervous system
DDU	Drug Discovery Unit
DFMO	α-Difluoromethylornithine
DHFR	Dihydrofolate reductase
dTMP	Deoxyuridine monophosphate
dUMP	Deoxyuridine monophosphate
EDTA	Ethylenediaminetetraacetic acid
ESAG	Expression site-associated gene
EtOH	Ethyl alcohol
FACS	Fluorescence-activated cell sorting
FBT	Folate biopterin transporter
FCS	Foetal calf serum
FDM	Folate deficient media

FMT	Methionyl-tRNA formyltransferase
FPGS	Folylpoly-γ-glutamate synthase
FR	Folate receptor
FT	Folate transporter
FTHFL	10-formyl-tetrahydrofolate ligase
GART	β-Glycinamide ribonucleotide transformylase
GCS	Glycine cleavage system
gDNA	Genomic DNA
GPI	Glycosylphosphatidylinositol
HAT	Human African Trypanosomiasis
IM	Intramuscularly
IMDM	Iscove's Modified Dulbecco's medium
IV	Intravenously
K_i	Inhibition constant
$K_{i\ app}$	Apparent inhibition constant
K_m	Michaelis-Menten constant
$K_{m\ app}$	Apparent Michaelis-Menten constant
LB	Luria Bertani
LC-MS/MS	Liguid chromatography tandem mass spectrometry
MCC	Minimum Cidal Concentration
MCP2	Mitochondrial carrier protein 2
MFT	Mitochondrial folate transporter
mMDH	Mitochondrial malate dehydrogenase

MOA	Mechansim of Action
MPXR	Melarsoprol/pentamidine cross resistance
MS	Methionine synthase
MTHFC	Methenyl-THF cyclohydrolase
MTHFD	Methylene-THF dehydrogenase
MTHFR	Methylene-THF reductase
MTP	Metoprine
MTX	Methotrexate
MTX R1	Methotrexate–resistant line 1
MTX R2	Methotrexate–resistant line 2
NECT	Nifurtimox-eflornithine combination therapy
NTD	Neglected tropical disease
NTR	Nitroreductase
NTX	Nolatrexed
ODC	Ornithine decarboxylase
PCF	Procyclic form
PCFT	Proton-coupled folate transporter
PGKA	Phosphoglycerate kinase A
PMX	Pemetrexed
PTR1	Pteridine reductase 1
PTR2	Pteridine reductase 2
PYR	Pyrimethamine
qDPR	Quinoid dihydropteridine reductase

RTX	Raltitrexed
RPMI	Roswell Park Memorial Institute medium
RPMI-BM	Roswell Park Memorial Institute medium- based media
RFC	Reduced folate carrier
SCX	Strong cation exchange
SD	Standard deviation
SDS	Sodium dodecyl sulphate
SDS-PAGE	Sodium dodecyl sulphate polyacrylamide gel electrophoresis
SHMT	Serine hydroxymethyl transferase
SILAC	Stable isotope labelling with amino acids in cell culture
TbAT1	*T. brucei* P2 adenosine transporter
TBM	*T. brucei* base media
TetR	Tetracycline repressor protein
THF	Tetrahydrofolate
TK	Thymidine kinase
TMP	Trimethoprim
TMX	Trimetrexate
TPP	Target product profile
TS	Thymidylate synthase
VSG	Variant surface glycoprotein
WBC	White blood cell
WHO	World Health Organization

Chapter 1: Introduction

1.1 Kinetoplastids and the neglected tropical diseases (NTDs)

The kinetoplastids are a group of flagellated, unicellular, protozoan organisms that contain a kinetoplast, and belong to the phylum Euglenozoa, order Kinetoplastida. The kinetoplast is a large network, inside the mitochondrion, consisting of a series of topologically interlocked DNA circles (mini or maxi-circles) containing copies of the mitochondrial genome (Shapiro and Englund, 1995). The *Trypanosomatidae* are distinguished by being uniflagellated and exclusively parasitic (Vickerman, 1976). They are divided into sub-genera *Blastocrithidia*, *Endotrypanum, Crithidia*, *Herpetomonas*, *Leptomonas*, *Rhynchoidomomas*, *Phytomonas*, *Leishmania* and the *Trypanosoma* (Stevens *et al*., 2001). Three distinct trypanosomatids cause human disease: African Trypanosomiasis (caused by *Trypanosoma brucei)*, South American Trypanosomiasis (Chagas disease, caused by *Trypanosoma cruzi*) and Leishmaniasis (caused by *Leishmania* species).

These trypanosomatid diseases have been classified as neglected tropical diseases (NTDs) of which they are 17 diseases in total, including viral, helminthic, bacterial and protozoan diseases (Yamey, 2002). NTDs mainly affect the poorest countries of the developing world; more than one billion people including half a billion children, but NTDs have traditionally been of limited interest to the pharmaceutical industry (2014). In recent years there has been renewed focus and interest in NTDs. There is now increased global awareness of their high disease burden and poverty-maintaining impact with recognition that these diseases can be prevented and treated. Indeed the World Health Organization (WHO) has set assertive targets for the control and elimination of NTDs by 2020 (World Health Organization, 2012a).

1.2 Chagas disease and Leishmaniasis

Trypanosoma cruzi (*T. cruzi*), the causative agent of Chagas disease, is primarily transmitted by the faeces of the triatomine bug (*Triatoma infestans*) and is endemic to Central and South America. Globally there are an estimated ~8 million infected individuals (World Health Organization, 2012b). Wide-spread emigration of chronic carriers of *T. cruzi* to North America, Europe, and Australia is to be noted with respect to the risk of reactivation of latent disease (Gascon *et al*., 2010). There are only two established medicines available for the treatment of Chagas disease, nifurtimox and benznidazole. These drugs are far from ideal with shortcomings such as lack of efficacy, side-effects and the danger of resistance emerging (Fairlamb *et al*., 2016; World Health Organization, 2012b).

Subspecies of *Leishmania* are the causative agents for a group of diseases known as the leishmaniases (visceral, cutaneous and mucocutaneous leishmaniasis). *Leishmania spp* are transmitted through the bite of an infected female sandfly (*Plebotominae spp*). Globally the disease currently threatens 350 million people in 88 countries (Scientific Working Group, 2004). Treatment of leishmaniasis is limited to four front-line medicines: pentavalent antimonials (sodium stibogluconate and meglumine antimonate), amphotericin B (deoxycholate or liposomal formulations), paromomycin and miltefosine**.** Oral azoles (ketoconazole, itraconazole, and fluconazole) have also been used to varying success (Croft *et al*., 2006). Again, current therapies are far from ideal and the need for new medicines is imperative.

1.3 Animal Trypanosomiases

Animal trypanosomiases have a high social and economic impact on the countries they affect and there is a great need for the development of new veterinary trypanocides. Animal African Trypanosomiasis (AAT and also called Nagana) is caused by the trypanosome species *T. congolense*, *T. vivax* and, to a lesser extent, *T. brucei brucei* (Giordani *et al.,* 2016). Nagana is present in sub-Saharan African countries and is transmitted by the teste fly. It mainly affects cattle and horses causing a fatal wasting disease, but, is also found in sheep and goats, having devastating consequences to livestock farming in affected countries. Of note *T. vivax* can be transmitted by vectors other than the teste fly, in particular horseflies (*Tabanus* spp.) and stable flies (*Stomoxys* spp.) and transmission has been found in Central and South America along with other regions (Giordani *et al.*, 2016). Surra, a wasting disease similar to Nagana, is caused by *T. evansi* and affects a large range of domestic and wild animals but is especially pathogenic in horses, camels and water buffalos (Giordani *et al.,* 2016). Like *T. vivax*, *T. evansi* can be transmitted by vectors other than the teste fly. It has the widest geographic distribution of the trypanasomatids. Dourine, a disease caused by *T. equiperdum,* is found in horses and other equine animals (e.g. donkeys, mules). It has no vectors and is transmitted through sexual intercourse (Claes *et al*., 2005). The trypanosome species *T. simiae* is pathogenic in pigs, causing a hyperacute and often fatal infection (Giordani *et al.,* 2016). Currently the most widely used compounds in the animal trypanosomiases are diminazene aceturate and isometamidium chloride; however, resistance to these compounds is well documented. Suramin is used to treat *T. evansi* but, again, resistance is commonly found (Giordani *et al.,* 2016).

1.4 Human African Trypanosomiasis

1.4.1 A brief introduction

The unicellular flagellated protozoan parasite *Trypanosoma brucei* is the causative agent of human African trypanosomiasis (HAT), also known as African sleeping sickness. HAT threatens approximately 70 million people in 24 sub-Saharan-African countries (Franco *et al*., 2014). There are two human pathogenic subspecies. *T. brucei gambiense* (*T. b. gambiense*) (98% of HAT cases) predominates in western and central Africa and is an anthroponotic disease primarily affecting humans with a small animal reservoir (an array of both domestic animals: pigs, sheep, dogs, and wild animals including reptilians and mammals) (Franco *et al*., 2014). The second human pathogenic subspecies, *T. brucei rhodesiense* (*T. b. rhodesiense*), predominates in southern-eastern Africa and causes a zoonotic disease primarily affecting animals (livestock and wild game) with humans inadvertently infected (Franco *et al*., 2014). The third subspecies of *T. brucei*, *T. b. brucei* is non-pathogenic to humans and causes the disease Nagana (it is a less common cause of Nagana than *T. congolense* and *T. vivax*). It is from this subspecies laboratory strains used in this thesis are derived.

In 2011 reported new cases of HAT fell to below 7,000; however, the disease carries a sizeable risk of resurgence with socio-economic and environmental variables such as epidemiological population shifts, civil unrest and climate change (Franco *et al*., 2014; Simarro *et al*., 2012). HAT also has an impact in sustaining the cycle of poverty in neglected communities. As part of the WHO target portfolio complete elimination of *gambiense* HAT by 2020 has been set (World Health Organization, 2012a). To facilitate the elimination of the disease, new medicines are

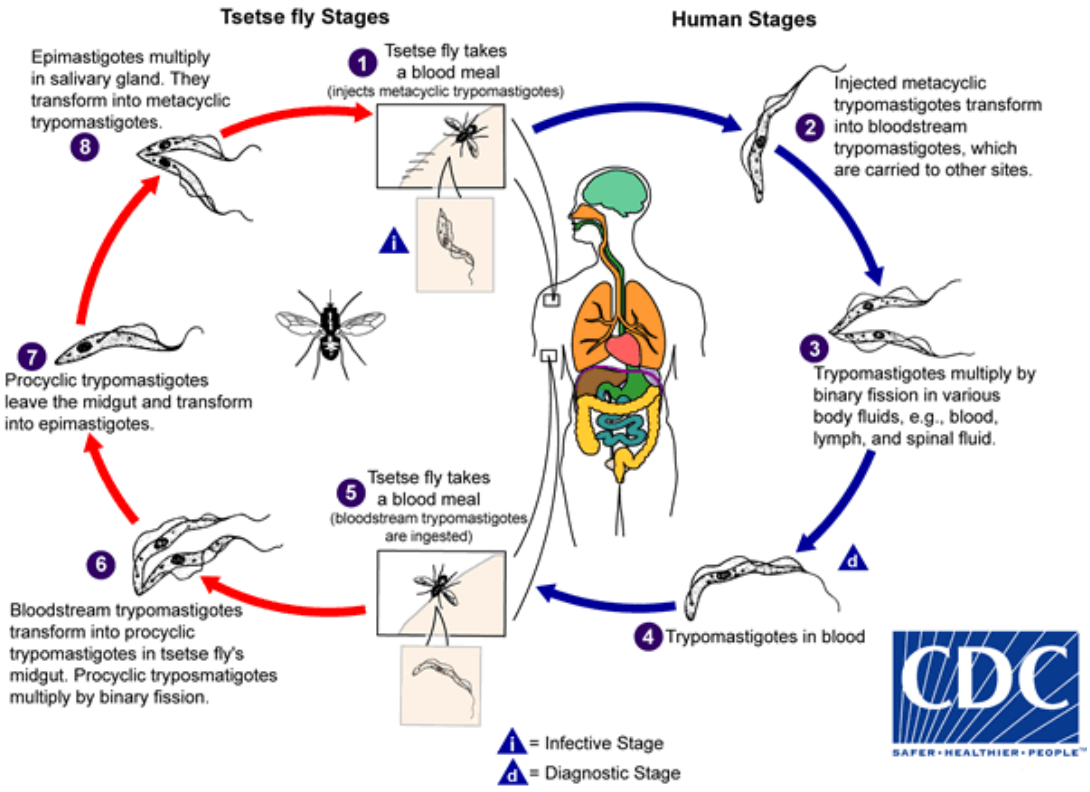

Figure 1.1 Life cycle of African Trypanosomes

Figure taken from Centre for Disease for Control and Prevention

required. However, in the current timescale elimination of HAT is a target that is not anticipated.

1.4.2 Life cycle of *T. brucei*

HAT is primarily transmitted by the bite of a tsetse fly (*Glossinidae spp*.) and the life-cycle of the causative agent, *T. brucei*, is depicted in Figure 1.1. In the human host stages, parasites initially multiply at the bite site before entering the bloodstream via the lymphatic system where they proliferate as long and slender trypomastigotes (Vickerman, 1976) – named blood stream form (BSF) parasites. It is these long and slender forms that can bridge the blood vessel epithelium and move into extracellular spaces, including the central nervous system (CNS) (Langousis and Hill, 2014). These cells rapidly proliferate by binary fission. During each wave of parasitaemia in the host, some parasites differentiate into non-proliferative short-stumpy forms, triggered and regulated by the metabolite stumpy inducing factor (Reuner *et al*., 1997). In the first stage in the vector's life cycle, these short-stumpy forms (taken up after the tsetse fly blood meal) differentiate into procyclic trypomastigotes in the fly's midgut (Matthews and Gull, 1998). In the fly's hindgut parasites differentiate into mesocyclic trypomastigotes before migration to the salivary gland where they differentiate into epimastigotes and then further into metacylic trypomastigotes (Van den Abbeele *et al*., 1999). The metacylic trypomastigotes are transferred from insect vector to human host by a bite of an infected tsetse fly into human skin, thus completing the life cycle of *T. brucei*. The predominant mode of transmission of HAT is vector-borne by the tsetse fly, but other less common routes have been described including vertical transmission, blood transfusion, sexual contact and accidental laboratory transmission (Franco *et al*.,

2014). Indeed looking at transmission routes other than teste fly is crucial if elimination targets are to be achieved (Welburn *et al*., 2016).

1.4.3 Immune evasion mechanisms

T. brucei BSF parasites are covered by a dense surface coat composed of variant surface glycoproteins (VSGs), attached via a Glycosylphosphatidylinositol (GPI) anchor, that protects the parasites from lytic factors in human plasma and host immune invasion (Cross, 1975; Fenn and Matthews, 2007). One of the main escape mechanisms to evade the immune response is the ability of *T. brucei* to undergo antigenic variation. Cells are covered by an estimated 5 million identical VSG dimers. However, the parasite can express a single antigenically distinct VSG from more than 2000 complete and partial (pseudogenes) VSG genes in a mono-allelic fashion (antigenic variation) thus enabling the parasite to deflect the immune response (Horn, 2014; Horn and Cross, 1997). Moreover, host antibodies that bind to the parasites cell surface can be cleared by clathrin-mediated endocytosis in the flagellar pocket (Allen *et al*., 2003). The flagellar pocket is an invagination of the membrane at the base of the parasites flagellum and is the sole site for exocytic and endocytic processes (Field and Carrington, 2009).

VSG, its protein anchor GPI and the flagellar pocket have been proposed as vaccination candidates for HAT. However due to the complex nature of the parasites' immune evasion, endeavours in vaccine development for HAT have not been successful (La and Magez, 2011). Indeed, *T. brucei* infection has an inhibitory effect on B-cell response. In a mouse HAT model, infection was found to nullify both anti-trypanosome responses and immunological memory in general (Radwanska *et al*., 2008). There was loss of B cell responsiveness to new antigens and loss of memory responses to previously encountered antigens, including VSGs. Also,

infection abrogated a non-related vaccine induced memory response, with loss of DTPa (diphtheria, tetanus and pertussis) vaccine protection against a later *B. pertussis* challenge.

1.4.4 Clinical Features and diagnosis of HAT

HAT clinically evolves in two stages, an early haemolymphatic stage and a secondary meningoencephalitic stage that is defined by invasion of the CNS. First stage illness is characterised by non-specific symptoms including fever, arthralgia and lymphadenopathy. A trypanosomal chancre (a localised reaction to the bite of the tsetse fly) is rarely seen in *T. b. gambiense* but occurs in around 20% of patients with *T. b. rhodesiense* (Brun *et al.,* 2010). If left untreated, first stage illness can cause anaemia and endocrine, kidney and cardiac dysfunction. Second stage illness (CNS stage) is associated with various progressive neuropsychiatric symptoms, disturbance of the sleep-wake cycle and progression to coma. *T. b. rhodesiense* HAT is typically an acute disease that leads to death within 6 months, in comparison *T. b. gambiense* HAT is typically a chronic disease with an average length of 3 years (Franco *et al*., 2014). Indeed, if left untreated, both subspecies have a fatality rate up to 100% (Franco *et al*., 2014). Rarely have asymptomatic chronic carriers (serologically positive patients, negative for parasites on microscopy, who are asymptotic and survive with no treatment) been found in HAT. These silent carriers are a potential human reservoir for HAT transmission (Welburn *et al*., 2016).

The non-specific clinical presentation of HAT means that a diagnosis requires laboratory evidence. The diagnosis of HAT follows a three-step pathway: screening, parasitic conformation and staging (Brun *et al.,* 2010). Antibody detection using the Card-Agglutination Trypanosomiasis Test (CATT) is used for population screening. Patients with a positive CATT on whole blood or serum (serum is

preferential as it is more specific) undergo parasite detection by microscopy of lymph node aspirate and blood (after either capillary tube centrifugation or mini-anion-exchange centrifugation of the blood sample) (Chappuis *et al.*, 2005). Differentiation of the stage of the infection can only be done by analysis of the cerebral spinal fluid (CSF), obtained by lumbar puncture. The number of parasites present in the CSF is often very low, which can lead to false negative results (Bonnet *et al*., 2015). An increased white blood cell (WBC) count (indicative of meningeal inflammation) is also used as a marker of infection to increase diagnostic sensitivity. The WHO diagnostic criteria for second stage HAT requires the presence of trypanosomes in the CSF and/or WBC > 5 cells μl^{-1} (Brun *et al.*, 2010).

Current diagnostic methods for HAT can often be challenging both to perform and interpret; therefore, alternative new diagnostic platforms are being examined. Lateral flow immunochromatographic devices (detection of antibodies targeted to specific antigens) are being progressed as rapid diagnostic tests (RDTs) for HAT. Standard Diagnostics (SD BIOLINE HAT) and Coris Bioconcept (Sero-K-SeT) have developed diagnostic instruments that use native VSG LiTat 1.3 and LiTat 1.5 to detect anti-trypanosome antibodies (Bonnet *et al*., 2015). In the field, both tests have sensitivity and specificity comparative to CATT (Bisser *et al*., 2016; Buscher *et al*., 2014). Moreover, DNA detection using loop-mediated isothermal amplification is highly specific and sensitive for HAT diagnosis (Kuboki *et al*., 2003; Njiru *et al*., 2008). This test is currently used in the Democratic Republic of Congo and Angola (Bonnet *et al*., 2015). As well as initial diagnosis, methods to determine second stage illness are being developed. These include CSF PCR *T. brucei* detection and measuring CSF IgM and/or neopterin levels (a biomarker for

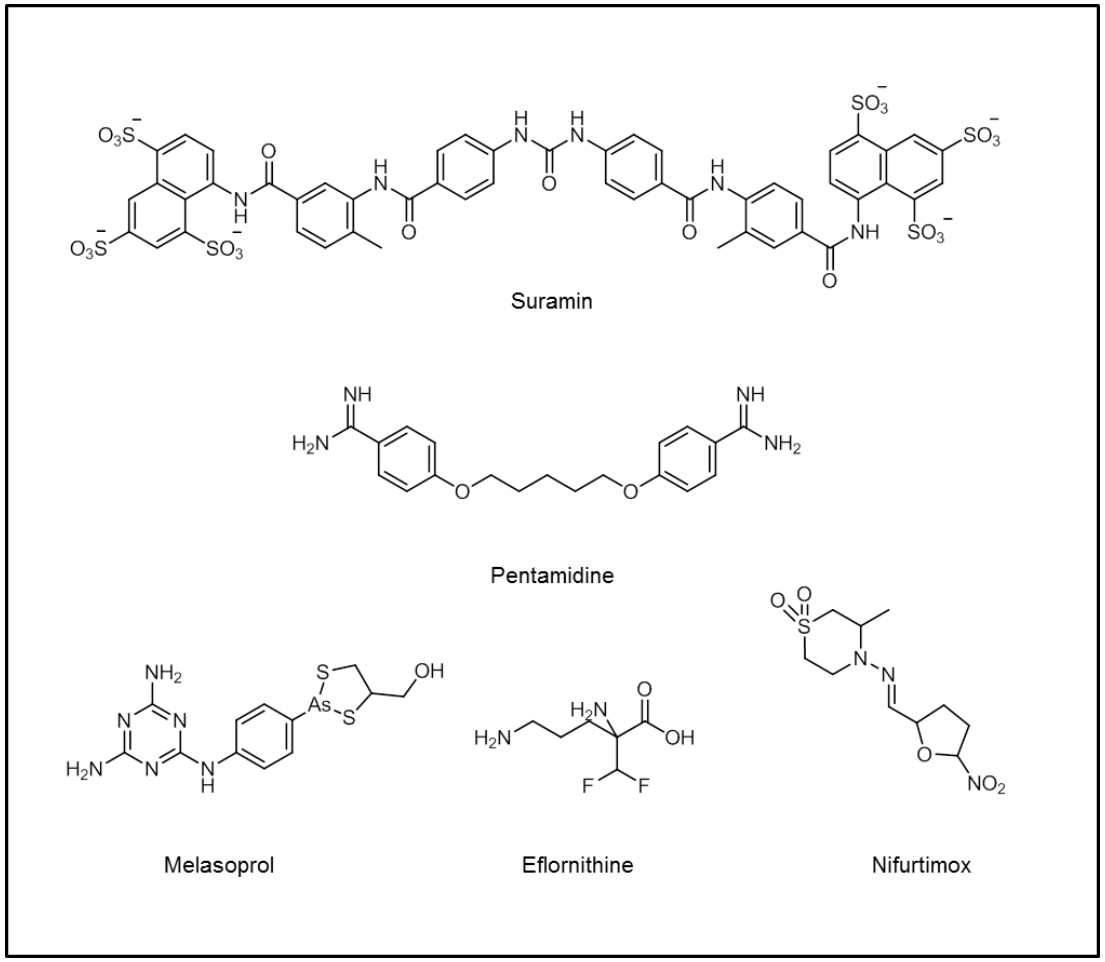

Figure 1.2 Chemical structures of HAT drugs in current use

Table 1.1 Key characteristics of current HAT drugs

Information for table taken from Fairlamb *et al*., 2016, Eperon *et al.*, 2012 and http://www.cdc.gov/parasites/sleepingsickness/health_professionals/

T.b.r = Trypanosoma brucei rhodesiense *T.b.g* = Trypanosoma brucei gambiense

Drug	Stage	Species	Mode of Action	Resistance Mechanisms	Significant Adverse Effects	Treatment Regime
Suramin	First Stage	*T.b.r* only.	Unknown	Laboratory-generated resistance - silencing of: invariant surface glycoprotein (ISG75), the AP1 adaptin complex, lysosomal proteases and major lysosomal transmembrane protein, also *N*-acetylglucosamine and spermidine	Skin reactions Fatal anaphylaxis	1 gm IV on days 1,3,5,14, and 21.
Pentamidine	First Stage	Inactive in some *T.b.r* cases	Unknown	Melarsoprol/pentamidine cross resistance (MPXR): 1. Laboratory and clinical resistance associated functional loss of P1 adenine/adenosine transporter (TbAT1). 2. Laboratory and clinical resistance associated with loss of AQP2 mediated transport and replacement with a chimeric AQP2/AQP3 gene	Hypoglycaemia, diarrhoea and vomiting	4 mg/kg/day IM or IV x 7-10 days
Melarsoprol	Second and First Stage	All species	Forms a cyclic complex with trypanothione (MelT). Inhibits trypanothione reductase along with other targets		Encephalitic syndrome Tremor Peripheral Neuropathy	2-3.6 mg/kg/day IV x 3 days. After 7 days, 3.6 mg/kg/day x 3 days. Give a 3rd series of 3.6 mg/kg/d after 7 days.
Eflornithine	Second stage	*T.b.g* only	Inhibition of ornithine decarboxylase	Laboratory-generated resistance due to loss of a non-essential amino acid transporter (*Tb*AAT6). Inherent resistance in some *T.b.r* field isolates	Headaches Seizures Anaemia	400 mg/kg/day IV in 4 doses x 14 days
Niufurtimox	Second stage as Eflornithine - Niufurtimox combination therapy (NECT)	Eflornithine *T.b.g* only	Progrug activated by nitroreductase (NTR) to form metabolites that kill parasites via unknown mechanism	Laboratory: RNAi screen and laboratory-generated resistant line identified NTR to be associated with resistance	Headaches Seizures Dizziness	As NECT: IV eflornithine 200 mg/kg every 12 h for 7 days, with oral nifurtimox 3 times daily for 10 days.

cellular immune response) (Lejon *et al*., 2002; Mugasa *et al*., 2012; Tiberti *et al*., 2013).

1.4.5 Current treatments for HAT

There are five treatment options for HAT: pentamidine, suramin, melarsoprol, eflornithine (α-difluoromethylornithine or DFMO) monotherapy and nifurtimox-eflornithine combination therapy (NECT). Drug structures are shown in Figure 1.2 with a summary of their characteristics in Table 1.1.

Suramin and pentamidine, both discovered in the early 20th century, are still used today to treat the first stages of HAT. Suramin (1916) is active against both HAT species; however, it cannot be used against *T. b. gambiense* in West and Central Africa because of a risk of severe reactions in patients co-infected with *Onchocerca volvulus* (the causative agent of river blindness) (Brun *et al.*, 2010). Suramin is given intravenously (IV) over a 3 week course and side effects include drug rash and nephrotoxicity, and in rare instances a severe hypersensitivity reaction. Its mechanism of action (MOA) is unknown. In the laboratory, resistance has been shown to be mediated by a number of mechanisms (Alsford *et al*., 2012) (Table 1.1), although resistance in the field has not been evident. Resistance to suramin, when used in animal trypanosomiasis (*T. evansi*), has been reported (Giordani *et al.*, 2016). Pentamidine (1937), a diamidine drug, is used for early stage *T. b gambiense* but not for *T. b. rhodesiense* where it has reduced activity (Wang, 1995). Pentamidine is administered intramuscularly (IM) or by IV infusion for 7-10 days and is overall well tolerated. Its MOA is also unknown and resistance emerging from pentamidine only use has not been detected. However, melarsoprol/pentamidine cross resistance (MPXR) is a well-known phenomenon and will be described when discussing the drug melarsoprol.

Second stage treatment options are melarsoprol, DFMO and NECT. Melarsoprol (1949), a trivalent melaminophenyl arsenical, is active against both *T. brucei* subspecies and both disease stages (Jacobs *et al*., 2011a). However, due to its extreme toxicity it is reserved as second line for late stage *T. b gambiense*, and is used for late stage *T. b. rhodesiense* for which no other options currently exist. The most severe adverse effect of melarsoprol is encephalitic syndrome. It occurs in 5-10% of treated patients, manifested by convulsions and coma, with a mortality rate of approximately 50% (Eperon *et al*., 2014). A prodrug, melarsoprol is rapidly converted to melarsen oxide. It reacts covalently with vicinal dithiols, both in the parasite and the host, and its toxicity likely results from these interactions. It is trypanocidal as it is known to react with the parasite-specific dithiol trypanothione, to form a cyclic complex known as MelT (Fairlamb *et al*., 2016; Fairlamb *et al*., 1989). Resistance to melarsoprol is a major concern with increasing numbers of treatment failures being reported in the field (Lutje *et al*., 2013; Robays *et al*., 2008). The functional loss of the P2 adenosine transporter (TbAT1) in drug uptake has been linked to MPXR both in the field and in the laboratory. Arsenicals (melarsoprol) and diamidines (pentamidine) are both imported into trypanosomes via TbAT1 (Carter and Fairlamb, 1993; Maser *et al*., 1999). *TbAT1* gene deletion and loss-of-function single nucleotide polymorphisms have been described in drug resistance in the laboratory (Graf *et al*., 2016; Maser *et al*., 1999; Stewart *et al*., 2010) and in melarsoprol-resistant clinical isolates (Kazibwe *et al*., 2009; Matovu *et al*., 2001). Also the aquaporin AQP2, synonymous with the high-affinity pentamidine transporter, is important in MPXR (Baker *et al*., 2012). Laboratory and clinical resistance was found to be consequential to a loss of AQP2 mediated transport and replacement with a chimeric *AQP2/AQP3* gene (Graf *et al*., 2015; Graf *et al*., 2016;

Graf *et al*., 2013; Munday *et al*., 2014; Pyana *et al*., 2014). Also the ATP-binding cassette (ABC) transporter, MRPA, is known to account for melarsoprol resistance in *T. brucei*, likely through efflux of MelT (Maser *et al*., 2003; Shahi *et al*., 2002).

DFMO, a fluorinated amino acid, is active against second stage *T. b. gambiense* HAT. In the 1980's DFMO was first discovered to have antitrypanosomal activity both *in vitro* and in the field, leading to its approval and registration for clinical use in 1990 (Eperon *et al*., 2014). In 1995 production was discontinued by its suppliers; however, advocacy efforts by Médecins Sans Frontières in 2000 lead to DFMO monotherapy being used in field projects (Eperon *et al*., 2014). Four daily 2-hour IV infusions for 14 days made the treatment regime logistically demanding. Side effects include headaches and seizures. DFMO is trypanostatic and is a selective irreversible inhibitor of ornithine decarboxylase (ODC), a key enzyme in polyamine synthesis. The slower turnover of ODC in *T. b. gambiense* compared to human cells may account for greater sensitivity in the parasite. Furthermore the innate resistance of *T. b. rhodesiense* to DFMO may be due to the swift turnover of ODC in this subspecies, as well as other mechanisms including decreased *S*-adenosylmethionine metabolism *(Bacchi et al., 1993; Iten et al., 1997).* TbAAT6 was first identified in the transport of DFMO by Vincent et al (Vincent *et al*., 2010). DFMO uptake was reduced in drug-resistant parasites which were found to have a deleted copy of the *TbAAT6* gene. Ectopic expression of *TbAAT6* in drug resistant-parasites, in which a copy of *TbAAT6* was deleted, restored DFMO sensitivity to that of wild type (Vincent *et al*., 2010). Moreover, two RNA interference (RNAi) library screens have further verified TbAAT6 as the major determinant of DFMO resistance in the laboratory (Baker *et al*., 2010; Schumann-Burkard G. *et al*., 2011). DFMO drug resistance in *T. b. gambiense* is not evident in the field.

Nifurtimox, an oral 5-nitrofuran, has been used since the 1970s for the treatment of Chagas Disease. It is a prodrug activated by mitochondrial nitroreductase (NTR) to form highly reactive drug metabolites which are toxic to trypanosomes (Hall *et al*., 2011). NTR is a key determinant of drug resistance in the laboratory; shown both in an RNAi library screen (Baker *et al*., 2010) and in drug resistant *T. brucei* cell lines (Wyllie *et al*., 2016). Nifurtimox monotherapy showed limited efficacy in HAT and it was a trial of the drug combination of Nifurtimox and DFMO (NECT) in 2001 (Priotto *et al*., 2006) that demonstrated high efficacy and good safety profile of this combination therapy. NECT has greatly improved HAT treatment and is phasing-out the use of melarsoprol. In NECT, DFMO is given 200mg/kg twice daily for 7 days (reduced frequency compared to monotherapy) and nifurtimox is given orally three times daily for 10 days (the only oral treatment for HAT). Resistance to NECT has not yet been reported in the field, but, with clear modes of inhibition demonstrated in the laboratory (NTR a determinant of nifurtimox resistance (Wyllie *et al*., 2016; Baker *et al*., 2010) and TbAAT6 a determinant of DFMO resistance (Vincent *et al*., 2010; Baker *et al*., 2010; Schumann-Burkard G. *et al*., 2011)), there are fears of clinical resistance developing and this may have implication for future chemotherapies. Indeed, nifurtimox-resistant *T. brucei* were found to be cross-resistant to other nitro drugs *in vitro* and, critically, cross-resistant to the clinical candidate fexinidazole (discussed in section 1.4.7) was evident both *in vitro* and *in vivo* (Sokolova *et al*., 2010). Should this finding be reproduced in the field, resistance to nifurtimox as part of NECT could preclude the future use of nitro drugs in HAT, including fexinidazole.

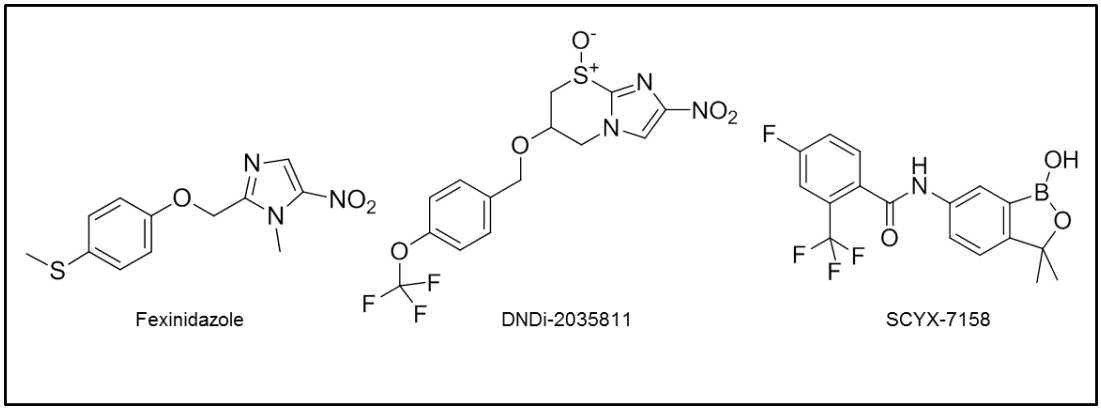

Figure 1.3 Chemical structures of HAT drugs in the pipeline

1.4.6 The drug discovery pipeline and continued endeavours

Whilst NECT has been successfully employed in nearly all endemic countries, its practical limitations restrict its use to hospital settings. Also, concerns regarding resistance to NECT developing in the field are growing. To enable the elimination of HAT, a WHO target by 2020, the development of new drugs is essential. Key characteristics in the target product profile (TPP) for HAT are that new medicines are oral, the administration period is of short duration, active against both *T. brucei* subspecies and both disease stages (penetrate CNS) and are cheaper compared to NECT (http://dndi.org). Two drugs are currently being assessed in HAT clinical trials: fexinidazole and SCYX-7158 (Figure 1.3). Fexinidazole is currently undergoing Phase II/III trials for HAT in the Democratic Republic of Congo and Central African Republic (Eperon *et al*., 2014). Fexinidazole, like nifurtimox, is a nitroaromatic compound. It is a prodrug that is quickly metabolised *in vivo* by two distinct pathways, flavin containing monooxygenease and cytochrome P450, into its two metabolites sulfone and sulfoxide. Despite modest *in vitro* activity the drug exhibited favourable *in vivo* activity in HAT mouse models (Tarral *et al*., 2014; Torreele *et al*., 2010). Fexinidazole-resistant trypanosomes have been generated *in vitro* and demonstrate cross resistance to other nitroimidazoles, including nifurtimox (Sokolova *et al*., 2010). In addition, reduced levels of *NTR* expression were found in drug-resistant trypanosomes implicating a role of NTR in MOA and mechanisms of resistance of fexinidazole (Wyllie *et al*., 2016). Pharmacokinetic/pharmacodynamic properties of fexinidazole are not ideal, with limited solubility, anticipated high human dose and food affecting oral bioavailability and so other nitroimidazoles with improved properties were explored. The lead compound from this endeavour, DNDi-

2035811 (Figure 1.3), is now a backup nitroimidazole (http://dndi.org) (Eperon *et al*., 2014).

Another drug in clinical trials is SCYX-7158, an orally available benzoxaborole. This drug was highly efficacious in pre-clinical studies and is currently in phase I trials, as a single dose treatment for both HAT stages (Jacobs *et al*., 2011b). This oral drug would be an ideal candidate for HAT elimination, if current clinical trials prove fruitful. Benzoxaborole compounds have been shown to kill bacteria and fungi through several mechanisms including inhibiting leucyl-tRNA synthetase (Rock *et al*., 2007); however, the mode of action in *T. brucei* remains unresolved. Benzoxaborole-resistant *T. brucei* cell lines have been generated *in vitro* and proteomic and genomic analysis of these lines provided an array of potential targets implicating a polypharmacological MOA (Jones *et al*., 2015).

A continued effort is still required to deliver new development candidates for HAT. Academic institutions and pharmaceutical companies, either as joint projects or separate endeavours, continue to explore new target-based and phenotypic screening-based approaches. Moreover, in 2013 Novartis and GlaxoSmithKline made substantial investments in HAT drug discovery (Eperon *et al*., 2014). Essential metabolic pathways of the parasite, such as polyamine (Taylor *et al*., 2008) and trypanothione biosynthesis (Torrie *et al*., 2009), glycolysis (Lakhdar-Ghazal *et al*., 2002) and *N*-myristoylation (Frearson *et al*., 2010) are being exploited to identify novel targets for the expansion of new treatments. Folate metabolism is one such pathway. An aim of this thesis is to further dissect folate metabolism in *T. brucei* and in doing so to identify areas that can be exploited for drug discovery endeavours.

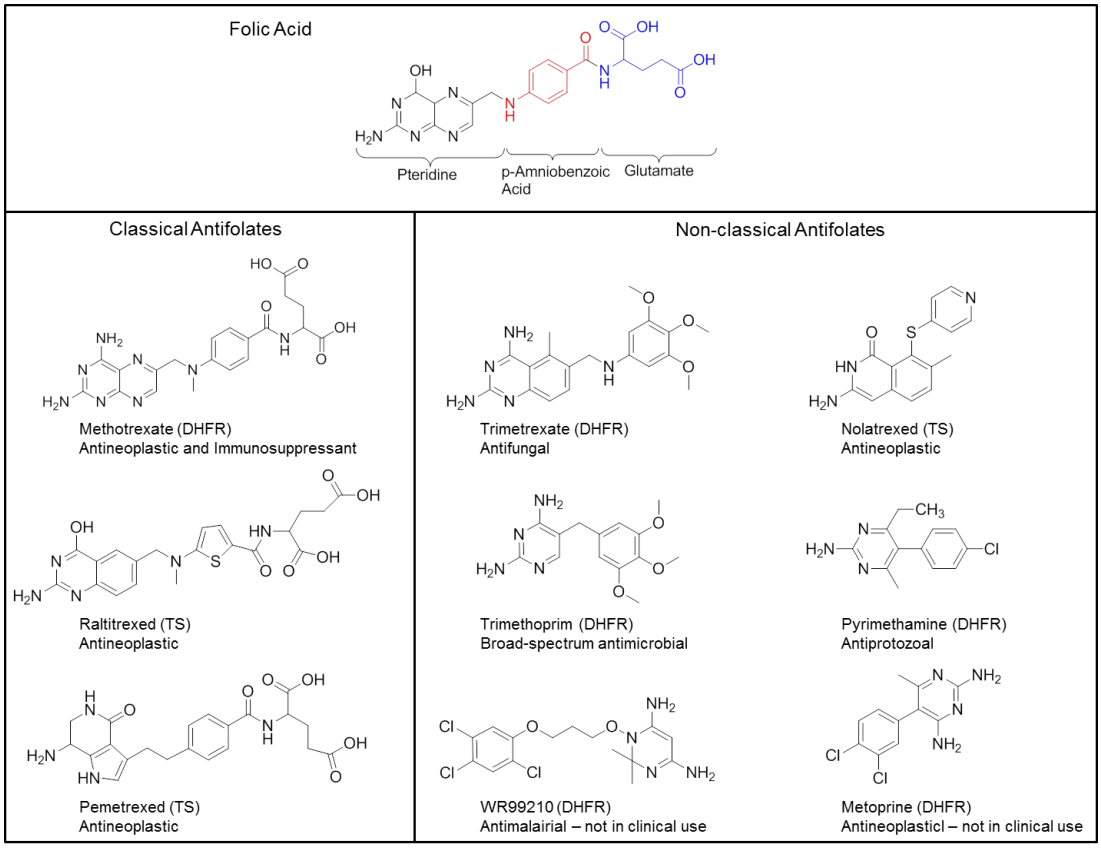

Figure 1.4 Chemical structures of folic acid and antifolate drugs used in this thesis.

1.5 Folate metabolism in mammalian cells

Folates are a family of B_9 vitamins that serve as one-carbon donors in multiple essential biosynthetic pathways. They play an essential role in nucleic acid synthesis, methionine regeneration, and mitochondrial protein synthesis crucial in a wide variety of organisms (Ulrich *et al*., 2008). Folates consist of three chemical components, a pterin ring, *p*–aminobenzoic acid (*p*ABA) and glutamic acid (Figure 1.4 shows the chemical structure of folic acid). They can be found in oxidised form, folic acid, or as naturally occurring reduced forms. Indeed the primary circulating folate in humans is a reduced form, 5-methyl-tetrahydrofolate (5-methyl-THF) (Antony, 1992). Plants and most bacteria are able to synthesize folates *de novo.* However mammalians cells and trypanosomes must obtain folates from their environment. The mammalian folate pathway has been researched in great detail and much can be learned from these studies.

1.5.1 Routes of folate uptake in mammalian cells

Ingested dietary folates primarily exist in polyglutamate forms and cannot cross the cell membrane as long chain (>3) polyglutamate derivatives (Zeng *et al*., 2001). In humans, hydrolysis from the ingested polyglutamate state to a monoglutamate form is accomplished by the enzyme glutamate carboxypeptidase II (GCPII) in the intestinal membrane (Chandler *et al*., 1986). Monoglutamate folates require specific uptake into cells as, under physiological pH, they are negatively charged owing to the ionization of the (dicarboxylic) glutamate moiety (Gonen and Assaraf, 2012).

In human, three transport systems are currently known to regulate folate uptake, the proton-coupled folate transporter (PCFT), the reduced folate carrier

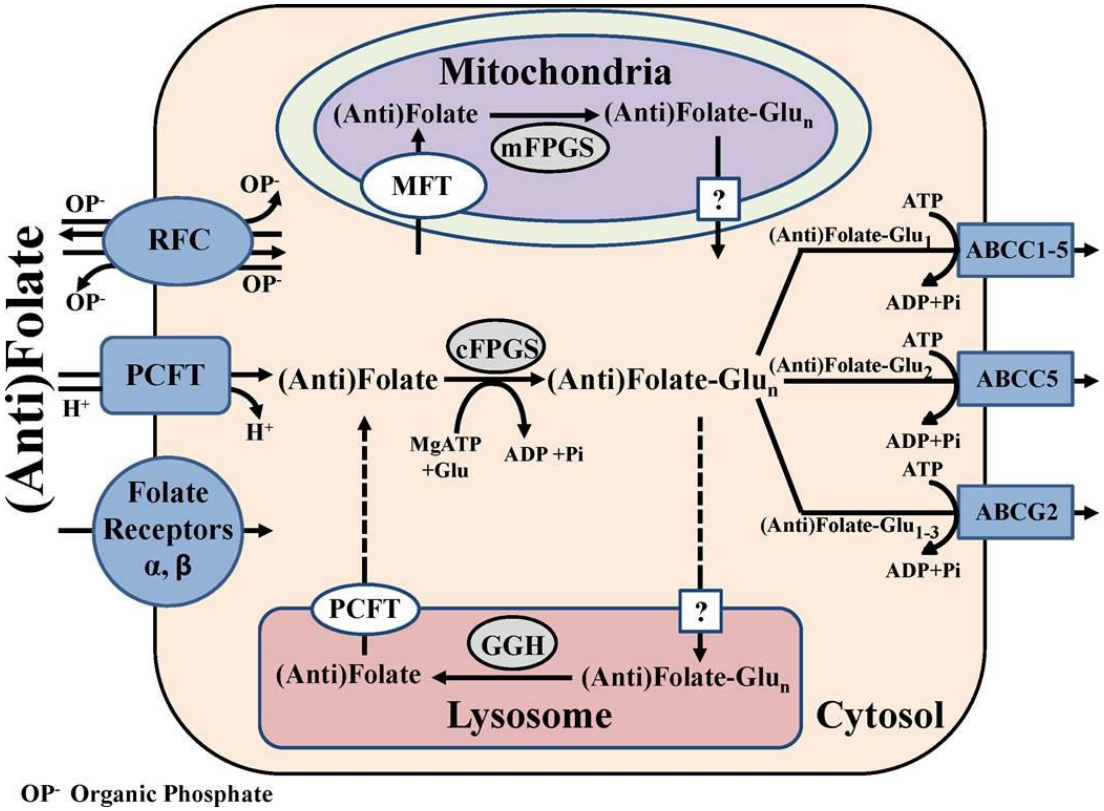

Figure 1.5 Folate metabolism and compartmentalisation in mammalian cells.

Fig 1.4 Taken from Gonen and Assaraf (2012).

Key:
RFC = reduced folate carrier
PCFT = proton-coupled folate transporter
cFPGS = cytosolic folypoly-γ-glutamate synthase
mFPGS = mitochondrial folypoly-γ-glutamate synthase
MFT = mitochondrial folate transporter
GGH = γ-glutamyl hydrolase
ABCC1-5= ATP-binding cassette (ABC) transporters C1-5
ABCG2 = ATP-binding cassette (ABC) transporters G2/breast cancer resistant protein

(RFC) and folate receptors (FRs) (Gonen and Assaraf, 2012) (Figure 1.5). PCFTs are principally expressed in the upper regions of the small intestine (proximal jejunum and duodenum). The PCFT is a unidirectional symporter of folate with H+ and the high concentrations of H+ in the acidic environment of the small intestine facilitates folate uptake (Qiu *et al*., 2006). At pH 5.5, PCFT has high affinity for folic acid, reduced folates (including 5-methyl-THF), and for classical antifolates such as methotrexate (MTX) and pemetrexed (PMX) (K_m largely in 0.5-3 μM range) (Wang *et al*., 2004; Zhao *et al*., 2008). Some transport activity has also been observed at physiological pH. Structurally, PCFT has 12 transmembrane domains with the N and C termini located in the cytoplasm (Zhao *et al*., 2010). In humans, PFCT is also expressed in a variety of other tissues including kidney, liver, splenic tissue and other tissues of the gastrointestinal tract (Qiu *et al*., 2006).

A second transport system, RFC, facilitates folate uptake predominantly in the lower intestine. RFC is a classic transmembrane facilitative carrier, and, like PFCT, has 12 transmembrane domains with the N and C termini located within the cytoplasm (Matherly and Hou, 2008). Deficient of an ATP-binding domain, it is a bidirectional anion antitransporter that facilitates the exchange of extracellular folates with intracellular organic phosphates (Goldman, 1971). It functions at physiological pH and also has high affinity for reduced folates (K_m 1-4 μM), has moderate affinity for MTX (range 2.3 to 26 μM) but has a low affinity for folic acid (K_m 200-400 μM) (Sirotnak, 1985; Sirotnak and Tolner, 1999). RFC can be expressed in virtually all tissues and cell lines and, in humans, it is also found in tissues including bone marrow, lung and coronary tissue (Visentin *et al*., 2014).

Of note, the pH values in different regions of the small intestine correlate with the optimal conditions for folate transport via PCFT and RFC. Intraluminal pH is rapidly changed from highly acid in the stomach to about pH 6 in the duodenum (Fallingborg, 1999), correlating with PCFT having an optimal pH of 5.5 and being primarily expressed in the proximal jejunum and duodenum. The pH gradually increases in the small intestine from pH 6 to about pH 7.4 in the terminal ileum (Fallingborg, 1999), correlating with RFC having optimal pH of 7.4 and being primarily expressed in terminal ileum.

A third route of folate uptake is via the family of high-affinity folate receptors (FRs). FRs are cysteine-rich glycoproteins that mediate folate uptake through endocytosis (Rijnboutt *et al*., 1996). In humans FRs are encoded by three closely located gene loci within chromosome 11q13.3-q13.5 region consisting of three isoforms, FRα, FRβ and FRγ. FRα and FRβ are GPI-anchored cell surface glycoproteins whereas FRγ is a secreted protein (Antony, 1996). Frα and FRβ display very high affinity for folic acid (K_d~: 0.1-1 nM) and reduced folates (K_d: 1-10 nM) and a relatively lower affinity for MTX (K_d >100 nM) (Antony, 1996; Rijnboutt *et al*., 1996). FRs are the main route of uptake of 5-methyl-THF, the most predominate circulatory form of folate. FRα is found on the membrane of epithelial tissues (in particular the uterus, placenta, choroid plexus, retina and kidney) and FRβ found in hematopoietic tissues (e.g. thymus and spleen) (Zhao *et al*., 2011).

1.5.2 Intracellular folate metabolism in mammalian cells

Following cellular uptake via the influx routes described above, folate metabolism can be compartmentalised into three main intracellular compartments, the cytosol,

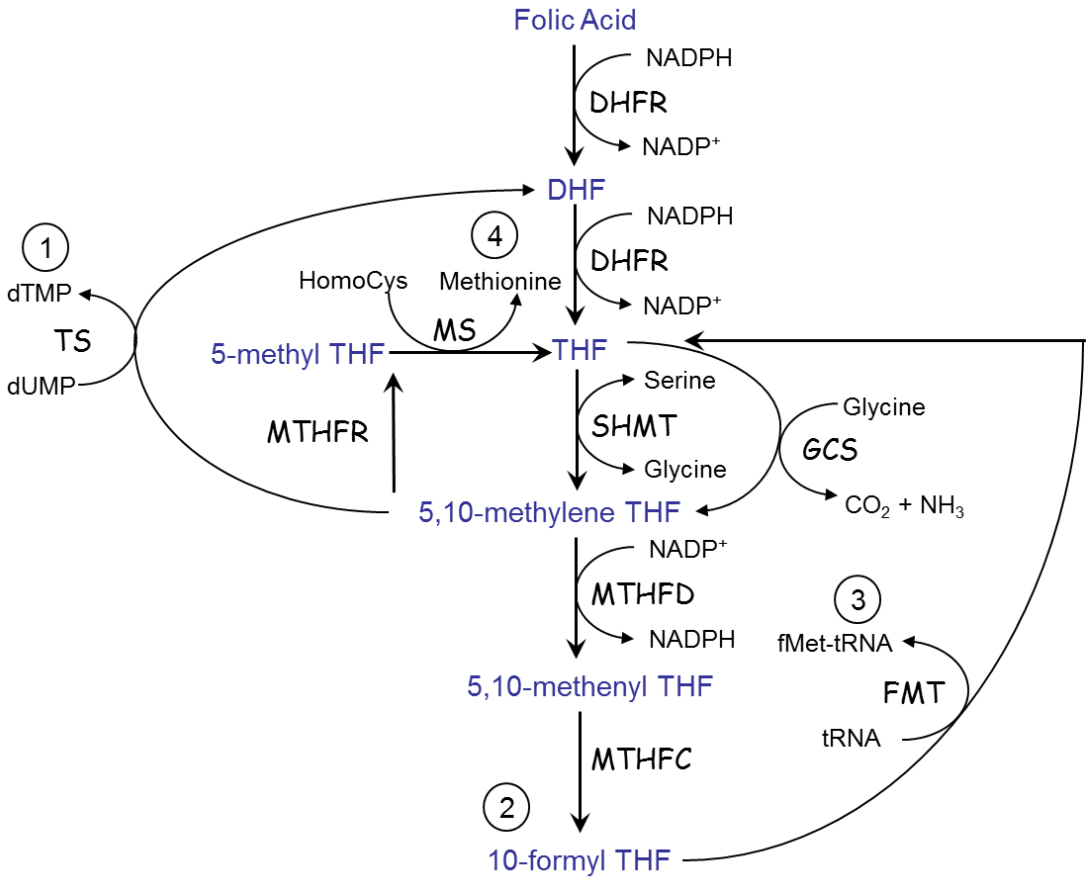

Figure 1.6 Folate metabolism and one-carbon transfer reactions in mammalian cells

Metabolic Reactions

1 = DNA synthesis
2 = Purine Synthesis
3 = Protein Synthesis
4 = AdoMet and methylation reactions

Enzyme Key:

DHFR	dihydrofolate reductase
GCS	glycine cleavage system
SHMT	serine hydroxymethyl transferase
MTHFD	methylene tetrahydrofolate dehydrogenase
MTHFC	methenyl tetrahydrofolate cyclohydrolase
FMT	methionyl-tRNA *formyltransferase*
MTHFR	methylene tetrahydrofolate reductase
MS	methionine synthase
TS	thymidylate synthase

the mitochondria and the lysosome (Figure 1.5). Polyglutamylation of intracellular folates occurs in the cytosol and mitochondria, whereas hydrolysis occurs in the lysosome (Gonen and Assaraf, 2012) (Figure 1.5). Polyglutamylation is regulated by the enzyme folylpoly-γ-glutamate synthase (FPGS). FPGS catalyses the sequential addition of glutamic acid to the γ-carboxyl group of reduced folates and classical antifolate drugs (Gonen and Assaraf, 2012). It plays a crucial role in intracellular folate regulation. Polyglutamylated folates cannot cross lipid bilayers and are no longer substrates for influx transporters (e.g. RFC) and efflux transporters, which enables intracellular retention (Zeng *et al*., 2001). Also, polyglutamylated folates are better substrate than monoglutamates for various intracellular folate dependent enzymes (Gonen and Assaraf, 2012). FPGS enables the accumulation of polyglutamates in the mitochondria, the site of key intracellular folate functions and the principal reservoir of intracellular folates (Lin *et al*., 1993). Counteracting the process of polyglutamylation is hydrolysis to monoglutamate folate forms, by the glycoprotein enzyme γ-glutamyl hydrolase located in the lysosome (Galivan *et al*., 2000; Gonen and Assaraf, 2012). This allows folates to be exported out of the cell by efflux mechanisms to be described later.

THF is the biologically active form of folate and its derivatives are utilised for a variety of one-carbon transfer reactions essential for cellular proliferation and maintenance both in the cytosol and mitochondria. Indeed, THF cofactors that originate in the cytosol can be transported into the mitochondrion by the mitochondrial folate transporter (MFT) (Lawrence *et al*., 2011). Various forms of THF have been identified intracellularly (e.g. 5-methyl-, 5,10-methylene- and 10-formyl-THF) (Figure 1.6). THF itself is a cofactor for the production of glycine from serine by serine hydroxymethyl transferase (SHMT) both in the cytosol and

mitochondrion (Stover and Schirch, 1990). Moreover it is also a cofactor in the mitochondrial glycine cleavage system (GCS) for the catabolism of glycine. The GCS is a multienzyme system comprised of four proteins: T-protein, P-protein, H-protein and L-protein. GCS–P protein (a pyridoxal phosphate-dependent glycine decarboxylase) catalyses the decarboxylation of glycine and the reductive methylamination of the lipoamide which is then covalently attached to GCS-H protein (a hydrogen carrier protein) and then shuttled to GCS-T protein and GCS-L protein. GCS-T protein (a tetrahydrofolate-requiring aminomethyltransferase) catalyses the transfer of methylene to THF and subsequent release of ammonia. GCS-L protein (a lipoamide dehydrogenase) is used in the oxidation of the dihydrolipoyl residue of H-protein.

5,10-Methylene-THF is exploited in the cytosol for the reductive methylation activity of thymidylate synthase (TS) that converts deoxyuridine monophosphate (dUMP) tothymidine monophosphate (dTMP) for DNA synthesis. The by-product of this reaction is dihydrofolate (DHF) which is reduced to THF by dihydrofolate reductase (DHFR) an abundant key cytosolic enzyme that maintains cellular THF. DHFR also sequentially reduces folic acid to DHF. 5,10-Methylene-THF is converted into 10-formyl-THF by the C1-THF synthase complex (which includes methylene-THF dehydrogenase (MTHFD) and methenyl-THF cyclohydrolase (MTHFC) (Hum *et al*., 1988). 10-Formyl-THF is used for cytosolic *de novo* purine synthesis as well as for the formation of methionyl-tRNA by methionyl-tRNA formyltransferase (FMT). Methionyl-tRNA is used for the initiation of mitochondrial protein synthesis. Methylene-THF reductase (MTHFR) catalyses the conversion of 5,10-methylene-THF to 5-methyl-THF . 5-Methyl-THF serves as a mitochondrial one carbon donor for methionine synthase (MS). MS converts

homocysteine to methionine, a precursor for the production of S-adenosylmethionine (AdoMet) which is utilised in the methylation of DNA and histones.

1.5.4 Folate efflux in mammalian cells

Efflux of folates is principally mediated by ATP-binding cassette (ABC) transporters. These are high capacity, low-affinity transmembrane transporters that couple ATP hydrolysis to transport substrates across the cell membrane. Multidrug resistant proteins (MRP/ABCC) compromise 13 members of the ABCC sub-family that are distinct by the conserved structure of the ATP-binding domain or nucleotide binding domains ((Zhou *et al*., 2008). Folates are amongst the various substrates of ABCC1-5, and these efflux pumps have been demonstrated to export THF, THF substrates and antifolate drugs out of the cell (Assaraf, 2006). Moreover, a low-capacity high-affinity ABC transporter capable of folate and antifolate drug export is the breast cancer resistant protein (BRCP/ABCG2) (Chen *et al*., 2003; Ifergan *et al*., 2004). ABC transporters are expressed in various tissues including the duodenum small intestine, biliary and liver tissue. Moreover, organic anion transporters (OAT1B1 and OATB3) present in the basolateral membrane of hepatocytes may also have a role in folate transport (Visentin *et al*., 2014). Folate export from the lysosome is thought to be mediated by PCFT and driven by the large pH gradient between endosome-lysosome and the cytosol (Zhao *et al*., 2007).

1.6 Folate metabolism in the Trypanosomatids

Trypanosomes, like mammalian cells, are auxotrophic for folates (Sienkiewicz *et al*., 2008; Vickers and Beverley, 2011). Research into parasite folate metabolism mainly

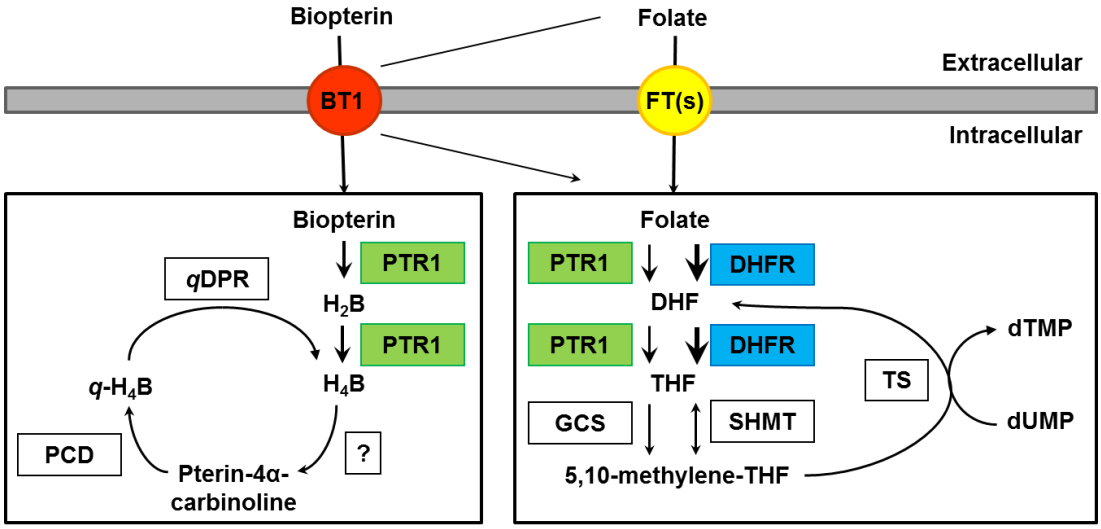

Figure 1.7 Folate and pteridine transport pathways in *Leishmania*

Figure modified and adapted from Vickers and Beverley (2011).

Key:

BT1	biopterin transporter 1
DHFR	dihydrofolate reductase
FT(s)	folate transporters
GCS	glycine cleavage system
PCD	pterin-4 alpha-carbinolamine dehydratase
PTR1	pteridine reductase 1
SHMT	serine hydroxymethyl transferase
TS	thymidylate synthase
qDPR	quinoid dihydropteridine reductase

examines the roles of specific folate-dependent enzymes (and transporters) in metabolism and virulence, and extrapolates targets for current and new antifolate drugs. Of the three distinct trypanosomatids, *T. brucei, T. cruzi* and *Leishmania* species, the majority of the underpinning knowledge in folate metabolism is derived from studies in *Leishmania*.

1.6.1 Folate metabolism in *Leishmania*

Leishmania transports folates via a novel superfamily of transporters known as Folate Biopterin Transporters (FBT). This class of transporter family was identified first in *Leishmania* (Kundig *et al*., 1999; Richard *et al*., 2002) and later found in the other kinetoplastids (Ouameur *et al*., 2008). *Leishmania* has 14 FBTs and the function of four members, BT1, FT1, FT5 and AdoMetT1 has been described. FT1 and FT5 specifically transport folates. FT1 is the predominant folate transporter in *Leishmania* and has a high affinity/high capacity for folate, (Richard *et al*., 2004), while FT5 is a high affinity/low capacity transporter (Richard *et al*., 2002). In contrast, BT1 is a biopterin transporter that mediates the uptake of folate but primarily mediates the uptake of the pteridine biopterin (Kundig *et al*., 1999) (Figure 1.7). AdomeT1, the fourth characterised member of the FBT family in *Leishmania*, is a high affinity transporter of AdoMet (Dridi *et al*., 2010a).

Intracellular oxidised folates are reduced sequentially to THF by the actions of pteridine reductase 1 (PTR1) and DHFR-TS (Vickers and Beverley, 2011) (Figure 1.7) with studies showing that DHFR-TS is responsible for the preponderance of THF production (Nare *et al*., 1997). PTR1 has a dual action in folate and pteridine metabolism. It reduces folic acid to DHF, and DHF to THF, and can also sequentially reduce biopterin to dihydrobiopterin and then to tetrahydrobiopterin

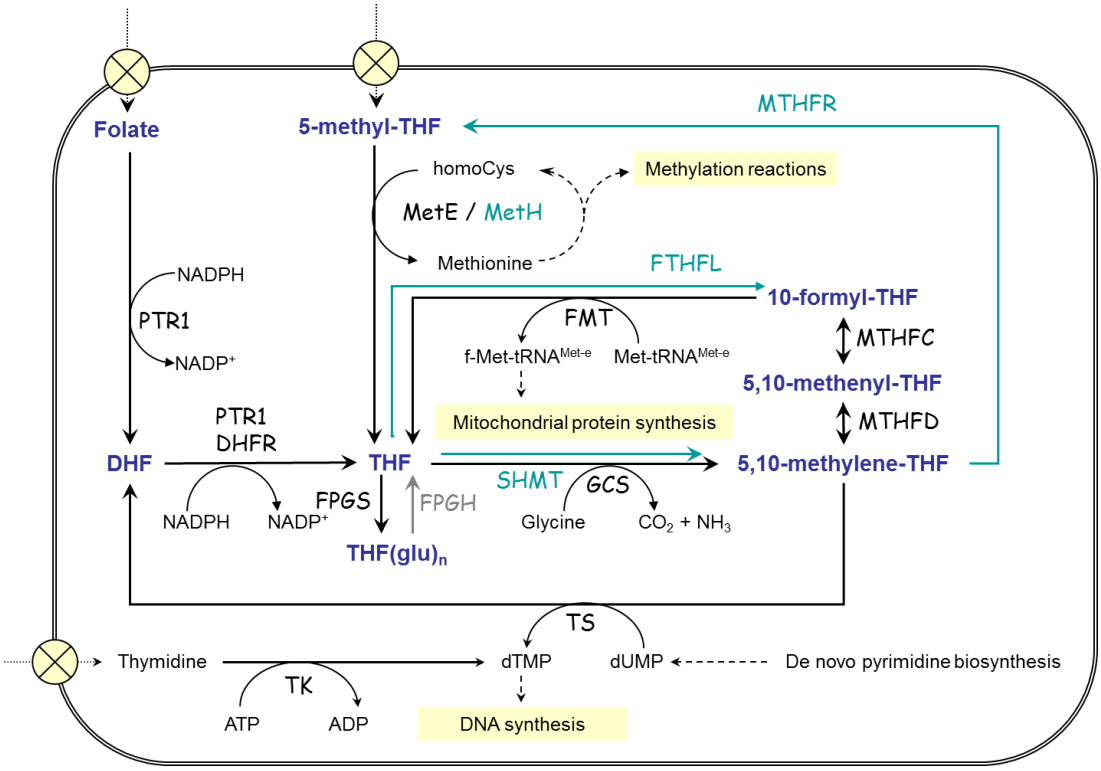

Figure 1.8 Folate metabolism in *T. brucei* and *Leishmania*

Enzyme Key:

DHFR	dihydrofolate reductase
FMT	methionyl-tRNA *formyltransferase*
FPGH	folylpoly-γ-glutamate hydrolase
FPGS	folylpoly-γ-glutamate synthase
FTHFL	10-formyl tetrahydrofolate ligase
GCS	glycine cleavage system
SHMT	serine hydroxymethyl transferase
MetE	vitamin B_{12}-independent methionine synthase
MetH	vitamin B_{12}-dependent methionine synthase
MTHFC	methenyl tetrahydrofolate cyclohydrolase
MTHFD	methylene tetrahydrofolate dehydrogenase
MTHFR	methylene tetrahydrofolate reductase
PTR-1	pteridine reductase - 1
TS	thymidylate synthase

(Bello *et al*., 1994). However, both *in vitro* (Bello *et al*., 1994) and *in vivo* (Cunningham *et al*., 2001) studies have shown PTR1 not to be essential in *Leishmania*, with the activity of other bypass enzymes in folate metabolism likely to account for this. In trypanosomatids, DHFR-TS is a homodimer constituting DHFR fused to TS using a linker peptide to form the bifunctional enzyme DHFR-TS. This is in contrast to humans where DHFR and TS are separate enzymes. In *Leishmania* DHFR has little activity in reducing unconjugated folate and has greater activity in reducing DHF (Nare *et al*., 1997) with PTR1 able to reduce folate to DHF (Bello *et al*., 1994). Unlike PTR1, DHFR-TS is essential both *in vitro* (Cruz and Beverley, 1990) and *in vivo* (Nare *et al*., 1997). Indeed DHFR-TS has been explored as a drug target in *Leishmania* (Gilbert, 2002).

The reduction of THF to 5,10-methylene-THF by mitochondrial GCS activity enables intracellular glycine catabolism. *Leishmania* and the other trypanosomatids possess close orthologues of the GCS P-protein, GCS T-protein and GCS H-protein (Vickers and Beverley, 2011). *GCVP* (which encoded GCS P-protein) null mutants lacked GCS activity *in vitro*; however parasites were viable, but their growth was reduced with serine depletion (Scott *et al*., 2008). In *GCVP*-null mice attenuation of *Leishmania* infection was found. *Leishmania* possesses the enzyme SHMT which, like GCS, reduces THF to 5,10-methylene-THF, but does so by converting serine to glycine (Figure 1.8). The fact that *GCVP* null mice had attenuated infectivity suggests that the parasites cannot scavenge sufficient serine *in vivo* to facilitate SHMT to fully recompense for loss of GCS activity. In *Leishmania* SHMT has two orthologues, located in the cytosol and the mitochondria respectively (Gagnon *et al*., 2006). SHMT inactivation, through knockdown of the two orthologues, demonstrated that it was not essential for parasite growth *in vitro* in a rich media

(Roy and Ouellette, 2015). When the media was serine deplete, parasite growth was substantially reduced with SHMT inactivation.

Unlike mammalian cells, trypanosomatids lack *de novo* purine synthesis (Bellofatto, 2007) and so the prime function of 10-formyl-THF is the formylation of methionyl-tRNA by FMT. In *Leishmania* 10-formyl-THF can be generated by enzymes of the C1-THF synthase complex, either by the sequential reduction of 5,10-methylene-THF by MTHFD and MTHFC, or directly from THF by the activity of 10-formyl-THF ligase (FTHFL) (Figure 1.8). FTHFL was shown to be non-essential *in vitro* and *in vivo*, likely due to the bypass actions of MTHFD and MTHFC (Murta *et al*., 2009). However, MTHFC was shown to be essential *in vitro* and the phenotype could be rescued by *FTHFL* overexpression (Murta *et al*., 2009). 5-Methyl-THF can be formed intracellularly from 5,10-methylene-THF by the action of methylenetetrahydrofolate reductase (MTHFR). MTHFR is not essential both *in vitro* and *in vivo* (Vickers *et al*., 2006), indeed the parasite can source extracellular 5-methyl-THF using FBT uptake as previously described. Polyglutamylation of intracellular folates is carried out by the enzyme FPGS. Studies in *Leishmania* found that overexpression of *FPGS* increased long chain glutamates (Glu_5) while in parasites where one *FPGS* allele was interrupted glutamates were predominantly short chained (Glu_3, Glu_4). Also, long term accumulation of folates was substantially increased with *FPGS* overexpression (El Fadili *et al*., 2002).

1.6.2 Folate metabolism in *T. brucei*

Comparatively, very little is known about folate metabolism in *T. brucei* and most of our understanding of folate metabolism in trypanosomatids is based on *Leishmania*. However, comparative genomics indicates that *T. brucei* lacks a number of genes in

folate-dependent pathways that are found in *L. major* (Berriman *et al.*, 2005). Indeed, folate metabolising enzymes such as SHMT, MTHFR and FTHFL, which have been studied in *Leishmania,* are not found in *T. brucei* (Figure 1.8). The lack of SHMT suggests *T. brucei* is entirely dependent on the GCS for generating 5,10-methylene-THF; moreover, the lack of MTHTR suggests that *T. brucei* is more reliant on uptake of host 5-methyl-THF via putative transporters. These differences between *T. brucei* and *Leishmania* suggest that folate metabolism in *T. brucei* may be more vulnerable to disruption and advocates greater potential for antifolate drug therapeutics in *T. brucei*.

When comparing folate uptake, *T. brucei* has 7 FBT homologues compared to the 14 FBT homologues found in *Leishmania* (Ouameur *et al*., 2008). Folate uptake and the function of FBTs have not been characterised in *T. brucei*. Two enzymes in folate metabolism which have been studied to a degree in *T. brucei* are PTR1 and the bifunctional DHFR-TS enzyme. In *T. brucei* PTR1 is essential for cell survival (Sienkiewicz *et al*., 2010), in contrast to *Leishmania* where it is not essential. *TbPTR1* knockdown by RNAi resulted in loss of viability *in vitro* and loss of virulence *in vivo*. *Tb*PTR1 is reported to display low activity in reducing folate and DHF (Ong *et al*., 2011) and so its essentiality may be based more on its function to reduce pterins. *T. brucei*, unlike *Leishmania*, lack quinoid dihydropteridine reductase (qDPR) genes and are solely dependent on PTR1 for H_4B production, thus explaining why PTR1 is essential in *T. brucei*. *Tb*PTR1 has been explored as a drug target. An in silico fragment screen was used to identify hits against PTR1 (Mpamhanga *et al*., 2009) and co-crystal structures were obtained from compounds containing a core benzimidazole scaffold to give a potent inhibitor (Spinks *et al*., 2011). Although potent inhibitors of the enzyme were identified this did not correlate

with *in vitro* potency and further work is required to understand lack of cellular activity (Gilbert, 2013).

The bifunctional enzyme DHFR-TS is also essential for *T. brucei* survival *in vitro* and *in vivo* (Sienkiewicz *et al.*, 2008). Nutritional recue was achieved *in vitro* with the addition of thymidine, highlighting thymidine scavenging as a bypass in dTMP production via the action of thymidine kinase (TK). Also, DHFR-TS$^{-/-}$ cells could not be rescued with an enzymatically active TS on a plasmid, demonstrating that both DHFR and TS are required for thymidylate synthesis. There was a lack of infectivity *in vivo* in DHFR-TS$^{-/-}$ mice. Sensitivity to classical antifolate drugs (including MTX) was substantially reduced in DHFR-TS$^{-/-}$ parasites, validating the enzyme as a drug target. TbDHFR-TS has recently been recombinantly produced, which was challenging as the TS activity of recombinant TbDHFR-TS was highly unstable (Gibson *et al*., 2016). TbDHFR-TS was unable to reduce folic acid, which is in agreement with *Leishmania* DHFR-TS, highlighting that in the trypanosomatids DHFR primarily functions to reduced DHF to THF.

1.6.3 Folate metabolism in *T. cruzi*

Of the trypanosomatids, least is known about folate metabolism in *T. cruzi*. There are three homologues of the FBT family that are annotated in the genome, but their function has yet to be characterised (Ouameur *et al*., 2008). Of note, as well as having PTR1 *T. cruzi* also has a second pteridine reductase, PTR2. PTR2 can reduce dihydrobiopterin and DHF, similar to the function of PTR1; however, it cannot reduce oxidised pteridines or folates (Robello *et al*., 1997; Senkovich *et al*., 2003). Crystal structures of an inhibitor (MTX) and a substrate (DHF)-complex with PTR2 have also been elucidated (Schormann *et al*., 2005). DHRF-TS has been studied in *T.*

cruzi. Single gene knockout *T .cruzi* parasites (TcDHFR-TS$^{+/-}$) have been generated (Xu *et al.,* 2009; Branadan *et al.,* 2011), however attempts to create a double null mutant (TcDHFR-TS$^{+/-}$) did not succeed (Branadan *et al.,* 2011). Also, thymidine supplementation to culture media did not aid in obtaining double null parasites, suggesting that DHFR-TS may be essential *in vitro*. Impaired parasite growth was observed in DHFR-TS$^{+/-}$ *in vitro* and also these mutants displayed reduced virulence in mice (Branadan *et al.,* 2011). There have been few endeavours in regards to DHFR-TS targeted drug discovery in *T. cruzi*. TcDHFR enzyme activity and whole cell activity (amastigote) has been assessed in a few chemical series with moderate results (Chowdhury *et al*., 1999; Chowdhury *et al*., 2002; Gilbert, 2002; Khabnadideh *et al*., 2005). 2-4 Diaminopyrimidine based compounds were also tested in mice; however, a lack of i*n vivo* activity was found (Pez *et al*., 2003). The crystal structure of TcDHFR-TS has been reported and docking sites and binding affinities of novel and known DHFR-TS inhibitors have been characterised (Schormann *et al*., 2008; Senkovich *et al*., 2009) gaining insight into the DHFR and TS active sites that can be exploited for the development of antifolate-based compounds for *T. cruzi*.

1.7 Antifolate drugs

Antifolate drugs, also known as folate antagonists, or antifols, are drugs that inhibit the intracellular actions of folic acid derivatives. Folate dependent processes such as purine and thymidylate biosynthesis are blocked, resulting in cell death. ‘Thymineless-death’ describes the phenomenon of cell death via inhibition of dTMP and DNA synthesis leading to cell cycle arrest in S phase (Khodursky *et al*., 2015).

Indeed antifolate drugs are known be cytotoxic during the S phase of the cell cycle (Di Gennaro E. *et al*., 2009; Taylor and Tattersall, 1981).

In the 1940s aminopterin was discovered to be an effective treatment in childhood acute leukaemia. It was replaced by MTX which was found to be less toxic and, decades after this, more rationally designed new generation antifolates have been developed. Today, antifolates are commonly used as adjuvant drugs with chemotherapy in the treatment of human malignant diseases (e.g. MTX, PMX, raltitrexed (RTX)) (Gonen and Assaraf, 2012; Wilson *et al*., 2014). Also, antifolates are used for non-malignant diseases. They are used clinically in the treatment of inflammatory diseases including rheumatoid arthritis and psoriasis (MTX); and are used in infectious diseases such as protozoal infections (pyrimethamine (PYR) used as an antimalarial agent and against toxoplasmosis), bacterial infections (trimethoprim (TMP) is a broad-spectrum antimicrobial) and fungal infections (trimetrexate (TMX) is used against *Pneumocystis* pneumonia) (Walling, 2006; Wright and Anderson, 2011).

Antifolates can generally be divided into two main categories, classical antifolates and non-classical antifolates. Classical antifolates, such as MTX and RTX, bear close structural resemblance to naturally occurring folates and contain a terminal glutamate residue and undergo intracellular polyglutamylation in mammalian cells. They also use the same mechanism as folates for cell entry via specific transporters (e.g. RFC, PCFT, FRs in mammalian cells) (Gonen and Assaraf, 2012). Non-classical antifolates, such as PYR and nolatrexed (NTX) are devoid of a glutamate moiety and are not polyglutamylated (Gonen and Assaraf, 2012). Non-classical antifolates are often termed lipophilic. However, in themselves they are not that lipophilic. Indeed, the clinically used non-classical antifolates that

have been tested in this thesis (Figure 1.4) have LogP values < 2. But these drugs are relatively lipophilic compared to classical antifolates that contain glutamate, a very hydrophilic moiety, and have LogP values < 0 (LogP values from http://chemspider.com). A further subdivision of antifolates can be made in regards to whether they are primarily selective for DHFR or TS. MTX is a potent competitive and reversible inhibitor of DHFR whereas newer antifolates such as RTX and NTX have been designed to directly inhibit TS. Structurally, compounds with a primary amine at position 4 favour DHFR inhibition and a carbonyl substituent in this position selects for TS inhibition (Phan *et al*., 2001). This change in selectivity is explained by the carbonyl oxygen providing extra hydrogen bonding. Moreover, TS-targeted classical antifolates have a terminal glutamyl moiety which results in polyglutamylation of the drug and better binding to TS (Synold *et al*., 1996). In this thesis a selection of both classical and non-classical antifolate drugs were used and within these groups compounds were either DHFR or TS selective (Figure 1.4). As well as primarily targeting DHFR and TS some antifolates also inhibit two key enzymes in *de novo* purine biosynthesis, β-glycinamide ribonucleotide transformylase (GART) and 5-aminoimidazole-4-carboxamide ribonucleotide transformylase (AICART). For the antifolates used in this thesis, PMX, primarily targeting TS, is also known to inhibit DHFR, GART and AICART (Wilson *et al*., 2014).

Antifolates are known to have a greater toxic effect in rapidly dividing cells, since their requirement for purines and thymidylate for DNA synthesis is high. Therefore, they are effective in killing malignant cells, but also have adverse effects on cells which divide rapidly such a bone marrow, skin, and hair. Indeed the folic acid derivative leucovorin (5-formyl-THF) is used as a folic acid supplement to

reduce the toxic side effects in patients receiving MTX treatment (Shiroky *et al*., 1993; Treon and Chabner, 1996). Resistance to antifolate drugs has emerged clinically, both in the treatment of malignant diseases (Gonen and Assaraf, 2012) and non-malignant diseases (inflammatory and infectious diseases) (Brolund *et al*., 2010; Gregson and Plowe, 2005; van der Heijden *et al*., 2007). Mechanisms of resistance include: decreased influx (via specific transporters for classical antifolates), impaired polyglutamylation (via FPGS), increased hydrolysis (via γ-glutamyl hydrolase), overexpression and mutations of enzyme targets (e.g. DHFR and TS), expanded intracellular folate pool and increased efflux (Assaraf, 2007; Gonen and Assaraf, 2012).

In light of this, new generation antifolates are being designed to overcome these drug resistance mechanisms. In *T. brucei* the bifunctional enzyme DHFR-TS was found to be a target of antifolate drugs and MTX was shown to have nanomolar whole cell potency (Sienkiewicz *et al.,* 2008). This has heightened the possible role of antifolate drugs as chemotherapeutic agents for HAT. Some antifolate drugs are available in oral preparations and also some have good CNS penetration, which confers well with the TPP for new compounds for HAT. However, there are many questions regarding the MOA of antifolates in *T. brucei* yet to be addressed (i.e. transport of drug, cell cycle effect and cidal/static effect). Understanding drug resistance mechanisms will help identify any problems if the drugs are used in the field, as well as giving insight into designing new and refining existing antifolates.

It should be noted that when testing antifolate drugs against *T. brucei* or investigating folate metabolic pathways *in vitro*, the utilisation of folate and thymidine depleted medium is essential. Standard culture for BSF *T. brucei*, based on HMI9, is very nutrient rich compared to the parasites natural *in vivo* environment.

This can hinder drug discovery endeavours as nutrient rich media could mask drugs that are potential pharmacologically active *in vivo*. Minimal media for *in vitro* culture have been used to create more physiologically relevant conditions (Baltz *et al*., 1985; Creek *et al*., 2013; Sienkiewicz *et al*., 2008). Indeed DHFR-TS inhibitors were shown to be most potent when tested in a folate deficient media 'FDM' (Sienkiewicz *et al*., 2008). High folate levels *in vitro* have been found to hinder antifolate drug potency in other systems (Nare *et al*., 1997; Peters *et al*., 1999). However, when testing antifolate drug potency in *T. brucei* media should be deficient of not only folate but also thymidine. Antifolates reduced the intracellular THF pool, which in turn circumvents dTMP and DNA synthesis resulting in 'thymineless-death', but, *T. brucei* can also salvage extra-cellular thymidine by-passing *de novo* dTMP synthesis (Sienkiewicz *et al*., 2008). In mammalian cells it is well-established that salvage nucleotide synthesis can hinder the inhibitory effects of antifolates (Jackman *et al*., 1991; Kinsella *et al*., 1997; Sobrero and Bertino, 1986). The standard media for *T. brucei* cell culture (HMI9) contains folate concentrations that are 150-2,000 times the plasma concentration in humans (Wahlin *et al*., 2002) and thymidine concentration 23-90 times that of humans (Howell *et al*., 1981). Consequently, this non-physiological high folate concentration could reduce the anti-trypanosomal potency of antifolate drugs through mechanisms such as competition for drug uptake, hindering cellular retention by competition for polyglutamylation by FPGS or through competition for the active site of target enzymes (e.g. DHFR-TS).

1.8 Aims and Objectives

The aim of this thesis is to expand upon the knowledge of the mechanism of action and resistance of antifolate drugs in *T. brucei brucei*, the model organism for HAT.

Mechanism of Action

- To establish a folate and thymidine depleted media that will enable studies to examine antifolate drug potencies under physiological conditions.
- To identify the nature of killing (cidal/static) and confirm mechanism of action (‘thymineless-death’) of antifolates.
- To screen a small library of DHFR-TS/PTR1 inhibitors of the Drug Discovery Unit (DDU).
- To describe the transport kinetics of folate and MTX in *T. brucei*. To determine whether antifolates and folate derivatives compete with folate uptake into cells.

Mechanism of Resistance

- To identify mechanism of resistance by a RIT-Seq study with selected classical antifolate drugs and to confirm hits from these screens by RNAi knockdown and phenotypic studies.
- To establish a MTX resistant cell line and identify key parameters involved in the mode of resistance by phenotypic studies, DNA and proteomic (stable isotope labelling with amino acids in cell culture (SILAC)) analysis.

Chapter 2: Material and Methods

2.1 Materials and chemicals

DHFR-TS inhibitors were obtained as follows: NTX, PMX and RTX from Sequoia Research Products; MTX, TMP, PYR and WR99210 from Sigma Aldrich; metoprine (MTP) from Toronto Research Chemicals; and TMX from Tocris Bioscience. Melarsoprol was purchased from Rhone-Poulenc. Solid stocks of compounds **1**, **2** and **4 - 16** from the "antifolate set" (see Fig 3.4) were sourced from the chemistry team of the Dundee Drug Discovery (DDU). Stocks were dissolved in DMSO and Dr Stephen Paterson confirmed purity and identity of the compounds by liquid chromatography - mass spectrometry and, when required, nuclear magnetic resonance. All compounds were of 90% purity or higher. Folic acid, p-aminobenzoyl-L-glutamic acid (*p*ABA-Glu) and biopterin were obtianed from Schircks Laboratories. ^{3}H-Folic acid (64 Ci mmol^{-1}) and ^{3}H-MTX (38.2 Ci mmol^{-1}) were purchased from Hartmann Analytical. Stable isotope-labelled amino acids were purchased from CK Gas Products.

2.2 Trypanosomatid cell cultures and culture media

Media and reagents used for culturing trypanosomes were filter sterilised using a Steriflip filtration unit (0.22 μm PES membrane, Millipore).

2.2.1 HMI9-T Media

HMI9-T was prepared based on HMI9 medium (Hirumi and Hirumi, 1989). However 56 μM 1-thioglycerol was substituted for 200 μM 2-mercaptoethanol as the reducing agent (Greig *et al*., 2009). Liquid IMDM (Thermo Fisher) was supplemented with 10% dialysed FCS (Gibco, Life Technologies), 10 % Serum Plus^{TM} (SAFC biosciences), 2 μM GIBCO ® GlutaMAX™ (Thermo Fisher), 110 μg

Table 2.1: Composition of HMI9-T, RPMI-BM and TBM

COMPONENTS	HMI9-T (mM)	RPMI-BM (mM)	TBM (mM)
Amino acids			
Hydroxy L-proline	0	0.153	0
Glycine	0.400	0.133	0.400
L-Alanine	0.281	0	0.281
L-Arginine	0.398	1.75	0.398
L-Asparagine	0.167	0.379	0.167
L-Aspartic acid	0.226	0.150	0.226
L-Cystine 2HCl	0.381	0.285	0.381
L-Glutamic Acid	0.510	0.136	0.510
L-Glutamine	4.00	2.05	2.00 [a]
L-Histidine	0.200	0.297	0.200
L-Isoleucine	0.802	0.782	0.802
L-Leucine	0.802	0.782	0.802
L-Lysine hydrochloride	0.798	0.670	0.798
L-Methionine	0.201	0.202	0.201
L-Phenylalanine	0.400	0.291	0.400
L-Proline	0.348	1.82	0.348
L-Serine	0.400	0.286	0.400
L-Threonine	0.798	0.568	0.798
L-Tryptophan	0.0784	0.745	0.0784
L-Tyrosine disodium salt	0.462	0.248	0.462
L-Valine	0.803	0.571	0.803
Vitamins			
Biotin	0.0000533	0.000820	0.0000533
Choline chloride	0.0286	0.0214	0.0286
D-Calcium pantothenate	0.00839	0.000524	0.00839
Folic Acid	0.00807[b]	0.0000309[c]	0[d]
i-Inositol	0.0400	0.194	0.0400
Niacinamide	0.0328	0.00820	0.0328
Pyridoxal / pyridoxine	0.0196[e]	0.00485[f]	0.0196[e]
Para-Aminobenzoic Acid	0	0.00730	0
Riboflavin	0.00106	0.000532	0.00106
Thiamine hydrochloride	0.0119	0.00297	0.0119
Vitamin B12	0.0000096	0.0000037	0.0000096
Salts			
Calcium ions	1.49[g]	0.424[h]	1.49[g]
Nitrate ions	0.000752[i]	0.8480[j]	0.000752[i]
Magnesium Sulphate ($MgSO_4$)	0.814	0.407	0.814
Potassium Chloride (KCl)	4.40	5.33	4.40
Sodium Bicarbonate ($NaHCO_3$)	36.00	23.81	36.00
Sodium Chloride (NaCl)	77.59	103.45	77.59
Sodium Phosphate	0.906	5.64	0.906
Sodium Selenite ($Na_2SeO_3.5H_20$)	0.0000658	0	0.0000658
Other components			
D-Glucose (Dextrose)	25.00	11.2 (25.1) [k]	25.00
HEPES	25.03	25	25.03
Phenol Red	0.0399	0.0133	0.0399
Sodium Pyruvate (total)	1.0 (2.0) [k]	0 (2.0) [k]	1.0 (2.0) [k]
Glutathione (reduced)	0	0.00326	0
Additional supplements			
D-Glucose	0	14.0	0
HEPES	0	25	0
Bathocuproine sulphonate	0.05	0.05	0.05
Cysteine	1.5	1.5	1.5
Thioglygerol	0.2	0	0
Hypoxanthine	1.0	1.0	1.0
Mercaptoethanol	0	0.2	0.2
Pyruvate	1.0 (see above)	2.0 (see above)	1.0 (see above)
Thymidine	0.16	0[l]	0[d]
Foetal bovine serum (%)	10	10	10
Serum Plus (%)	10	0.5	0

Key:

a) As GIBCO ® GlutaMAX™, L-alanyl-L- glutamine, a dipeptide substitute for L-glutamine
b) From Iscove's Modified Dulbecco's Media and 10% Serum Plus, excluding any contribution from FBS
c) From 0.5% Serum Plus and folate free RPMI medium, excluding any contribution from FBS
d) Excluding any contribution from FBS
e) As pyridoxal hydrochloride
f) As pyridoxine hydrochloride
g) As $CaCl_2$
h) As $Ca(NO_3)_2$
i) As KNO_3
j) As $Ca(NO_3)_2$
k) Values in parentheses include additional supplements
l) Excluding any contribution from 0.5% Serum Plum Plus, folate free RPMI medium and FBS.

ml^{-1} pyruvic acid, 39 μg ml^{-1} thymidine, 2.8 μg ml^{-1} bathocuproine disulfonic acid, 182 μg ml^{-1} L-cysteine and 13.6 μg ml^{-1} hypoxanthine, and reduced with 56 μM 1-thioglycerol.

2.2.2 Folate and Thymidine Depleted Media

Folate (as folic acid) and thymidine depleted media is not commercially available and in-house nutrient depleted media was prepared by hand. Initially a folate and thymidine deficient media, based upon 'FDM', was prepared as previously described (Sienkiewicz *et al*., 2008) and named RPMI-based media (RPMI-BM). This media was made using a folate-free RPMI 1640 medium (Thermo Fisher), supplemented with 50 x MEM amino acid solution (Thermo Fisher), and addition of 0.5% Serum Plus™ (SAFC biosciences). A second nutrient depleted media was prepared based on HMI9-T (Greig *et al*., 2009), lacking Serum Plus™, folate and thymidine, and using 2-mercaptoethanol instead of thioglycerol as the reducing agent. This was named *T. brucei* base media (TBM) (Gibson *et al*., 2016). A comparison of media types is shown in Table 2.1. In TBM residual folate is only provided by the 10% foetal calf serum (FCS, GE Healthcare) component.

2.2.3 SILAC Media

SILAC media was prepared essentially as described (Urbaniak *et al*., 2013) but without the addition of excess folate. SILAC IMDM depleted of L-arginine and L-lysine (Thermo Fisher) was supplemented with 10% dialysed FCS (Gibco, Life Technologies) and 110 μg ml^{-1} pyruvic acid, 39 μg ml^{-1} thymidine, 2.8 μg ml^{-1} bathocuproine disulfonic acid, 182 μg ml^{-1} L-cysteine and 13.6 μg ml^{-1} hypoxanthine and reduced with 200 μM 2-mercaptoethanol.

2.2.4 Culture Conditions

For routine culture, blood stream-form (BSF) *T. brucei* 'single marker' S427 (Wirtz *et al*., 1999) and 2T1 strains (Alsford *et al*., 2005) were cultured in TBM and HMI9-T medium. S427 cells were supplemented with 2.5 μg ml^{-1} neomycin (G418) to maintain expression of T7 RNA polymerase and a tetracycline repressor protein (TetR) and 2T1 cells supplemented with 1 μg ml^{-1} phleomycin (TetR) and 1 μg ml^{-1} puromycin (PAC resistance cassette). Trypanosomes were incubated at 37 ^{o}C in the presence of 5% CO_2. Cultures were routinely passaged into fresh media every 48 or 72 h and cell density kept below 5 x 10^6 cells ml^{-1}.

2.2.5 Cell counting

Cells were counted using a CASY cell counter model DT according to manufacturers' instruction. For cell densities below 5 x 10^5 cells ml^{-1} (below comfortable limit of detection) trypanosomes were manually counted using a Haemocytometer (Neubauer).

2.3 General Molecular Biology

2.3.1 Isolation of genomic DNA

Mid-log cells (a total of ~ 4 x 10^7) were pelleted by centrifugation (800g, 10 min, 25 ^{o}C) and resuspended in 250 μl of gDNA lysis buffer (10mM Tris-HCl, pH 8, 100nM NaCl, 25nM EDTA, 0.1 mg ml^{-1} proteinase K, 0.5% (w/v) SDS) and incubated at 56 ^{o}C overnight. Four volumes of 95% EtOH were added to the lysate and the tube inverted several times to mix. DNA was spooled and precipitated in 90% EtOH followed by a further precipitation in 70% EtOH. After ensuring the remaining EtOH was drained off, isolated gDNA was resuspended overnight at RT in 100 μl elution

Table 2.2 Primers used in this study

Primer Name	Primer Sequence	Primer Purpose
LIB2f	5′-TAGCCCCTCGAGGGCCAGT	Sequencing RNAi library fragments
LIB2r	5′-GGAATTCGATATCAAGCTTGGC	Sequencing RNAi library fragments
TbFT1-3 stem loop fwd	5’-GATCGGGCCCGGTACCGCTTGTGAGTTGGGTTTGGT	Generate FT1-3 RNAi construct
TbFT1-3 stem loop rev	5’-GATCTCTAGAGGATCCCGATCACAAGTGGAAGAGC	Generate FT1-3 RNAi construct
Stem loop seq fwd	5’-AATAGTGGACTCTTGTTCCA	Sequencing stem loop construct
Stem loop seq rev	5’-AAAGGGGGATGTGCTGCAAG	Sequencing stem loop construct
FT Fw	5’-ATGACCACGTCACCGAAC	Southern Blot
FT Rx	5’-CTAATTGGCTGTGGGTTC	Southern Blot
TR Fw	5’-ATGTCCAAGGCCTTCG	Southern Blot
TR Rev	5’-TCACAGGTTAGAGTCCG	Southern Blot
TbTERT fwd	5′-GAGCGTGTGACTTCCGAAGG	RT qPCR
TbTERT rev	5’-AGGAACTGTCACGGAGTTTGC	RT qPCR
TbFT1-3 qPCR fwd	5′-GAATTGCTGACAACATCATT	RT qPCR
TbFT1-3 qPCR rev	5′-TCACTGCGTAACCAAATGTA	RT qPCR
TbFT1 fwd	5’-GATGCCTTGATGATACTGC	Sequencing MTX line
TbFT 1 rev	5’-CGCTTCTACATGTACTTAC	Sequencing MTX line
TbFT 2 fwd	5’-GCGTAACATTATACAATAC	Sequencing MTX line
TbFT 2 rev	5’-GAATATAGTCCACCTGCTC	Sequencing MTX line
TbFT 3 fwd	5’-GAGGTAACCCTTCCATTTTG	Sequencing MTX line
TbFT 3 rev	5’-ACATACACACACACACAC	Sequencing MTX line
TbFT Univ fwd 1	5’-CTTCCACTTGTGATCGCGAAG	Sequencing MTX line
TbFT Univ rev 1	5’-GACGCGGCGAATCAAGCG	Sequencing MTX line
TbFT Univ fwd 2	5’-CACCCTCGCTATTGTGTACG	Sequencing MTX line
TbFT Univ rev 2	5’-GACATTGTCGATTGCGCCAG	Sequencing MTX line

buffer (Qiagen) and confirmed to be pure by spectrophotometry (260:280 ratio >1.8) using a NanoDrop (Thermo Scientific) .

2.3.2 Agarose-gel electrophoresis.

DNA was analysed using agarose gels (0.8% (w/v), VWR) containing 20 μg ethidium bromide per 100 ml and made in TAE buffer (40 nM Tris, 20 mM acetic acid, and 1 mM EDTA). Electrophoresis was carried out at 100 V in TAE buffer until the desired separation was attained. The separation of a DNA marker (1 kbp plus DNA ladder, Promega) enabled DNA bands to be compared and estimated using UV transillumination for visualisation.

2.3.3 Quantitative RT-PCR

T. brucei RNA was isolated from ~ 1 x 10^7 parasites using an RNeasy purification kit (Qiagen) as per manufacturer's instructions and cDNA was then synthesised from these samples using a high capacity RNA-to-cDNA kit (Applied Biosystems). Primers were designed by Dr Natasha Sienkiewicz using Premier Biosoft's Beacon Designer 6 to amplify a 117 bp region that is common to all three *FT* genes, but different from the region that is targeted by RNAi (primer sequence Table 2.2). qRT-PCR reactions included 1 μl (40 ng) cDNA, 1 μl (500 nM) each of the forward and reverse primers, 10 μl Brilliant III Ultra-Fast QPCR Master Mix (Agilent Technologies), 0.3 μl (30 nM) of reference dye and the remaining volume nuclease free PCR grade-treated water. Cycling conditions were: 95 °C for 3 min followed by 40 cycles of 95 °C for 20 s; 60 °C for 20 s, and analysis was conducted using an Agilent Mx3005P machine. The reference gene *TERT* (Tb927.11.10190, telomerase

reverse transcriptase) allowed normalization of the data by providing a baseline of transcription levels (primer sequence Table 2.2). Relative quantification of cDNA was determined using the ΔΔCt method and a student's unpaired *t*-test was used to dtermine significance. Statistical analyses were performed using Microsoft Excel 2010.

2.3.4 Synthesis of Southern blot probes

PCR DIG synthesis kit (Roche) was used to make DIG labelled probes for Southern blotting. Primers designed against FT1-3 (Table 2.2) were used to amplify the target region of DNA from plasmid DNA, as described in the manufacturers' protocol. To test label incorporation, DIG labelled product was ran on an agarose gel and exhibited a decrease in electrophoretic mobility compared to the unlabelled control.

2.3.5 Southern blot

Samples of gDNA (5 μg) were digested with EcoR1 overnight at 37 ^{o}C. The digested products were separated on a 0.8 % agarose gel (containing 20 μg ethidium bromide in 200 ml) for 3 h at 80 V in TAE buffer. The gel was washed in 0.25 M HCl for 10 min to de-purinate the DNA prior to equilibrating in 0.4 M NaOH for 2 min. The DNA was transferred onto a positively charged nylon membrane (Roche) by capillary mechanism for ~ 90 min using 0.4 M NaOH as the transfer buffer. The membrane was pre-incubated with DIG Easy Hyb solution for 2 h at 42 ^{o}C followed by overnight incubation with fresh DIG Easy Hyb solution containing 2 μl of the denatured DIG labelled probe. The probe was denatured by heating at 100 ^{o}C for 10 min before rapidly cooling on ice. Following overnight incubation, the membrane

was washed twice in low-stringency conditions (25^{o}C, 5 min, 2 x saline sodium citrate (SSC) with 0.01% (w/v) sodium dodecyl (SDS)) followed by two high-stringency washes (68 ^{o}C, 15 min, 0.5 x SCC with 0.01% SDS) to remove any excess probe (20 x SSC (Ambion) compromises 3M sodium chloride and 0.3 M sodium citrate, pH 7.0). The blot was prepared for development using DIG block and wash buffer set (Roche) as per manufactures' instructions and detected using Anti-DIG AP-Conjugate Antibody (Roche) with the chemiluminescent substrate, CSPD (Roche). Films were exposed (Hyperfilm^{TM}, Amersham) from 1 min to 5 min and developed with a KODAK film developer.

2.4 EC_{50} and resazurin assay

EC_{50} values (drug concentration that gives half-maximal response) of antifolates against BSF trypanosomes were determined in 96-well microtitre plates. Serial doubling dilutions of drugs (5-50 mM stocks prepared in DMSO) were prepared in 100 μl of TBM and parasites, routinely cultured in HMI9-T, were added in 100 μl TBM with a final cell density of 2.5×10^3 cells ml^{-1} in 96-well plates. A final volume of 0.5% DMSO was in all wells, including controls. After a 72 h incubation cell density was determined using a resazurin-based assay (Jones *et al*., 2010; Raz *et al*., 1997) with fluorescence measured using a Biotec Instruments FLX 800 fluorescent plate reader (excitation of 528 nm and emission of 590 nm). Resazurin (20 μl of a 500 μM stock, giving 45.5 μM final concentration) was added at 68 h for 4 hours of incubation prior to fluorescence being measured at 72 h Data was corrected for background fluorescence. EC_{50} values were calculated using GraFit v 5.0.13 with a 3-parameter fit (see below) from triplicate readings.

$$y = \frac{Range}{1 + \left(\frac{x}{EC_{50}} \right)^{s}}$$

In this equation *Range* is the fitted uninhibited value, *x* is the inhibitor concentration and *s* is the Hill slope of the curve.

2.5 Static-Cidal Assay

2.5.1 Limit of detection

The static-cidal assay was adapted from a previously published method (De Rycker *et al*., 2012). Briefly, 200 µl of *T. brucei* cells grown in TBM were dispensed in triplicate into a 96-well plate at the following densities: 0, 5×10^3, 1×10^4, 2×10^4, 5×10^4, 1×10^5 and 2×10^5 cells ml^{-1}. Resazurin (Sigma) was then added at a 45.5 µM final concentration and the plates were incubated for 4 h and florescence measured as previously described in section 2.4. Using linear regression, cell number versus fluorescence signal was plotted. The limit of detection was determined as the cell density with a signal higher than the mean, plus three times the standard deviation (SD) of the mean, of the blank wells (no cells).

2.5.2 Growth assays

Three replicate 96-well plates of serial doubling dilutions of each compound were prepared and trypanosomes were seeded into each plate at a final concentration of 4×10^5 ml^{-1} (200 µl final volume in TBM). All wells, including controls (no drug), contained a final volume of 0.5% DMSO. Immediately resazurin (45.5 µM final concentration) was added to plate 1, and all plates (plates 1-3) were then incubated.

After 4 h, florescence of the time zero plate (plate 1) was measured. At 20 h and 44 h plates 2 and 3 respectively were processed in the same manner. A growth curve was taken from triplicate readings of florescence signal and calculated as a percentage against the no drug control. The Minimum Cidal Concentration (MCC) was determined as the lowest drug concentration that causes a reduction in fluorescence signal at 48 h relative to time zero (De Rycker *et al*., 2012).

2.6 Cell-Cycle Analysis

T. brucei cultures in TBM were seeded at 3×10^5 cells ml^{-1} and treated with varying concentrations of MTX and RTX and supplemented with either excess 160 µM or 1 µM thymidine (the physiological level found in mouse plasma (Clarke *et al*., 2000b)). After 20 h cells were harvested by centrifugation (10 min, 800 g, 25 ^{o}C), washed in FACS buffer (1 x PBS pH 7.0, 5 mM EDTA and 1% FCS) and supernatant removed. Cells were fixed in 1% formaldehyde in FACS buffer, in a drop-wise fashion while gently vortexing to reduce cell clumping, incubated at RT for 10 min and stopped by centrifugation. Cells were then permeabilized with 0.01% Triton X-100 in FACS buffer, incubated at RT for 30 min and stopped by centrifugation. Cells were resuspended in 400 µl staining solution (FACS buffer, 10 µg ml^{-1} propidium iodide, 100 µg ml^{-1} RNase A), stained for 45 min at 37 ^{o}C in the dark before being analysed by flow cytometry. Samples were analysed and data acquired on a FACS Canto (Becton Dickinson, BD) using BD FACSDiva Software. Pulse-width analysis was used to ensure the exclusion of doublets and clumps (Garcia-Martinez *et al*., 2009). Triplicate or duplicate samples were used in each analysis. Data was visualized using FlowJo software (Tree Star). Evaluation of cell

cycle distribution using the Watson-Pragmatic model (Watson *et al*., 1987) or the Dean-Jett-Fox model (Dean and Jett, 1974; Fox, 1980) could not be attained for drug treated cells. These models assume that data is distributed in normal cell cycle phases; however, cell cycle was greatly disturbed in treated cells to an extent that distribution could not fit these algorithms.

2.7 Transport Experiments

2.7.1 Transport Assay

Prior to transport being measured, trypanosomes routinely grown in HMI9-T media were split to 5×10^3 cells ml^{-1} in TBM and then cultured in TBM for 72 h. Cells were pelleted by centrifugation (800 g, 10 min, 4 ^oC), washed twice and resuspended in ice-cold transport buffer (33 mM HEPES, 14 mM glucose, 4.6 mM KCl, 0.07 mM $MgSO_4$, 0.3 mM $MgCl_2$, 23 mM $NaHCO_3$, 98 mM NaCl, 0.55 mM $CaCl_2$, 5.8 mM NaH_2PO_4, pH 7.3) (Ali *et al*., 2013a) at a density of 2.5 x 10^8 cells ml^{-1}. Transport was carried based on a method previously described (Ong *et al*., 2013). Uptake was determined by mixing 100 µl of trypanosomes with 100 µl of transport buffer that contains the radiolabelled ligand (0.5µCi) and, when required, potential inhibitors of transport. This mixture is layered over 100 µl of dibutyl phthalate (Sigma Aldrich) and uptake was stopped by centrifugation (16,000g, 1 min) of the mixture through the dibutyl phthalate layer. Microcentrifuge tubes were then immediately flash frozen in liquid nitrogen. The bottom of the tubes (containing the cell pellet) were cut straight into scintillation vials and then solubilized in 150 µl of 1 M NaOH overnight. Scintillation fluid (2 ml) was added the following day and radioactivity was measured using a liquid scintillation counter (Beckman LS 6500).

2.7.2 Rate and $K_{m\ app}$ analysis

Uptake of [^{3}H]-folic acid (0.04 μM) was measured in the presence of varying concentrations of unlabelled folate, in the same way, uptake of [^{3}H]-MTX (0.07 μM) was measured in the presence of varying concentrations of unlabelled MTX. Linear uptake of both folate and MTX was assessed over 150 s with five 30 s time points (30, 60, 90, 120 and 150 s). Data was then fitted using a robust non-linear fitting to the linear equation y = mx + c. In a similar manner, non-specific binding of radiolabeled ligand (folate or MTX respectfully) to trypanosomes at 4 ^oC (on ice) was determined. Uptake of folate or MTX in pmol 10^8 cells^{-1} was calculated using their [^{3}H] specific activities, cell number and dilution factor of unlabelled substrate. As these transport experiments reflect the activity of multiple transporters (FT1-3) the $K_{m\ app}$ (apparent $K_{m\ app}$ of multiple, distinct transport activities) of folate and methotrexate transport was calculated. To calculate $K_{m\ app}$, data was fitted by non-linear regression to the Michaelis–Menten equation and a weighted mean from three independent experiments was calculated.

2.7.3 Folate and MTX inhibition studies

Linear rate of uptake was determined as described but with the addition of 100 μM of competing inhibitor and standard assay mixture modified to contain approximately [S] = $K_{m\ app}$ (folate at 2.0 μM and MTX at 13 μM) and corrected for additional DMSO (0.4%). To measure IC_{50} (inhibitor concentrations giving 50% inhibition) uptake of the substrate was determined over a range of inhibitor concentrations across 7-8 point serial doubling dilutions. Data was expressed as 0-100% of the no drug control. Using GraFit 5.0, data was fitted by non-linear regression to a two-parameter IC_{50} equation:

$$y = \frac{100\%}{1 + \left(\frac{x}{\mathrm{IC}_{50}} \right)^{s}}$$

In this equation, *x* is the inhibitor concentration and *s* is the Hill slope of the curve.

To determine the mode of inhibition of both MTX to folate uptake, and vice versa, the linear rate of uptake was measured as described but with three different inhibitor concentrations and four different substrate concentrations. The resulting data was plotted as a Lineweaver-Burke transformation and the graphs inspected to confirm competitive inhibition mode (intersection on *y*-axis). An *F*-test confirmed the mode of inhibition as linear competitive. The entire data set was globally fitted to the competitive-mode equation 1.

$$v = \frac{V_{\max}.[\mathrm{S}]}{K_{\mathrm{m}}\left(1 + \frac{[\mathrm{I}]}{K_{\mathrm{i}}}\right) + [\mathrm{S}]} \qquad \text{Equation 1}$$

If folate and MTX are competitive substrates for the same transporter then:

for folate $$v_{\mathrm{F}} = \frac{V^{\mathrm{F}}_{\max}[\mathrm{F}]}{K^{\mathrm{F}}_{\mathrm{m}}\left(1 + \frac{[\mathrm{M}]}{K^{\mathrm{M}}_{\mathrm{m}}}\right) + [\mathrm{F}]} = \frac{(V^{\mathrm{F}}_{\max} / K^{\mathrm{F}}_{\mathrm{m}})[\mathrm{F}]}{1 + \frac{[\mathrm{M}]}{K^{\mathrm{M}}_{\mathrm{m}}} + \frac{[\mathrm{F}]}{K^{\mathrm{F}}_{\mathrm{m}}}}$$ Equation 2

for MTX: $$v_{\mathrm{M}} = \frac{V^{\mathrm{M}}_{\max}[\mathrm{M}]}{K^{\mathrm{M}}_{\mathrm{m}}\left(1 + \frac{[\mathrm{F}]}{K^{\mathrm{F}}_{\mathrm{m}}}\right) + [\mathrm{M}]} = \frac{(V^{\mathrm{M}}_{\max} / K^{\mathrm{M}}_{\mathrm{m}})[\mathrm{M}]}{1 + \frac{[\mathrm{F}]}{K^{\mathrm{F}}_{\mathrm{m}}} + \frac{[\mathrm{M}]}{K^{\mathrm{M}}_{\mathrm{m}}}}$$ Equation 3

[M] and [F] refer to the concentrations of MTX and folate respectively

Dividing equation 3 by equation 2 constitutes:

$$\left(\frac{v_{\mathrm{M}}}{v_{\mathrm{F}}}\right)=\left(\frac{(V_{\max}^{\mathrm{M}}/K_{\mathrm{m}}^{\mathrm{M}})[\mathrm{M}]}{(V_{\max}^{\mathrm{F}}/K_{\mathrm{m}}^{\mathrm{F}})[\mathrm{F}]}\right) \qquad \text{Equation 4}$$

The IC_{50} for MTX occurs when: $\left(\frac{v_{\mathrm{M}}}{v_{\mathrm{F}}}\right)=0.5$ Equation 5

By substituting equation 5 into equation 4 and rearranging:

$$\mathrm{IC}_{50}^{\mathrm{M}}=\frac{0.5(V_{\max}^{\mathrm{F}}/K_{\mathrm{m}}^{\mathrm{F}})[\mathrm{F}]}{(V_{\max}^{\mathrm{M}}/K_{\mathrm{m}}^{\mathrm{M}})} \qquad \text{Equation 6}$$

In the same way, the IC_{50} for folate can be calculated:

$$\mathrm{IC}_{50}^{\mathrm{F}}=\frac{0.5(V_{\max}^{\mathrm{M}}/K_{\mathrm{m}}^{\mathrm{M}})[\mathrm{M}]}{(V_{\max}^{\mathrm{F}}/K_{\mathrm{m}}^{\mathrm{F}})} \qquad \text{Equation 7}$$

2.7.4 Folate uptake in high and low folate conditions.

The transport assay was performed as previously described in section 2.7.1, except cells were either cultured for 72 h in TBM (low folate conditions) or TBM supplemented with 9 μM folate (high folate conditions) prior to assay. Folate uptake was assessed at either 2 μM ($K_{\mathrm{m\ app}}$) or 20 μM (saturating concentrations) of folate. Uptake was measured over 10 min at 8 time points (30, 60, 90, 120, 150, 300, 450 and 600 s), with linearity of uptake fitted using a robust non-linear fitting to the linear equation y = mx + c for the first 5 time points.

2.8 RNAi library

2.8.1 Cell culture and extraction of genomic DNA

The RNAi library screen was performed in TBM and carried out based on the protocol previously described (Glover *et al*., 2015). On day 0, a frozen RNAi library stock was thawed in media, maintained under blasticidin (1 μg ml^{-1}) and phleomycin (1 μg ml^{-1}) control, expanded to a cell density of 2.5×10^7 cells in 150 ml media and then induced with tetracycline (1 μg ml^{-1}). Following induction for 24 h, 15 nM MTX or 10 nM RTX were added. Starting drug concentration is normally approximately 2 × EC_{50} (Glover *et al*., 2015). EC_{50} data is usually generated from cells routinely passaged in HMI9-T and then diluted in TBM at the start of the assay (EC_{50} MTX = 12 nM and RTX 38 nM). However, in RNAi library screening, cells will be maintained in TBM for up to 48 h before drug being added. To have a better impression of EC_{50} in this scenario, parasites were cultured in TBM for 48 h prior to EC_{50} being measured (EC_{50} MTX = 5.7 nM and RTX 2.5 nM). Starting drug concentrations of 15 nM MTX and 10 nM RTX were derived to reflect these differences in EC_{50}. Throughout the screen, cultures were split and supplemented with fresh drug as required. After 4 days, concentrations of MTX and RTX were increased to 30 nM to select a resistant population. 2 days after recovery of the resistant population (day 11) gDNA was extracted using the Qiagen DNeasy Blood & Tissue Kit, as per manufactures instructions.

2.8.2 PCR amplification of fragments and mapping

RNAi target fragments were amplified by PCR using LIB2f and LIB2r primers and protocol from Glover *et al* (Glover *et al*., 2015). For low through-put identification

of fragments, PCR products were separated on an agarose gel and individual bands were excised using a QIA quick Gel Extraction Kit (Qiagen), as per manufactures instructions, and sequenced by the DNA sequencing service at the University of Dundee using the Lib2f and Lib2r primers (Table 2.2). Sequencing results were BLAST searched against the *T. brucei* 927 reference genome using v9.0, (http://tritrypdb.org) to identify hits. For high through-put identification of fragments the PCR products were PCR purified (QIAquick PCR Purification Kit, Qiagen), made to 10 μg DNA, and sent to BGI (Beijing Genomics Institute) to be fragmented and sequenced using an Illumina HiSeq platform. Using Bowtie 2 (Langmead and Salzberg, 2012) and the parameters very-sensitive-local–phred33, reads were mapped to the *T. brucei* 927 reference genome. The generated alignment files were then manipulated with SAMtools (Li *et al*., 2009) and a custom script used to identify reads containing identifying barcodes (GCCTCGCGA). Using the Artemis genome browser (Carver *et al*., 2012) total and barcode only reads were mapped to the *T. brucei* 927 reference genome. Dr Richard Wall assisted with computational alignment work.

2.9 Generation of RNAi knockdown cell line.

2.9.1 Polymerase Chain reaction (PCR)

PCR was carried out using template *T. brucei* genomic DNA (100 ng), Platinum Taq polymerases (Invitrogen) as per manufacturer's standard protocol, and primers designed using RNAit (Redmond *et al*., 2003) to generate a 536 kb PCR fragment, conferring specific knockdown to Tb927.8.3620, Tb927.8.3630 and Tb927.8.3650 genes (*FT1*, *2* and *3* respectively). The PCR product was confirmed by agarose-gel

electrophoresis and purified using the QIAquick PCR Purification Kit (Qiagen), eluting in 30 µl of elution buffer.

2.9.2 pRPa^{SLi} vector and PCR insert preparation and ligation

For cloning in a sense orientation both the pRPa^{SLi} vector (Alsford and Horn, 2008) and PCR product were digested with the sense fragment cloning restriction enzymes Acc65I (25 U, NEB) and BamH1 (25 U, NEB) for 90 min at 37 ^{o}C, then both PCR purified. Digested vector and digested PCR product were ligated with T4 DNA Ligase (400 U, NEB) for 120 min at room temperature with the following cocktail (1 µl of insert, 7 µl vector, 1 µl T4 DNA Ligase, 1 µl T4 DNA Ligase Reaction Buffer).

2.9.3 Transformation of competent cells

The total ligation reaction (10 µl) was added into 25 µl of One-Shot TOP-10 cells (Invitrogen) and incubated on ice for 30 min. Cells were then subjected to heat shock for 45 s at 42 ^{o}C in a water bath, followed by a further incubation on ice for 2 min. 250 µl of SOC media (Invitrogen) was added and the resulting culture was incubated at 37 ^{o}C for 1 h with agitation at 200 rpm. Cells were plated out on Luria Bertani (LB) agar plates supplemented with ampicillin (50 µg ml^{-1}) and incubated at 37 ^{o}C overnight, resultant colonies were picked and grown overnight at 37 ^{o}C with agitation at 200 rpm in 10 ml of LB media with ampicillin. Cells were pelleted by centrifugation (3000g, 10 min at 4 ^{o}C) and purified using the Qiagen Miniprep kit as per manufacturer's instructions.

2.9.4 Confirming the organisation of stem loop cassette

DNA prepared from individual colonies was digested with the restriction enzymes Acc65I and Bam H1 and analysed by agarose-gel electrophoresis to determine whether the integration of this insert into the pRPa^{SLi} vector had occurred. Positive colonies were sequenced, using the respective primers (Table 2.2), by the DNA sequencing service at the University of Dundee.

Steps 2.9.2 and 2.9.4 were repeated with the anti-sense cloning restriction enzymes XbaI (NEB) and Bsp120I (NEB) for full construction of the stem loop plasmid.

2.9.5 Transfection into BSF *T. brucei*

The final plasmid was linearized with AscI (50 U, NEB) overnight at RT and EtOH precipitated and suspended in sterile water (1 μg ml^{-1}). Twenty four hours prior to transfection 2T1 strains, in HMI9-T, were split and kept of puromycin selection to reduce selection of puromycin resistant clones. Parasites, at 2 x 10^7 cells, were electroporated using programme X-001 of the Nucleofector II electroporator (Amaxa, Cologne, Germany) (Burkard *et al*., 2007) following the addition of 5 μg of linearized DNA suspended in 100 μl cytomix (van den Hoff *et al*., 1992). Subsequent to electroporation, cells were transferred into a flask of 25 ml HMI9-T media and after 6 h transformants were cloned by limiting dilution and maintained under phleomycin (1 μg ml^{-1}) and hygromycin (2.5 μg ml^{-1}) selection. Puromycin sensitivity (1 μg ml^{-1}) was tested for full integration of the construct (double homologous recombination) and RNAi was induced with 1 μg ml^{-1} tetracycline (tet).

2.10 MTX-resistant cell lines

2.10.1 Generation of MTX-resistant cell lines

These cell lines were kindly generated by Dr Natasha Sienkiewicz and described as follows. MTX resistant *T. brucei* cell lines were generated using S427 cells continuously grown in TBM for 4 weeks prior to resistance generation. Lines were generated in two independent flasks. Starting at a sublethal concentration of 0.05 μM MTX, trypanosomes were sub-cultured in the presence of increasing concentrations of drug. After 72 days when cells were able to survive and grow at 800 nM, cells were cloned by limiting dilution in the absence of drug. EC_{50} determinations to confirm resistance was carried out by myself and the clone from each independent cell lines that displayed the highest rate of resistance was selected for further studies (named MTX R1 and MTX R2). Cell lines were maintained in TBM without MTX. EC_{50} were carried out four months later to determine whether resistance had been maintained in the absence of MTX.

2.10.2 Sequencing of DNA

To attain full and unique coverage of Tb927.8.3620, Tb927.8.3630 and Tb927. 8.3650 (*FT1-3*) primers were designed (Table 2.2). PCR was carried out using Platinum Taq polymerases (Invitrogen) as per manufacturer's standard protocol. The template concentrations ranged from 200-2 ng of gDNA from the parental cell line (WT), MTX R1 and MTX R2, and PCR conditions optimised for each target of interest. PCR products were PCR purified (Qiagen Kit) and sequenced in-house (Dundee Sequencing Unit) and CLC Main Workbench 6 used for analysis. Sequences were aligned using Clustal Omega (http://www.ebi.ac.uk/Tools/msa/) (Li

et al., 2015). Topological models of FT1-3 were visualised using the web-based Protter software (http://wlab.ethz.ch/protter/start/) (Omasits *et al*., 2014).

2.10.3 Transport Studies in MTX-resistant cell lines

Uptake of [^{3}H]-folic acid (0.04 μM) and of [^{3}H]-MTX (0.07 μM) was determined as 2.3.2 but at a set concentration of unlabelled substrate (5 μM folate and 20 μM MTX respectively) instead of at varying concentrations. One transport experiment was undertaken each for folic acid and MTX. Linear rate of uptake was determined in triplicate and the weighted mean of the experimental triplicate was calculated. Weighted mean was used, where each value is "weighted" according to the probability of it being correct. This method takes into account the uncertainty in any given experimental calculation and does not introduce bias (Young, 1962). *p* values were calculated using a Student's unpaired *t*-test.

2.11 Proteomic Profiling

2.11.1 Cell labelling

SILAC-labelling was carried out in prepared SILAC media (section 2.2.4). WT, MTX R1 and MTX R2 cells were harvested at log-phase and washed twice in PBS to remove exogenous L-Arginine and L-Lysine from the TBM. Cells were resuspended in PBS and seeded at a density of 3×10^4 ml^{-1} in the SILAC media. L-Arginine and L-Lysine (light, medium and heavy labels) amino acids were added at a concentration of 120 nM and 240 nM respectively (30% of the original HMI11 concentration) to the prepared SILAC media. WT cells were labelled with light L-

Arginine and L-Lysine (HMI11-R_0K_0), MTX R1 with medium L-Arginine U - $^{13}C_6$ and L-Lysine 4,4,5,5 - $^{2}H_4$ (HMI11-R_6K_4) and MTX R2 with heavy L-Arginine U - $^{13}C_{10}$ and L-Lysine 4,4,5,5 - $^{2}H_6$ (HMI11-$R_{10}K_8$).

Following 5 days passage (cells split on d 2) and growth to approx. 16-18 cell divisions, cells were harvested at ~ 1-2×10^6 cells ml^{-1} by centrifugation (800g, 10 min, RT). Cells were washed twice in ice-cold PBS and finally resuspended in PBS containing 1X Complete Mini Protease Inhibitor Cocktail (Roche). WT cells (HMI11-R_0K_0) were equally mixed (1:1) with either MTX R1 (HMI11-R_6K_4) or MTX R2 (HMI11-$R_{10}K_8$) to a total concentration of 1.4 x 10^8 cells. Cells were suspended in 140 µl of Laemmli buffer containing 1 mM dithiothreitol (BioRad). Samples were boiled for 10 min and stored at -80^oC until further processing. In addition, the remaining unmixed MTX R1 cells (HMI11-R_6K_4) and MTX R2 cells (HMI11-$R_{10}K_8$) were harvested as described previously to be used as controls separated for label incorporation.

2.11.2 Sodium dodecyl sulphate polyacrylamide gel electrophoresis (SDS-PAGE).

Aliquots of WT (R_0K_0) v Res 1 (R_6K_4) and WT (R_0K_0) v Res 2 ($R_{10}K_8$) were made up to 2.0 x 10^7 cells and medium and heavy isotope controls were aliquoted to 2.0 x 10^6 cells. Proteins were separated on a NuPAGE bis-tris 4–12% gradient polyacrylamide gel (Invitrogen) at 200 V with NuPAGE MES SDS running buffer (0/1% SDS, 1mM EDTA, 50mM MES, 50nM Tris Base, pH 7.3) for 20 min. The gel was washed in H_20 three times (10 min per wash), with agitation, before staining

with Instant-Blue (Expedeon) at RT for 1-2 h. The stain was removed and a further three 10 min H_20 washes were undertaken to de-stain the gel.

2.11.3 Mass spectrometry

All in-gel digestion and mass spectrometry was carried by the FingerPrints proteomics service at the University of Dundee (http://proteomics.lifesci.dundee.ac.uk). The protocol was provided by Douglas Lamont and the key steps from this are described. Reduction and alkalisation of cysteine residues was performed by adding dithiothreitol then 2-iodoacetamide respectively to the gel preparation. The protein was trypsinized, lyophilised and resuspended in 5% formic acid. Samples were fractionised by C18 reverse phase into 6 fractions prior to LC-MS/MS analysis. Analysis of peptides was performed on an Ultimate 3000 RSLCnano system (Thermo Scientific) coupled to a LTQ OrbiTrap Velos Pro (Thermo Scientific). Samples were loaded in 0.1% formic acid (buffer A) and separated using a binary gradient consisting of buffer A and buffer B (80% acetonitrile, 0.08% formic acid). Peptides were initially trapped on an Acclaim PepMap 100 (C18, 100 μM x 2 cm) and then separated on an Easy-Spray PepMap RSLC C18 column (75 μM x 50 cm) (Thermo Scientific). Samples were transferred to ms via an Easy-Spray source with temperature set at 50^{o}C and a source voltage of 1.9kV.

2.11.4 Data Analysis

Mass spectra was analysed by the FingerPrints proteomics service using MaxQuant version 1.5.2.8 which incorporates the Andromeda search engine (Cox and Mann, 2008; Cox *et al.*, 2011). Proteins were identified by searching the *T. brucei* 927

annotated protein from TriTrypDB (v9.0, http://tritrypdb.org). Search parameters specified a MS tolerance of as 4.5 ppm with the MS/MS tolerance set at 0.6 Da. SILAC ratios of H/L based on R_0K_0 and either R_6K_4 or $R_{10}K_8$ were calculated then normalised to adjust for loading difference based on identification of peptides using 1% False Discovery Rate. SILAC ratios were calculated using uniquely mapped peptides that were a minimum of 7 amino acids in length. Data was visualized by myself, using Perseus 1.3.0.4 (http://perseus-framework.org). Differential expression was determined using a significance B test (Cox and Mann, 2008).

Chapter 3

Dissecting the mechanism of action and transport of antifolate drugs in *Trypanosoma brucei*

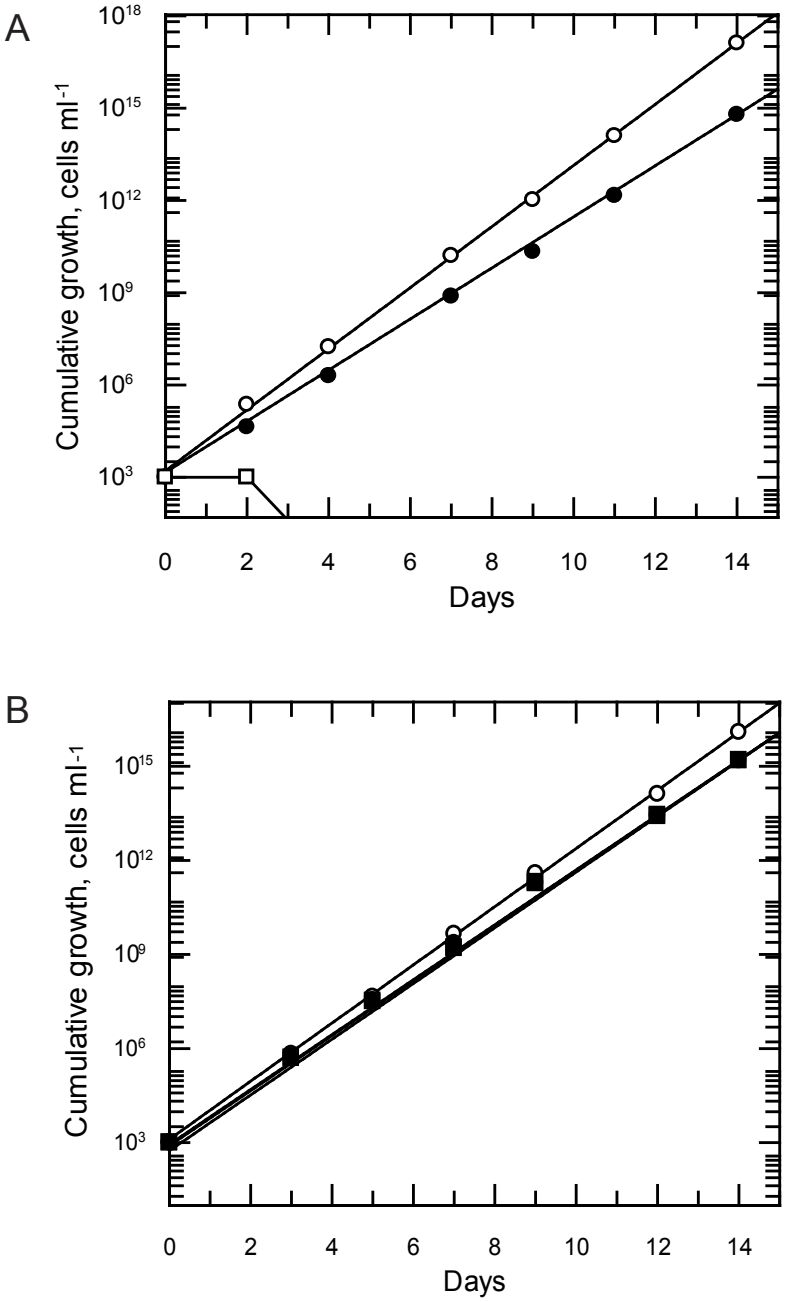

Fig 3.1 Cumulative growth of BSF *T. brucei* in different media.

(A) Cultured in RMPI-BM and HMI9-T. Open circle, HMI9-T; closed circles, RMPI-BM plus thymidine; open squares, RMPI-BM.

(B) Cultured in TBM. Open circle, TBM plus thymidine and folate: closed circle, TBM plus thymidine; open square, TBM plus folate; closed square, TBM only.

Media was supplemented with 160 μM thymidine and 9 μM folate, as required. Cumulative growth over 14 days. Doubling times were determined by linear regression and analysed using GraFit.

3.1 Growth of BSF *T. brucei* in different media

In 1989, Hirumi & Hirumi published the HMI9 medium, based on IMDM, where continuous *in vitro* culture could be maintained by the inclusion of reducing and chelating agents (2-mercaptoethanol and bathocuproine sulfonate) (Hirumi and Hirumi, 1989). Today, HMI9 is now most widely utilised for BSF *T. brucei* cell culture, with variants such as HMI9-T (thioglycerol instead of 2-mercaptoethanol as a reducing agent) and HMI911 (lacks Serum Plus^{TM}) adopted as well (Creek *et al*., 2013; Greig *et al*., 2009). Indeed in our research group and in the DDU HMI9-T medium is used for standard *in vitro* culture. However, HMI9-T medium contains high concentrations of folate, as folic acid (7.9 μM from IMDM), and thymidine (160 μM added to IMDM) (Sienkiewicz *et al*., 2008). Additionally folate concentrations are ~ 9 μM when including the contributions of Serum Plus^{TM} (0.62 μM when supplied by SAFC Biosciences (Sienkiewicz *et al*., 2008)) and FCS (~3 nM when supplied by GE Healthcare (personal communication)). In order to characterise the properties of drugs acting on folate metabolism, an objective of this thesis, folate and thymidine depleted medium was made and cumulative growth analysed.

BSF *T. brucei* S427 cells failed to grow when cultured in RPMI-BM (made as per section 2.2.3) and died after 72 h (Figure 3.1 A). However, cells grew in RPMI-BM supplemented with thymidine (160 μM), demonstrating that thymidine serves as a nutritional rescue in these cells. Cell growth in a media deficient in both thymidine and folate was required for inhibitor studies and as a consequence TBM was prepared, as per section 2.2.3. Cells grew in TBM, indeed cells grew to a similar rate regardless of supplementation with thymidine and/or folate (Figure 3.1 B). Cells grew slightly slower when cultured in TBM (doubling time 8.2 h) and RPMI-BM

Table 3.1. **Effect of folate and thymidine on sensitivity of *T. brucei* to DHFR-TS inhibitors *in vitro*.** Cells were cultured in TBM with the addition of thymidine (160 μM) and/or folate (9μM). Results are the weighted means ± standard error of 3 independent experiments

Inhibitor	No addition		+ Thymidine		+ Folate		+ Thymidine + Folate	
	EC_{50} μM	Hill Slope	EC_{50} μM	Hill Slope	EC_{50} μM	Hill Slope	EC_{50} μM	Hill Slope
Methotrexate (MTX)	0.012 ± 0.001	4.8	0.12 ± 0.03	1.2	1.31 ± 0.13	1.3	8.16 ± 2.78	1.4
Raltitrexed (RTX)	0.038 ± 0.001	4.7	> 250	-	64.8 ± 4.3	4.8	> 250	-
Pemetrexed (PMX)	0.020 ± 0.001	5.2	> 250	-	12.9 ± 1.1	3.2	>250	-
Trimetrexate (TMX)	0.32 ± 0.02	5.2	2.82 ± 0.36	1.4	1.23 ± 0.06	4.8	4.09 ± 0.35	1.9
Pyrimethamine (PYR)	2.26 ± 0.32	0.9	2.01 ± 0.34	0.8	6.32 ± 0.71	1.1	6.87 ± 0.33	1.0
Trimethoprim (TMP)	48.8 ± 3.7	1.4	59.8 ± 8.6	0.8	170 ± 28	0.7	145 ± 22	0.6
Nolatrexed (NTX)	33.8 ± 3.7	2.9	32.7 ± 4.7	1.8	21.8 ± 2.0	2.0	39.6 ± 7.2	1.8

plus thymidine (doubling time 8.5 h) compared to when cultured in standard HMI9-T medium (doubling time 7.3 h). TBM was carried forward for further *in vitro* studies in this thesis.

3.2 *In vitro* effects of known DHFR and TS inhibitors on *T. brucei*

To assess the specificity of a range of known DHFR and TS inhibitors, EC_{50} values for growth inhibition against *T. brucei* were compared in TBM where supplementation of folate could potentially reduce drug potency by competing with a drug for its target and thymidine could serve as a by-pass mechanism for inhibition of DHFR or TS (Table 3.1 and structures shown in Figure 1.4).

Antifolates had highest potency against BSF *T. brucei* when tested in a medium depleted in folate and thymidine (TBM), apart from NTX where there was no real change detected. In TBM, MTX, RTX, and PMX showed nanomolar potencies and have high Hill slope (*s*) values, ~5, indicative of an 'all or nothing' type of concentration effect. TMX also possessed high nanomolar potency in TBM with a similar Hill slope. With the exception of NTX, supplementation with folate and thymidine to TBM reduced the parasites' susceptibility to the antifolate drugs. For MTX, PYR and TMP the addition of folate alone had a more substantial effect in reducing susceptibility than addition of thymidine alone. For MTX, supplementing with folate or thymidine substantially decreased the Hill slope to a similar extent. MTX is known to inhibit both DHFR-TS and PTR1 in *T. brucei* (Shanks *et al*., 2010; Spinks *et al*., 2011; Gibson *et al*., 2016). The monoglutamate form of MTX has been shown to have picomolar K_i values against TbDHFR enzyme (K_i 95 pM) (Gibson *et al*., 2016), micromolar K_i values against TbTS (463 μM) (Gibson *et al*., 2016) (polyglutamylation of MTX likely increasing TS affinity) and nanomolar values

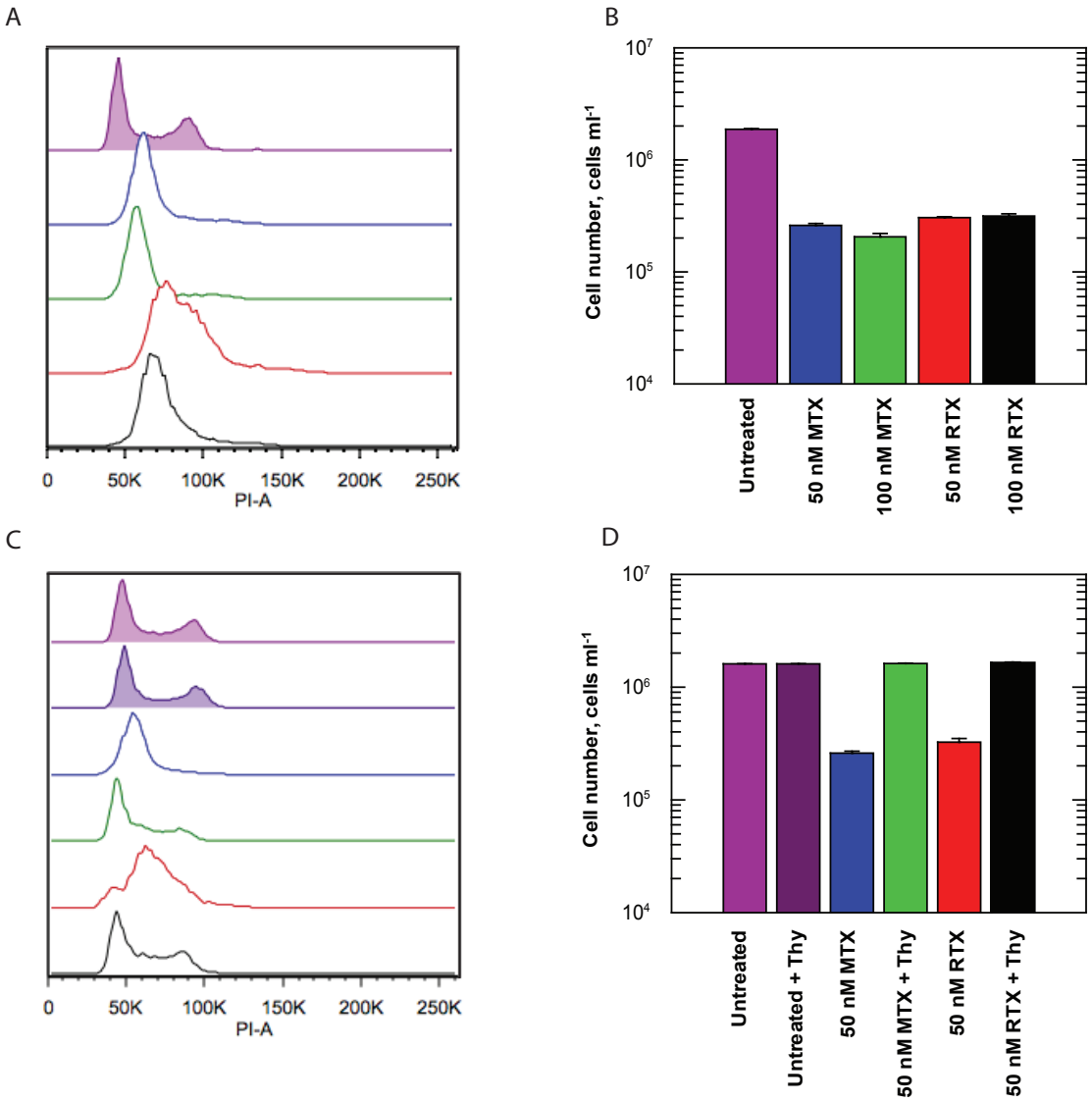

Fig 3.2 Cell cycle analyses of MTX and RTX treated cells.

(A) and **(B)** Cells cultured in TBM plus 1 µM thymidine. (A) Cell count of untreated cell compared to 20 hrs treatment with MTX or RTX. (B) The histogram from the FACs analysis is presented as; light purple, untreated cells; blue, 50 µM MTX; green, 100 µM MTX; red, 50 µM RTX; black, 100 µM RTX. The Y-axis on the overlay histogram is "% of Max". The x-axis is DNA content measured using Propidium Iodine (PI) staining and pulse area (A).

(C) and **(D)** Cells cultures in TBM plus either 1 µM thymidine or excess 160 µM thymidine. **(C)** Cell count of untreated cells compared to 20 hrs treatment with MTX or RTX in 1 µM or excess 160 µM thymidine. The histogram from the FACs analysis is presented as; light purple, untreated cells; dark purple; untreated cells plus excess thymidine; blue, 50 µM MTX; green, 50 µM MTX plus excess thymidine; red, 50 µM RTX; black, 50 µM RTX plus excess thymidine. The Y-axis on the overlay histogram is "% of Max". The x-axis is DNA content measured using Propidium Iodine (PI) staining and pulse area (A).

against TbPTR1 ($K_{i\ app}$ 11.1 nM) (Spinks *et al*., 2011). Indeed *in vitro* low concentrations of MTX may inhibit DHFR and higher concentrations PTR1. A steep Hill slope is characteristic of DHFR (or TS) inhibition (unpublished from Sienkiewicz *et al*., 2008) and a shallow Hill slope of PTR1 inhibition (Spinks *et al*., 2011). Therefore abolishing the effect of thymidine and/or folate starvation would reveal the second mode of action, lowering the Hill slope. Thymidine addition did lower the Hill slope of TMX which is consistent with the above hypothesis. For RTX and PMX growth inhibition was completely abolished with thymidine supplementation and folate addition resulted in a substantial reduction in susceptibility while the Hill slope remained high, indicative of inhibition primarily through TS. For TMX, supplementation with either folate or with thymidine had a comparable effect on reducing drug potency and with supplementation of thymidine alone the Hill slope was reduced. Melarsoprol was used as a control and there was no change in EC_{50} (2 nM) and Hill slope value (~3) across all media types (results not shown). MTX (targeting DHFR) and RTX (targeting TS) were taken forward as lead compounds from these cell-based potency tests.

3.3 Cell Cycle Analysis

With results of *in vitro* potency suggesting 'thymineless-death' to be a mechanism of MTX toxicity (susceptibility to MTX reduced with thymidine addition) and more-so RTX toxicity (RTX potency abolished with thymidine addition) (Table 3.1) cell cycle analysis was undertaken to confirm this mode of action. Untreated cells showed a normal distribution of G1, S (DNA synthesis) and G2/M phase; however with both MTX and RTX treatment this distribution was substantially disrupted (Figure 3.2 A). With both 50 nM and 100 nM MTX treatment cells were arrested in

S phase and, with the higher MTX concentration, cells were distributed earlier in S phase. With 50 nM RTX treatment cells were distributed in S phase into G2/M phase, and with 100 nM RTX cells were distributed more prominently in S phase. With both MTX and RTX treatment parasites were unable to complete DNA synthesis from 2N (G1) to 4N (G2/M) with arrest within S phase. Moreover total cell density was reduced with 20 h drug treatment compared to the untreated control, MTX; 50 nM ~ 7 fold and 100 nM ~ 9 fold, RTX; 50 nM and 100 nM both ~ 6 fold. (Figure 3.2 B).

Figure 3.2 C demonstrates that excess thymidine supplementation can reverse the cell-cycle effects of both MTX and RTX. Untreated cells showed a normal distribution of G1, S and G2/M phase with 1μM thymidine (physiological levels in mice (Clarke *et al*., 2000b) or excess 160 μM thymidine. In MTX and RTX treated parasites with excess thymidine supplementation, cell cycle distribution changes from that of arrest in S phase to that of a more normal cell cycle distribution with cells distributed in G1, S and G2/M phase. Returning to 'normal' distribution with thymidine supplementation is most prominently seen in RTX treated cells. Figure 3.2 D illustrates that with the addition of excess thymidine the total cell density of MTX or RTX treated cells returned to that of the untreated controls (MTX = 2.6×10^5 cells ml^{-1}, MTX plus excess thymidine = 1.6×10^6 cells ml^{-1}, RTX = 3.3×10^5 cells ml^{-1}, RTX plus excess thymidine = 1.6×10^6 cells ml^{-1}).

3.4 Static-cidal assay for MTX and RTX

In *T. brucei* drug discovery, compounds with trypanocidal activity are more desirable than compounds with trypanostatic activity and therefore an objective was

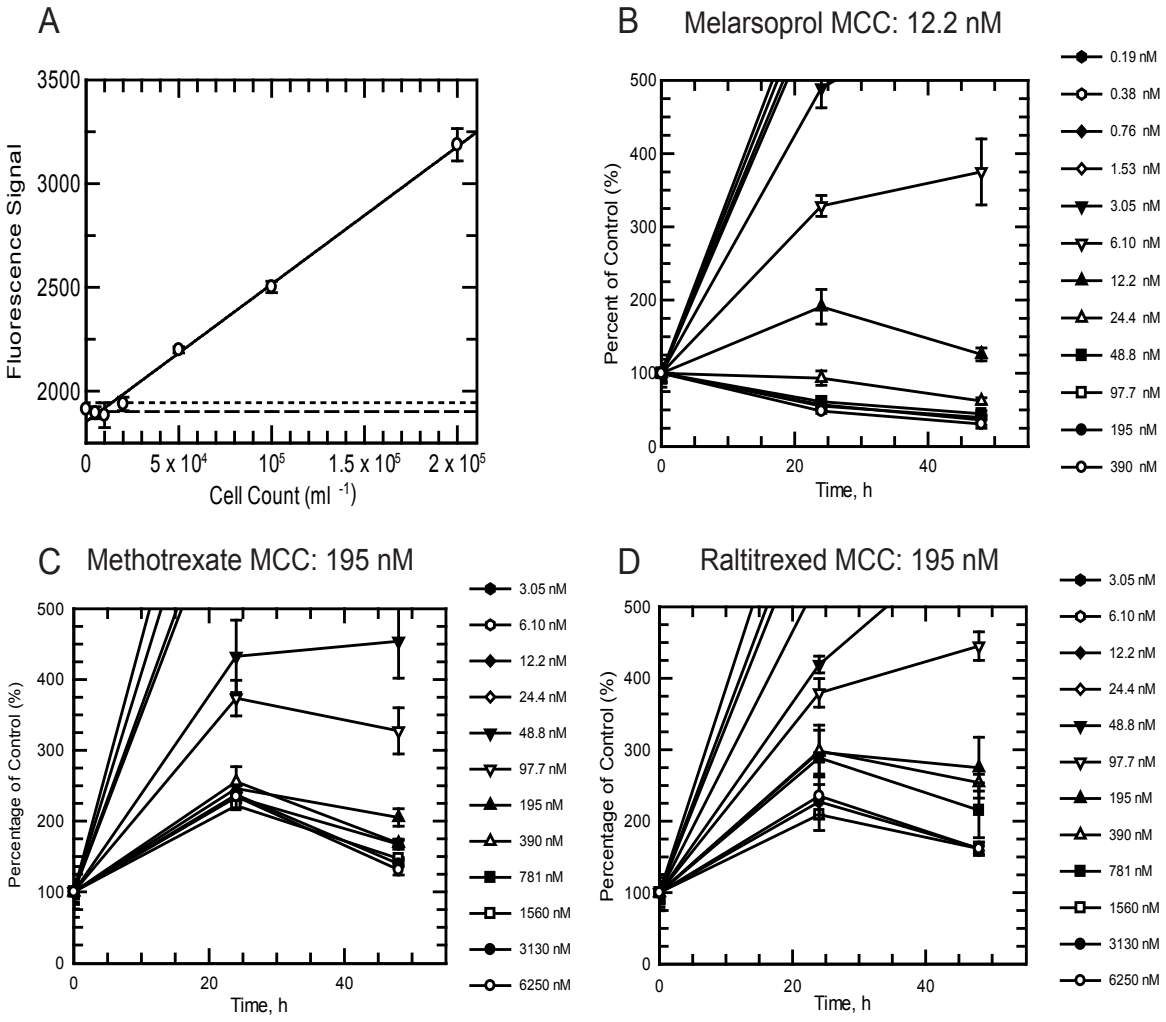

Fig 3.3 Static-cidal assay for drugs tested in TBM.

(A) Detection limit of static-cidal assay**.** Solid line, linear regression of cell count against fluorescence signal; dashed line, mean value of blanks; dotted line, assay detection limit (2 x 10^4 cells ml^{-1}).

(B, C, D) Growth curves and MCC are shown for melarsoprol **(B)**, MTX **(C)** and RTX **(D)**. Growth is calculated as a percentage against the no drug control. Error bars represent standard deviation**.**

to determine the static/cidal nature of MTX and RTX, the lead compounds from *in vitro* potency testing.

In a standard EC_{50} analysis over 72 h, the initial parasite cell density is below the limit of detection of the assay, which means one cannot discriminate between drugs with a cidal effect from drugs with a static effect. Indeed, the limit of detection of the resazurin assay was measured to be 2.0×10^4 cell ml^{-1} (Figure 3.3 A) and the starting density of 2.5×10^3 cells ml^{-1} (as described in section 2.4) used for standard EC_{50} assays is below this limit of detection. To determine the cidal nature of MTX and RTX, parasite starting density was increased to 4.0×10^5 cell ml^{-1} as previously described (De Rycker *et al*., 2012).

A decline in parasite density after drug exposure (reduction in fluorescent signal) is indicative of trypanocidal activity. Cidal activity is observed in the melarsoprol control after 48 h with a Minimum Cidal Concentration (MCC) of 12.2 nM (Figure 3.3 B). For all concentrations of MTX and RTX the signal at 48 h was not equal to or less than the starting signal (t= zero), compared to melarsoprol where some concentrations at 48 h were less than t = zero (Figure 3.3 C + D). Melarsoprol would therefore be described as rapidly cidal at 48 h whereas MTX and RTX were not fully cidal at 48 h, albeit due to the limitations of the assay MTX and RTX showed static activity.

3.5 MTX and RTX potency in folate and thymidine ranges found in mouse plasma

With MTX and RTX showing nanomolar potencies in TBM further *in vitro* potency studies were carried out in view of potential future *in vivo* testing. Previous studies have demonstrated that plasma folate levels in mice can vary from ~71 nM to ~350

Table 3.2 Modulation of folate and thymidine levels to mimic physiological ranges found in mouse plasma: Effect on MTX and RTX treatment *in vitro*. Results are the weighted means ± standard error of triplicate readings. MTX, methotrexate; RTX, raltitrexed.

Drug	+ Folate (nM)	+ Thymidine (nM)	EC_{50} (nM)	Hill slope
MTX	~30	1,000	16.1 ± 0.6	5.2
MTX	~30	-	17.7 ± 0.7	3.9
MTX	~80	1,000	29.2 ± 1.5	5.6
MTX	~80	-	30.5 ± 1.3	5.7
MTX	~300	1,000	118 ± 10	8.3
MTX	~300	-	82.3 ± 5.0	4.7
RTX	~30	1,000	122 ± 6	3.8
RTX	~30	-	175 ± 8	4.4
RTX	~80	1,000	315 ± 15	5.2
RTX	~80	-	421 ± 23	4.5
RTX	~300	1,000	1830 ± 104	4.6
RTX	~300	-	1760 ± 124	6.7

nM dependent on whether mice are fed a folate-depleted or folate-replete diet (Wang *et al*., 2010) with thymidine levels ~ 1 μM (Clarke *et al*., 2000b). MTX and RTX potency was tested in trypanosomes with the addition of 1 μM thymidine and either 30, 80 or 300 nM folate comparable to the ranges detected in mice, with 30 nM folate being the lower limit of detection.

Modulation of folate concentration, rather than thymidine, affected the potency of both MTX and RTX as depicted in Table 3.2. Increasing folate levels only (without thymidine addition) from 30 to 300 nM shifts MTX potency 5 fold, and RTX potency 14 fold. The addition of 1 μM thymidine does not substantially change the EC_{50} values of both MTX and RTX at the respective folate concentrations. This is compared to results in section 3.1 where the addition of excess thymidine (160 μM) to TBM reduced MTX susceptibility by 10 fold and abolished the effect of RTX. Hill slopes are not substantially changed with the addition of mice physiological levels of thymidine or folate, with MTX and RTX retaining their 'all or nothing' concentration effect.

3.6 "Antifolate set" drug screen in various media

Known DHFR-TS inhibitors (MTX, RTX and PEM) displayed nanomolar potencies against *T. brucei* when tested in TBM, a media which is deficient in both folate and thymidine (result in section 3.2). In *T. brucei* drug screening programmes, standard HMI9-T media is routinely used (Brand *et al*., 2012; Oduor *et al*., 2011; Pena *et al*., 2015); however, this media would not accurately assess the potency of drugs acting on folate metabolism due to the excessive amount of folate and thymidine present in the media. An objective of this thesis was to assess whether TBM would be a good media candidate for *in vitro T. brucei* screening of chemicals with potential

Figure 3.4 Chemical structures of "antifolate set"

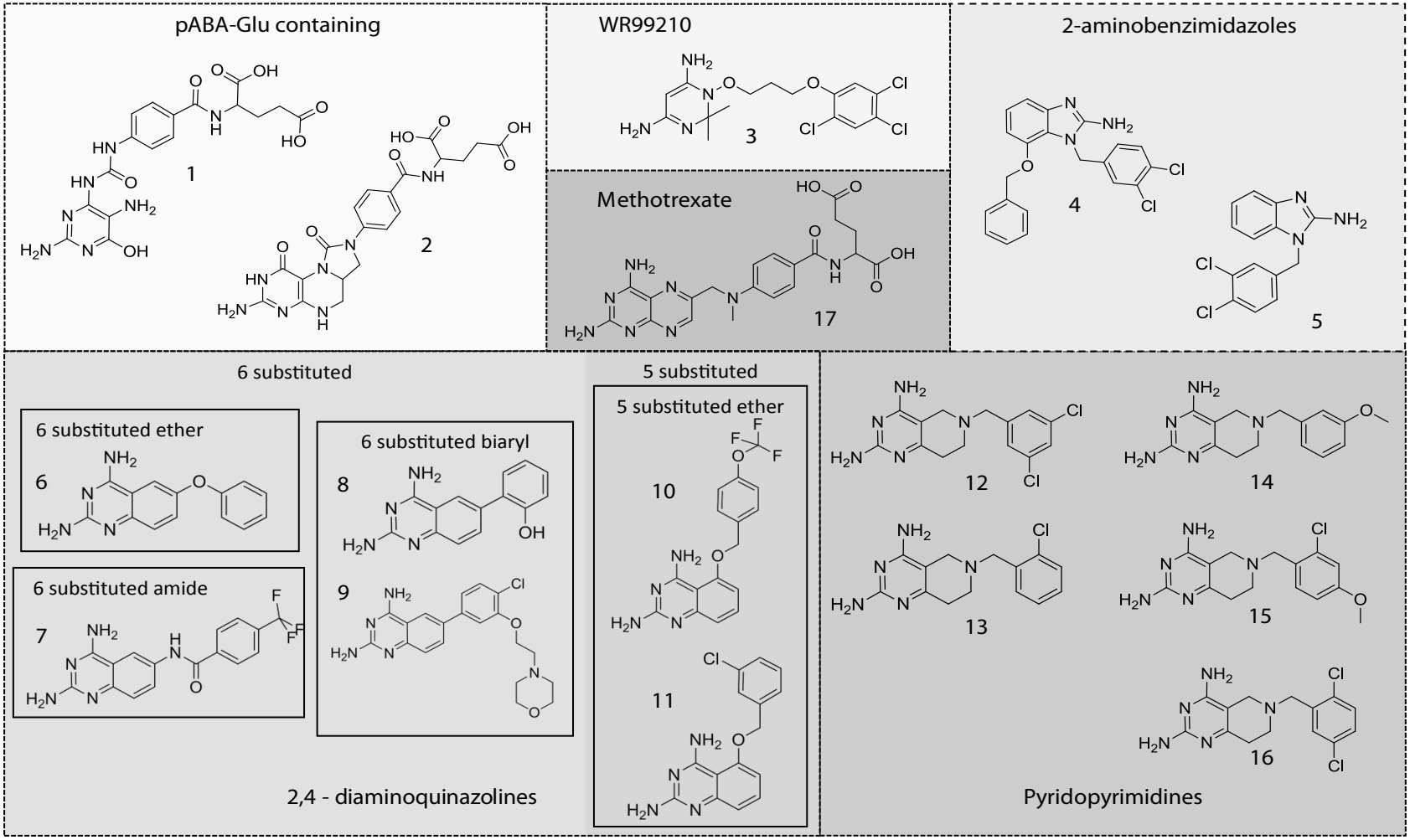

Table 3.3 Screen of "antifolate set" across media types.

Cells were cultured in TBM with the addition of thymidine (160 μM) or folate (9 μM), or in HMI9T. PTR1 and DHFR enzyme activity measured by biologists of the DDU using a cystochrome c-coupled assay as per previously described (Shanks *et al*., 2010). [a] = K_i as of (Vanichtanankul *et al*., 2011) [b] = K_i as of (Spinks *et al*., 2011). NT = not tested. Results of *in vivo* potency testing are the weighted means ± standard error of 3 (n = 3) or 2 (n =2) independent experiments.

Compound	Enzyme Activity EC_{50} (nM)		TBM (n=3)		TBM + Thymidine (n=2)		TBM + Folate (n=2)		HMI9T (n=2)	
	PTR1	DHFR	EC_{50} (nM)	Hill Slope (s)	EC_{50} (nM)	Hill Slope (s)	EC_{50} (nM)	Hill Slope (s)	EC_{50} (nM)	Hill Slope (s)
1	-	-	18500 ± 4700	1.7	27100 ± 2600	2.7	45300 ± 22300	1.6	23600 ± 5020	1.9
2	-	-	31800 ± 8440	1.0	22200 ± 1780	2.4	>25000	-	>25000	-
3	-	[a]1.1	4210 ± 379	8.0	5590 ± 2630	23.6	4150 ± 601	7.5	6220 ± 501	3.4
4	[b]98	[b]>50	3360 ± 209	3.5	3290 ± 251	3.3	3170 ± 284	4.0	6260 ± 255	6.1
5	[b]800	[b]>50	6720 ± 382	6.4	6570 ± 550	5.6	6830 ± 1030	9.9	7350 ± 180	3.0
6	4	60	6.67 ± 1.71	0.47	7.52 ± 1.89	0.44	28.1 ± 5.08	0.61	47.5 ± 6.05	0.92
7	6	NT	130 ± 15.0	1.2	141 ± 18.5	1.3	167 ± 13.2	3.0	187 ± 17.7	1.7
8	2	40	58.6 ± 12.8	0.45	134 ± 32.4	0.60	210 ± 61.1	0.36	177 ± 34.8	0.61
9	3	3500	203 ± 13.7	1.4	132 ± 16.7	1.1	231 ± 21.5	1.3	323 ± 21.4	3.3
10	60	600	131 ± 13.7	0.74	59.6 ± 9.97	0.55	62.1 ± 8.62	0.51	149 ± 9.05	0.79
11	20	40	91.2 ± 5.75	1.1	71.1 ± 9.23	0.85	112 ± 8.71	1.3	133 ± 17.6	1.7
12	5.3	250	240 ± 33.8	0.60	392 ± 119	0.68	240 ± 78.4	0.43	625 ± 56.4	0.89
13	3.6	83	478 ± 76.4	0.76	643 ± 119	0.68	838 ± 161	0.80	666 ± 60.8	0.74
14	11	1020	569 ± 90.2	0.61	568± 19.9	0.58	980 ± 137	0.73	866 ± 137	0.87
15	11	1010	387 ± 76.6	0.67	384 ± 109	0.49	951 ± 144	0.86	1080 ± 177	0.76
16	6.6	52	278 ± 46.0	0.68	199 ± 102	0.37	662 ± 133	0.91	507 ± 105	0.67
17	7.4	0.8	13.8 ± 0.80	3.0	104 ± 45.9	0.98	1220 ± 102	1.46	7070 ± 987	0.87

antifolate properties. In addition, it would be beneficial to elucidate whether testing drug potency in TBM with thymidine or folate supplementation could give an insight into the mode of action of inhibitors, specifically if they are targeting DHFR-TS.

A compound set was established containing inhibitors known to possess potency against the *T. brucei* DHFR enzyme: MTX (compound **17**) with DHFR activity in *T. brucei* (Gibson *et al*., 2016) and WR99210 (compound **3**) with established DHFR enzyme activity in *Plasmodium falciparum* (Winstanley *et al*., 1995) and evidence to suggest DHFR activity in *T. brucei* (Vanichtanankul *et al*., 2011). The set also included compounds known to inhibit DHFR to a lesser extent than their primary enzyme target. It was known from an in-house DDU drug discovery programme against *T. brucei* PTR1 that there were a number of compounds that, as well as primarily targeting the PTR1 enzyme, also inhibited DHFR to varying degrees, as an off-target effect (Shanks *et al*., 2010; Spinks *et al*., 2011). Compounds (**4** to **16**) were selected from this programme for this cell based drug screen and these compounds covered a variety of different chemical series (Figure 3.4). Compound selection was limited by availability, however compounds from four different chemical classes were included; 2-aminobenzimidazoles, 6 and 5 substituted 2,4- diaminoquinazolines, and tetrahydropyridopyrimidines. This set also included 2 compounds (compounds **1** and **2**) containing a *p*ABA-Glu moiety, mainly to assess the *p*ABA-Glu moiety in antifolate drug discovery. This compound set (total of seventeen compounds) was known as the "antifolate set".

The "antifolate set" were tested in TBM, TBM supplemented with thymidine and folate respectively, and standard HMI9-T media (Table 3.3). Compounds **1** and **2** (*p*ABA-Glu containing) displayed weak potency (high micromolar) across all media types (Table 3.3). For the remaining compounds (**3-17**) there was a marked

increase in potency when tested in TBM compared to HMI9-T media. Compound **3** (WR99210) and compounds **4** and **5** (2-aminobenzimidazoles) displayed micromolar potencies across all media types but had a high Hill slope ($\geq$ 3) suggesting inhibition of DHFR-TS (see section 3.2). WR99210 had previously been shown to have an *in vitro* EC_{50} of 0.09 $\pm$ 0.02 μM in *T. brucei* (Vanichtanankul *et al*., 2011), however this could not be replicated in this drug screen where EC_{50} were ~ 4 - 6 μM across media types.

The addition of folate had a greater effect in increasing EC_{50} than the addition of thymidine for compounds **6**-**9**. In particular compounds **6** and **9** have low nanomolar enzyme activity against both PTR1 and DHFR and the addition of folate reduced whole cell susceptibility by ~ 4 fold for these compounds. There was no substantial change in EC_{50} in compounds **10** and **11** with thymidine or folate supplementation. Compound **11** has nanomolar enzyme activity against both PTR1 and DHFR. In the tetrahydropyridopyrimidines group (compounds **12**-**16**) supplementation with folate and thymidine did not change whole cell EC_{50} to any great extent. Of note a shallow Hill slope (<1) is a characteristic of PTR1 inhibition (compounds 4-16) and this is evident in whole cell potencies with the exception of compounds **7**, **9** and **11** were Hill slopes are >1, this could suggest other off-target effects for these three compounds (e.g. DHFR-TS). The MTX control behaved as expectedly with folate supplementation having a more substantial effect in increasing EC_{50} than thymidine supplementation (88 fold and 8 fold respectively) which highlights selectivity of DHFR inhibition over TS inhibition.

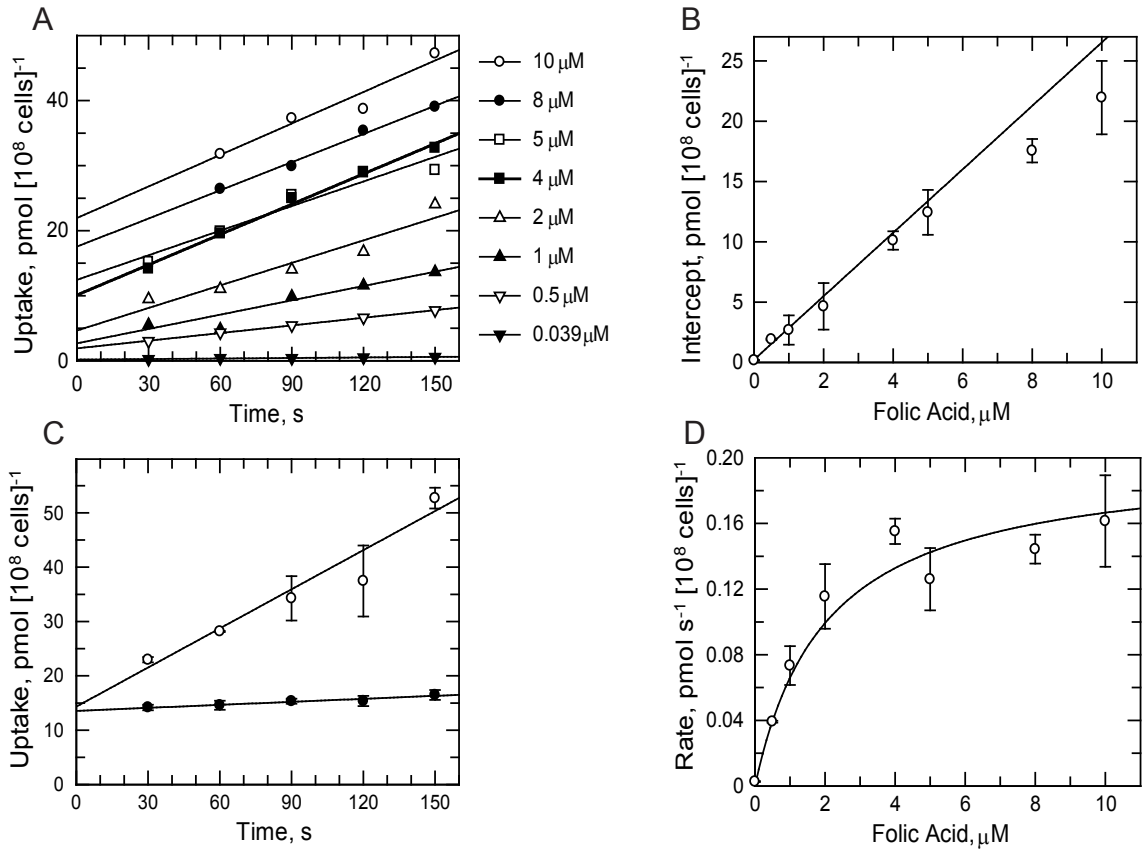

Figure 3.5 Folate transport

(A) Linearity of folate uptake at 23 ^{o}C. Time point at 30 s for 10 μM and 8 μM not plotted due to loss of pellet during experiment. **(B)** Intercepts (from panel **(A)** at time zero) as a function of folate concentration **(C)** Effect of temperature on folate uptake. Uptake of 10 μM folate at 23 ^{o}C (open circles) or 4 ^{o}C (closed circles). Time points were done in triplicate and the mean and SEM are shown. **(D)** Uptake of folate fitted by Michaelis-Menten equation using rates obtained from the slopes of data in panel **(A)**

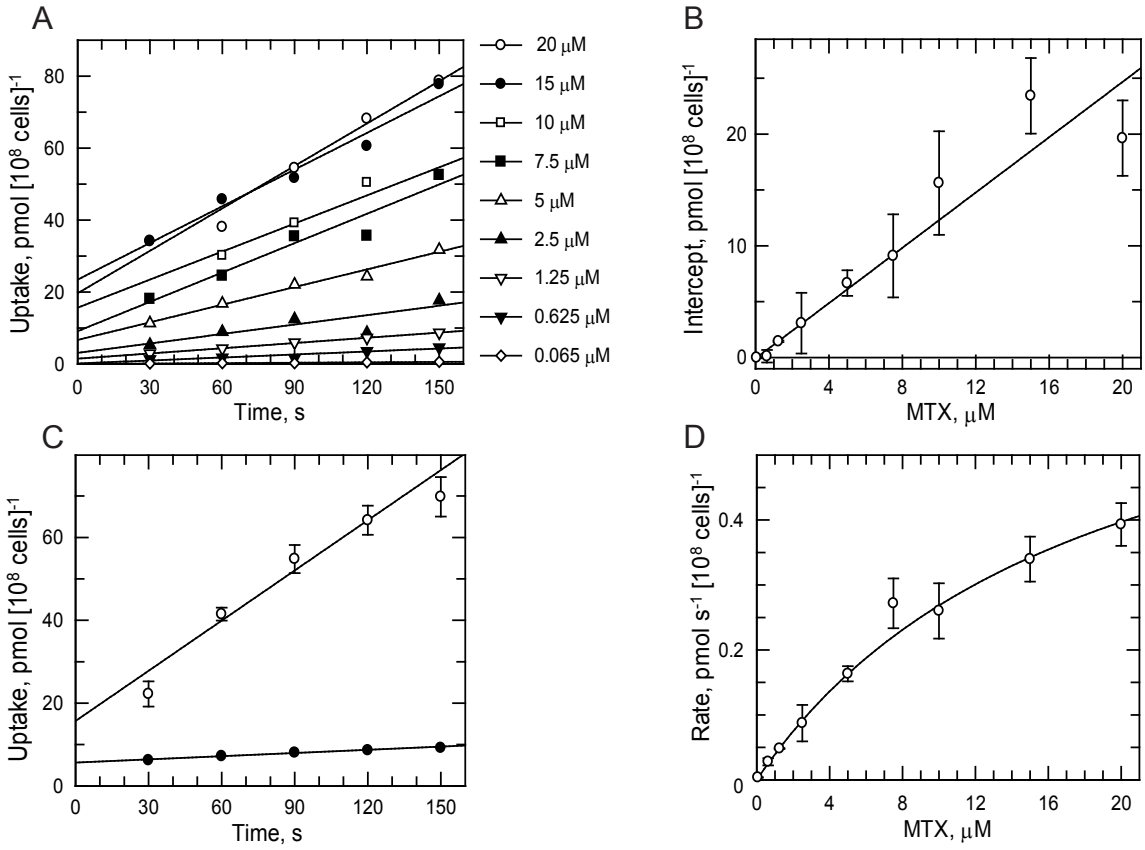

Figure 3.6 MTX transport

(A) Linearity of MTX uptake at 23 ^{o}C. Time point at 30 s for 20 μM not plotted due to loss of pellet during experiment. **(B)** Intercepts (from panel (A) at time zero) as a function of MTX concentration **C**. Effect of temperature on MTX uptake. Uptake of 20 μM MTX at 23 ^{o}C (open circles) or 4 ^{o}C (closed circles). Time points were done in triplicate and the mean and SEM are shown. **(D)** Uptake of MTX fitted by Michaelis-Menten equation using rates obtained from the slopes of data in panel **(A)**

3.7 Transport Studies

A core objective to this thesis was to determine how folate and antifolate drugs are transported into cells. This will expand the current knowledge around the mode of action of these drugs.

3.7.1 Folate Uptake and $K_{m\ app}$ analysis

To address the transport kinetics of folate (folic acid) uptake in BSF *T. brucei* the linearity of folate uptake over time was first determined. The linearity of the assay was based on previous studies which demonstrated that folate uptake was rapid and linear over 2-3 minutes in *Leishmania* parasites (Ellenberger and Beverley, 1987). Indeed in *T. brucei* the rate of folate uptake was found to be linear over 150 seconds up to 10 μM at 23 ^{o}C (Figure 3.5 A). A plot of the y-axis intercepts (time zero) of the varying concentrations of folate is linear (Figure 3.5 B), which demonstrates non-specific binding of folate. The rate of uptake of folate is temperature-dependent with a 10-fold higher rate at 23 ^{o}C (0.24 $\pm$ 0.03 pmol s^{-1} $[10^8$ cells$]^{-1}$) compared to 4 ^{o}C (0.02 $\pm$ 0.01 pmol s^{-1} $[10^8$ cells$]^{-1}$) (Figure 3.5 C). It was found that the uptake of folate in BSF *T. brucei* obeys simple Michaelis-Menten kinetics with a $K_{m\ app}$ of 2.07 $\pm$ 0.63 μM and V_{max} of 0.19 $\pm$ 0.02 pmol s^{-1} $[10^8$ cells$]^{-1}$ (Figure 3.5 D).

3.7.2 MTX Uptake and $K_{m\ app}$ analysis

In the same way as folate uptake was established, MTX uptake was found to be linear and directly proportional over 150 s up to 20 μM (Figure 3.6 A) at 23 ^{o}C with evidence of non-specific binding (Figure 3.6 B). The rate of uptake of 20 μM MTX at 23 ^{o}C was determined to be 0.40 $\pm$ 0.06 pmol s^{-1} $[10^8$ cells$]^{-1}$ compared to 0.03 $\pm$ 0.01 pmol s^{-1} $[10^8$ cells$]^{-1}$ at 4 ^{o}C, indicative of temperature-dependent uptake (Figure

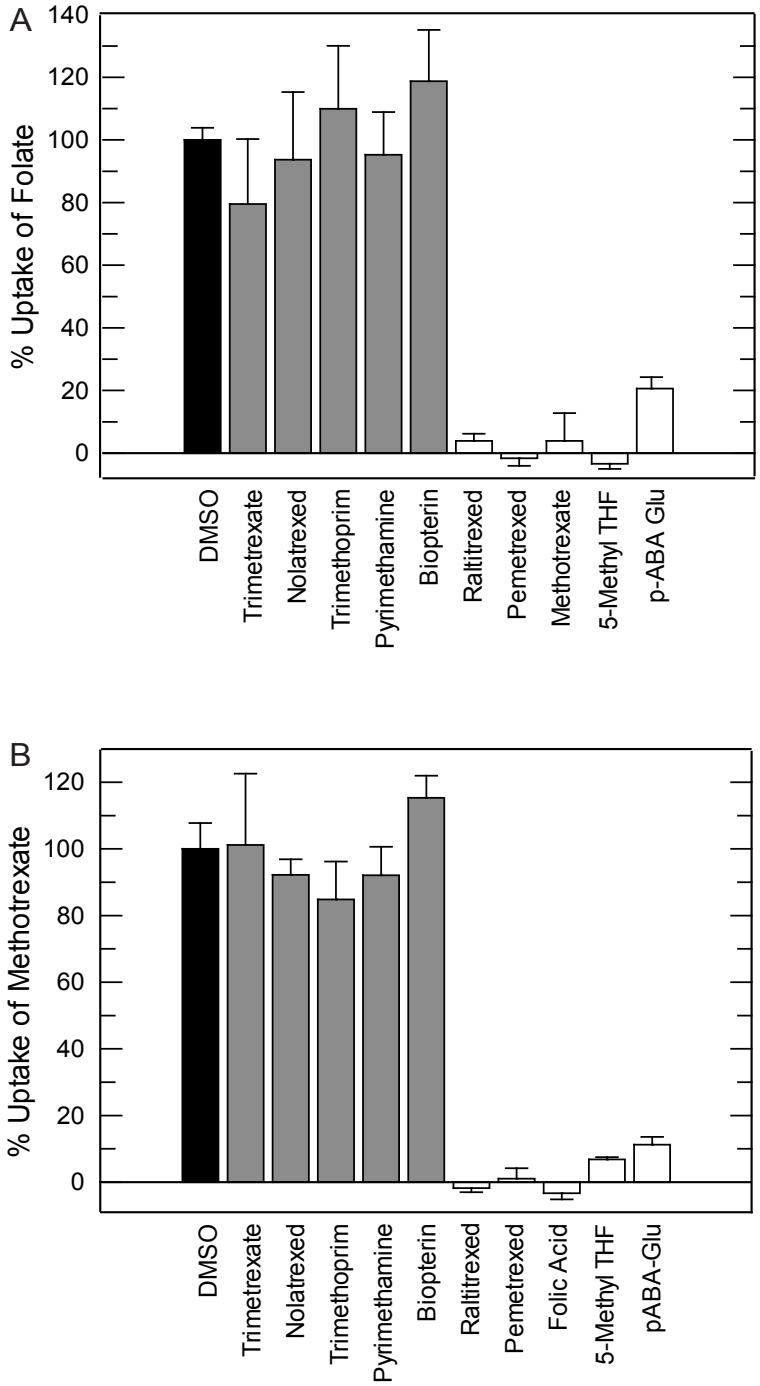

Figure 3.7. Effect of antifolates and folate metabolites on uptake of folate or MTX.

Uptake of folate **(A)** and MTX **(B)** is measured in the presence of 100 μM of each inhibitor. Black bar, DMSO control; grey bars, 'non-folate-like' structures; white bars, 'folate-like' structures. Assay mixture corrected for additional DMSO (0.4 %.) and modified to contain approx. [S] ≅ $K_{m\ app}$ (folate at 2 μM and MTX at 13 μM). Uptake was determined over a 150s incubation peroid.

Table 3.4 Uptake of folate and MTX is measured in the presence of varying concentrations of inhibitor. The standard assay mixture is modified to contain approx. [S] = K_m and corrected for additional DMSO (0.4 %.). IC_{50} is calculated using a two-parameter fit. ND, not determined. Results are IC_{50} value ± standard error.

Substrate	IC_{50} against folate (μM)	Hill Slope	IC_{50} against MTX (μM)	Hill Slope
Methotrexate	3.4 ± 0.4	1.2	-	
Folic Acid	-		1.9 ± 0.4	1.0
5 –Methyl THF	6.3 ± 1.0	0.9	8.0 ± 0.8	0.9
pABA-Glu	30.8 ± 3.7	0.8	33.5 ± 4.6	1.0
Pemetrexed	3.2 ± 0.3	0.8	ND	
Raltitrexed	1.8 ± 0.4	0.8	ND	

3.6 C). MTX uptake also obeys simple Michaelis-Menten kinetics (Figure 3.6 D) with a $K_{m\ app}$ of 16.5 $\pm$ 3.0 μM and V_{max} of 0.68 $\pm$ 0.11 pmol s^{-1} $[10^8$ cells$]^{-1}$.

3.7.3 Inhibitor Studies

After establishing the kinetics parameters of folate and MTX uptake, uptake was measured in the presence of other folate derivatives (metabolites and antifolates) to establish if they had any effect on substrate uptake. Folate uptake was found to be inhibited by the classical antifolates MTX, RTX and PTX and the folate metabolite 5-methyl-THF (principal form found in human plasma) (Figure 3.7 A). Conversely, uptake of folate does not appear to be inhibited by the non-classical antifolates TMX, NTX, TMP, PYR nor biopterin. *p*ABA-Glu had a substantial effect in inhibiting folate uptake (~21% residual folate uptake).

Furthermore, MTX uptake was found to be inhibited by classical antifolates (RTX, PMX) and folic acid, but not inhibited by non-classical antifolates (TMX, NTX, TMP, PYR) or biopterin (Figure 3.7 B). *p*ABA-Glu also had a substantial effect in inhibiting MTX uptake (~11% residual uptake).

3.7.4 Potency of Inhibition

'Folate-like molecules', at a set concentration (100 μM), where shown to inhibit folate and MTX uptake. The potency of inhibition was further characterised by measuring the compounds IC_{50} against substrate uptake. The IC_{50}'s for MTX and folate against folate and MTX uptake were 3.4 μM and 1.9 μM respectively. RTX and PMX had comparative potencies to MTX in inhibiting folate uptake (Table 3.4).

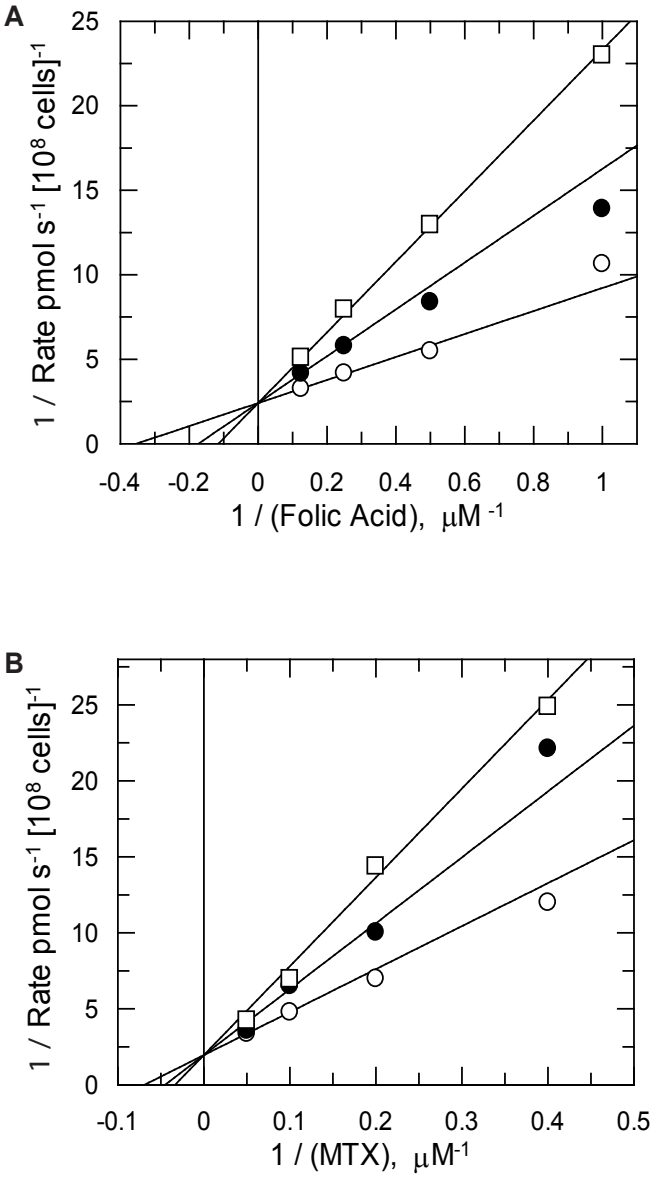

Figure 3.8 Mode of inhibition of folate transport by MTX and vice versa

(A) K_i determination of MTX with respect to folate. Folate concentrations were varied in the presence of fixed concentrations of MTX. MTX was added at 0 μM (open circles); 0.5 μM (closed circles) and 1 μM (open squares). **(B)** Folate was added at 0μM (open circles); 0.5 μM (closed circles) and 1 μM (open squares) and MTX was the variable concentration to determine K_i of folate with respect to MTX.

5-methyl-THF inhibited both FA and MTX uptake to the same extent but at a lower potency than the classical antifolates. *p*ABA-Glu was the weakest inhibitor of both folate (30.8 μM) and MTX (33.5 μM) uptake. For all substrates Hill slopes were, within experimental error, 1. This is indicative of simple binding of one ligand to one transporter. Indeed IC_{50} curves appear to go down towards zero and therefore it is unlikely that other transporters are involved.

3.7.5 Mode of Inhibition

To determine the mode of inhibition of MTX to folate uptake the rate of uptake of folate was measured whilst varying folate concentrations in combination with a set range of MTX concentrations resulting in a double reciprocal plot, or Lineweaver – Burk plot, of the data (Figure 3.8 A). In a similar way, the mode of folate inhibition of MTX uptake was also determined (Figure 3.8 B). Plotting $1/v$ against 1/[S] gives an intercept of $1/V_{max}$ on the *y* axis, $1/[S] = -1/K_{m\ app}$ on the *x* axis and the slope factor is $K_{m\ app}/V_{max}$. Presenting the data in this way, the mode of inhibition was confirmed to be competitive. With changes in [I], competitive inhibition affects $K_{m\ app}$ (*x* intercept and slope factor) only and not V_{max} (*y* intercept) since infinitely high concentrations of [S] displace [I].

In addition, an F-test in GraFit confirmed that data fitted best to competitive inhibition. Using the competitive-mode equation (Section 2.7.3) the inhibition constant (K_i) of MTX competing with folate uptake was calculated to be 0.48 μM. and folate competing with MTX uptake was 0.94 μM. If two substrates compete for the same target (folate transporter) then an IC_{50} can be determined using equations 6 and 7 of section 2.7.3. By applying experimental derived values to these equations an

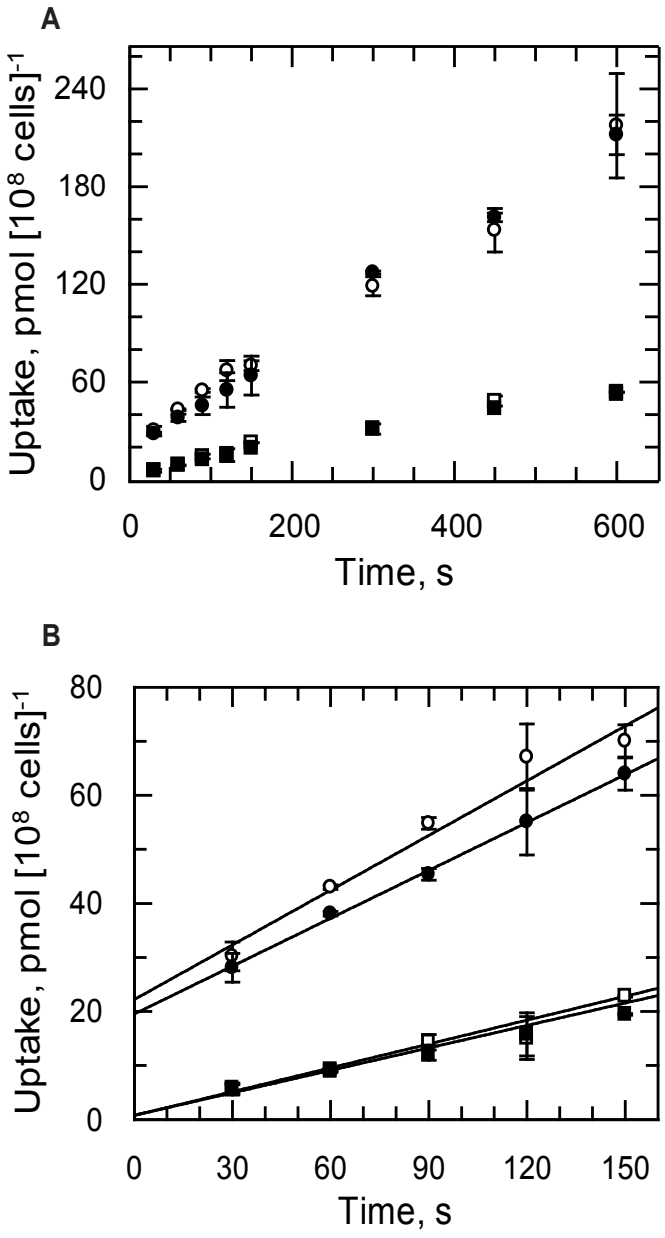

Figure 3.9 Folate uptake in low and high folate conditions.

Folate transport was measured in 'low folate' conditions (TBM) at 20 µM (open circles) and 2 µM (open squares); and in 'high folate' conditions (TBM plus 9 µM folate) at 20 µM (closed circles) and 2 µM (closed squares). Data points are the mean of two biological replicates with error bars indicative of SEM. (**A)** Folate uptake over 10 mins. (**B)** Linearity of folate uptake over 150 s.

IC_{50} of MTX against folate uptake was found to be 2.2 μM and the reverse for folate against methotrexate uptake was 2.9 μM. These values are comparable to the actual EC_{50} values found, 3.4 μM for MTX against folate uptake and 1.9 μM for folate against MTX uptake (Table 3.4), giving good evidence of a competitive substrate model for folate and MTX transport.

K_i (K_d) values cannot be calculated for RTX, PMX and pABA-Glu as V_{max} for these competing substrates is required in order to do so (see section 2.7.3, equations 6 and 7). If these compounds were competitive inhibitors (and do not undergo transport) and not competitive substrates then $K_i = 0.5IC_{50}$ as experiments were performed at [S] = K_m. However, based on the structural similarity of these compounds to folate and MTX and the fact that they inhibit DHFR-TS (therefore get into the cell) it is likely that these compounds are competitive substrates in the same way that folate and MTX were found to be.

3.7.6 Folate transport in high and low folate conditions

To establish whether high extracellular folate conditions affects folate transport into cells, folate transport was measured at 2 μM ($K_{m\ app}$), and 20 μM (saturating concentrations, indicative of V_{max}) in TBM and TBM supplemented with excess folate (9 μM). Over 10 mins, folate transport at 2 μM and 20 μM does not appear to be affected by folate conditions (Figure 3.9 A). Looking more closely at linear transport over 150 s, transport at 2 μM and 20 μM also does not appear to be affected, to any great extent, by low or high folate growth conditions (0.15 and 0.14 for 2 μM compared to 0.34 and 0.30 for 20 μM respectively, measured in pmol s^{-1} $[10^8$ cells$]^{-1}$) (Figure 3.9 B).

Of note, this experiment also confirms steady state Michaelis-Menten kinetics for folate transport, as when [S] = $K_{m\ app}$, then $v = V_{max}/2$. Indeed the rate, measure at pmol s^{-1} [10^8 cells]$^{-1}$, at 2 μM ($K_{m\ app}$) is half that of the rate at 20 μM (indicative of V_{max}) for both high and low folate conditions respectively, 0.15 compared to 0.34 and 0.14 compared to 0.30 (low and high folate respectively).

Chapter 4

Dissecting the mechanism(s) of resistance of antifolate drugs in *Trypanosoma brucei*

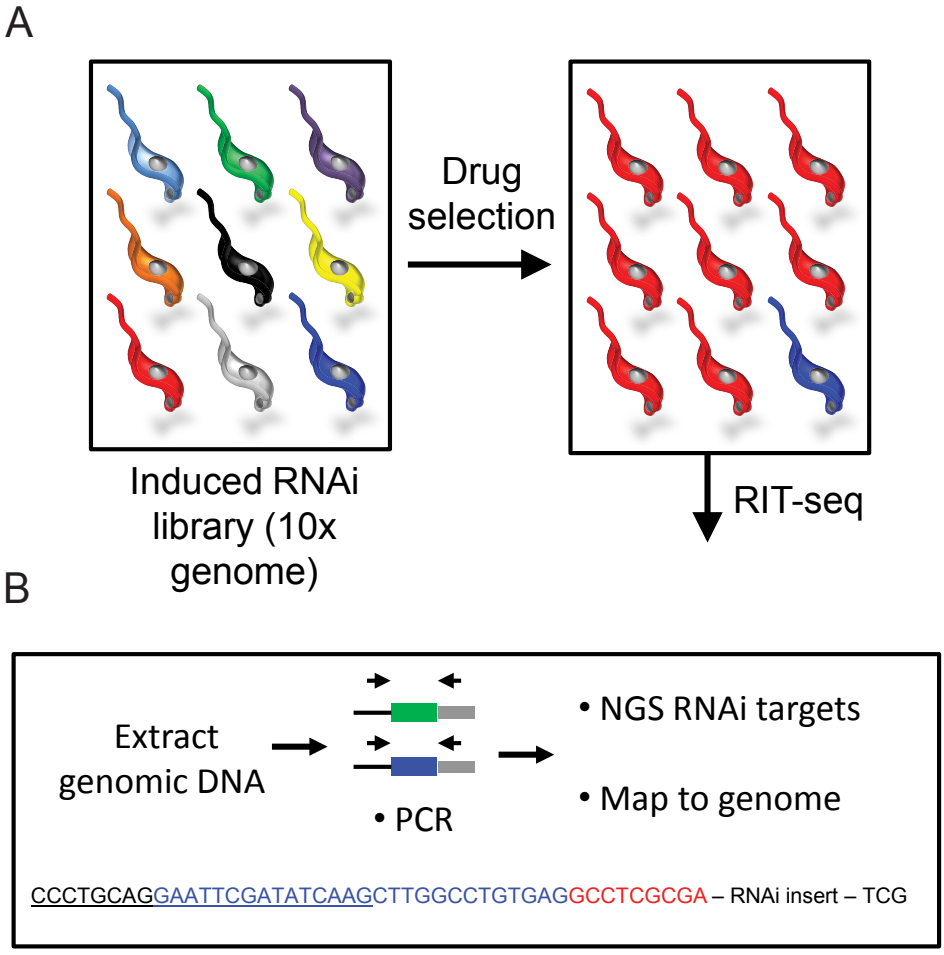

Figure 4.1 RIT-seq schematic

Figure 4.1 Adapted from Glover *et al* 2015.

(A) *T. brucei* dsRNA expression and RNAi is induced by tetracycline (tet). Knockdown has the potential to confer a selective advantage under drug pressure. With drug exposure to a heterogeneous population (multi-coloured) gene knockdowns display a growth defect (red), whereas the surviving population does not (blue). (**B**) RIT-seq comprises amplification of RNAi target fragments. In red, signature barcode used to identify sequence; in blue, sequencing primer TbrR1SF1; underlined, RNAi cassette component of the TbrF1 primer.

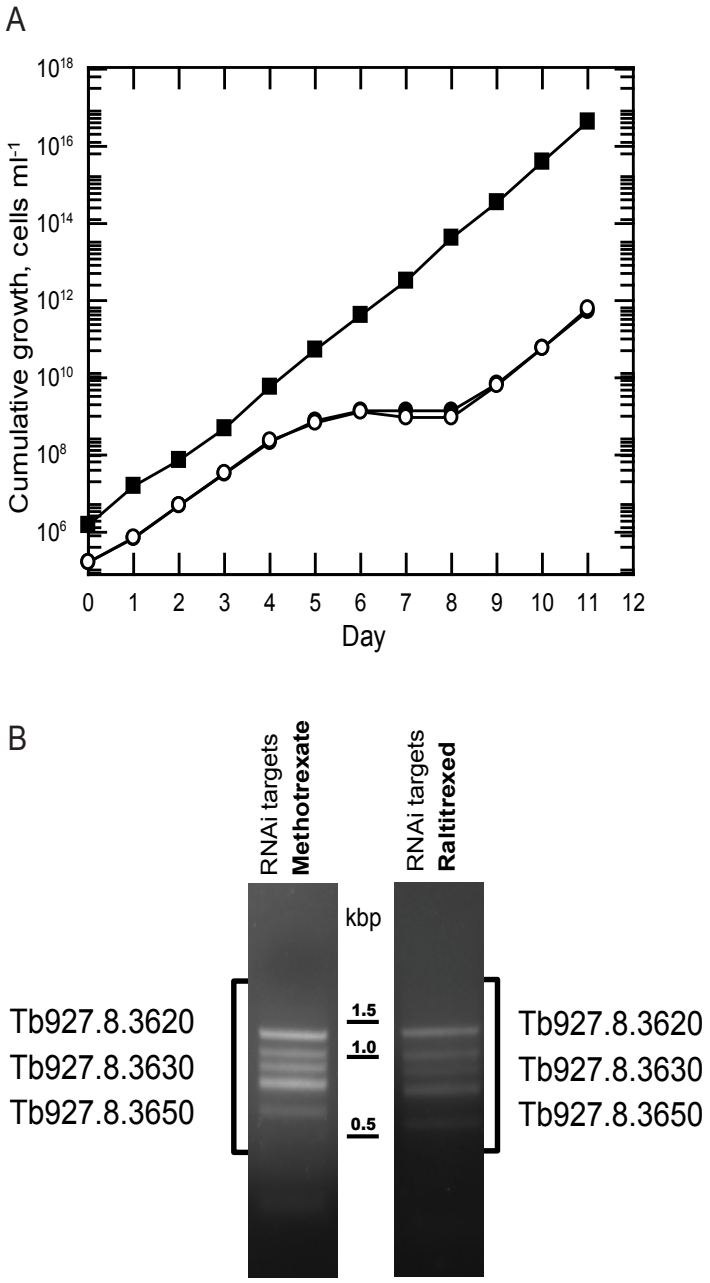

Figure 4.2 Selection of drug resistance by RNAi and low-throughput RIT-seq

(A) Growth phenotype of RNAi library cells treated with MTX or RTX. Closed squares, untreated control; closed circles, MTX treated and open circles RTX treated. (**B)** Low throughput RIT-seq. PCR products representing RNAi target fragments, derived from the RNAi screen, were separated on an agarose gel. Highlighted FT family ID's in both screens.

4.1 RIT-seq Analysis

4.1.1 Selection of drug resistance by RNAi

A *T. brucei* RNAi library screen was used to investigate the putative mechanism of resistaFigurence of two inhibitors of the bifunctional *T. brucei* DHFR-TS enzyme using MTX, which targets DHFR, and RTX which targets TS. Parasites were exposed to a sub-lethal dose of each drug to select a resistant phenotype. With tetracycline induction, each cell produces dsRNA from the integrated RNAi target fragment. Knockdown has the potential to facilitate parasite survival under drug treatment (Figure 4.1 A) and from the surviving population RIT-seq is used to generate a read-out (Figure 4.1 B). Figure 4.2 A demonstrates the growth phenotype of RNAi library cells treated with MTX or RTX. After 4 days, concentrations of MTX and RTX were increased from 15 nM and 10 nM, respectively, to 30 nM for both drugs and resistant populations were isolated for RIT-seq analysis.

4.1.2 Low-throughput RIT-seq

Low-throughput RIT-seq identified DNA fragments that were subsequently sequenced in-house and mapped to the *T. brucei* 927 reference genome (http://tritrypdb.org). PCR fragments seen in both the MTX and RTX screens are shown in Figure 4.2 B and the genes identified by sequencing are shown in Table S1 and Table S2. In both screens two PCR fragments strongly mapped to putative folate transporter genes *FT1-3*: Tb927.8.3620, Tb927.8.3630 and Tb927.8.3650 (Figure 4.2 B, Table S1 and S2). The putative folate transporter orphan gene Tb11.v5.0766 was also implicated. For some PCR fragments, no or poor sequence data was generated through ‘mis-priming’ on gDNA in such *T. brucei* RNAi library screens

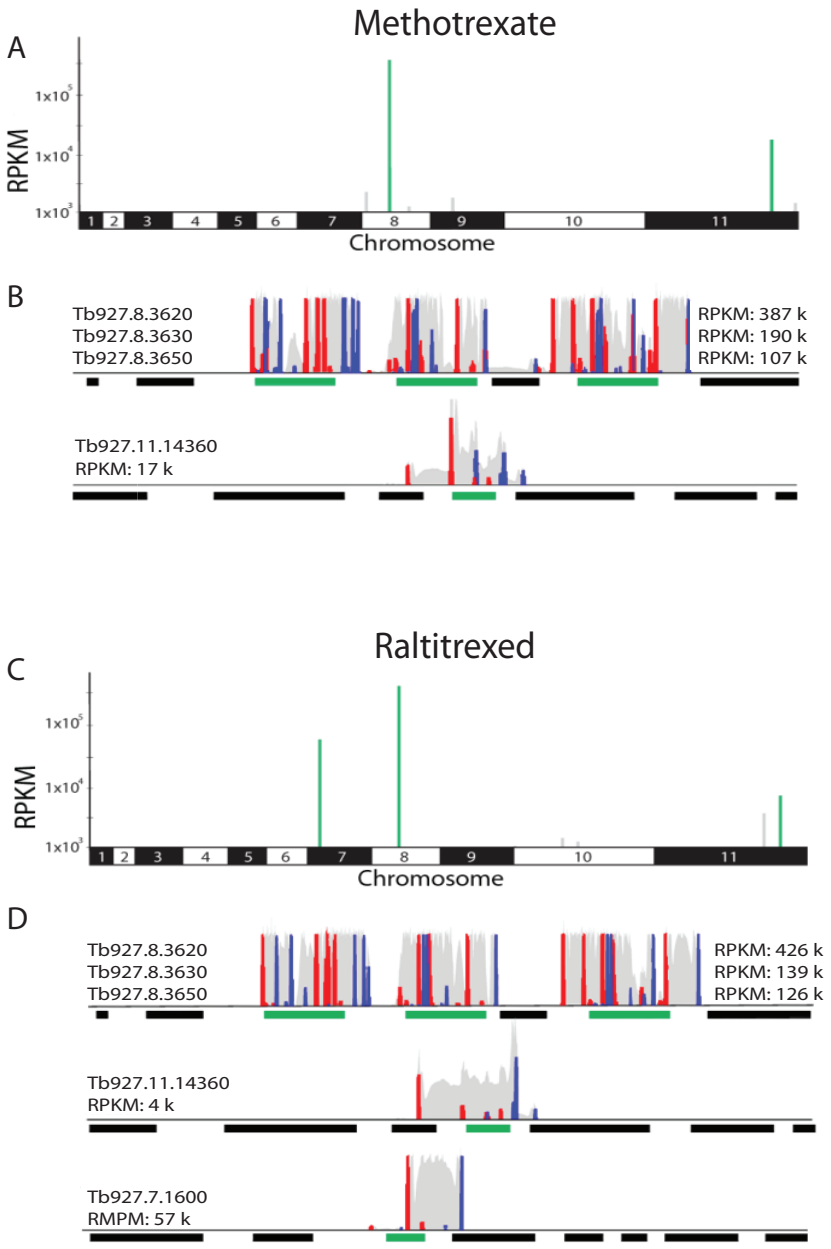

Figure 4.3 High-throughput RIT-seq

(A, C) Hits from the MTX and RTX antifolate RNAi screens are displayed in genome-wide RIT-seq maps. Hits are loci identified by fragments that map with > 1000 reads per kilobase per million (RPKM). 'High confidence' hits, indicated in green, are characterised by multiple RIT-seq fragments. Other 'low confidence' loci with mapped reads are highlighted in grey.

(B, D) The Artemis screen-shots of 'high confidence' hits identified for MTX and RTX. Hits in green and flanking protein coding sequences indicated as black bars. Red peaks, forward reads with RNAi-construct barcodes; blue peaks, reverse reads with RNAi-construct barcodes; grey peaks, all other reads.

Table 4.1: Extended hit list for MTX RIT-seq analysis

(>1000 RPKM 'barcoded reads' and >200 RPKM 'all mapped reads' cut-offs)

Gene ID	Gene description	Barcoded reads only		All mapped reads	
		RPKM	Total reads	RPKM	Total reads
Tb927.8.3620	folate transporter, expression site-associated gene 10 (ESAG10) protein, putative	387390	310399	159467	1000562
Tb927.8.3650	folate transporter, expression site-associated gene 10 (ESAG10) protein, putative	190118	146668	71770	450315
Tb927.8.3630	folate transporter, expression site-associated gene 10 (ESAG10) protein, putative	106956	82928	83978	526914
Tb11.v5.0766	folate transporter, putative	85370	41033	91104	350379
Tb927.11.14360	mitochondrial carrier protein (MCP2)	16568	7047	15474	52150
Tb927.11.14350	mitochondrial carrier protein (MCP22)	5637	2323	2664	9163
Tb927.8.3640	JAB1/Mov34/MPN/PAD-1 ubiquitin protease, putative	5491	2571	3133	11459
Tb927.8.1040	protein phosphatase inhibitor, putative	2096	361	934	1343
Tb927.9.5960	succinate dehydrogenase, putative	1671	375	724	1356
Tb927.11.14370	hypothetical protein, conserved	1388	1694	438	4072
Tb927.8.5840	hypothetical protein, conserved	1182	278	431	846

Primary 'hit' >1 fragment per gene
Secondary 'hit' ≤ 1 fragment per gene
Adjacent to 'hit'

Table 4.2: Extended hit list for RTX RIT-seq analysis

(>1000 RPKM 'barcoded reads' and >200 RPKM 'all mapped reads' cut-offs)

Gene ID	Gene description	Barcoded reads only		All mapped reads	
		RPKM	Total reads	RPKM	Total reads
Tb927.8.3620	folate transporter, expression site-associated gene 10 (ESAG10) protein, putative	425569	352755	176660	1245838
Tb927.8.3650	folate transporter, expression site-associated gene 10 (ESAG10) protein, putative	139362	113541	58099	409726
Tb927.8.3630	folate transporter, expression site-associated gene 10 (ESAG10) protein, putative	125517	99759	91451	644928
Tb11.v5.0766	folate transporter, putative	78888	39418	87613	378723
Tb927.7.1600	C-1-tetrahydrofolate synthase, cytoplasmic, putative	57287	20709	21075	70202
Tb927.7.1610	6-phosphofructo-2-kinase/fructose-2,6-biphosphatase, putative	12920	11529	4807	34755
Tb927.11.14350	mitochondrial carrier protein (MCP22)	6967	2917	3117	12050
Tb927.11.14360	mitochondrial carrier protein (MCP2)	3962	1686	8384	31759
Tb927.11.12460	hypothetical protein, conserved	3598	4672	931	10650
Tb927.10.7520	folylpolyglutamate synthase, putative (FPGS)	1242	855	816	4556

Primary 'hit' >1 fragment per gene
Secondary 'hit' ≤ 1 fragment per gene
Adjacent to 'hit'

(Tb927.10.1740 and Tb927.10.1750, personal communication David Horn). Moreover, a fragment mapping to Tb927.10.2430 (putative- receptor-type adenylate cyclase GRESAG 4) was identified but not validated by high-throughput RIT-seq (see below).

4.1.3 High-throughput RIT-seq

High-throughput RIT-seq, with sequencing generated by the Beijing Genomics Institute, confirmed and extended the preliminary analysis above. Genome coverage was adequate for both drug screens. For the MTX screen, 2.4 million paired reads were generated of which 70% mapped to the reference genome (Table 4.1) and for the RTX screen, 2.6 million paired read were generated of which 71% mapped to the reference genome (Table 4.2). Of note, further analysis of the MTX and RTX screens against a reference genome including the *T. brucei* 427 telomeric and metacyclic VSG expression site regions mapped 95% of the reads for both drugs. The vast majority of the other reads map to expression site associated genes (*ESAG10*) genes in the VSG expression sites, which share 90-94% gene identity to the chromosome 8 tandem folate transport genes *FT1-3*.

Hits implicated from high-throughput RIT-seq are depicted in Figure 4.3. The putative folate transporters, *FT1-3*, and a redundant orphan folate transporter gene, Tb11.v5.0766, are the predominant 'hits' in both the MTX and RTX screens accounting for 91% and 89% of all mapped reads respectively (Fig 4.3 B and D Table 4.1, Table 4.2). Other 'hits' include a mitochondrial carrier protein (MCP2, Tb927.11.14360), found in both MTX and RTX screens (Fig 4.3 B and D) and C-1-THF synthase (Tb927.7.1600) specific to the RTX screen (Fig 1 D). Another

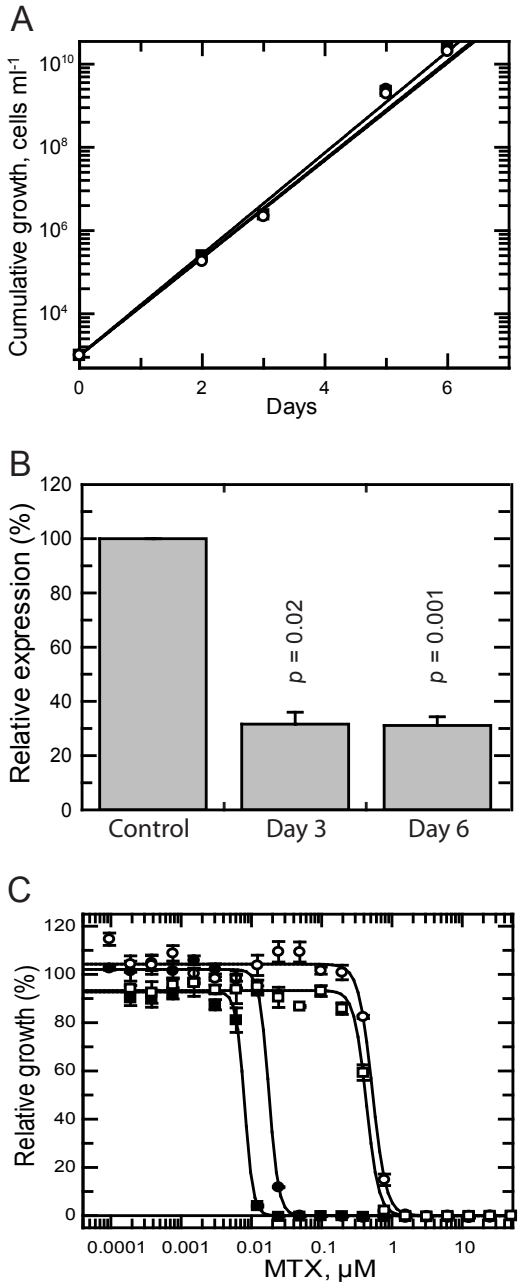

Figure 4.4 Evidence of RNAi knockdown of *FT1-3*

(A) Cumulative growth of WT cells and *FT1-3* RNAi line + or - tet induction. Doubling times were determined by linear regression and analysed using GraFit. Closed squares, WT 2T1 cells; closed circles, RNAi knockdown - tet; open circles, RNAi knockdown + tet.

(B) qRT-PCR shows down regulation of FT RNA in RNAi line. Data is mean $\pm$ SEM of four experimental replicates. *p* values shown.

(C) Representative drug sensitivity (EC_{50}) plots for MTX. Closed circles, day 3 RNAi knockdown- tet; open circles, day 3 RNAi knockdown + tet; closed squares, day 6 RNAi knockdown - tet and open squares; day 6 RNAi knockdown + tet.

Table 4.3 Potency shifts of DHFR-TS Inhibitors in FT RNAi knockdown.

EC_{50} values (nM) of antifolates against un-induced and induced knockdown cells Results are weighted means ± associated error of 3 independent experiments.

Drug	3 days			6 days		
	- Tet	+ Tet	Fold Shift	- Tet	+ Tet	Fold Shift
Methotrexate	14.5 ± 0.4	444 ± 17	30.6	8.73 ± 0.39	321 ± 13	36.8
Raltitrexed	11.2 ± 0.3	368 ± 14	32.9	5.83 ± 0.20	227 ± 10	38.9
Pyrimethamine	2,500 ± 100	200 ± 11	0.08	2,040 ± 165	142 ± 10	0.07
Nolatrexed	36,200 ± 1,900	16,700 ± 1,000	0.46	39,900 ± 2,500	15,600 ± 900	0.39
Melarsoprol	1.73 ± 0.09	1.70 ± 0.08	0.98	1.26 ± 0.60	1.29 ± 0.59	1.02

noteworthy ‘hit’ in the RTX screen, supported by only a single RIT-seq fragment was FPGS (Tb927.10.7520) (Fig 4.3 D, Table 4.2) implicated in folate polyglutamylation. It should be noted that no hits appeared in either MTX or RTX screens for the putative pteridine transporter genes (*BT1-4*), members of the FBT family, suggesting that they are not implicated in antifolate drug transport.

4.2 RNAi knockdown of putative folate transporters (*FT1-3*)

Findings from the RIT-seq analysis strongly implicated *FT1-3* genes in antifolate drug resistance. To validate *FT1-3*, an RNAi knockdown transgenic mutant was generated and phenotypic studies were performed.

4.2.1 Evidence of RNAi knockdown of *FT1-3*

Figure 4.4 A demonstrates that with knock-down of *FT1-3*, by induction with tetracycline (tet), there was no substantial change in cell growth compared to both WT and un-induced cells (Figure 4.4 A). Doubling times were determined to be 6.2 h, 6.1 h and 5.9 h for WT, un-induced and induced cells respectively. qRT-PCR was used to determine a quantitative measure of knockdown. RNA transcription analysis of RNAi mutant confirmed a down-regulation of mRNA levels to 32 % relative to un-induced cells after 3 days of tet induction (p = 0.02) and to 31 % relative to un-induced cells after 6 days induction (p = 0.001) (Figure 4.4 B). MTX potency was used to determine phenotypic changes associated with *FT1-3* RNAi knockdown. There was a substantial reduction in MTX potency after induction for 3 days (31-fold) and 6 days (37-fold) induction (Figure 4.4 C and EC_{50} values in Table 4.3).

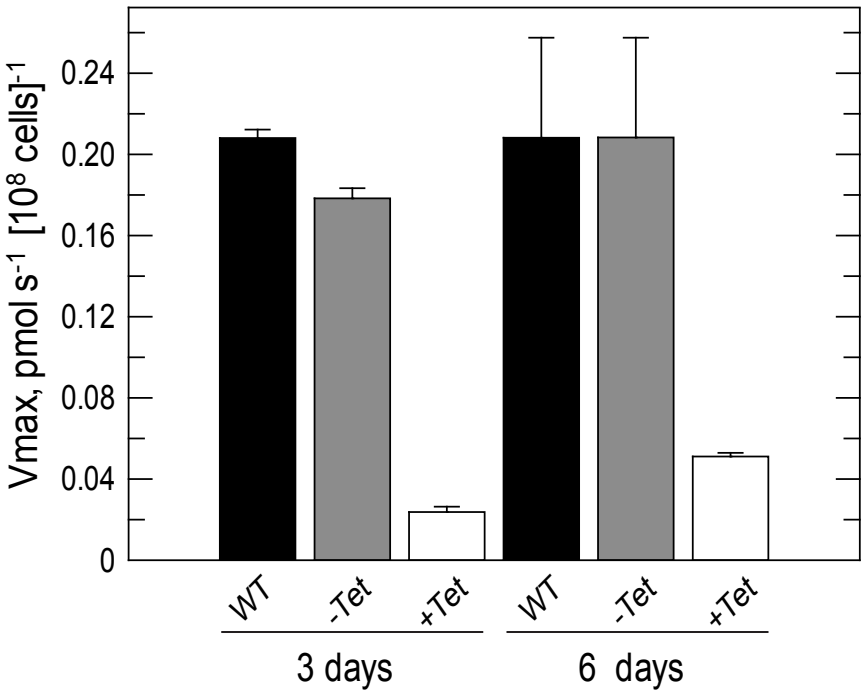

Figure 4.5 V_{max} of folate transport in FT RNAi line

Folate transport kinetics measured at day 3 and day 6 in WT cells and FT RNAi strains + or - tet, at day 3 and day 6

4.2.2 Potency shifts of DHFR-TS inhibitors with RNAi knockdown of *FT1-3*

As *FT1-3* knockdown in *T. brucei* parasites was shown to affect sensitivity to MTX, other antifolates were tested to determine whether there is a similar effect. After both 3 days and 6 days induction EC_{50} studies demonstrated a > 30 fold reduction in parasite sensitivity to RTX (Table 4.3). This is indicative of cross resistance between classical antifolates MTX and RTX. However, parasites were hypertensive to the non-classical DHFR inhibitor PYR with potency increasing by 12-fold and 14-fold after 3 days and 6 days induction respectively. Similarly, a hypersensitivity to the non-classical TS inhibitor, NTX, was evident; a 2-fold reduction in EC_{50} after both 3 days and 6 days induction. This is indicative of increased sensitivity of *T. brucei* to the non-classical antifolates with knockdown of *FT1-3*. No marked change in sensitivity for the control, melarsoprol, was found after 3 or 6 days induction.

4.2.3 Transport of folate with RNAi knockdown of *FT1-3*

As shown earlier in this thesis, folate and MTX are competitive substrates for transport into cells (section 3.7.5) and FTs were indicated from an RIT-seq screen (section 4.1) to be involved in MTX-resistance mechanisms. It seemed prudent therefore to determine folate transport in the RNAi knockdown cell line. Indeed, V_{max} of folate uptake was substantially reduced with RNAi knockdown (Figure 4.5). After 3 days, the V_{max} of induced cells was reduced by 10-fold and 9-fold compared to WT and un-induced cells respectively. Likewise, after 6 days, the V_{max} of induced cells was reduced by 4-fold compared to both WT and un-induced cells. No changes in folate $K_{m\ app}$ was detected between induced, un-induced and WT after 3 days (2.56 $\pm$ 0.20 μM, 3.43 $\pm$ 0.24 μM and 3.47 $\pm$ 0.77 μM, respectively) or 6 days (2.77 $\pm$ 1.68 μM, 2.68 $\pm$ 1.68 μM and 2.67 $\pm$ 0.26 μM, respectively).

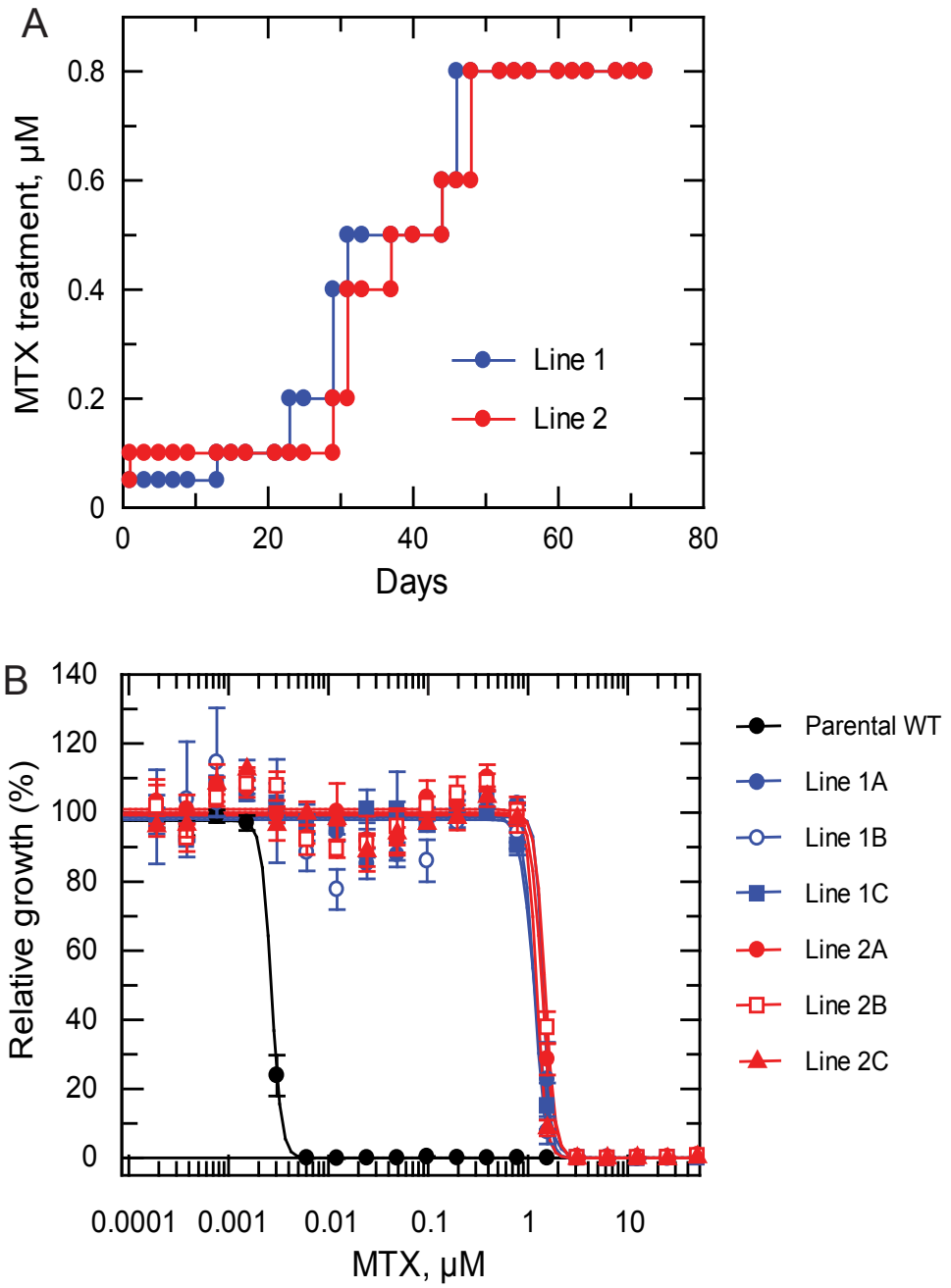

Figure 4.6 Generation of MTX-resistant trypanosomes and EC_{50} confirmation

(A) Stepwise generation of resistance to MTX (**B)** Representative drug sensitivity (EC_{50}) plots. The parental WT line had an EC_{50} value of 3.90 $\pm$ 0.10 nM and the resistant clones: line 1A, 1380 $\pm$ 80 nM; line 1B, 1170 $\pm$ 180 nM; line 1C, 1280 $\pm$ 50 nM; line 2A, 1350 $\pm$ 90 nM; line 2B 1490 $\pm$ 70 nM; line 2C, 1320 $\pm$ 90 nM. Data are the weighted mean of two independent experiments.

4.3 MTX Resistant Cell Line

4.3.1 Generation of MTX resistance

To investigate the ease in which resistance to MTX could occur in *vitro*, two independent cell lines of BSF *T. brucei* were cultured in the continuous presence of MTX in TBM until they were able to sustain normal growth in 800 nM MTX. This process took 72 days to achieve (Figure 4.6 A). Three clones were selected from each independent resistant line (6 in total), and MTX sensitivity was determined. A comparable EC_{50} was found in all six clones (1.17 to 1.49 μM) and the resultant EC_{50} shifts were >300-fold compared to the sensitivity of the parental cell line (WT EC_{50} = 3.9 nM) (Figure 4.6 B). From each independent cell line the clone displaying the greatest resistance to MTX was selected for further studies. For cell line 1 this was clone A with EC_{50} = 1.38 μM (now named MTX R1) and for cell line 2, clone B with EC_{50} = 1.39 μM (named MTX R2). Of note, cumulative growth for MTX R1 and MTX R2 was similar to the parental cell line (doubling times of 6.2 h for WT, 6.2 h for MTX R1 and 6.4 h for MTX R2). Moreover, after 4 months of continual passage in the absence of MTX, resistance in MTX R1 and MTX R2 was retained (EC_{50} 1.0 μM and 1.1 μM respectively).

4.3.2 Potency shifts of DHFR-TS inhibitors in MTX-resistant trypanosomes

MTX R1 and MTX R2 demonstrated cross-resistance to the classical antifolates as depicted in Table 4.4. For the classical TS inhibitors RTX and PMX there was a substantial reduction in sensitivity in both cell lines compared to the parental line (~ 200-fold and ~ 50-fold respectively). The opposite effect was seen with non-classical antifolates, where MTX R1 and MTX R2 parasites became more sensitive to these

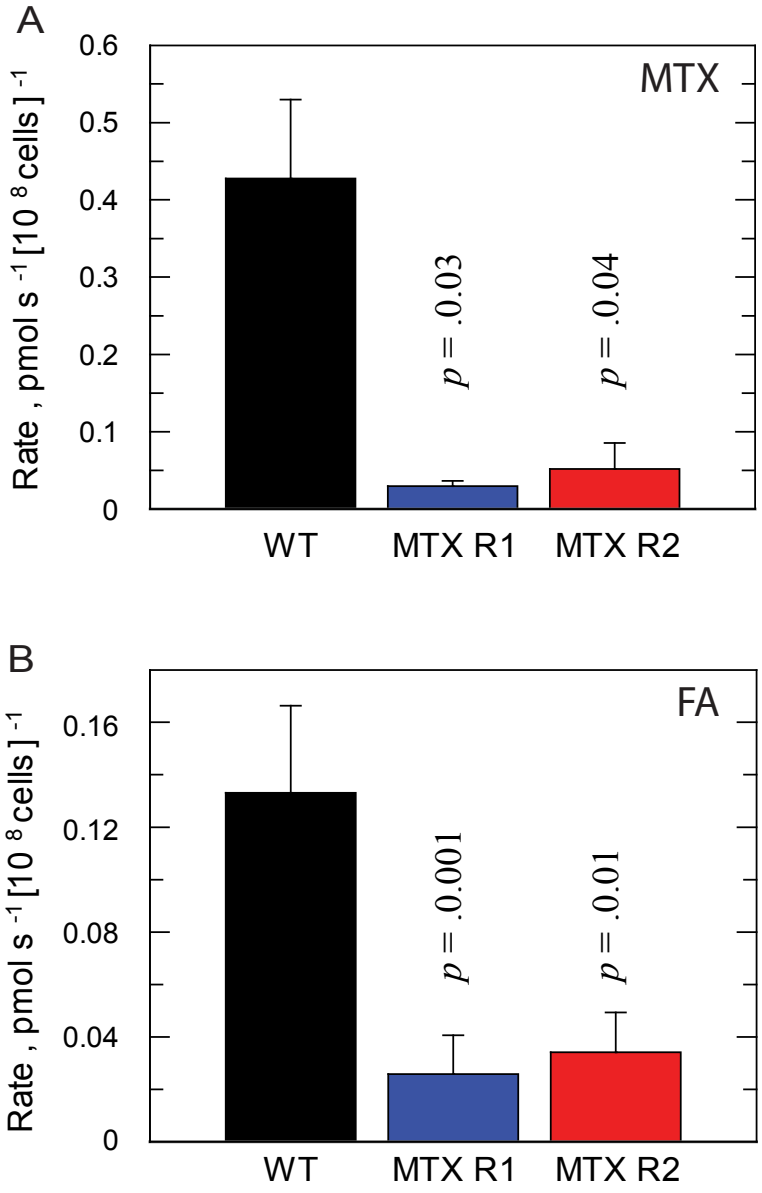

Figure 4.7 MTX and folate tranport studies in MTX-resistant trypanosomes

Uptake of [^{3}H]-folate and [^{3}H]-MTX was determined at a set concentraion of unlabelled subtrate (5 μM folate and 20 μM MTX). Linear rate of uptake was determined in triplicate and the weighted mean of the experimental triplicate was calculated. *p* values were calculated using a student's unpaired t-test. **(A) (B)** Data is meighted means + SEM. **(A)** MTX uptake, measures at 20 μM MTX. **(B)** Folate uptake, measures at 5 μM folate.

compounds. Sensitivity to the non-classical DHFR inhibitors, PYR, TMP and MTP, increased to a similar extent (between 6 and 13-fold) in MTX R1 and MTX R2 cells, apart from TMX where sensitivity increased by ~40-fold. There was a slight increase in sensitivity to the non-classical TS inhibitor NTX in MTXR1 and MTXR2 (~1.4-fold). No change in melarsoprol sensitivity was detected compared to the parental cell line for either clone.

4.3.3 Transport of MTX and folate in MTX-resistant trypanosomes

As FTs had been established to be involved in MTX drug resistance mechanisms by RIT-Seq, transport of the FTs substrates, MTX and folate, was determined in MTX resistant trypanosomes. For this, transport was determined at fixed concentration of unlabelled substrate (20 μM MTX and 5 μM folate) instead of at varying concentration (Figure 4.7). For MTX and folate, the rate of transport was substantially reduced in both clones compared to the parental WT cells. For MTX uptake there was a 15-fold reduction in MTX R1 (p = 0.03) and an 8-fold reduction in MTX R2 (p = 0.04). For folate uptake there was a 5 fold reduction in MTX R1 (p = 0.001) and a 4-fold reduction in MTX R2 (p = 0.01). This data suggests that the rate of folate uptake may be affected less than MTX uptake in MTX-resistant trypanosomes.

4.3.4 Sequencing of *FT1-3* in MTX-resistant trypanosomes

Results illustrate that there is a substantial transport deficit for folate and MTX in both resistant cell lines, thus sequencing of FT genes was undertaken to establish if any mutations had arisen that may account for these phenotypes. Putative *FT* genes (*FT1-3*) are each 1899 bp in length and share 96% nucleotide identity. They are

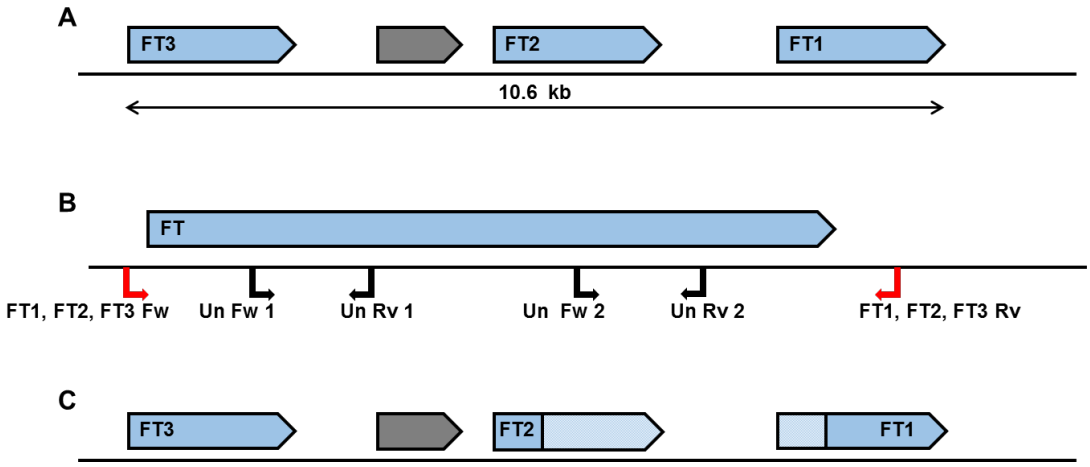

Figure 4.8 Schematic of *FT1-3* sequencing

(A) Schematic of 927 FT1-3: Tb927.8.3620, Tb927.8.3630, Tb927.8.3650 (blue bars) in tandem interrupted by Tb927.8.3640 (grey bar)

(B) Primer design for FTs. universal primers in intragenic regions common to the FTs depicted in black, unique primers specific for the upstream and downstream regions near the ORF of each individual gene depicted in red.

(C) Sequence coverage of FT1-3 in MTX-resistant trypanosomes. Gene coverage represented by blue bars and areas not covered by light blue bars.

Figure 4.9 PCR products of *FT1* and *FT2* in MTX-resistant trypanosomes

PCR products separated on an agarose gel.

Lanes 1-3: PCR reactions using primers FT1 Fw and Un Rv 1. ~900 bp band in lane 1 (WT); not evident in lane 2 (MTXR1) and lane 3 (MTXR2).

Lanes: 4-6 PCR reactions using primers FT2 Rv and Un Fw 2 ~1900 bp band in lane 4 (WT); not evident in lane 5 (MTXR1) and lane 6 (MTXR2)

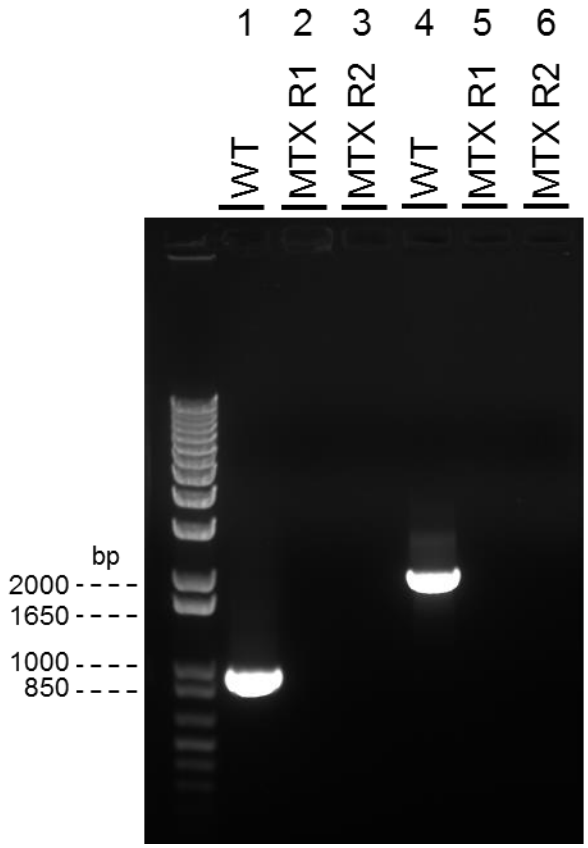

Table 4.5 Amino acid changes in FT1-3 in MTX-resistant cell lines

Position		MTX R1 and R2	WT	927 Reference
FT1	216	valine	leucine	leucine
	218	threonine	valine	valine
FT3	216	leucine	valine	leucine
	218	valine	threonine	valine
	278	glutamate	lysine	lysine
	282	arginine	histidine	histidine
	523	tyrosine	serine	serine
	526	alanine	methionine	methionine
	530	valine	leucine	leucine
	536	histidine	asparagine	asparagine

arranged in tandem on chromosome 8 and interrupted by an unrelated gene (Tb927.8.3640, putative JAB1/Mov34/MPN/PAD-1 ubiquitin protease) (Figure 4.8 A). In order to individually sequence these highly homologous genes, unique primers were designed that were specific for the upstream and downstream regions near the ORF of each individual gene. To attain full sequencing coverage of the genes, primers were also designed in the intragenic regions common to the *FT*s (Figure 4.8 B illustrates primer coverage and all primer sequences are given in Table 2.2).

In the WT parental line sequence coverage was attained for all three *FT* genes (1899 bp of each gene). However, full coverage was not attained for the MTX resistant clones with segments missing from *FT1* and *FT2*. Specifically, coverage was not attained for the first 548 bp of *FT1* for both MTX-resistant lines (coverage 549-1899 bp), for the last 1354 bp of *FT2* in MTX R1 (coverage 1-545 bp) and for the last 1345 bp of FT2 in MTX R2 (coverage 1-546 bp) (Figure 4.8 C). This is due failure to obtain PCR products for these regions using the unique primers (see Figure 4.8 C, Figure 4.9) despite attempts to optimise PCR conditions. Indeed, no PCR product was generated for PCR reactions using the *FT1* Fw primer for MTX R1 and MTX R2 and reactions using the *FT2* Rev primer for MTX R1 and MTX R2 (Figure 4.9 as an example). The DNA and protein sequences of MTXR1, MTXR2 and WT were aligned with *T. brucei* 927 reference genome sequences using Clustal Omega and are shown in the supplementary materials (Figures S1 and S2). Two predicted amino acid changes were seen encoded by *FT1* for both MTX-resistant lines compared to WT and the 927 reference genome (V216L, T218V). For *FT3*, eight amino acid changes were predicted in both MTX-resistant lines (L216V, V218T, E278K, R282H, Y523S, A526M, V530L, H536N) (Table 4.5). Of note, for the first two mutations in *FT3* (L216V, V218T) although there are mutations in the MTX-

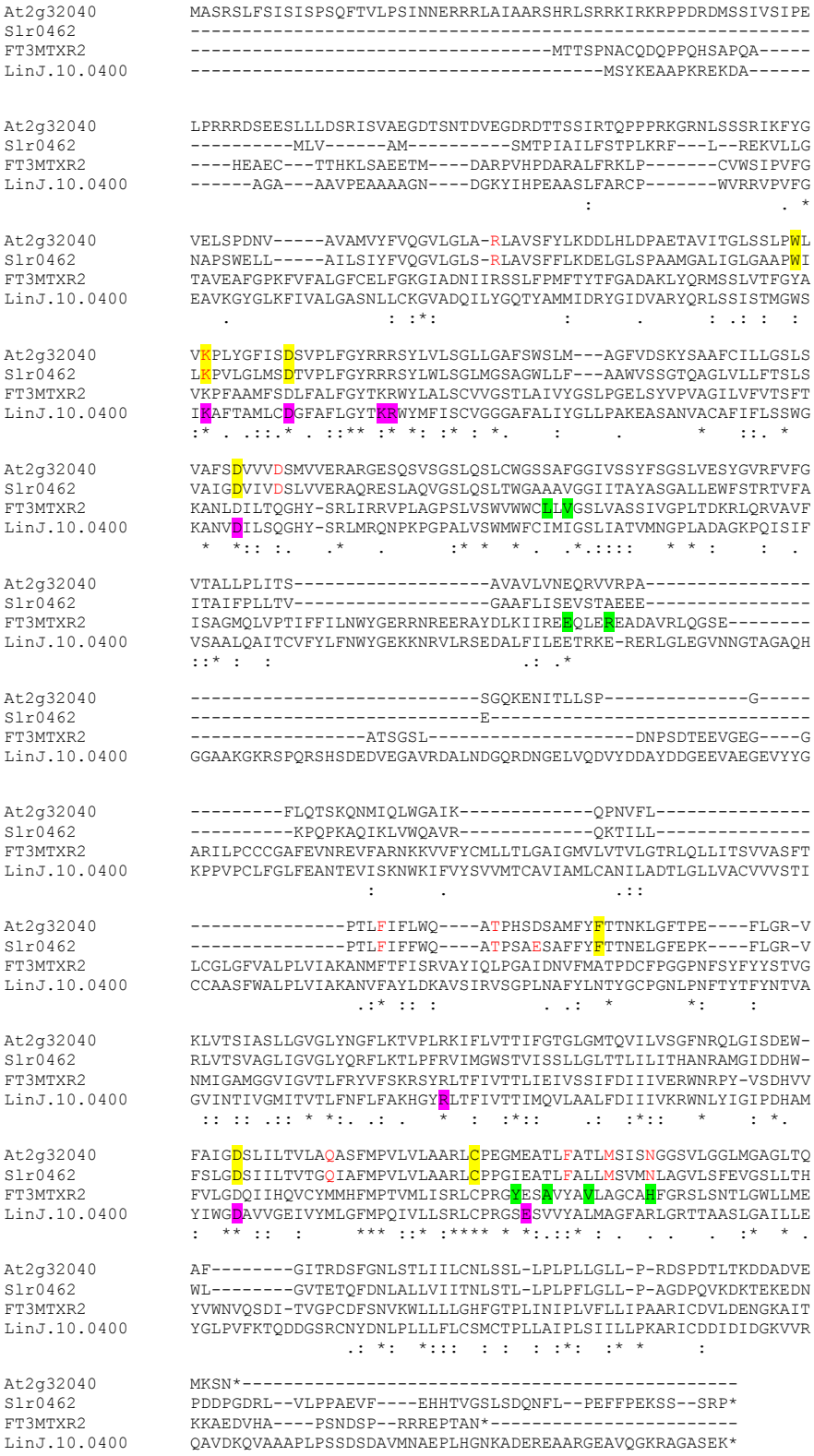

Figure 4.10 Protein sequence alignment of FT3 MTX R2 compared to FBTs in *Leishmania*, cyanobacteria and plant. Highlighted in yellow: residues shown to be critical to folate transport by mutagenesis studies in *Synechocystis*, highlighted in purple: residues shown to be critical to folate transport by mutagenesis studies in *Leishmania*, red font: residues found to be critical to folate transport by bioinformatics modelling in *Synechocystis*, highlighted in green: mutations present in *T. brucei* FT3 in MTX R2.

resistant cell lines compared to WT (leucine to valine, valine to threonine respectively) this is not the case when compared to the 927 reference genome (leucine to leucine and valine to valine respectively). This is an anomaly as one may expect WT and 927 reference strain to have the same amino acids and changes evident in MTX R1 and MTX R2, as is the case for *FT1*. With this anomaly in mind, the PCR reaction was repeated and also fresh genomic DNA from the MTX-resistant lines was isolated and the experiment repeated. The same result was returned. The cause of this discrepancy with FT1 is not known; it could have been due to a mix up of the primers, cell lines or genomic DNA. Further work is required to resolve this issue. In contrast, there was no ambiguity in the sequence data for FT3. Out of the eight mutations in *FT3*, three of these represent a change in either polarity or size. For E278K the side group changes to being negatively charged (E) from positively charged (K), for R282H an increase in size from (H) to (R) is evident, and Y523S changes to an aromatic side group (Y) from a polar side group (S).

4.3.5 Structure-function analysis of *FT1-3* mutations

To identify if mutations found in MTX resistant-cell lines could be critical to folate transport activity, the protein sequence of MTX R2 for *T. brucei* FT3 was aligned to protein sequences of other members of the FBT family in which critical residues responsible for folate transport have been identified (Figure 4.10). The novel FBT superfamily was identified first in *Leishmania* (Richard *et al*., 2002) and is present in other kinetoplastids (Ouameur *et al*., 2008) (including *T. brucei*), malaria (Wang *et al*., 2007), *Toxoplasma* (Massimine *et al*., 2005), plants and in cyanobacteria (Klaus *et al*., 2005) The *Synechocystis* slr0642 gene and its closest *Arabidopsis* homolog, At2g32040 gene, have been expressed in *E.coli* and shown to

mediate uptake of folate and MTX (Klaus *et al*., 2005). Studies of FBT mediated folate transport in *Synechocystis* and *Leishmnia* have identified key transporter residues implicated in folate transport (Dridi *et al*., 2010b; Eudes *et al*., 2010). A protein sequence alignment of *Synechocystis* slr0642, *Arabidopsis* At2g32040 and *L. infantum* LinJ.10.0400 (FT1 in *Leishmania*) with MTX R2 for *T. brucei* FT3 is shown in Figure 4.10. In this alignment, the group of four mutations found in MTX R2 (Y523S, A526M, V530L, H536N) are in very close proximity to critical residues shown to mediate folate uptake in FBT genes. Nearby cysteine and glutamic acid residues, conserved in all four FBT genes (position 519 and 524 in *T. brucei* FT3 respectively) were shown to be critical to folate transport in *Synechocystis* and *Leishmnia* respectively (Dridi *et al*., 2010b; Eudes *et al*., 2010). Also, three residues conserved in *Synechocystis* slr0642 and *Arabidopsis* At2g32040 that were implicated in folate transport by bioinformatics modelling (using the PSIPRED bioinformatics tool) (Eudes *et al*., 2010) aligned closely to this group of four mutations found in MTX R2 (phenylalanine, methionine and asparagine aligning to positions 528, 532 and 536 in *T. brucei* FT3).

A topological model of FT1-3 was rendered in order to visualise and identify the location of these mutations in the transmembrane transporters. FT1-3 are predicted by the TMHMM server v 2.0 348 to contain 12 transmembrane helices (http://www.cbs.dtu.dk/services/TMHMM/) (Krogh *et al*., 2001). FT1-3 are family members of FBT which belongs to the major facilitator superfamily. Transporters in this family typically consist of 12 transmembrane helices with both N and C terminus located intracellularly (Paulsen, 2003), so the model predicted by TMHMM is consistent with this. Topological models of FT1-3 were visualised using the web-based Protter software. Using TriTryp DB (http://tritrypdb.org) and the post

Figure 4.11 Topological models of FT1-FT3. **A)** Predicted phosphorylation sites in FT3 for parental WT line. **(B, C, D)** PCR coverage and mutations in FT1-3 for MTX-resistant cell lines. Models made using the web-based Protter software.

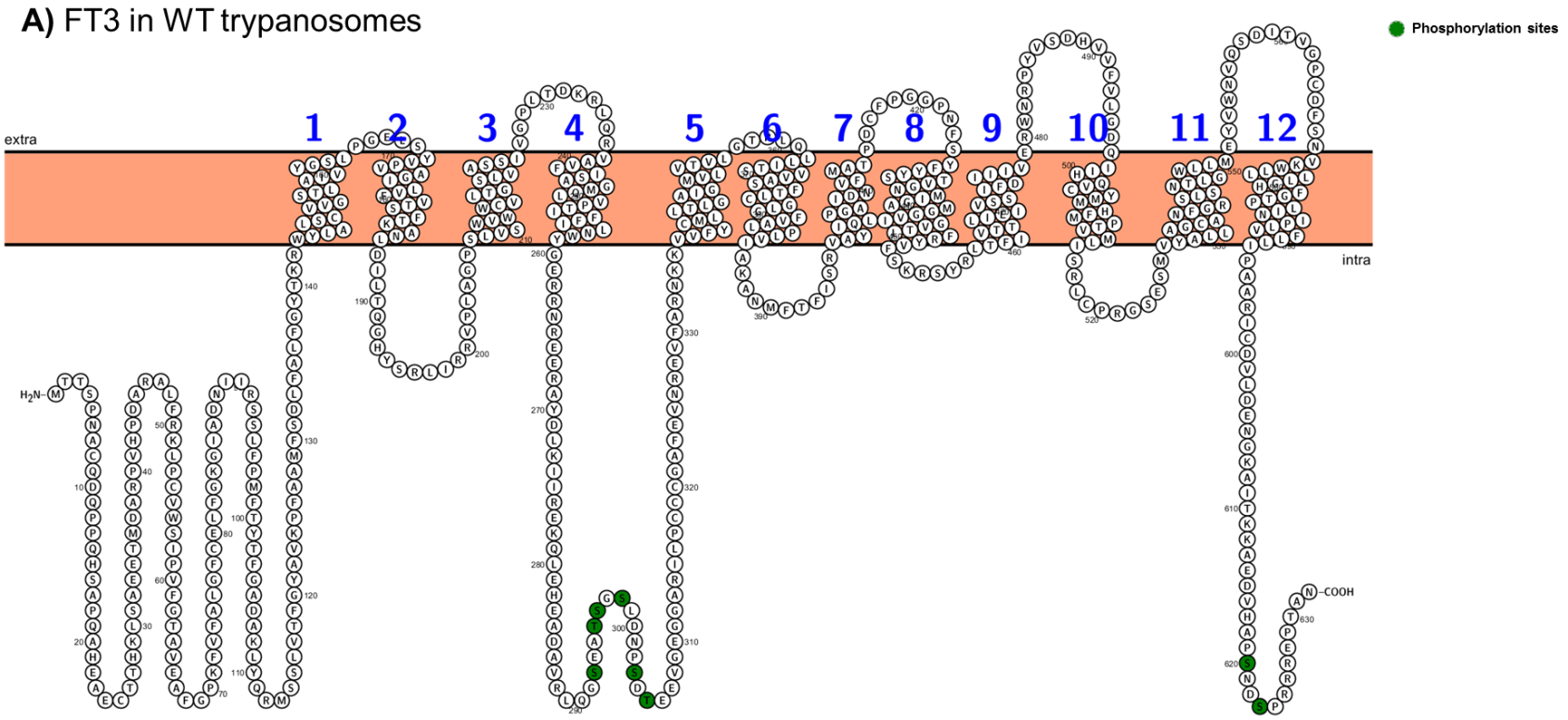

B) FT1 in MTX-resistant trypanosomes

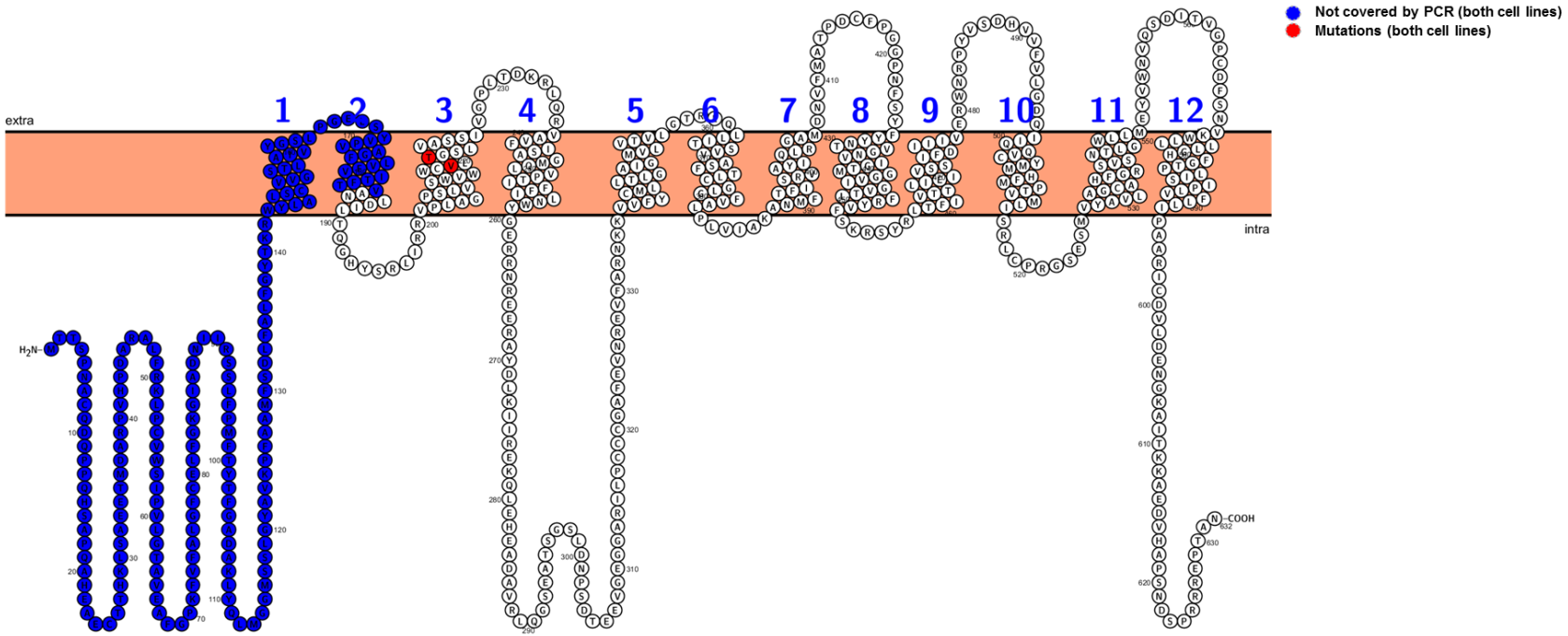

C) FT2 in MTX-resistant trypanosomes

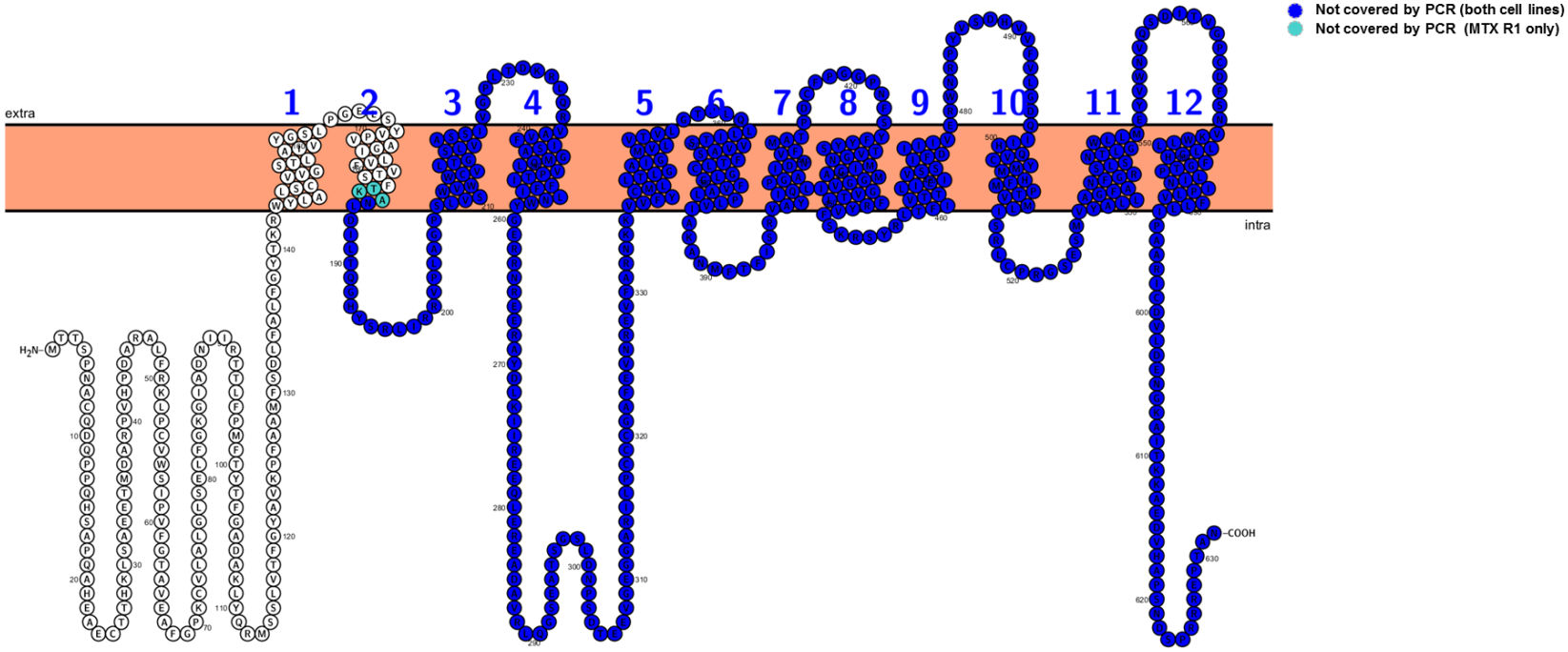

D) FT3 in MTX-resistant trypanosomes

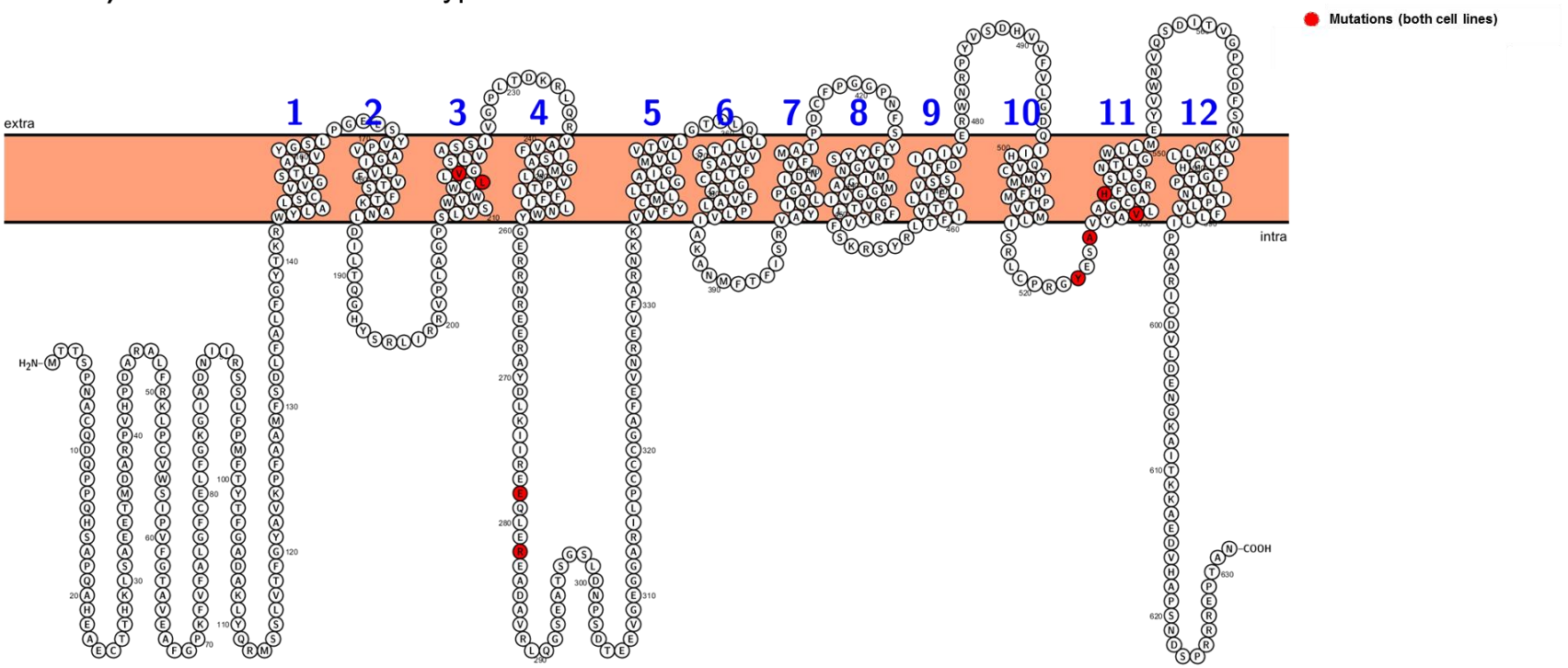

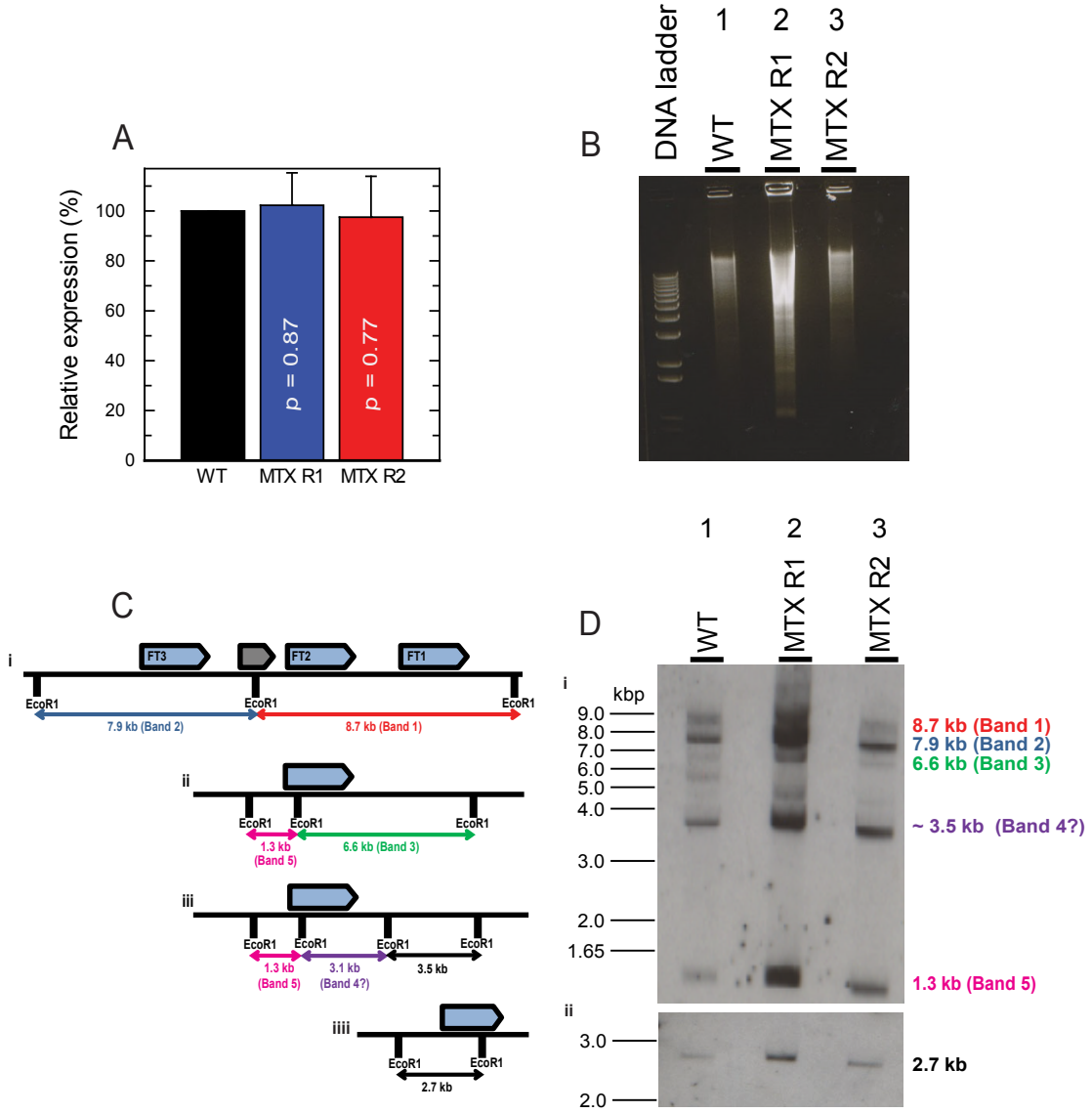

Figure 4.12 RNA and DNA detection of *FT1-3* in MTX-resistant trypanosomes

(A) qRT-PCR shows no change in FT RNA in WT and MTX-resistant cell lines: normalised against endogenous control gene TERT. Data are the mean ± SEM of three experimental replicates. *p* values shown.

(B) Agarose gel showing overloading of lane 2 (MTX R1).

(C) Schematic of EcoRI sites and expected Southern blot bands associated with 427 *FT1-3*, *ESAG10* genes and trypanothione reductase. i) 427 in reverse compliment FT1-3; Tb427.8.3620, Tb427.8.3630, Tb427.8.3650 (blue bars) in tandem interrupted by Tb427.8.3640 (grey bar) ii) *ESAG10* genes; Tb427.BES15.1, Tb427.BES51.1, Tb427.BES56.1, Tb427.BES59.1 and Tb427.BES126.1 (represented by blue bar) that share common EcoRI sites. iii) *ESAG10* genes; Tb427.BES134.1 and Tb427.BES153.1 (represented by blue bar) that share common EcoRI sites iiii) Tb427.10.10390 (blue bar)

(D) Sothern blot, (i) *FT1-3* and *ESAG10* genes (ii) trypanothione reductase

translation model from Urbaniak *et al* (Urbaniak *et al*., 2013), eight serine/threonine residues conserved in *FT1-3* are predicted phosphorylation sites. Applying WT FT3 as an example, Figure 4.11 A demonstrates the cytoplasmic location of these sites, further giving evidence of this topology model. Figure 4.11 B-D demonstrates the amino acid mutations found in FTs and the coverage of each transporter attained by PCR. Of note the four mutations in FT3 found in close proximity (Y523S, A526M, V530L, H536N) are clustered around the cytoplasmic loop close to the 11 transmembrane α helix and in the α helix itself.

4.3.6 qRT-PCR and Southern blot in MTX-resistant trypanosomes

To identify if there was any change in transcription and/or copy number of *FTs* in the MTX-resistant cell lines qRT-PCR and Southern blot experiments were performed respectively. qRT-PCR showed no change in transcription of *FT1-3* in MTX R1 and MTX R2 compared to the parental WT cell lines (Figure 4.12.A). To determine if copy number is changed a Southern blot was performed. After digestion with EcoRI, DNA from WT, MTX R1 and MTX R2 were separated on an agarose gel. There is DNA overloading for MTX R1 (Figure 4.12 B). The MTX-resistant cell line was grown in *T. brucei* S427 and there are 7 *ESAG10* genes in this strain that share up to 90-94% gene identify with 927 *FT1-3* and 91-95% gene identify with 427 *FT1-3*. Although these genes may not be expressed (Hertz-Fowler *et al*., 2008), they need to be considered when analysing the Southern blot. Figure 4.12.C illustrates the cutting sites of EcoRI in 427 *FT1-3* and the 7 *ESAG10* genes. Five *ESAG10* genes share common EcoRI cutting sites (1.27 kb and 6.6 kb either side) and the two others also share common cutting sites (1.27 kb and 3.1 kb either side). The Southern blot identified bands associated with *FT1-3* and the *ESAG10* genes and

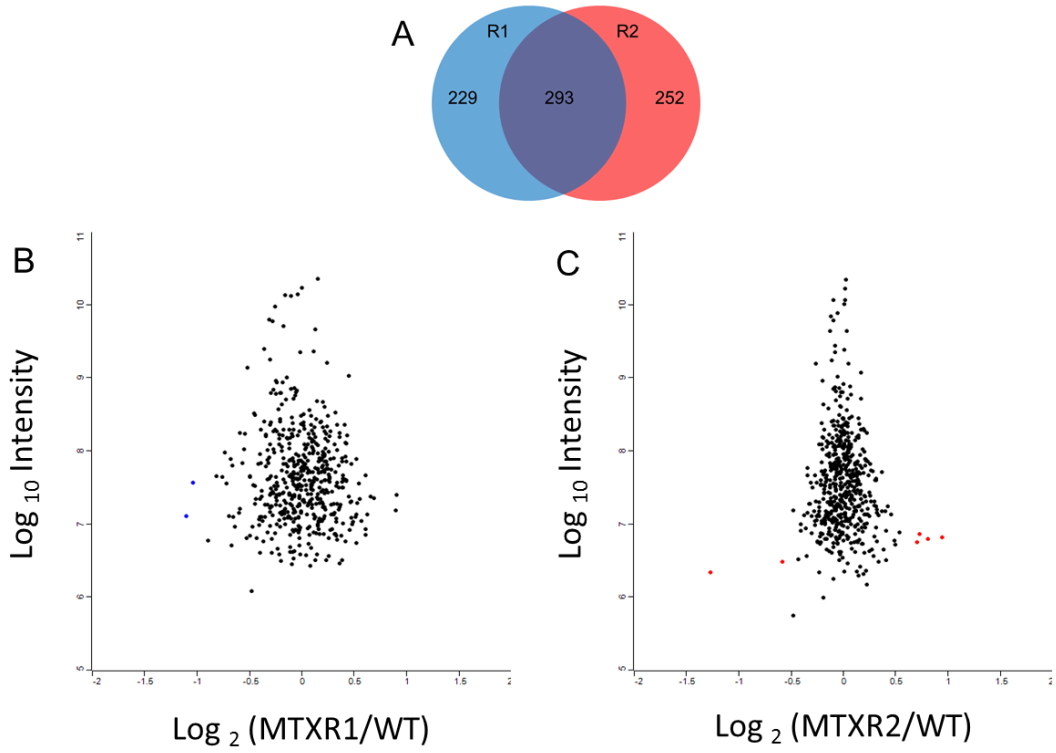

Figure 4.13 Proteomic analysis of MTX-resistant trypanosomes

(A) Venn diagram showing proteins with a quantifiable expression change between resistant lines and WT in order to calculate an H/L SILAC ratio. Blue circle, MTX R1; red circle, MTX R2.

(B,C) Plot of the proteomics data from **(B)** MTX R1 and **(C)** MTX R2. Protein is represented by a point plotted as the Log_2 of the H/L SILAC ratio against the Log_{10} value of the intensities of peptides that belonging to each protein. Proteins plotted in blue **(B)** and red **(C)** were found to have significant changes in H/L SILAC ratio.

there is no substantial change in the banding patterns between WT and MTX-resistant trypanosomes (Figure 4.12.D). There is a stronger signal with MTX R1 which can be attributed to gel overloading (Fig 4.12.B). The *T. brucei* 427 genome is only partially assembled and this may account for band 3 not completely corresponding with the expected band size of 3.1 kb. Trypanothione reductase (Tb427.10.10390) was used as a control with the EcoRI sites illustrated and the expected banding pattern found on Southern blot (Figure 4.12 C,D). Again a stronger signal was evident for MTX R1 consistent with unequal loading of the gel.

4.3.7 Proteomic analysis of MTX-resistant trypanosomes

Examining folate/MTX transport in the MTX-resistant parasites gave a targeted approach to identify resistance mechanisms. A more global perspective using a SILAC proteomic approach may facilitate the identification of other candidates implicated in MTX resistance. Such SILAC approaches have been successfully utilised in identifying the actions of anti-kinetoplastid compounds including oxaboroles in *T. brucei* (Jones *et al*., 2015) and nitro-drugs in *Leishmania* (Fairlamb group, unpublished).

MTX-resistant cell lines and the parental WT line were SILAC labelled, mixed in a 1:1 ratio and analysed by LC-MS/MS. For MTX R1/WT 721 proteins were identified and of these 522 had a quantifiable expression change between MTX R1 and WT in order to calculate a H/L SILAC ratio. For MTX R2/WT 702 proteins were identified with 545 quantifiable for a SILAC ratio. Between both cell lines only 744 proteins could be quantified for SILAC ratios, with 293 proteins present in both drug-resistant lines (Figure 4.13.A).

Table 4.6 Proteins found to be significantly over- or under- expressed in MTX-resistant trypanosomes

Blue columns, MTX R1; Red Columns, MTX R2

Gene ID	Product	Log_2 Res/WT
Tb927.8.7950	flagellar member 4 (FLAM4)	-1.10
Tb927.10.2560	mitochondrial malate dehydrogenase (mMDH)	-1.04
Tb927.6.2420	p22 protein precursor	-1.27
Tb927.1.720	phosphoglycerate kinase (PGKA)	-0.59
Tb927.1.3060	unspecified product	0.95
Tb927.8.6240	STOP axonemal protein	0.81
Tb927.3.5020	flagellar member 6 (FLAM6)	0.73
Tb927.5.1400	hypothetical protein	0.70

Proteins that are more abundant in the resistant populations compared to WT will have a SILAC ratio greater than 1 (or $\log_2 > 0$) whereas less abundant proteins will have a SILAC ratio less than 1 (or $\log_2 < 0$). Proteins that are not changed will have a ratio = 1 (or $\log_2 = 0$). Only one protein related to folate metabolism was identified in this SILAC experiment, namely DHFR-TS. No change in DHFR-TS was seen in the resistant cell lines compared to WT ($\log_2 = 0.07$ for MTXR1 and $\log_2 = -0.09$ for MTX R2). Moreover FTs were not identified in these experiments. Eight proteins were identified with significantly altered expression levels in resistant lines compared to WT (statistical significance was assessed using significance B) (Figure 4.13.B, C and Table 4.6). Two proteins were identified in MTX R1 that were significantly under-expressed compared to WT, and six proteins were identified in MTX R2, two of which were under-expressed and four of which were over-expressed (Figure 4.13.B,C Table 4.6). There was no striking change in abundance of any of the proteins identified with the top hit, p22 protein precursor (Tb927.6.2420), only demonstrating ~2.4 fold lower abundance in MTX R2.

Chapter 5: Discussion

5.1 Mechanism of action of antifolates

5.1.1 Effects of thymidine and folate on antifolate cell potencies

To fully assess the effects of thymidine and folate on antifolate drug potency a medium deficient of folate and thymidine was established. The first attempt to make a folate and thymidine depleted medium (named RPMI-BM) was based on 'FDM' (Sienkiewicz *et al*., 2008) but the medium was modified to contain no additional thymidine. FDM was prepared using RPMI 1640, supplemented with 50x MEM amino acid solution, with amino acids and other nutrient concentrations comparable to HMI9-T (Table 2.1). Also it contained 0.5% Serum Plus™ and 10% FCS. Unfortunately parasites could only survive in this medium with thymidine supplementation; a finding shared with others members of the Fairlamb group and the DDU (personal communication). A second attempt was to create a media based on HMI9-T, but without additional folate and thymidine, named TBM. This media contained no Serum Plus™ with serum provided by 10% FCS (Table 2.1). Parasites survived and grew at a normal rate in this medium, without the need for thymidine supplementation. It is interesting that cells did not grow in RPMI-BM despite this media having extra serum (provided by 0.5% Serum Plus™) and therefore extra folate; as opposed to TBM that did not contain Serum Plus™ where cells survived without the need for thymidine supplementation. Perhaps, some of the amino acids provided by MEM in RPMI-BM were insufficient level support growth and thymidine served as nutritional rescue in the medium. Thymidine is synthesised de novo from aspartate and glutamine to form dUMP and then 5,10-MeTHF provides the methyl group to form dTMP. In turn 5,10-MeTHF is formed from THF with the methylene moiety derived from either glycine or serine. Comparison of amino acid levels in these media (Table 2.1) reveals that amino acid composition is essentially

the same. However, glutamine is supplied as L-alanyl-L-glutamine in TBM and L-glutamine in FDM. It is well known that glutamine is unstable in solution and possibly became limiting in FDM. It would be of value to measure the thymidine and folate levels (e.g. by HPLC) in both RPMI-BM and TBM to provide an accurate comparison of these media.

Antifolate drugs were tested in TBM with the addition of thymidine and/or folate. MTX has been shown to have picomolar K_i values against TbDHFR enzyme and micromolar K_i values against TbTS (Gibson *et al*., 2016). The addition of folate had a greater effect in reducing whole cell potency than the addition of thymidine confirming that MTX is selective for TbDHFR over TbTS. Moreover, the absence of thymidine improved MTX cell potency confirming that 'thymineless death' is part of the mode of action (MOA) of MTX. However, excess thymidine did not totally nullify MTX toxicity suggesting that MTX has intracellular targets other than DHFR-TS. One probable candidate is PTR1, as MTX have been previously shown to be active against this enzyme in *T. brucei* ($K_{i\ app}$ 11.1 nM) (Spinks *et al*., 2011). The fact that MTX is structurally similar to folate metabolites means that MTX could inhibit other targets in the folate metabolic pathway such as FPGS, MS or C1-THF synthase. In mammalian cells, as well as targeting DHFR, MTX is also known to inhibit the enzymes MTHFR and MS resulting in diminished intracellular 5-methyl-THF levels and a reduction in homocysteine remethylation to methionine (Broxson, Jr. *et al*., 1989; Fiskerstrand *et al*., 1997).

The addition of thymidine completely abrogated the actions of classical antifolates RTX and PMX suggesting that these drugs are TS- specific. This suggests that 'thymineless death' is their primary MOA and that there are minimal off-target effects. The monoglutamate forms of RTX and PMX are more selective for

TbDHFR than TbTS in an enzyme assay (Gibson *et al*., 2016); this has also been reported in the monofunctional human enzymes (Jackman *et al*., 1991; Shih *et al*., 1997). However, these drugs contain a terminal glutamyl moiety which enables polyglutamylation by FPGS (Synold *et al*., 1996). In mammalian cells, polyglutamylation of RTX and PMX enables better binding to TS with minimal effect on binding to DHFR (Jackman *et al*., 1991; Shih *et al*., 1997). In *T. brucei*, RTX and PMX display better whole cell potencies than against the TbDHFR and TbTS enzyme activities, implying that polyglutamylation of these drugs probably happens.

The non-classical antifolates that were tested included the TbDHFR-specific inhibitors TMX, PYR and TMP; and also the TbTS-specific inhibitor NTX. TMX has picomolar K_i values against TbDHFR (Gibson *et al*., 2016), but unlike MTX, this does not translate into whole cell potency, possibly due to TMX not containing a terminal glutamyl moiety for polyglutamylation and subsequent intracellular retention (Jackson *et al*., 1984). Results showed that PYR and TMP have intermediate potency against TbDHFR (Gibson *et al*., 2016) and display a marked drop-off in potency from enzyme target to cell when cultured in TBM. The addition of thymidine had little effect in reducing whole cell potency compared to the addition of folate, where drug potency was reduced, confirming that PYR and TMP are DHFR specific in *T. brucei* as they are in mammalian, bacterial and protozoan cells (Benkovic *et al*., 1988; Chio and Queener, 1993). Although NTX has nanomolar K_i values against TbTS (Gibson *et al*., 2016) it displayed only moderate whole cell potencies with no change in drug potencies with the addition of folate or, notably, thymidine. Again, NTX is a non-classical antifolate; non-classical antifolates lack a terminal glutamate and therefore are unlikely to enter the cell via

folate transporters and cannot be polyglutamylated. Polyglutamylation may facilitate compound concentration in a cell. The drop-off in cell potency may also be due to drug efflux, or non-specific binding to proteins in the medium.

5.1.2 Cell cycle studies

Previously, DHFR-TS$^{-/-}$ BSF *T. brucei* parasites have been shown to undergo cell cycle arrest in S-phase when grown in the absence of thymidine (Sienkiewicz *et al*., 2008). S-phase arrest has been linked to 'thymineless death', in both prokaryote and eukaryotic systems (Ahmad *et al*., 1998). Analysis of DHFR-TS inhibitors RTX and MTX confirmed cell cycle arrest in S phase. Indeed this phenotype was rescued with excess thymidine supplementation, with a greater 'rescue' for RTX than MTX treated cells, indicating that 'thymineless death' is a more prominent MOA for RTX (targeting TS) than MTX (targeting DHFR and PTR1). In *T. brucei* PTR1 is essential both *in vitro* and *in vivo* (Sienkiewicz *et al*., 2010) and displays a low activity in reducing folate to DHF (Ong *et al*., 2011). Histograms of parasites treated with MTX and RTX were non-canonical with cell cycle distribution unquantifiable. This non-canonical histogram profile has also been previously found with the TS inhibitor 5-fluorouracil (5FU) in yeast (Hoose *et al*., 2012). Furthermore, the cytotoxic effect during the S phase of the cell cycle has also been observed in mammalian cells treated with antifolates, including MTX and RTX (Di Gennaro E. *et al*., 2009; Taylor and Tattersall, 1981). Cell cycle arrest in S phase caused by MTX treatment has been previously shown to be partially rescued by supplementation with excess thymidine. In these cancer cell line studies complete rescue was seen when both thymidine and hypothanxine were added, suggesting that MTX toxicity was associated with inhibition of DNA synthesis from suppression of both thymidine and purine synthesis (Taylor and Tattersall, 1981). Unlike mammalian cells,

trypanosomatids lack *de novo* purine synthesis (Bellofatto, 2007) and so MTX toxicity via suppression of purine synthesis is not applicable to *T. brucei*.

The TS inhibitor fluorouracil (5FU) modulated by folinic acid (5FU-FA) is widely used in the treatment of metastatic colorectal cancer. The 5FU metabolite FdUMP forms a stable tertiary complex with TS and methyl donor 5-10-Methylene-THF which inhibits TS function (Longley *et al*., 2003). Folinic acid (leucorovin) is known to modulate the effects of 5FU. Leucorovin enters the mammalian cell via the RFC and is converted to 5-10-Methylene-THF. Polyglutamylation of 5-10-Methylene-THF, by FPGS, increases its cellular intracellular retention and also improves the stabilization of its tertiary complex with FdUMP and TS (Longley *et al*., 2003). 5FU with leucorovin lead to improved clinical response rates in colorectal cancer compared to treatment with 5FU only (Thirion et al., 2004). In cell cycle studies, it has been found that supplementation with the drug vorinostat increased the magnitude of S phase arrest by 5FU-FA in cancer cell lines (Di Gennaro E. *et al*., 2009). Vorinostat is a histone deacetylase inhibitor; this action affects multiple pathways that cause cell death including the expression of cell cycle regulation, differentiation and/or apoptosis (Xu *et al*., 2007). It has been shown that TS activity is reduced by vorinostat and it has a synergistic anti-proliferative effect when combined with either 5FU-FA or RTX leading to a reversal of chemo-resistance to both these drugs (Di Gennaro E. *et al*., 2009). It would be interesting to determine if vorinostat, or other histone deacetylase inhibitors, had any supplementary effect on cell cycle disruption caused by antifolates in *T. brucei* and whether a combination regime can indeed enhance antifolate parasite toxicity. Moreover vorinostat could block the ability of thymidine to both rescue S phase arrest associated with RTX and MTX treatment and reverse its ability to reduce drug potency *in vitro*.

5.1.3 Determining the trypanocidal nature of MTX and RTX

Compounds that are cytostatic against *T. brucei* inhibit parasite growth, whilst not killing them, are unlikely to clear parasite burden completely. Furthermore, these agents are often not effective in animal models of HAT and so should be identified and eliminated from drug discovery pipelines as early as possible (De Rycker *et al*., 2012). Of the current drugs used in HAT there is a spectrum of cidal activity e.g. melarsoprol is rapidly cidal, pentamidine slow-cidal and DFMO is typically trypanostatic ((De Rycker *et al*., 2012; Sykes *et al*., 2012). MTX and RTX were not fully cidal at 48 h, in fact only static activity was shown in this time frame. Cell density dropped after 48 hours drug exposure but did not fall to below the starting concentration, in contrast to the rapidly cidal melasoprol. However if the assay was modified to have a longer duration of drug exposure (> 48 hours) it is possible that cidal activity of MTX and RTX might have been seen. Also, if drug washout was done at the end of the assay one could determine whether the MTX and RTX effect was reversible (static effect) or if cell death had occurred (cidal effect). In DHFR-TS $^{-/-}$ studies, null mutants died on removal of thymidine from the medium (100% inhibition of the target is lethal not static) and this occurred after 72 hours (Sienkiewicz *et al.*, 2008). 72 hours may be the best time frame to determine cidal activity of the DHFR-TS inhibitors MTX and RTX. Furthermore, cidal/static activity may be dose dependent. 100% inhibition of DHFR-TS may be lethal (as seen in DHFR-TS $^{-/-}$ studies) whereas a lower dose (90% inhibition) may give growth arrest. Another assay used in HAT drug discovery determines *T. brucei* cidal activity by measuring parasite numbers after 24, 48 and up to 72 hour exposure to compounds at Minimal Inhibitory Concentrations (MIC) (Sykes *et al*., 2012). In this assay, cidal nature is identified by parasite burden being completely cleared and puromycin is

used as a positive control for 100% cell death. An assay like this could be adopted for determining MTX and RTX cidal activity.

Work on current antifolates used against infectious diseases has shown some interesting results regarding their nature of killing. The DHFR inhibitor PYR is known to act in a 'slow-cidal' antiparasitic manner against *P. falciparum* (Le Manach C. *et al.,* 2013). PYR was shown to have a stage-specific profile with activity against schizont formation and no activity against younger ring stages (Le Manach C. *et al*., 2013). In mammalian cells, parasite DNA synthesis takes place during erythrocytic schizogony (approx. 48 hours after infection) and after the parasite invades the hepatocytes (White and Kilbey, 1996). Slow–cidal activity of PYR could be explained by its activity against schizonts where DNA synthesis takes place. Of note, the most widely used antimicrobial antifolate, TMP, is likely to have both bacteriostatic (catabolic effects) and bacteriocidal (folic acid effects) actions (Quinlivan *et al*., 2000). This further highlights that categorising drugs into merely static or cidal can often be an oversimplification.

5.1.4 MTX and RTX *in vitro* potencies as precursor for *in vivo* studies

As a precursor for *in vivo* work, MTX and RTX potency was tested *in vitro* in parasites supplemented with thymidine and folate levels comparative to physiological levels seen in mice. It was found that supplementation with physiological thymidine concentrations did not affect drug potency; however, when physiological folate concentrations were increased MTX and RTX potency was reduced. However the 1 μM of thymidine used for supplementation is likely to have been used up very rapidly by the parasite (Ali *et al*., 2013b), whereas folate is stored

and recycled intracellularly and therefore low concentrations of folate (30-300 nM used here) are more likely to reverse antifolate drug effects. The 1 μM of thymidine used was not based on a steady state concentration but a pre-treatment concentration in Balb/c mice (Clarke *et al*., 2000b).

Reversal of antifolate potency due to modulation of intracellular folate levels has been demonstrated in a number of studies relating not only to cancer but also infectious disease models both *in vitro* and *in vivo* (Peters *et al*., 1999; Schmitz *et al*., 1994; van der Wilt *et al*., 2001; Wang *et al*., 2010). Studies in *P. falciparum* have shown that the addition of folate, or its derivatives, decreases the activity of antifolates (Carter *et al*., 2005; Ouma *et al*., 2006). Indeed, while MTX lacked any antimalarial activity against the murine infection, this was partially explained by the high content of folate in these mice (Irungu *et al*., 2009). Also, in humans it has been found that there was reduced efficacy of the antimalarial treatment sulfadoxine-pyrimethamine when used in patients receiving folic acid supplementation for anaemia (Carter *et al*., 2005). There is a balance between high folate levels inhibiting the actions of antifolates and antifolate toxicity with low folate levels. Moreover, leucorovin is often given to patients who are receiving MTX, for the treatment of cancer or inflammatory diseases, in order to reduce the toxic side effects of MTX (Shea *et al*., 2014; Treon and Chabner, 1996). For HAT animal model testing of antifolates it would be necessary to consider the effect of folate in the diet of mice and how this may impact the drug effect, both high folate levels inhibiting drug potency and low folate levels contributing to drug toxicity. Moreover, studies in cancer murine models have found that thymidine levels modulate RTX potency *in vivo*. Potency could be abrogated by thymidine supplementation (Jackman *et al*., 1991), and drug toxicity caused when thymidine levels were lowered by the inhibitor

methoxypolyethyleneglycol-conjugated thymidine phosphorylase (MPEG-TPase) (Cao *et al*., 1999). Physiological levels of folate and thymidine in mice are still higher than those found in humans, with studies showing four times the folate concentrations in mice ((71 nM in low-folate diet (Wang *et al*., 2010)) compared to humans (17.91 nM (Wahlin *et al*., 2002)) and eight times thymidine concentrations in mice (1 μM) (Clarke *et al*., 2000b) compared to humans (0.13 μM) (Howell *et al*., 1981) indicating that animal models may not give a true representative of antifolate drug activity.

With this information in hand, *T. brucei in vivo* studies of antifolate drugs would be the next step. However, MTX has already been tested in a HAT animal model by the Fairlamb group (personal communication). It was found that a standard regime of twice daily 5mg/kg MTX did not reduced parasite burden in mice fed a standard diet. However, in mice fed a low folate diet the same dose led to low levels of parasitemia but the mice had to be terminated due to toxicity. Folate levels were not examined in the mice and it could be that these were at a level that negated any MTX potency in mice fed a normal diet; moreover toxicity in the mice fed a low folate diet could be reflective of the narrow therapeutic index of MTX (Lennard, 1999). Moreover, thymidine levels were not measured and this may have impacted on MTX activity. Rescue with leucorovin circumvented MTX toxicity but it also increased levels of parasitemia, suggesting that the active reduced metabolites of leucorovin can be utilized by *T. brucei in vivo*. Previously, it has been demonstrated that after administration of leucorovin the predominant elevated metabolic forms after 2 hours were 5,10-methylene-THF and THF in mouse plasma (Bunni *et al*., 1994). It is likely that in *T. brucei* these folate forms could be taken up and utilised. Studies show favourable preclinical RTX pharmacology (Clarke *et al*., 2000a) and

RTX appears a credible candidate for HAT animal model studies. However, RTX has limitations in the clinical setting including poor oral bioavailability and lack of CNS penetration (Clarke *et al*., 2000a). Also with current anitfolates there is a lack of specificity against the parasite DHFR-TS and human enzyme (Gibson *et al*., 2016) which may account for toxicity seen in the animal mouse model with MTX. Designing new or refining existing antifolates may help reduce toxicity in the animal model and be necessary if this drug class are to be used in *T. brucei*. With this in mind a small phenotypic screen of "antifolate" DDU compounds was undertaken.

5.1.5 The "antifolate set"

In this "antifolate set" compounds with known activity against folate-dependent enzymes displayed better *in vitro* potencies against *T. brucei* when tested in TBM compared to when tested in HMI9-T. This small-scale compound screen suggests that using routine nutrient-rich media in phenotypic drug screening can mask the potency of certain compounds. It has been previously reported that selective TbPTR1 inhibitors, 2-aminobenzimidazoles, showed a lack of whole cell *T. brucei* potency despite having nanomolar TbPTR1 enzyme activity (Spinks *et al*., 2011). Indeed, the 2-aminobenzimidazoles in our "antifolate set" showed moderate whole cell potencies across media types with EC_{50} values in the low micromolar range. Moreover, when tested in HMI9-T media, the EC_{50} of compounds **4** and **5** were comparable to the EC_{50} values previously reported (Spinks *et al*., 2011). Further work is required to explain the lack of cellular activity for selective TbPTR1 inhibitors, with proposed reasons including lack of cellular penetration , efflux of the drug, high non-specific protein binding, and high lipophilicity of compounds (leading to sequestration into lipid compartments which may negate activity against

a likely cytosol drug target) (Gilbert, 2013). In addition, it has been deduced that PTR1 inhibitors require very high levels of enzyme inhibition in order to translate to respectable whole cell potencies (K_i < 1 nM, based on the physiological levels of substrate and the need for >90% enzyme inhibition) (Gilbert, 2013). This drop off in potency from target to cell is a common problem encountered in target-based *T. brucei* drug discovery endeavours; targets such as fructose 1,6-bisphosphate aldolase (Dax *et al*., 2006) and trypanothione synthase (Spinks *et al*., 2012) are two examples of this. Continued medicinal chemistry efforts are required but it may be that cell potency cannot be achieved despite potent target activity.

The 2,4-diaminoquinazolines and pyridopyrimidines (Figure 3.4) are TbPTR1 inhibitors that were also shown to display 'off target' TbDHFR activity. These compounds had nanomolar whole cell potencies when tested in TBM and for some of these compounds the addition of thymidine and folate moderately reduced drug potency. The moderate potency shift with folate supplementation suggests that DHFR activity alone does not account for whole cell potencies. It also suggests that these PTR1 inhibitors are not transported into the cell via folate transporters (as opposed to MTX where folate supplementation negated drug activity likely due to competition for drug uptake into the cell). A previous study has investigated the *in vitro* efficacy of 2,4 diaminoquinazolines in *Leishmania*, *T. cruzi* and *T. brucei* moreover compounds were also assayed against recombinant *L. major* DHFR (Khabnadideh *et al*., 2005). Correlation with inhibition of *L. major* DHFR and *in vitro* cell potencies for *Leishmania*, *T. cruzi* and *T. brucei* was often not found for this compound set, which suggests that compounds may be killing parasites other than by DHFR activity. 2,4-diaminopyrimidines also have activity against *L. major* DHFR with scaffolds based on this core leading to the 5-benzyl-2,4-

diaminopyrimidines series being explored further (Gilbert, 2002). This series was found to have activity against TbDHFR with promising *in vitro* potencies; however, *in vivo* these lead compounds showed poor potency and were toxic (Chowdhury *et al*., 2002). The authors postulated that activity against other enzymes involved in folate metabolism may account for disappointing *in vivo* results. The results of this thesis suggest that both pyridopyrimidines and 2,4-diaminoquinazolines do indeed have targets other than DHFR in trypanosomes (e.g. PTR1). This is not a surprising finding as pyridopyrimidines and 2,4-diaminoquinazolines were known to inhibit TbPTR1 from an in-house DDU drug discovery programme (personal communication). It is likely that the *in vitro* potency of these compounds is primarily due to PTR1 activity with some potency attributed to TbDHFR activity.

In this "antifolate set" compounds **1** and **2** were chosen for potency determination because they contain a *p*ABA-Glu moiety. However, these two compounds showed disappointing whole cell potencies against *T. brucei*. Activity against TbPTR1 and TbDHFR has not been determined so it may be that these compounds, although structurally similar to classical antifolates, do not inhibit enzymes in the folate metabolic pathway to any great extent. WR99210 has been previously shown to have very good binding affinity to TbDHFR (K_i 0.9 $\pm$ 0.1 nM); moreover, it had potent whole cell *in vitro* activity (EC_{50} of 0.09 $\pm$ 0.02 μM) (Vanichtanankul *et al*., 2011). However, in this assay WR99210 had only moderate whole cell potency with EC_{50} ~ 4 - 6 μM across media types. The previous work on WR99210 was carried out on a strain of *T.b. rhodesiense*, whereas *T.b. brucei* was used in these studies potentially explaining the difference. However, *T.b. rhodendiense* and *T.b. brucei* are morphologically indistinguishable and genetically near equivalent. It has been demonstrated than they can differ by as little as the expression of a single gene,

serum resistance-associated (SRA) gene, the gene that confers *T. b. rhodendiense* its human infective phenotype (Gibson, 2003: Sistrom *et al*., 2016). Also, whole cell potencies of WR99210 against *T.b rhodesiense* were performed in nutrient deplete medium (with no thymidine and folate). It would be prudent to test WR99210 activity against T.b.b DHFR and T.b.b TS to determine if results do represent subspecies variation. If enzyme activity is found it would be worth revaluating why a lack of potency was observed in these whole cell studies.

5.1.6 Transport Studies

The folate transport properties of *T. brucei* BSF, evident in this thesis, are comparable to *Leishmania.* Uptake is rapid and linear for 2 to 3 min in both parasites, the rate of folate uptake is concentration dependent indicating carrier-mediated transport, and transport in both kinetoplastids exhibits Michaelis-Menten kinetics (Ellenberger and Beverley, 1987). The K_m for folate uptake in *Leishmania* is in the sub micromolar range for all the species examined: K_m of 0.7 μM for *L. major* (Ellenberger and Beverley, 1987), K_m of 0.23 μM in *L. donovani* (Kaur *et al.*, 1988) and $K_{m\ app}$ of 0.26 μM in *L. tarentolae* (Kundig *et al*., 1999). The $K_{m\ app}$ of folate transport found in *T. brucei* BSF 427 strain (2.1 μM) is comparatively higher than that found in *Leishmania*. Also the $K_{m\ app}$ for MTX transport in *T. brucei* (16 μM) is higher than that found in Leishmania: K_m of 1.8 μM in *L. major* (Ellenberger and Beverley, 1987), 0.41 μM in *L. donovani* (Kaur *et al.*, 1988) and 0.45 μM in *L. tarentolae* (Richard *et al*., 2002). The promastigote form (insect vector form) of the *Leishmania* parasite was used for these transport experiments. It may be that the environment of the insect stage of *Leishmania* accounts for a higher affinity of folate

transport. It would be interesting to determine if affinity for folate transport changes in relation to the stage of parasite development.

Similar to *T. brucei*, the potency of MTX in *Leishmania* is dependent on the concentration of folate in the culture medium (Nare *et al*., 1997; Richard *et al*., 2002). Studies in *L. tarentolae* have found that MTX has an EC_{50} of 25 μM in SDM79 (high folate media) compared to 0.25 μM in M-199 (low folate media) (El Fadili *et al*., 2003). Overexpression of the enzyme FPGS increased MTX potency by four fold in M-199 compared to WT, highlighting the role of polyglutamylation in increasing intracellular antifolate potency (El Fadili *et al*., 2003). It is possible that in *T. brucei* although MTX has a moderate $K_{m\ app}$ of drug transport, polyglutamylation by FPGS, as in *Leishmania*, may be responsible for its potent intracellular activity.

In these transport studies substrate uptake is measured at pH 7.3, which is close to physiological pH. In mammalian cells, folate and MTX transport at physiological pH is primarily carrier mediated via the RFC and so a comparison to this mode of transport in mammalian cells is most relevant. Mammalian cells display a lower affinity for folate transport via RFC (100-fold less compared to *T. brucei*) but have a high affinity for 5-methyl-THF (the predominant folate form in serum) (Sirotnak, 1985). Indeed, the K_m or K_i values for 5-methyl-THF transport via RFC (range 1 to 4 μM) (Sirotnak and Tolner, 1999) are similar to the $K_{m\ app}$ for folate in *T. brucei* (2.1 μM). The lower affinity for MTX uptake found in *T. brucei* ($K_{m\ app}$ 16 μM) is comparable to the affinity for RFC mediated MTX transport (range 2.3 to 26 μM) (Sirotnak and Tolner, 1999).

The substrate competition assay provided further understanding into the structural recognition of folate for its uptake in *T. brucei*. *p*ABA-Glu and 5-methyl-

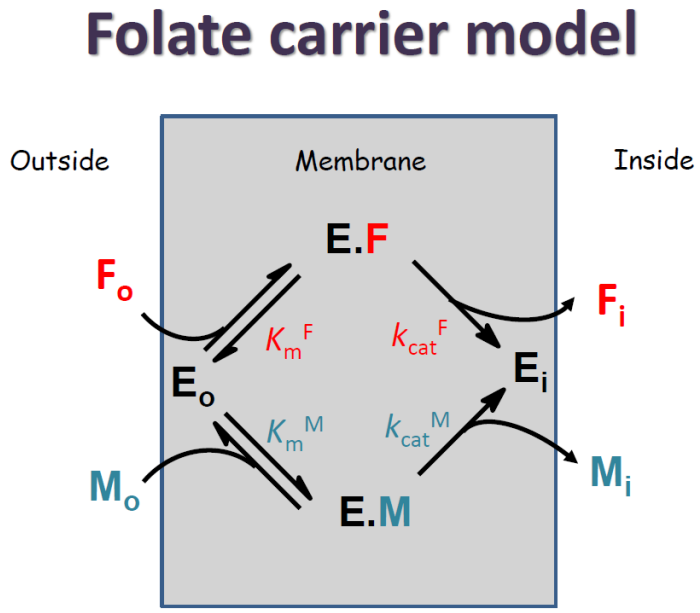

Figure 5.1: Folate carrier model

Cell entry is defined by affinity to the membrane transporter (s) (K_m), a confirmation change in the transporter, and then substrate turnover (k_{cat}) into the cell. F = folate. M = methotrexate, E = enzyme (transporter (s))

THF inhibited folate and MTX uptake whereas biopterin had no effect on uptake. *p*ABA-Glu and 5-methyl-THF have also been shown to competitively inhibit folate and MTX uptake in *Leishmania* (Ellenberger and Beverley, 1987). Results demonstrate that compounds containing *p*ABA-Glu (folate, 5-methy-THF) or a *p*ABA-Glu-like moiety (classical antifolates) compete for transport in trypanosomes. Adding a *p*ABA-Glu moiety to a non-classical antifolate, e.g. PYR, could potentially lead to improved drug uptake. In competing with folate for uptake this may lead to reduced intracellular folate levels and potentially improve drug potency by outcompeting for the target enzyme (DHFR).

Folate and MTX were found to be competitive substrates for uptake in *T. brucei*, comparable to studies in *Leishmania* (Ellenberger and Beverley, 1987). In this 'folate carrier model' (Figure 5.1) folate and MTX are mutually competing substrates for uptake into the cell. Cell entry is defined by binding to the membrane transporter(s) (K_m), a conformational change in the transporter, and then substrate turnover (k_{cat}) into the cell (Figure 5.1). This is an active transport model. It would also be prudent to determine if folate transport is dependent on protomotive forces and whether it is ATP-driven. Transport could be measured in the presence of ionophores: e.g. valinomycin, K^+; carbonyl cyanide *m*-chlorophenyl hydrazine (CCCP), H^+; monensin, Na^+; gramicidin, Na^+/K^+; and nigericin, K^+/H^+; and also in the presence of ATPase inhibitors e.g. N-ethylmaleimide (NEM), H^+-ATPase; ouabain, Na^+/K^+-ATPase; N,N′-dicyclohexyl-carbodiimide (DCCD), H^+-ATPase. In *T. brucei* BSF purine transport has been shown to be dependent on protomotive forces, which was confirmed by a linear relationship between protomotive forces (intracellular pH and membrane potential) and rate of hypoxanthine uptake (De

Koning and Jarvis, 1997). Similar studies could be carried out to determine if promotive forces act upon folate transport.

Of interest, growing cells in a higher folate concentration had little or no effect on folate uptake in *T. brucei*. At saturating concentrations (V_{max}) there was a slight reduction (12%) in the rate of folate transport in cells grown in high folate medium. In *Leishmania* it has been found that there was a 30% decrease in the V_{max} of folate uptake for cells grown in a high folate medium, which appeared to be independent of the intracellular folate concentration (Ellenberger and Beverley, 1987). These results demonstrate that folate transport does not appear to regulate intracellular folate in *T. brucei* and *Leishmania*. Indeed, polyglutamylation of folates by FPGS has been found to regulate intracellular folate levels in *Leishmania* (El Fadili *et al.*, 2002). Similar studies could be initiated to determine whether FPGS plays a pivotal role in folate retention in *T. brucei*.

5.2 Mechanisms of antifolate resistance

5.2.1 RIT-seq Studies

An RNAi library screen implicated *FT1-3* in parasite resistance to antifolate drugs MTX and RTX. *FT1-3* belong to the FBT family of which *T. brucei* has seven homologues. The *T. brucei* FBT family consists of three putative folate transporters (*FT1-3*) that share 96 % gene identity and are clustered on chromosome 8 (Tb927.8.3620, Tb927.8.3630 and Tb927.8.3650); three putative pteridine transporters (*BT1-3*) that share 99% gene identify and are clustered on chromosome 1 (Tb927.1.2820, Tb927.1.2850 and Tb927.1.2880), and a putative pteridine transporter (*BT4*) on chromosome 10 (Tb927.10.9080) that shares 68% gene identity

with *BT1-3*. In addition, the genome includes a folate transporter orphan fragment (Tb11.v5.0766) that shares 97 to 100% gene identity to *FT1-3* (position 736 -1899 of ORF). This orphan gene is likely to be non-functional. It encodes a protein that does not contain the first 245 residues that are predicted to encode the first 4 transmembrane portions of the transporter (based on topology modelling). Of note, in the *T. brucei* S427 strain there are 7 *ESAG10* genes that share 90-94% gene identity with *FT1-3*. *ESAG10* genes are found in approximately half of the telomeric transcription units (Bloodstream Expression Sites, BES) that regulate the expression of VSGs (Hertz-Fowler *et al*., 2008) and only one BES is transcribed at any time. The cell lines used in these thesis express VSG221 from BES1 in which *ESAG10* is not transcribed (Hertz-Fowler *et al*., 2008). From evidence in this thesis, in BSF *T. brucei*, *FT1-3* are likely the only expressed and functional genes for folate transport. In *Leishmania* there are 14 FBT and one of these transporters, *BT1*, primarily mediates the uptake of biopterin but also has a low affinity for folate uptake (Kundig *et al*., 1999). Indeed, in Leishmania folate, but not MTX, can be taken up by BT1, providing the folate requirements in cells lacking functional high-affinity folate transport (Kundig et al., 1999). The putative biopterin transporters in *T. brucei* (*BT1-4*) have not been characterised and it would be prudent to determine if these transporters have any folate transport activity. Also, it would be worth determining if *FT1-3* are responsible for any biopterin transport in *T. brucei*.

RIT-seq experiments, with MTX and RTX, revealed other hits of interest. Both drug screens identified the mitochondrial carrier protein 2 (*MCP2*), (Tb927.11.14360) as a hit. MCPs are a group of structurally conserved proteins that are known to modulate the transport of metabolic intermediates across the mitochondrial membrane. Twenty four MCP homologues have been found in *T.*

brucei (Colasante *et al*., 2009). TbMCP2 has been described to be on a phylogenetic branch with the human mitochondrial folate transporter (*MFT*) (Colasante *et al*., 2009). MFT is known to regulate the transport of THF cofactors from the cytosol to the mitochondria (Lawrence *et al*., 2011). Moreover, TbMCP2 has been l localised to the mitochondria by Myc-tagging (Colasante *et al*., 2009). The subcellular localisation of folate metabolic enzymes has not been fully characterised in *T. brucei*; however, some enzymes have localised to the mitochondria, illustrating that folates are indeed imported into this organelle. Methionyl-tRNA^{Met} formyltransferase, needed for mitochondrial protein biosynthesis, has been mitochondrially localised (Tan *et al*., 2002). Also, components of the GCS were determined to be mitochondrial by proteomic analysis (Panigrahi *et al*., 2009).

RTX specific hits were C1-THF synthase and the ‘minor hit’ FPGS. Reduced C1-THF synthase activity could result in accumulation of 5,10-Methylene-THF. TS, the target of RTX, utilises 5,10-Methylene-THF to convert dUMP to dTMP. Accumulation of 5,10-Methylene-THF could compete with RTX for its activity against TS thus providing a mechanism of drug resistance. Polyglutamylation of RTX, by FPGS, is known to account for its potency in mammalian cells (Jackman *et al*., 1991; Shih *et al*., 1997). Moreover, it is probable that polyglutamylation occurs in *T. brucei*. Reduced TbFGPS activity could impair RTX potency and lead to drug resistance. Of the hits identified in RIT-seq experiments FT1-3 were validated to account for MTX and RTX drug resistance. Further work would be to establish if additional hits seen in these screens; MCP2, FPGS and C1-THF synthase are also part of drug resistance mechanisms. Although targeting the mitochondrial transporter MCP2 for drug discovery would be technically extremely challenging.

Using a RIT-seq approach, gene down regulation (loss of function) confers a selective advantage to parasites under drug pressure. However, not all drug resistance mechanisms are due to loss of function; drug efflux is an example of this. Moreover a RIT-seq approach is unlikely to identify essential genes as RNAi of these genes may be lethal, even without drug selection. A genome-wide overexpression approach, looking at gain-of-function, would complement the current RIT-seq loss-of-function approach. Overexpression libraries are currently being developed in *T. brucei* (Begolo *et al*., 2014) (personal communication, Mechanism of Action Team, DDU). Testing antifolate drugs using such overexpression approaches may identify intracellular targets of these drugs, e.g. DHFR-TS, PTR1 and potential drug efflux mechanisms.

Most *Leishmania* species lack functional RNAi machinery and therefore an RNAi based drug screening approach is not viable (Lye *et al*., 2010). But, an overexpression cosmid library approach, "Cos-Seq", has recently proved successfully in identifying resistance mechanism of antileishmanial drugs (Gazanion *et al*., 2016). Resistance to MTX was tested in these studies and DHFR–TS and PTR1 were identified as drug resistance determinants; confirming what had been previously found in MTX-resistance *Leishmania* cell lines (Arrebola *et al*., 1994; Callahan and Beverley, 1992; Coderre *et al*., 1983; Papadopoulou *et al*., 1992). Also, enriched genomic regions of chromosomes 21 and 34 were identified and two phosphatase-related genes emerged as candidates (LinJ.34.2310 and LinJ.34.2320). Consequently, transfected parasites with these genes showed a reduced susceptibility to MTX. Of note, MTX is known to inhibit protein phosphatase 2A in mammalian cells (Fernandez-Perez *et al*., 2013). It would be interesting if future studies in *T .brucei* identified protein phosphatases in antifolate action and resistance.

5.2.2 Folate transport in drug resistance– RNAi knockdown and MTX-resistant trypanosomes

Studies in this thesis have confirmed *FT1-3* in parasite resistance to antifolate drugs. Folate transport was substantially reduced with *FT1-3* RNAi knockdown; also in a MTX-resistance cell line, displaying both a deficit in MTX and folate transport, amino acid changes in *FT1-3* were identified by PCR. Looking at antifolate drug potency, the same phenotype was found with *FT1-3* RNAi knockdown and MTX-resistant lines; there was a reduced potency to classical antifolates and hypersensitivity to non-classical antifolates. Results indicate that folate and classical antifolates share a common transport system, via FT1-3, which is not the case for non-classical antifolates. When FT1-3 function is reduced, folates and classical antifolates have diminished cell uptake (causing reduced antifolate potency) whereas uptake of non-classical antifolates is not disturbed (less intracellular folate to compete with drug target causing increased sensitivity).

Studies in *Leishmania* have also identified a deficit of folate and MTX transport in MTX-resistant cells lines and found folate transporters to be implicated in MTX resistant (Kundig *et al*., 1999; Richard *et al*., 2002; Richard *et al*., 2004). MTX-resistant cell lines were generated by transfection with a genomic cosmid bank, functional cloning, and genes determined through fragment identification. BT1 (originally known as ORFG but later termed BT1 (Lemley *et al*., 1999)) was characterised as a high affinity biopterin transporter and a low affinity folate transporter, but was not found to transport MTX (Kundig *et al*., 1999). Overexpression of *BT1* and a *BT1*-null mutant showed resistance or hypersensitivity to MTX, respectively. An increase in folate transport with no change in MTX transport was evident with *BT1* overexpression which is likely to account for MTX

resistance developing. FT5 was later discovered to be a high affinity/low capacity transporter of folate and MTX (Richard *et al*., 2002). *FT5* was expressed in a MTX-resistance cell line which resulted in increased folate and MTX transport. Moreover the *FT5* transfectant improved MTX sensitivity in the resistant line. Conversely in a *FT5* null mutant, folate and MTX transport was reduced. Interestingly the *FT5* null was hypertensive to MTX. A third transporter, FT1, was found to improve folate and MTX transport and restore MTX sensitivity in MTX-resistant *Leishmania* (Richard *et al*., 2004). FT1 was characterised as a high affinity/high capacity folate/MTX transporter. In a *FT1* null mutant, folate and MTX transport was reduced and also MTX sensitivity was diminished. These *Leishmania* studies included localisation experiments of BT1 and FT1 using GFP tagging and fluorescent microscopy (Kundig *et al*., 1999; Richard *et al*., 2004). Transporters were found to localise to the plasma membrane and also there was some localisation to an area corresponding to the flagellar pocket. Such localisation studies for FT1-3 in *T. brucei* would be worthwhile.

It would be beneficial to determine which of the folate transporters FT1-3 are responsible for folate transport. A strategy would be to express *FT1*, *FT2* and *FT3* separately in the MTX-resistant cell lines and establish any recovery of folate/MTX transport and drug sensitivity. This could be done by using an overexpression vector such as pLEW100 (Kelly *et al*., 2007). However, with such a vector, integration is on an ectopic locus and expression levels can be variable. It has also been found that protein expression from such loci can be affected by cell density (Ali and Field, 2013). This does not mean it is not useful as expression in multiple clones can be screened by qPCR. Alternatively one could use a vector that enables constitutive expression at the genes' native locus which is more stable (Alsford and Horn, 2008).

Moreover such a vector also has an epitope tag (GFP and cMyc) that allows for localisation studies (Alsford and Horn, 2008). Knockout strategies of the individual transporters could be attempted however this may prove challenging due to the close genetic homology between them.

The studies in *Leishmania* did not examine the potency of other antifolate drugs in MTX-resistant cell lines and overexpression/knockdown transporter constructs (Kundig *et al*., 1999; Richard *et al*., 2002; Richard *et al*., 2004). It would be interesting to determine if such studies would find the juxtapositioning of classical and non-classical antifolates that were seen in *T. brucei.* In cancer cells, it was found that in MTX-resistance, through a transport deficit via RFC, there was no real change in sensitivity to the classical antifolate PMX because of compensatory depletion of intracellular THF-cofactors (Zhao *et al*., 2000). Here, EC_{50} values were compared to a cell line deficient in FPGS. It may be that if potency was assessed against a cell line with normal FGPS activity there could actually be hyper resistance to PMX, as FPGS is known to polyglutamylate PMX to a greater extent than MTX (Zhao *et al*., 2000). Indeed, it may be that in MTX-resistant *T. brucei* there is no change in FPGS activity. If FPGS activity was reduced, the hyper resistance to RTX and PMX may not have been seen. Measuring antifolate polyglutamylation, via strategies like High-performance liquid chromatography (El Fadili *et al*., 2003), may help elucidate the activity of FPGS in the MTX-resistant line. FPGS was not identified in RIT-seq studies for MTX, but was identified for RTX, which may account for the differences in the drugs dependency on polyglutamylation for activity. Studies in other MTX-resistance cancer cells, which display a transport deficiency, showed hypersensitivity to non-classical DHFR targeted non-classical antifolates TMX and MTP, compared to WT (Diddens *et al*., 1983). In contrast,

when MTX-resistance was due to DHFR overexpression cross-resistance to TMX and MTP was evident, demonstrating that different mechanisms of resistant may reflect different resistance patterns of antifolate drugs (Diddens *et al*., 1983). Results in *T. brucei* suggest that DHFR activity may not be changed in MTX-resistant parasites as a clear hypersensitivity to non-classical antifols was found (including TMX and MTP), which is likely explained by a folate transport deficit. Experimentally evaluating TbDHFR activity in our MTX-resistant line would be a way to test this hypothesis (Gibson *et al*., 2016; Shanks *et al*., 2010).

Of note, biopterin transport was not measured in studies of FT1 and FT5 in *Leishmania* (Richard *et al*., 2002; Richard *et al*., 2004) so the co-transport of biopterin, folate and MTX has not been fully elucidated in this organism. From the results in this thesis, it can be deduced that in *T. brucei* folate and MTX share the same transporter system, FT1-3 (within this gene cluster), which is not shared by biopterin. In our competition assay biopterin did not inhibit MTX or folate transport and pteridine transporters were not identified in our RIT-seq studies of MTX and RTX. To fully exclude any co-transport of biopterin with MTX/folate, biopterin transport could be measured both in the *FT1-3* RNAi knockdown mutants and MTX-resistant cells lines. Also, one could establish whether biotperin is indeed mediated by the other four members of the *T. brucei* FBT family (BT1-4) in a similar manner that FT1-3 was found to mediate folate transport (e.g. through transport studies and RNAi knockdown).

5.2.3 Identifying molecular mechanisms of transport mediated MTX-resistance

In MTX-resistant cell lines sequencing of *FT1-3* was determined using a PCR approach. This revealed two amino acid changes in *FT1* and eight amino acid changes in *FT3* in MTX-resistant trypanosomes. It is surprising that the same mutations were found in independent clones. This could occur if a rare variant was present in the original "WT" clone and this was selected out during culture rather than by mutation. However, WT clone was 99 % identical on the gene level to the FT1, FT2 and FT3 927 reference genome. It may be that these MTX-resistant cell lines are not true independent lines and cross-contamination cannot be ruled out. Also to find eight amino acid changes is unusual indeed in a mutant line. A single point mutation of a critical residue may be sufficient to disrupt transporter function. Moreover, other drug transporters in *T. brucei*, e.g. AQP2 and AT1, are not essential and therefore a single point mutation could be sufficient to bring about drug resistance without a cost to fitness. Indeed a single-point mutation in AT1 was found in a pentamidine-resistant cell line with no fitness cost (Graf *et al*., 2016). Essentiality of FT1-3 would be worth assessing.

The protein sequence of MTX R2 FT3 was aligned with FBT family members in *Leishmania*, cyanobacteria and plants in which key residues associated with folate transport have been identified (Dridi *et al*., 2010b; Eudes *et al*., 2010). Mutagenesis studies of *Synechocystis* slr0642 found seven amino acid residues, conserved with *Arabidopsis* At2g32040, that were critical to folate uptake function (Eudes *et al*., 2010). Bioinformatics modelling identified several other conserved residues in the central cavity of the transporters also thought to be critical to transport. A study in *Leishmania* aligned thirty seven hypothetical FBT proteins across the species mentioned above and targeted the 10 most conserved charged

amino acids (Dridi *et al*., 2010b). These 10 residues were mutated to neutral amino acids and were all found to reduce FT1 folate transport activity in *Leishmania*. A group of mutations found in *T. brucei FT3*: Y523S, R526M, V530L and H536N are in close proximity to conserved C519 and E524 residues determined to be critical to FBT mediated folate transport in *Synechocystis* and *Leishmania* respectively (Dridi *et al*., 2010b; Eudes *et al*., 2010). Moreover this group of four mutations in *T .brucei* lies close to regions determined to be critical to folate transport by bioinformatics modelling in *Synechocystis* (Eudes *et al*., 2010). A topological model of FT3 (Figure 4.11 D) showed that these four mutation are clustered around the cytoplasmic loop close to the 11 transmembrane α helix and in the α helix itself. Out of the eight mutations in FT3, three of these represent a change in either polarity or amino acid structure. Further structural analysis, by computational modelling or even through crystal structures, may elucidate how these mutations could affect the integrity of the transporter and ultimately substrate binding. Disabling mutation may not necessarily be associated with ligand binding and could cause abnormal transporter function through other mechanisms including defective post-translational protein processing (e.g. misfolded protein), defective protein regulation (e.g. increased degradation) and alternations in RNA processing. Computational modelling and crystallography may help elucidate mutations in FT1-3 that may affect ligand binding.

Such structural analysis has been useful in identifying substrate binding motifs in the pentamidine/melasoprol transporters TbAT1 and AQP2. An ‘amide’ motif in TbAT1, enabling the selectivity of aminopurines but not oxopurines (De Koning and Jarvis, 1999), was further explored using computational modelling (Collar *et al*., 2009). Computational modelling of AQPs has also enabled the further exploration of a key pore-forming residue in AQP2 implicated in substrate binding

(Munday *et al*., 2015). In an *AQP2/AQP3* chimera, mutations in this residue led to amino acids with bulkier side-chains that protrude into the pore channel, possibly accounting for lack of drug transport and resulting in drug resistance. Moreover, mutagenesis studies of this key pore forming residue in *AQP2* abolished pentamidine binding and resulted in parasites with reduced sensitivity to pentamidine (Song *et al*., 2016). In relation to folate transporters, one could do similar computational modelling and mutagenesis studies to validate the amino acid changes that were evident in MTX-resistant trypanosomes. By introducing one mutation at a time the mutations responsible for any drug resistance could be determined. Indeed a change in folate/MTX transport and drug sensitivity may be seen in the mutant transfectants.

It should be noted that full sequence coverage of *FT1-3* was not attained for the MTX-resistant trypanosomes. This was due to the fact that PCR product could not be attained for reactions using the unique FT1 Fw and FT2 Rev primers despite varying PCR conditions. This translated into a segment of the first ~550 bp of *FT1* and the last ~1350 bp of *FT2* not being covered. Given the alignment of these genes (Figure 4.8) it could be considered that a homologous recombination event had taken place between *FT1* and *FT2* with a chimeric *FT1/FT2* locus being formed. This mechanism has been seen with AQP mediated melarsoprol/pentamidine cross resistance (MPXR), with evidence of homologous recombination between *AQP2* and *AQP3* in laboratory and clinical strains likely due to the high degree of sequence identity between the genes (Graf *et al*., 2016; Munday *et al*., 2015). It is important to note that *FT1* and *FT2* also share high sequence identify. Further experiments in this thesis showed no change in transcription (qPCR) or copy number/banding pattern (Southern blot) of *FT1-3* between WT and drug-resistant parasites, suggesting that gene deletion has not occurred. If gene rearrangement with a chimeric *FT1/FT2*

locus had occurred a change in banding would have been illustrated in the Southern blot. The band representing *FT1* and *FT2* (8.7 bkb) would be smaller by ~ 3.4 kb (inclusive of intergenic region) however this was not clearly evident as a band of 8.7 kb was seen in all three samples (Figure 4.12 D). Indeed there is currently no evidence to suggest gene rearrangement with a chimeric locus. The restriction enzyme EcoR1 was used as this was the only unique cutter which was able to differentiate the location of *FT1-2* to *FT3*; moreover none of the commercially available rare cutters had recognitions sites spanning the tandem repeats of *FT1-3*. Of note Southern blot banding also revealed the *ESAG10* genes in *T. brucei* S427 that share close homology to *FT1-3.* As the intergenic regions of *FT1-3* are highly homologous attempts to identify other unique primers within these regions were not fruitful. It may also be that point mutations have taken place in *FT1* and *FT2* in regions that could account for an inability of primer binding and thus lack of PCR product. Whole-genome deep sequencing of the MTX-resistant cell lines may be worthwhile in identifying and confirming the underlying mutations in *FT1-3*. Moreover this approach could identify, or help exclude, other gene candidates implicated in MTX-resistance (e.g. *DHFR, PTR1, FPGS*). This approach has been used to great effect in studying drug-resistance mechanisms in *T .brucei*; examples include the oxaboroles, nitro-compounds and MPXR (Graf *et al*., 2016; Jones *et al*., 2015; Wyllie *et al*., 2016). With more time and resources whole-gene sequencing would be the investigation of choice to help elucidate the molecular mechanisms of drug resistance

5.2.4 SILAC studies in MTX-resistant trypanosomes

A very low number of proteins were identified from this SILAC experiment. SILAC ratios were determined for 6% of the *T. brucei* 927 proteome from each MTX-resistant cell line and combining the two populations this represented 9% proteome coverage. This proteome coverage is very low and reasons why this may have occurred will be discussed. Due to time constraints for thesis submission this experiment could not be repeated. However future repetition and development of this SILAC work would be invaluable to give a better understanding of any protein changes associated with MTX-resistant trypanosomes. There are only a handful of published studies using the SILAC proteomic method in BSF *T. brucei* (Jones *et al*., 2015; Urbaniak *et al*., 2013; Zoltner *et al*., 2015). In Zolter *et al* the authors had up to 22% proteome coverage (Zoltner *et al*., 2015); Urbaniak *et al* had up to 39% proteome coverage (peptides were separated by strong cation exchange (SCX) and an enrichment step was carried out for phosphopeptides) (Urbaniak *et al*., 2013)); and in Jones *et al* up to 9% proteome coverage was seen (note this was a pull-down chemo-proteomics experiment) (Jones *et al*., 2015). Given the different methodologies and aims of each paper, Zoltner *et al* is the most comparable by sample and analytic methods (no enrichment, no pull-down, and protein ran on SDS-PAGE). It is therefore timely to consider why protein identification was quite low in SILAC experiments in this thesis.

Looking at cell culture and label incorporation it is unlikely that these contributed to poor proteome depth. Cells were grown in a SILAC media previously shown to be compatible with *T. brucei* culture (Jones *et al*., 2015; Urbaniak *et al*., 2013; Zoltner *et al*., 2015). This SILAC medium normally contains a total of 18 μM of folate; however, because resistance to antifolates was examined the media was

modified to only contain 9 μM of folate (ideally folate levels would be even lower than this). Cells grew at a normal rate in this media with no morphological changes. It has been found that 11 −12 cell divisions would provide sufficient label incorporation (>95%) which must be attained in such SILAC experiments (Urbaniak *et al*., 2013). Indeed cells were passaged for 16-18 cell divisions and label incorporation was 99.3% for R_6K_4 for and 99.2% for $R_{10}K_8$. Therefore culture conditions enabled sufficient label incorporation.

Around of 200 μg protein (2 x 10^7 cells) from the harvested trypanosomes was used for further protein separation and MS. This is comparable with other BSF *T. brucei* studies (Urbaniak *et al*., 2013; Zoltner *et al*., 2015) (cell number not recorded in the other study (Jones *et al*., 2015). It could be that an error in cell counting or in loading the NuPAGE gel may have resulted in a lower volume of protein than was initially estimated. Enrichment steps may also have been useful to increase proteome depth; indeed, mitochondrial enrichment may help identify mitochondrial folate-dependent enzyme of lower abundance. Various biological mitochondrial enrichment methods have been used in *T. brucei* procyclic form (PCF) (Acestor *et al*., 2009; Acestor *et al*., 2011; Schneider *et al*., 2007). However these methods all use ultracentrifugation for subcellular fractionation at some point, which ultimately leads to loss of material. Higher cell densities in PCF make it more practical compared to low density BSF, however using more starting material (protein) may solve the problem of losses due to ultracentrifugation. Also, it may be that mitochondrial separation techniques with more moderate centrifugation forces, such as those used in plants (Abas and Luschnig, 2010) could be adapted for BSF *T. brucei.*

In this SILAC study, although protein was separated by SDS-PAGE, instead of individual gel slices being taken the whole gel was pooled for fractionation by chromatography. This however was not intentional; SDS-PAGE was performed by myself and the gel then given to the Fingerprints Proteomics facility to further processing. It was intended that fractionation would be done by taking individual gel slices rather than pooling for chromatography. It is likely that miscommunication resulted in this different processing, highlighting the importance of clear and careful communication between service provider and user. This pooling of the gel may cause suppression of the less represented proteins and result in bias towards the more dominant ones (Mostovenko et al 2013). Previously, in *T. brucei* BSF, two orthogonal techniques have been used to fractionate SILAC samples; either at the protein level (SDS-PAGE) or at the peptide level (SCX) (Jones *et al*., 2015; Urbaniak *et al*., 2013; Zoltner *et al*., 2015). In *T. brucei* PCF the two different fractionation approaches have been used for the same sample set (Urbaniak *et al*., 2012). It was found that fractionation at the peptide level (SCX), rather than the protein level (SDS-PAGE) identified more proteins. However, the authors noted that the higher number of peptides identified by SCX fractionation was likely due to higher capacity; about 10 times as much material was loaded on the SCX column. In this case, it is likely that the method of fractionation (peptide level rather than the protein level) did not result in less proteins being identified.

With the small proteome coverage and lack of organelle enrichment, only one protein related to folate-metabolism was identified through this proteomic SILAC approach, namely DHFR-TS. Interestingly this was not changed in MTX-resistant parasites. This result further highlights that MTX-resistance in these cell lines is primarily through a deficit in drug transport. As discussed previously, cell potency

patterns of antifolates in the MTX resistant trypanosomes also suggest DHFR-TS activity is not changed. Strategies like whole-gene sequencing, a gain-of function overexpression library screen, assessing enzyme activity and measuring transcription may be helpful in fully assessing whether DHFR-TS does have a role in drug resistance. This SILAC experiment did not identify FPGS and therefore changes in protein abundance could not be assessed. Results in this thesis have shown that modulating extracellular folate levels did not affect folate uptake into cells, highlighting the likely role of polyglutamylation of folates, by FPGS, in regulating folate metabolism through intracellular retention. FPGS was also a 'hit' in RIT-Seq studies with RTX but not MTX. It would be prudent to examine FPGS further as this may be another mechanism of drug resistance, as well as transport mediated resistance. In these SILAC studies eight proteins were identified that displayed a significant difference in abundance between the resistant parasites and the parental WT; three of which may play important roles in parasite biology, mitochondrial malate dehydrogenase (mMDH) (Blattner *et al*., 1998), phosphoglycerate kinase A (PGKA) (Anderson *et al*., 1998) and p22 protein precursor (Hayman *et al*., 2001; Sprehe *et al*., 2010). Of note, protein 'hits' identified in these SILAC studies were only identified in either MTXR1 or MTXR2 and there were no hits present in both MTX-resistance cell lines. It is essential to validate any SILAC 'hits' e.g. by reverse genetics and showing a phenotypic effect (change in drug EC_{50}). Also repeating these experiments with the modifications discussed above will help verify the significance of the 'hits' that were found in these initial results.

5.3 Concluding remarks

In conclusion, since the 1940s antifolates have been used successfully in the treatment of a number of human diseases ranging from cancer to bacterial infections.

Expanding the knowledge of the mechanism of action and resistance of antifolate drugs in *T. brucei* has enabled a better assessment of their potential use in HAT treatment. Encouragingly, classical antifolates displayed excellent *in vitro* potency. For HAT animal testing, modulation of serum folate and thymidine levels may be needed to accurately assess *in vivo* potency. Oral bioavailability and CNS penetration are two properties that are desirable in determining a clinical candidate for HAT (http://dndi.org). Although lack of CNS penetration is a concern for some antifolate drugs (e.g. RTX, PMX) others have been found to have adequate CNS penetration (e.g. MTX, PYR, TMP) (Clarke *et al*., 2000a; Kumthekar *et al*., 2013; Nau *et al*., 2010; Treon and Chabner, 1996). Although MTX is available in an oral form, it is high dose MTX, through IV infusion that achieves adequate CNS penetration to treat malignancy (Treon and Chabner, 1996). The disadvantages of high dose MTX include long dosing schedules, the need for IV infusion, and toxicity (Treon and Chabner, 1996), and these are likely to limit its use in a HAT setting. A key characteristic in the target product profile (TPP) for a new HAT medicine is that it can be given orally (http://dndi.org). Oral PYR, a crucial part of cerebral toxoplasmosis treatment, has good CNS penetration (McLeod *et al*., 1992; Weiss *et al*., 1988). Although PYR was found to have modest *in vitro* potency against *T. brucei*, adding a *p*ABA-Glu moiety to PYR could lead to improved potency by becoming a substrate for folate transporters. Current clinical antifolates are disappointing candidates for HAT and it may be through designing new or refining existing antifolates that antifolate based therapeutic agents may be exploited for use. Moreover this thesis has explored, and aided in the understanding of, the biological processes involved in folate transport and metabolism, with is beneficial to drug discovery endeavours in the *T .brucei* folate pathway.

Reference List

(2014). Neglected tropical diseases: becoming less neglected. *Lancet 383*, 1269

Abas, L. and Luschnig, C. (2010). Maximum yields of microsomal-type membranes from small amounts of plant material without requiring ultracentrifugation. *Analytical Biochemistry 401*, 217-227

Acestor, N., Panigrahi, A.K., Ogata, Y., Anupama, A. and Stuart, K.D. (2009). Protein composition of *Trypanosoma brucei* mitochondrial membranes. *Proteomics 9*, 5497-5508

Acestor, N., Zikova, A., Dalley, R.A., Anupama, A., Panigrahi, A.K. and Stuart, K.D. (2011). *Trypanosoma brucei* mitochondrial respiratome: composition and organization in procyclic form. *Molecular & Cellular Proeomics 10*, M110

Ahmad, S.I., Kirk, S.H. and Eisenstark, A. (1998). Thymine metabolism and thymineless death in prokaryotes and eukaryotes. *Annual Review of Microbiology 52*, 591-625

Ali, J.A.M., Tagoe, D.N., Munday, J.C., Donachie, A., Morrison, L.J. and De Koning, H.P. (2013a). Pyrimidine biosynthesis is not an essential function for *Trypanosoma brucei* bloodstream forms. *Plos One 8*, e58034

Ali, J.A.M., Creek, D.J., Burgess, K., Allison, H.C., Field, M.C., Maser, P., and De Koning, H.P. (2013b). Pyrimidine salvage in *Trypanosoma brucei* bloodstream forms and the trypanocidal action of halogenated pyrimidines. *Molecular Pharmacology 83*, 439-453.

Ali, M. and Field, M.C. (2013). Cell density-dependent ectopic expression in bloodstream form *Trypanosoma brucei*. *Experimental Parasitology 134*, 249-255

Allen, C.L., Goulding, D. and Field, M.C. (2003). Clathrin-mediated endocytosis is essential in *Trypanosoma brucei*. *EMBO Journal 22*, 4991-5002

Alsford, S., Eckert, S., Baker, N., Glover, L., Sanchez-Flores, A., Leung, K.F., Turner, D.J., Field, M.C., Berriman, M. and Horn, D. (2012). High-throughput decoding of antitrypanosomal drug efficacy and resistance. *Nature 482*, 232-236

Alsford, S. and Horn, D. (2008). Single-locus targeting constructs for reliable regulated RNAi and transgene expression in *Trypanosoma brucei*. *Molecular and Biochemical Parasitology 161*, 76-79

Alsford, S., Kawahara, T., Glover, L. and Horn, D. (2005). Tagging a *T.brucei RRNA* locus improves stable transfection efficiency and circumvents inducible expression position effects. *Molecular and Biochemical Parasitology 144*, 142-148

Anderson, S.A., Carter, V. and Parsons, M. (1998). *Trypanosoma brucei*: Molecular cloning and stage-regulated expression of a malate dehydrogenase localized to the mitochondrion. *Experimental Parasitology 89*, 63-70

Antony, A.C. (1992). The biological chemistry of folate receptors. *Blood 79*, 2807-2820

Antony, A.C. (1996). Folate receptors. *Annaual Review of Nutrition 16*, 501-521

Arrebola, R., Olmo, A., Reche, P., Garvey, E.P., Santi, D.V., Ruiz-Perez, L.M. and Gonzalez-Pacanowska, D. (1994). Isolation and characterization of a mutant dihydrofolate reductase-thymidylate synthase from methotrexate-resistant *Leishmania* cells. *Journal of Biological Chemistry 269*, 10590-10596

Assaraf, Y.G. (2006). The role of multidrug resistance efflux transporters in antifolate resistance and folate homeostasis. *Drug Resistance Updates 9*, 227-246

Bacchi, C.J., Garofalo, J., Ciminelli, M., Rattendi, D., Goldberg, B., McCann, P.P. and Yarlett, N. (1993). Resistance to DL-α-difluoromethylornithine by clinical isolates of *Trypanosoma brucei rhodesiense*. Role of *S*-adenosylmethionine. *Biochemical Pharmacology 46*, 471-481

Backus, H.H., Pinedo, H.M., Wouters, D., Kuiper, C.M., Jansen, G., van Groeningen, C.J. and Peters, G.J. (2000). Differences in the induction of DNA damage, cell cycle arrest, and cell death by 5-fluorouracil and antifolates. *Oncology Research 12*, 231-239

Baker, N., Alsford, S. and Horn, D. (2010). Genome-wide RNAi screens in African trypanosomes identify the nifurtimox activator NTR and the eflornithine transporter AAT6. *Molecular and Biochemical Parasitology 176*, 55-57

Baker, N., Glover, L., Munday, J.C., Aguinaga, A.D., Barrett, M.P., De Koning, H.P. and Horn, D. (2012). Aquaglyceroporin 2 controls susceptibility to melarsoprol and pentamidine in African trypanosomes. *Proceedings of the National Academy of Sciences of the United States of America 109*, 10996-11001

Baltz, T., Baltz, D., Giroud, Ch. and Crockett, J. (1985). Cultivation in a semi-defined medium of animal infective forms of *Trypanosoma brucei*, *T.equiperdum*, *T.evansi*, *T.rhodesiense* and *T.gambiense*. *EMBO Journal 4*, 1273-1277

Begolo, D., Erben, E. and Clayton, C. (2014). Drug target identification using a trypanosome overexpression library. *Antimicrobial Agents and Chemotherapy 58*, 6260-6264

Bello, A.R., Nare, B., Freedman, D., Hardy, L. and Beverley, S.M. (1994). PTR1: a reductase mediating salvage of oxidized pteridines and methotrexate resistance in the protozoan parasite *Leishmania major*. *Proceedings of the National Academy of Sciences of the United States of America 91*, 11442-11446

Bellofatto, V. (2007). Pyrimidine transport activities in trypanosomes. *Trends in Parasitology 23*, 187-189

Berriman, M., Ghedin, E., Hertz-Fowler, C., Blandin, G., Renauld, H., Bartholomeu, D.C., Lennard, N.J., Caler, E., Hamlin, N.E., Haas, B., Bohme, U., Hannick, L., Aslett, M.A., Shallom, J., Marcello, L., Hou, L., Wickstead, B., Alsmark, U.C., Arrowsmith, C., Atkin, R.J., Barron, A.J., Bringaud, F., Brooks, K., Carrington, M., Cherevach, I., Chillingworth, T.J., Churcher, C., Clark, L.N., Corton, C.H., Cronin, A., Davies, R.M., Doggett, J., Djikeng, A., Feldblyum, T., Field, M.C., Fraser, A., Goodhead, I., Hance, Z., Harper, D., Harris, B.R., Hauser, H., Hostetler, J., Ivens, A., Jagels, K., Johnson, D., Johnson, J., Jones, K., Kerhornou, A.X., Koo, H., Larke, N., Landfear, S., Larkin, C., Leech, V., Line, A., Lord, A., MacLeod, A., Mooney, P.J., Moule, S., Martin, D.M., Morgan, G.W., Mungall, K., Norbertczak, H., Ormond, D., Pai, G., Peacock, C.S., Peterson, J., Quail, M.A., Rabbinowitsch, E., Rajandream, M.A., Reitter, C., Salzberg, S.L., Sanders, M., Schobel, S., Sharp, S., Simmonds, M., Simpson, A.J., Tallon, L., Turner, C.M., Tait, A., Tivey, A.R., Van Aken, S., Walker, D., Wanless, D., Wang, S., White, B.,

White, O., Whitehead, S., Woodward, J., Wortman, J., Adams, M.D., Embley, T.M., Gull, K., Ullu, E., Barry, J.D., Fairlamb, A.H., Opperdoes, F., Barrell, B.G., Donelson, J.E., Hall, N., Fraser, C.M., Melville, S.E. and El Sayed, N.M. (2005). The genome of the African trypanosome *Trypanosoma brucei*. *Science 309*, 416-422

Bisser, S., Lumbala, C., Nguertoum, E., Kande, V., Flevaud, L., Vatunga, G., Boelaert, M., Buscher, P., Josenando, T., Bessell, P.R., Bieler, S. and Ndung'u, J.M. (2016). Sensitivity and specificity of a prototype rapid diagnostic test for the detection of *Trypanosoma brucei gambiense* infection: a multi-centric prospective study. *PLoS Neglected Tropical Diseases 10*, e0004608

Blattner, J., Helfert, S., Michels, P. and Clayton, C. (1998). Compartmentation of phosphoglycerate kinase in *Trypanosoma brucei* plays a critical role in parasite energy metabolism. *Proceedings of the National Academy of Sciences of the United States of America 95*, 11596-11600

Bonnet, J., Boudot, C. and Courtioux, B. (2015). Overview of the diagnostic methods used in the field for human African trypanosomiasis: What could change in the next years? *Biomed Research International 2015*, 583262

Brand, S., Cleghorn, L.A.T., McElroy, S.P., Robinson, D.A., Smith, V.C., Hallyburton, I., Harrison, J.R., Norcross, N.R., Spinks, D., Bayliss, T., Norval, S., Stojanovski, L., Torrie, L.S., Frearson, J.A., Brenk, R., Fairlamb, A.H., Ferguson, M.A.J., Read, K.D., Wyatt, P.G. and Gilbert, I.H. (2012). Discovery of a novel class of orally active trypanocidal *N*-myristoyltransferase inhibitors. *Journal of Medicinal Chemistry 55*, 140-152

Brandan, C.P, Padilla, A.M, Xu, D., Tarleton, R.L and Basombrio, M.A. (2011). Knockout of the *dhfr-ts* gene in *Trypanosoma cruzi* generates attenuated parasites able to confer protection against a virulent challenge. *PLoS Neglected Tropical Diseases 5*, e1418

Brolund, A., Sundqvist, M., Kahlmeter, G. and Grape, M. (2010). Molecular characterisation of trimethoprim resistance in *Escherichia coli* and *Klebsiella pneumoniae* during a two year intervention on trimethoprim use. *Plos One 5*, e9233

Broxson, E.H., Jr., Stork, L.C., Allen, R.H., Stabler, S.P. and Kolhouse, J.F. (1989). Changes in plasma methionine and total homocysteine levels in patients receiving methotrexate infusions. *Cancer Research 49*, 5879-5883

Brun, R., Blum, J., Chappuis, F. and Burri, C. (2010). Human African Trypanosomiasis. *Lancet 375*, 148-159

Bunni, M.A., Sirotnak, F.M., Otter, G.M. and Priest, D.G. (1994). Disposition of leucovorin and Its metabolites in the plasma, intestinal epithelium, and intraperitoneal L1210 cells of methotrexate-pretreated mice. *Cancer Chemotherapy and Pharmacology 34*, 455-458

Burkard, G., Fragoso, C.M. and Roditi, I. (2007). Highly efficient stable transformation of bloodstream forms of *Trypanosoma brucei*. *Molecular and Biochemical Parasitology 153*, 220-223

Buscher, P., Mertens, P., Leclipteux, T., Gilleman, Q., Jacquet, D., Mumba-Ngoyi, D., Pyana, P.P., Boelaert, M. and Lejon, V. (2014). Sensitivity and specificity of HAT Sero-K-SeT, a rapid diagnostic test for serodiagnosis of sleeping sickness caused by Trypanosoma brucei gambiense: a case-control study. *Lancet Global Health 2*, e359-e363

Callahan, H.L. and Beverley, S.M. (1992). A member of the aldoketo reductase family confers methotrexate resistance in *Leishmania*. *Journal of Biological Chemistry 267*, 24165-24168

Cao, S., McGuire, J.J. and Rustum, Y.M. (1999). Antitumor activity of ZD1694 (tomudex) against human head and neck cancer in nude mouse models: role of dosing schedule and plasma thymidine. *Clinical Cancer Reearch. 5*, 1925-1934

Carter, J.Y., Loolpapit, M.P., Lema, O.E., Tome, J.L., Nagelkerke, N.J.D. and Watkins, W.M. (2005). Reduction of the efficacy of antifolate antimalarial therapy by folic acid supplementation. *American Journal of Tropical Medicine and Hygiene 73*, 166-170

Carter, N.S. and Fairlamb, A.H. (1993). Arsenical-resistant trypanosomes lack an unusual adenosine transporter [published erratum appears in Nature 1993 Jan 28; 361(6410):374]. *Nature 361*, 173-176

Carver, T., Harris, S.R., Berriman, M., Parkhill, J. and McQuillan, J.A. (2012). Artemis: an integrated platform for visualization and analysis of high-throughput sequence-based experimental data. *Bioinformatics 28*, 464-469

Chandler, C.J., Wang, T.T. and Halsted, C.H. (1986). Pteroylpolyglutamate hydrolase from human jejunal brush borders. Purification and characterization. *Journal of Biological Chemistry 261*, 928-933

Chappuis, F., Loutan, L., Simarro, P., Lejon, V. and Buscher, P. (2005). Options for field diagnosis of human African trypanosomiasis. *Clinical Microbiology Reviews 18*, 133-146

Chen, Z.S., Robey, R.W., Belinsky, M.G., Shchaveleva, I., Ren, X.Q., Sugimoto, Y., Ross, D.D., Bates, S.E. and Kruh, G.D. (2003). Transport of methotrexate, methotrexate polyglutamates, and 17β-estradiol 17-(β-D-glucuronide) by ABCG2: effects of acquired mutations at R482 on methotrexate transport. *Cancer Research 63*, 4048-4054

Chowdhury, S.F., Villamor, V.B., Guerrero, R.H., Leal, I., Brun, R., Croft, S.L., Goodman, J.M., Maes, L., Ruiz-Perez, L.M., Pacanowska, D.G. and Gilbert, I.H. (1999). Design, synthesis, and evaluation of inhibitors of trypanosomal and leishmanial dihydrofolate reductase. *Journal of Medicinal Chemistry 42*, 4300-4312

Chowdhury, S.F., Guerrero, R.H., Brun, R., Ruiz-Perez, L.M., Pacanowska, D.G. and Gilbert, I.H. (2002). Synthesis and testing of 5-benzyl-2,4-diaminopyrimidines as potential inhibitors of leishmanial and trypanosomal dihydrofolate reductase. *Journal of Enzyme Inhibition and Medicinal Chemistry 17*, 293-302

Claes, F., Buscher, P., Touratier, L. and Goddeeris, B. M. (2005). Trypanosoma equiperdum: master of disguise or historical mistake? *Trends in Parasitology 21*, 316–321.

Clarke, S.J., Beale, P.J. and Rivory, L.P. (2000a). Clinical and preclinical pharmacokinetics of raltitrexed. *Clinical Pharmacokinetics 39*, 429-443

Clarke, S.J., Farrugia, D.C., Aherne, G.W., Pritchard, D.M., Benstead, J. and Jackman, A.L. (2000b). Balb/c mice as a preclinical model for raltitrexed-induced gastrointestinal toxicity. *Clinical Cancer Research 6*, 285-296

Coderre, J.A., Beverley, S.M., Schimke, R.T. and Santi, D.V. (1983). Overproduction of a bifunctional thymidylate synthetase-dihydrofolate reductase and DNA amplification in methotrexate-resistant *Leishmania tropica*. *Proceedings of the National Academy of Sciences of the United States of America 80*, 2132-2136

Colasante, C., Pena, D.P., Clayton, C. and Voncken, F. (2009). Mitochondrial carrier family inventory of *Trypanosoma brucei brucei*: Identification, expression and subcellular localisation. *Molecular and Biochemical Parasitology 167*, 104-117

Collar, C.J., Al-Salabi, M.I., Stewart, M.L., Barrett, M.P., Wilson, W.D. and De Koning, H.P. (2009). Predictive computational models of substrate binding by a nucleoside transporter. *Journal of Biological Chemistry 284*, 34028-34035

Cox, J. and Mann, M. (2008). MaxQuant enables high peptide identification rates, individualized p.p.b.-range mass accuracies and proteome-wide protein quantification. *Nature Biotechnology 26*, 1367-1372

Cox, J., Neuhauser, N., Michalski, A., Scheltema, R.A., Olsen, J.V. and Mann, M. (2011). Andromeda: a peptide search engine integrated into the MaxQuant environment. *Journal of Proteome Research 10*, 1794-1805

Creek, D.J., Nijagal, B., Kim, D.H., Rojas, F., Matthews, K.R. and Barrett, M.P. (2013). Metabolomics guides rational development of a simplified cell culture medium for drug screening against *Trypanosoma brucei*. *Antimicrobial Agents and Chemotherapy 57*, 2768-2779

Croft, S.L., Sundar, S. and Fairlamb, A.H. (2006). Drug Resistance in Leishmaniasis. *Clinical Microbiology Reviews 19*, 111-126

Cross, G.A.M. (1975). Identification, purification and properties of clone-specific glycoprotein antigens constituting the surface coat of *Trypanosoma brucei*. *Parasitology 71*, 393-417

Cruz, A. and Beverley, S.M. (1990). Gene replacement in parasitic protozoa. *Nature 348*, 171-173

Cunningham, M.L., Titus, R.G., Turco, S.J. and Beverley, S.M. (2001). Regulation of differentiation to the infective stage of the protozoan parasite *Leishmania major* by tetrahydrobiopterin. *Science 292*, 285-287

Dax, C., Duffieux, F., Chabot, N., Coincon, M., Sygusch, J., Michels, P.A. and Blonski, C. (2006). Selective irreversible inhibition of fructose 1,6-bisphosphate aldolase from *Trypanosoma brucei*. *Journal of Medicinal Chemistry 49*, 1499-1502

De Koning, H.P. and Jarvis, S.M. (1997). Purine nucleobase transport in bloodstream forms of *Trypanosoma brucei brucei* is mediated by two novel transporters. *Molecular and Biochemical Parasitology 89*, 245-258

De Koning, H.P. and Jarvis, S.M. (1999). Adenosine transporters in bloodstream forms of *Trypanosoma brucei brucei:* Substrate recognition motifs and affinity for trypanocidal drugs. *Molecular Pharmacology 56*, 1162-1170

De Rycker, M., O'Neill, S., Joshi, D., Campbell, L., Gray, D.W. and Fairlamb, A.H. (2012). A static-cidal assay for *Trypanosoma brucei* to aid hit prioritisation for progression into drug discovery programmes. *PLoS Neglected Tropical Diseases 6*, e1932

Dean, P.N. and Jett, J.H. (1974). Mathematical analysis of DNA distributions derived from flow microfluorometry. *Journal of Cell Biology 60*, 523-527

Di Gennaro E., Bruzzese, F., Pepe, S., Leone, A., Delrio, P., Subbarayan, P.R., Avallone, A. and Budillon, A. (2009). Modulation of thymidilate synthase and p53 expression by HDAC inhibitor vorinostat resulted in synergistic antitumor effect in combination with 5FU or raltitrexed. *Cancer Biololgy& Therapy 8*, 782-791

Diddens, H., Niethammer, D. and Jackson, R.C. (1983). Patterns of cross-resistance to the antifolate drugs trimetrexate, metoprine, homofolate, and CB3717 in human lymphoma and osteosarcoma cells resistant to methotrexate. *Cancer Research 43*, 5286-5292

Dridi, L., Ouameur, A.A., Ouellette, M. (2010a) High affinity S-Adenosylmethionine plasma membrane transporter of Leishmania is a member of the folate biopterin transporter (FBT) family. *Journal of Biological Chemistry 285*, 19767–19775.

Dridi, L., Haimeur, A. and Ouellette, M. (2010b). Structure-function analysis of the highly conserved charged residues of the membrane protein FT1, the main folic acid transporter of the protozoan parasite Leishmania. *Biochemical Pharmacology 79*, 30-38

Duszenko, M., Ferguson, M.A.J., Lamont, G.S., Rifkin, M.R. and Cross, G.A.M. (1985). Cysteine eliminates the feeder cell requirement for cultivation of *Trypanosoma brucei* bloodstream forms in vitro. *Journal of Experimental Medicine 162*, 1256-1263

El Fadili, A., Kundig, C. and Ouellette, M. (2002). Characterization of the folylpolyglutamate synthetase gene and polyglutamylation of folates in the protozoan parasite Leishmania. *Molecular and Biochemical Parasitology 124*, 63-71

El Fadili, A., Richard, D., Kundig, C. and Ouellette, M. (2003). Effect of polyglutamylation of methotrexate on its accumulation and the development of resistance in the protozoan parasite *Leishmania*. *Biochemical Pharmacology 66*, 999-1008

Ellenberger, T.E. and Beverley, S.M. (1987). Biochemistry and regulation of folate and methotrexate transport in *Leishmania major*. *Journal of Biological Chemistry 262*, 10053-10058

Eperon, G., Balasegaram, M., Potet, J., Mowbray, C., Valverde, O. and Chappuis, F. (2014). Treatment options for second-stage gambiense human African trypanosomiasis. *Expert Review of Anti- infectective Therapy 12*, 1407-1417

Eudes, A., Kunji, E.R.S., Noiriel, A., Klaus, S.M.J., Vickers, T.J., Beverley, S.M., Gregory, J.F. and Hanson, A.D. (2010). Identification of transport-critical residues in a folate transporter from the folate-biopterin transporter (FBT) family. *Journal of Biological Chemistry 285*, 2867-2875

Fairlamb, A.H., Gow, N.A.R., Matthews, K.R. and Waters, A.P. (2016). Drug resistance in eukaryotic microorganisms. *Nature Microbiology 1*, e16092

Fairlamb, A.H., Henderson, G.B. and Cerami, A. (1989). Trypanothione is the primary target for arsenical drugs against African trypanosomes. *Proceedings of the National Academy of Sciences of the United States of America 86*, 2607-2611

Fallingborg, J. (1999). Intraluminal pH of the human gastrointestinal tract. *Danish Medical Buletin. 46*, 183-196

Fenn, K. and Matthews, K.R. (2007). The cell biology of *Trypanosoma brucei* differentiation. *Current Opinion In Microbiology 10*, 539-546

Fernandez-Perez, M.P., Montenegro, M.F., Saez-Ayala, M., Sanchez-del-Campo, L., Pinero-Madrona, A., Cabezas-Herrera, J. and Rodriguez-Lopez, J.N. (2013). Suppression of antifolate resistance by targeting the myosin Va trafficking pathway in melanoma. *Neoplasia. 15*, 826-839

Field, M.C. and Carrington, M. (2009). The trypanosome flagellar pocket. *Nature Reviews Microbiology 7*, 775-786

Fiskerstrand, T., Ueland, P.M. and Refsum, H. (1997). Folate depletion induced by methotrexate affects methionine synthase activity and its susceptibility to inactivation by nitrous oxide. *Journal of Pharmacology and Experimental Therapeutics 282*, 1305-1311

Fox, M.H. (1980). A model for the computer analysis of synchronous DNA distributions obtained by flow cytometry. *Cytometry 1*, 71-77

Franco, J.R., Simarro, P.P., Diarra, A. and Jannin, J.G. (2014). Epidemiology of human African trypanosomiasis. *Clinical Epidemiology 6*, 257-275

Frearson, J.A., Brand, S., McElroy, S.P., Cleghorn, L.A.T., Smid, O., Stojanovski, L., Price, H.P., Guther, M.L.S., Torrie, L.S., Robinson, D.A., Hallyburton, I., Mpamhanga, C.P., Brannigan, J.A., Wilkinson, A.J., Hodgkinson, M., Hui, R., Qiu, W., Raimi, O.G., van Aalten, D.M.F., Brenk, R., Gilbert, I.H., Read, K.D., Fairlamb, A.H., Ferguson, M.A.J., Smith, D.F. and Wyatt, P.G. (2010). *N*-myristoyltransferase inhibitors as new leads to treat sleeping sickness. *Nature 464*, 728-732

Gagnon, D., Foucher, A., Girard, I. and Ouellette, M. (2006). Stage specific gene expression and cellular localization of two isoforms of the serine hydroxymethyltransferase in the protozoan parasite *Leishmania*. *Molecular and Biochemical Parasitology 150*, 63-71

Galivan, J., Ryan, T.J., Chave, K., Rhee, M., Yao, R. and Yin, D.Z. (2000). Glutamyl hydrolase: pharmacological role and enzymatic characterization. *Pharmacology and Therapeutics 85*, 207-215

Garcia-Martinez, J.M., Moran, J., Clarke, R.G., Gray, A., Cosulich, S.C., Chresta, C.M. and Alessi, D.R. (2009). Ku-0063794 is a specific inhibitor of the mammalian target of rapamycin (mTOR). *Biochemical Journal 421*, 29-42

Gascon, J., Bern, C. and Pinazo, M.J. (2010). Chagas disease in Spain, the United States and other non-endemic countries. *Acta Tropica 115*, 22-27

Gazanion, E., Fernandez-Prada, C., Papadopoulou, B., Leprohon, P. and Ouellette, M. (2016). Cos-Seq for high-throughput identification of drug target and resistance

mechanisms in the protozoan parasite *Leishmania*. *Proc. Natl. Acad. Sci. U. S. A 113*, E3012-E3021

Gibson, M.W., Dewar, S., Ong, H.B., Sienkiewicz, N. and Fairlamb, A.H. (2016). *Trypanosoma brucei* DHFR-TS revisited: characterisation of a bifunctional and highly unstable recombinant dihydrofolate reductase-thymidylate synthase. *PLoS Neglected Tropical Diseases 10*, e0004714

Gibson, W. (2003).Species concepts for trypanosomes: from morphological to molecular definitions? Kinetoplastid Biology and Disease 2, 10

Gilbert, I.H. (2002). Inhibitors of dihydrofolate reductase in leishmania and trypanosomes. *Biochimica et Biophysica Acta 1587*, 249-257

Gilbert, I.H. (2013). Drug discovery for neglected diseases: molecular target-based and phenotypic approaches. *Journal of Medicinal Chemistry 56*, 7719-7726

Giordani, F., Morrison, L.J., Rowan, T.G., De Koning H.P. and Barrett, M.P. (2016).The animal trypanosomiases and their chemotherapy: a review. *Parasitology 143*, 1862-1889

Glover, L., Alsford, S., Baker, N., Turner, D.J., Sanchez-Flores, A., Hutchinson, S., Hertz-Fowler, C., Berriman, M. and Horn, D. (2015). Genome-scale RNAi screens for high-throughput phenotyping in bloodstream-form African trypanosomes. *Nature Protocols 10*, 106-133

Goldman, I.D. (1971). The characteristics of the membrane transport of amethopterin and the naturally occurring folates. *Annals of the New York Academy of Sciences 186*, 400-422

Goldman, I.D., Lichtenstein, N.S. and Oliverio, V.T. (1968). Carrier-mediated transport of the folic acid analogue, methotrexate, in the L1210 leukemia cell. *Journal of Biological Chemistry 243*, 5007-5017

Gonen, N. and Assaraf, Y.G. (2012). Antifolates in cancer therapy: structure, activity and mechanisms of drug resistance. *Drug Resistance Updates 15*, 183-210

Graf, F.E., Baker, N., Munday, J.C., De Koning, H.P., Horn, D. and Maser, P. (2015). Chimerization at the *AQP2-AQP3* locus is the genetic basis of melarsoprol-pentamidine cross-resistance in clinical *Trypanosoma brucei gambiense* isolates. *International Journal for Parasitology: Drugs and Drug Resistance 5*, 65-68

Graf, F.E., Ludin, P., Arquint, C., Schmidt, R.S., Schaub, N., Kunz, R.C., Munday, J.C., Krezdorn, J., Baker, N., Horn, D., Balmer, O., Caccone, A., De Koning, H.P. and Maser, P. (2016). Comparative genomics of drug resistance in *Trypanosoma brucei rhodesiense*. *Cellular and Molecular Life Sciences 73*, 3387-3400

Graf, F.E., Ludin, P., Wenzler, T., Kaiser, M., Brun, R., Pyana, P.P., Buscher, P., De Koning, H.P., Horn, D. and Maser, P. (2013). Aquaporin 2 mutations in *Trypanosoma brucei gambiense* field isolates correlate with decreased susceptibility to pentamidine and melarsoprol. *PLoS Neglected Tropical Diseases 7*, e2475

Gregson, A. and Plowe, C.V. (2005). Mechanisms of resistance of malaria parasites to antifolates. *Pharmacological Reviews 57*, 117-145

Greig, N., Wyllie, S., Patterson, S. and Fairlamb, A.H. (2009). A comparative study of methylglyoxal metabolism in trypanosomatids. *FEBS Journal 276*, 376-386

Hall, B.S., Bot, C. and Wilkinson, S.R. (2011). Nifurtimox activation by trypanosomal type I nitroreductases generates cytotoxic nitrile metabolites. *Journal of Biological Chemistry 286*, 13088-13095

Hayman, M.L., Miller, M.M., Chandler, D.M., Goulah, C.C. and Read, L.K. (2001). The trypanosome homolog of human p32 interacts with RBP16 and stimulates its gRNA binding activity. *Nucleic Acids Research 29*, 5216-5225

Hertz-Fowler, C., Figueiredo, L.M., Quail, M.A., Becker, M., Jackson, A., Bason, N., Brooks, K., Churcher, C., Fahkro, S., Goodhead, I., Heath, P., Kartvelishvili, M., Mungall, K., Harris, D., Hauser, H., Sanders, M., Saunders, D., Seeger, K., Sharp, S., Taylor, J.E., Walker, D., White, B., Young, R., Cross, G.A., Rudenko, G., Barry, J.D., Louis, E.J. and Berriman, M. (2008). Telomeric expression sites are highly conserved in *Trypanosoma brucei*. *Plos One 3*, e3527

Hirumi, H., Doyle, J.J. and Hirumi, K. (1977). Cultivation of bloodstream *Trypanosoma brucei*. *Bulletin of the World Health Organization 55*, 405-409

Hirumi, H. and Hirumi, K. (1989). Continuous cultivation of *Trypanosoma brucei* blood stream forms in a medium containing a low concentration of serum protein without feeder cell layers. *Journal of Parasitology 75*, 985-989

Hoose, S.A., Duran, C., Malik, I., Eslamfam, S., Shasserre, S.C., Downing, S.S., Hoover, E.M., Dowd, K.E., Smith, R., III and Polymenis, M. (2012). Systematic analysis of cell cycle effects of common drugs leads to the discovery of a suppressive interaction between gemfibrozil and fluoxetine. *Plos One 7*, e36503

Horn, D. (2014). Antigenic variation in African trypanosomes. *Molecular and Biochemical Parasitology 195*, 123-129

Horn, D. and Cross, G.A.M. (1997). Analysis of Trypanosoma brucei vsg expression site switching in vitro. *Molecular and Biochemical Parasitology 84*, 189-201

Howell, S.B., Mansfield, S.J. and Taetle, R. (1981). Thymidine and hypoxanthine requirements of normal and malignant human cells for protection against methotrexate cytotoxicity. *Cancer Research 41*, 945-950

Hum, D.W., Bell, A.W., Rozen, R. and Mackenzie, R.E. (1988). Primary structure of a human trifunctional enzyme. Isolation of a cDNA encoding methylenetetrahydrofolate dehydrogenase-methenyltetrahydrofolate cyclohydrolase-formyltetrahydrofolate synthetase. *Journal of Biological Chemistry 263*, 15946-15950

Ifergan, I., Shafran, A., Jansen, G., Hooijberg, J.H., Scheffer, G.L. and Assaraf, Y.G. (2004). Folate deprivation results in the loss of breast cancer resistance protein (BCRP/ABCG2) expression. A role for BCRP in cellular folate homeostasis. *Journal of Biological Chemistry 279*, 25527-25534

Irungu, B., Kiboi, D., Langat, B., Rukunga, G., Wittlin, S. and Nzila, A. (2009). Methotrexate and aminopterin lack in vivo antimalarial activity against murine malaria species. *Experimental Parasitology 123*, 118-121

Iten, M., Mett, H., Evans, A., Enyaru, J.C.K., Brun, R. and Kaminsky, R. (1997). Alterations in ornithine decarboxylase characteristics account for tolerance of *Trypanosoma brucei rhodesiense* to D,L-alpha-difluoromethylornithine. *Antimicrobial Agents and Chemotherapy 41*, 1922-1925

Jackman, A.L., Taylor, G.A., Gibson, W., Kimbell, R., Brown, M., Calvert, A.H., Judson, I.R. and Hughes, L.R. (1991). ICI D1694, a quinazoline antifolate thymidylate synthase inhibitor that is a potent inhibitor of L1210 tumor cell growth *in vitro* and *in vivo*: a new agent for clinical study. *Cancer Research 51*, 5579-5586

Jackson, R.C., Fry, D.W., Boritzki, T.J., Besserer, J.A., Leopold, W.R., Sloan, B.J. and Elslager, E.F. (1984). Biochemical pharmacology of the lipophilic antifolate, trimetrexate. *Advances in Enzyme Regulation 22*, 187-206

Jacobs, R.T., Nare, B. and Phillips, M.A. (2011a). State of the art in African trypanosome drug discovery. *Current Topics in Medicinal Chemistry 11*, 1255-1274

Jacobs, R.T., Plattner, J.J., Nare, B., Wring, S.A., Chen, D., Freund, Y., Gaukel, E.G., Orr, M.D., Perales, J.B., Jenks, M., Noe, R.A., Sligar, J.M., Zhang, Y.K., Bacchi, C.J., Yarlett, N. and Don, R. (2011b). Benzoxaboroles: a new class of potential drugs for human African trypanosomiasis. *Future Medicinal Chemistry 3*, 1259-1278

Jones, D.C., Foth, B.J., Urbaniak, M.D., Patterson, S., Ong, H.B., Berriman, M. and Fairlamb, A.H. (2015). Genomic and proteomic studies on the mode of action of oxaboroles against the African trypanosome. *PLoS Neglected Tropical Diseases 9*, e0004299

Jones, D.C., Hallyburton, I., Stojanovski, L., Read, K.D., Frearson, J.A. and Fairlamb, A.H. (2010). Identification of a kappa-opioid agonist as a potent and selective lead for drug development against human African trypanosomiasis. *Biochemical Pharmacology 80*, 1478-1486

Kaur, K., Coons, T., Emmett, K. and Ullman, B. (1988). Methotrexate-resistant *Leishmania donovani* genetically deficient in the folate-methotrexate transporter. *Journal of Biological Chemistry 263*, 7020-7028

Kazibwe, A.J., Nerima, B., De Koning, H.P., Maser, P., Barrett, M.P. and Matovu, E. (2009). Genotypic status of the TbAT1/P2 adenosine transporter of *Trypanosoma brucei gambiense* isolates from Northwestern Uganda following melarsoprol withdrawal. *PLoS Neglected Tropical Diseases 3*, e523

Kelly, S., Reed, J., Kramer, S., Ellis, L., Webb, H., Sunter, J., Salje, J., Marinsek, N., Gull, K., Wickstead, B. and Carrington, M. (2007). Functional genomics in *Trypanosoma brucei*: a collection of vectors for the expression of tagged proteins from endogenous and ectopic gene loci. *Molecular and Biochemical Parasitology 154*, 103-109

Khabnadideh, S., Pez, D., Musso, A., Brun, R., Perez, L.M., González-Pacanowska, D. and Gilbert I.H. (2005). Design, synthesis and evaluation of 2,4-diaminoquinazolines as inhibitors of trypanosomal and leishmanial dihydrofolate reductase. *Bioorganic and Medicinal Chemistry 13*, 2637- 2649

Khodursky, A., Guzman, E.C. and Hanawalt, P.C. (2015). Thymineless death lives on: new insights into a classic phenomenon. *Annual Review of Microbiology 69*, 247-263

Kinsella, A.R., Smith, D. and Pickard, M. (1997). Resistance to chemotherapeutic antimetabolites: a function of salvage pathway involvement and cellular response to DNA damage. *British Journal of Cancer 75*, 935-945

Klaus, S.M., Kunji, E.R., Bozzo, G.G., Noiriel, A., de la Garza, R.D., Basset, G.J., Ravanel, S., Rebeille, F., Gregory, J.F., III and Hanson, A.D. (2005). Higher plant plastids and cyanobacteria have folate carriers related to those of trypanosomatids. *Journal of Biological Chemistry 280*, 38457-38463

Krogh, A., Larsson, B., von, H.G. and Sonnhammer, E.L. (2001). Predicting transmembrane protein topology with a hidden Markov model: application to complete genomes. *Journal of Molecular Biology 305*, 567-580

Kuboki, N., Inoue, N., Sakurai, T., Di, C.F., Grab, D.J., Suzuki, H., Sugimoto, C. and Igarashi, I. (2003). Loop-mediated isothermal amplification for detection of African trypanosomes. *Journal of Clinical Microbiology 41*, 5517-5524

Kumthekar, P., Grimm, S.A., Avram, M.J., Kaklamani, V., Helenowski, I., Rademaker, A., Cianfrocca, M., Gradishar, W., Patel, J., Mulcahy, M., McCarthy, K. and Raizer, J.J. (2013). Pharmacokinetics and efficacy of pemetrexed in patients with brain or leptomeningeal metastases. *Journal of Neuro-Oncology 112*, 247-255

Kundig, C., Haimeur, A., Legare, D., Papadopoulou, B. and Ouellette, M. (1999). Increased transport of pteridines compensates for mutations in the high affinity folate transporter and contributes to methotrexate resistance in the protozoan parasite *Leishmania tarentolae*. *EMBO Journal 18*, 2342-2351

L'Hostis, C., Geindre, M. and Deshusses, J. (1993). Active transport of L-proline in the protozoan parasite Trypanosoma brucei brucei. *Biochemical Journal 291*, (pp 297-301)

La, G.F. and Magez, S. (2011). Vaccination against trypanosomiasis: can it be done or is the trypanosome truly the ultimate immune destroyer and escape artist? *Human Vaccines 7*, 1225-1233

Lakhdar-Ghazal, F., Blonski, C., Willson, M., Michels, P. and Perie, J. (2002). Glycolysis and proteases as targets for the design of new anti-trypanosome drugs. *Current Topics in Medicinal Chemistry 2*, 439-456

Langmead, B. and Salzberg, S.L. (2012). Fast gapped-read alignment with Bowtie 2. *Nature Methods 9*, 357-359

Langousis, G. and Hill, K.L. (2014). Motility and more: the flagellum of *Trypanosoma brucei*. *Nature Reviews Microbiology 12*, 505-518

Lawrence, S.A., Hackett, J.C. and Moran, R.G. (2011). Tetrahydrofolate recognition by the mitochondrial folate transporter. *Journal of Biological Chemistry 286*, 31480-31489

Le Manach C., Scheurer, C., Sax, S., Schleiferbock, S., Cabrera, D.G., Younis, Y., Paquet, T., Street, L., Smith, P., Ding, X.C., Waterson, D., Witty, M.J., Leroy, D., Chibale, K. and Wittlin, S. (2013). Fast in vitro methods to determine the speed of action and the stage-specificity of anti-malarials in *Plasmodium falciparum*. *Malaria Journal 12*, 424

Lejon, V., Legros, D., Richer, M., Ruiz, J.A., Jamonneau, V., Truc, P., Doua, F., Dje, N., N'Siesi, F.X., Bisser, S., Magnus, E., Wouters, I., Konings, J., Vervoort, T., Sultan, F. and Buscher, P. (2002). IgM quantification in the cerebrospinal fluid of sleeping sickness patients by a latex card agglutination test. *Tropical Medicine and International Health 7*, 685-692

Lemley, C., Yan, S.F., Dole, V.S., Madhubala, R., Cunningham, M.L., Beverley, S.M., Myler, P.J. and Stuart, K.D. (1999). The *Leishmania donovani* LD1 locus gene ORFG encodes a biopterin transporter (BT1). *Molecular and Biochemical Parasitology 104,* 93-105

Lennard, L. (1999). Therapeutic drug monitoring of antimetabolic cytotoxic drugs. *British Journal of Clinical Pharmacology 47*, 131-143

Li, H., Handsaker, B., Wysoker, A., Fennell, T., Ruan, J., Homer, N., Marth, G., Abecasis, G. and Durbin, R. (2009). The Sequence Alignment/Map format and SAMtools. *Bioinformatics 25*, 2078-2079

Li, W., Cowley, A., Uludag, M., Gur, T., McWilliam, H., Squizzato, S., Park, Y.M., Buso, N. and Lopez, R. (2015). The EMBL-EBI bioinformatics web and programmatic tools framework. *Nucleic Acids Research 43*, W580-W584

Lin, B.F., Huang, R.F. and Shane, B. (1993). Regulation of folate and one-carbon metabolism in mammalian cells. III. Role of mitochondrial folylpoly-γ-glutamate synthetase. *Journal of Biological Chemistry 268*, 21674-21679

Longley D.B., Harkin, D.P and Johnstone, P.G. (2003). 5-flourouracil: mechanisms of action and clinical strategies. *Nature Reviews Cancer 3,* 330-338

Lutje, V., Seixas, J. and Kennedy, A. (2013). Chemotherapy for second-stage human African trypanosomiasis. *Cochrane Database Syst. Rev. 6*, CD006201

Lye, L.F., Owens, K., Shi, H., Murta, S.M., Vieira, A.C., Turco, S.J., Tschudi, C., Ullu, E. and Beverley, S.M. (2010). Retention and loss of RNA interference pathways in trypanosomatid protozoans. *PLoS Pathogens 6*, e1001161

Maser, P., Luscher, A. and Kaminsky, R. (2003). Drug transport and drug resistance in African trypanosomes. *Drug Resistance Updates 6*, 281-290

Maser, P., Sutterlin, C., Kralli, A. and Kaminsky, R. (1999). A nucleoside transporter from *Trypanosoma brucei* involved in drug resistance. *Science 285*, 242-244

Massimine, K.M., Doan, L.T., Atreya, C.A., Stedman, T.T., Anderson, K.S., Joiner, K.A. and Coppens, I. (2005). *Toxoplasma gondii* is capable of exogenous folate transport. A likely expansion of the BT1 family of transmembrane proteins. *Molecular and Biochemical Parasitology 144*, 44-54

Matherly, L.H. and Hou, Z. (2008). Structure and function of the reduced folate carrier a paradigm of a major facilitator superfamily mammalian nutrient transporter. *Vitamins and Hormones 79*, 145-184

Matovu, E., Enyaru, J.C.K., Legros, D., Schmid, C., Seebeck, T. and Kaminsky, R. (2001). Melarsoprol refractory *T.b. gambiense* from Omugo, north-western Uganda. *Tropical Medicine and International Health 6*, 407-411

Matthews, K.R. and Gull, K. (1998). Identification of stage-regulated and differentiation-enriched transcripts during transformation of the African trypanosome from its bloodstream to procyclic form. *Molecular and Biochemical Parasitology 95*, 81-95

McGuire, J.J., Russell, C.A. and Balinska, M. (2000). Human cytosolic and mitochondrial folylpolyglutamate synthetase are electrophoretically distinct. Expression in antifolate-sensitive and -resistant human cell lines. *Journal of Biological Chemistry 275*, 13012-13016

McLeod, R., Mack, D., Foss, R., Boyer, K., Withers, S., Levin, S. and Hubbell, J. (1992). Levels of pyrimethamine in sera and cerebrospinal and ventricular fluids from infants treated for congenital toxoplasmosis. Toxoplasmosis Study Group. *Antimicrobial Agents and Chemotherapy 36*, 1040-1048

Mpamhanga, C.P., Spinks, D., Tulloch, L.B., Shanks, E.J., Robinson, D.A., Collie, I.T., Fairlamb, A.H., Wyatt, P.G., Frearson, J.A., Hunter, W.N., Gilbert, I.H. and Brenk, R. (2009). One scaffold, three binding modes: novel and selective pteridine reductase 1 Inhibitors derived from fragment hits discovered by virtual screening. *Journal of Medicinal Chemistry 52*, 4454-4465

Mugasa, C.M., Adams, E.R., Boer, K.R., Dyserinck, H.C., Buscher, P., Schallig, H.D. and Leeflang, M.M. (2012). Diagnostic accuracy of molecular amplification tests for human African trypanosomiasis--systematic review. *PLoS Neglected Tropical Diseases 6*, e1438

Munday, J.C., Eze, A.A., Baker, N., Glover, L., Clucas, C., Aguinaga, A.D., Natto, M.J., Teka, I.A., McDonald, J., Lee, R.S., Graf, F.E., Ludin, P., Burchmore, R.J., Turner, C.M., Tait, A., MacLeod, A., Maser, P., Barrett, M.P., Horn, D. and De Koning, H.P. (2014). *Trypanosoma brucei* aquaglyceroporin 2 is a high-affinity transporter for pentamidine and melaminophenyl arsenic drugs and the main genetic determinant of resistance to these drugs. *Journal of Antimicrobial Chemotherapy 69*, 651-663

Munday, J.C., Settimo, L. and De Koning, H.P. (2015). Transport proteins determine drug sensitivity and resistance in a protozoan parasite, *Trypanosoma brucei*. *Frontiers in Pharmacology 6*, 32

Murta, S.M., Vickers, T.J., Scott, D.A. and Beverley, S.M. (2009). Methylene tetrahydrofolate dehydrogenase/cyclohydrolase and the synthesis of 10-CHO-THF are essential in *Leishmania major*. *Molecular Microbiology 71*, 1386-1401

Nare, B., Hardy, L.W. and Beverley, S.M. (1997). The roles of pteridine reductase 1 and dihydrofolate reductase-thymidylate synthase in pteridine metabolism in the protozoan parasite *Leishmania major*. *Journal of Biological Chemistry 272*, 13883-13891

Nau, R., Sorgel, F. and Eiffert, H. (2010). Penetration of drugs through the blood-cerebrospinal fluid/blood-brain barrier for treatment of central nervous system infections. *Clinical Microbiology Reviews 23*, 858-883

Njiru, Z.K., Mikosza, A.S.J., Armstrong, T., Enyaru, J.C., Ndung'u, J.M. and Thompson, A.R.C. (2008). Loop-mediated isothermal amplification (LAMP) method for rapid detection of *Trypanosoma brucei rhodesiense*. *PLoS Neglected Tropical Diseases 2,* e147

Oduor, R.O., Ojo, K.K., Williams, G.P., Bertelli, F., Mills, J., Maes, L., Pryde, D.C., Parkinson, T., Van Voorhis, W.C. and Holler, T.P. (2011). *Trypanosoma brucei* glycogen synthase

kinase-3, a target for anti-trypanosomal drug development: a public-private partnership to identify novel leads. *PLoS Neglected Tropical Diseases 5*, e1017

Omasits, U., Ahrens, C.H., Muller, S. and Wollscheid, B. (2014). Protter: interactive protein feature visualization and integration with experimental proteomic data. *Bioinformatics 30*, 884-886

Ong, H.B., Sienkiewicz, N., Wyllie, S. and Fairlamb, A.H. (2011). Dissecting the metabolic roles of pteridine reductase 1 in *Trypanosoma brucei* and *Leishmania major*. *Journal of Biological Chemistry 286*, 10429-10438

Ong, H.B., Sienkiewicz, N., Wyllie, S., Patterson, S. and Fairlamb, A.H. (2013). *Trypanosoma brucei* (UMP synthase null mutants) are avirulent in mice, but recover virulence upon prolonged culture in vitro while retaining pyrimidine auxotrophy. *Molecular Microbiology 90*, 443-455

Ouameur, A.A., Girard, I., Legare, D. and Ouellette, M. (2008). Functional analysis and complex gene rearrangements of the folate/biopterin transporter (FBT) gene family in the protozoan parasite *Leishmania*. *Molecular and Biochemical Parasitology 162*, 155-164

Ouma, P., Parise, M.E., Hamel, M.J., Ter Kuile, F.O., Otieno, K., Ayisi, J.G., Kager, P.A., Steketee, R.W., Slutsker, L. and van Eijk, A.M. (2006). A randomized controlled trial of folate supplementation when treating malaria in pregnancy with sulfadoxine-pyrimethamine. *PloS Clinical Trials 1*, e28

Panigrahi, A.K., Ogata, Y., Zikova, A., Anupama, A., Dalley, R.A., Acestor, N., Myler, P.J. and Stuart, K.D. (2009). A comprehensive analysis of *Trypanosoma brucei* mitochondrial proteome. *Proteomics 9*, 434-450

Papadopoulou, B., Roy, G. and Ouellette, M. (1992). A novel antifolate resistance gene on the amplified H circle of *Leishmania*. *EMBO Journal 11*, 3601-3608

Paulsen, I.T. (2003). Multidrug efflux pumps and resistance: regulation and evolution. *Current Opinion In Microbiology 6*, 446-451

Pena, I., Pilar, M.M., Cantizani, J., Kessler, A., Alonso-Padilla, J., Bardera, A.I., Alvarez, E., Colmenarejo, G., Cotillo, I., Roquero, I., de Dios-Anton, F., Barroso, V., Rodriguez, A., Gray, D.W., Navarro, M., Kumar, V., Sherstnev, A., Drewry, D.H., Brown, J.R., Fiandor, J.M. and Julio, M.J. (2015). New compound sets identified from high throughput phenotypic screening against three kinetoplastid parasites: an open resource. *Scientific Reports 5*, 8771

Peters, G.J., Smitskamp-Wilms, E., Smid, K., Pinedo, H.M. and Jansen, G. (1999). Determinants of activity of the antifolate thymidylate synthase inhibitors Tomudex (ZD1694) and GW1843U89 against mono- and multilayered colon cancer cell lines under folate-restrided conditions. *Cancer Research 59*, 5529-5535

Pez, D., Leal, I., Zuccotto, F., Boussard, C., Brun, R., Croft, S.L., Yardley, V., Ruiz Perez, L.M., Gonzalez-Pacanowska, D. and Gilbert I.H. (2003). 2,4-Diaminopyrimidines as inhibitors of Leishmanial and Trypanosomal dihydrofolate reductase. *Bioorganic and Medicinal Chemistry 11*, 4693- 4711

Phan, J., Koli, S., Minor, W., Dunlap, R.B., Berger, S.H. and Lebioda, L. (2001). Human thymidylate synthase is in the closed conformation when complexed with dUMP and raltitrexed, an antifolate drug. *Biochemistry 40*, 1897-1902

Priotto, G., Fogg, C., Balasegaram, M., Erphas, O., Louga, A., Checchi, F., Ghabri, S. and Piola, P. (2006). Three drug combinations for late-stage *Trypanosoma brucei gambiense* sleeping sickness: a randomized clinical trial in Uganda. *PloS Clinical Trials 1*, e39

Pyana, P.P., Van Reet, N., Mumba, N.D., Ngay, L.I., Karhemere, B.S.S. and Buscher, P. (2014). Melarsoprol sensitivity profile of *Trypanosoma brucei gambiense* isolates from cured and relapsed sleeping sickness patients from the Democratic Republic of the Congo. *PLoS Neglected Tropical Diseases 8*, e3212

Qiu, A.D., Jansen, M., Sakaris, A., Min, S.H., Chattopadhyay, S., Tsai, E., Sandoval, C., Zhao, R.B., Akabas, M.H. and Goldman, I.D. (2006). Identification of an intestinal folate transporter and the molecular basis for hereditary folate malabsorption. *Cell 127*, 917-928

Quinlivan, E.P., McPartlin, J., Weir, D.G. and Scott, J. (2000). Mechanism of the antimicrobial drug trimethoprim revisited. *FASEB Journal 14*, 2519-2524

Radwanska, M., Guirnalda, P., De, T.C., Ryffel, B., Black, S. and Magez, S. (2008). Trypanosomiasis-induced B cell apoptosis results in loss of protective anti-parasite antibody responses and abolishment of vaccine-induced memory responses. *PLoS Pathogens 4*, e1000078

Raz, B., Iten, M., Grether-Buhler, Y., Kaminsky, R. and Brun, R. (1997). The Alamar Blue assay to determine drug sensitivity of African trypanosomes (*T.b.rhodesiense* and *T.b.gambiense*) in vitro. *Acta Tropica 68*, 139-147

Redmond, S., Vadivelu, J. and Field, M.C. (2003). RNAit: an automated web-based tool for the selection of RNAi targets in Trypanosoma brucei. *Molecular and Biochemical Parasitology 128*, 115-118

Reuner, B., Vassella, E., Yutzy, B. and Boshart, M. (1997). Cell density triggers slender to stumpy differentiation of *Trypanosoma brucei* bloodstream forms in culture. *Molecular and Biochemical Parasitology 90*, 269-280

Richard, D., Kundig, C. and Ouellette, M. (2002). A new type of high affinity folic acid transporter in the protozoan parasite *Leishmania* and deletion of its gene in methotrexate-resistant cells. *Journal of Biological Chemistry 277*, 29460-29467

Richard, D., Leprohon, P., Drummelsmith, J. and Ouellette, M. (2004). Growth phase regulation of the main folate transporter of *Leishmania infantum* and its role in methotrexate resistance. *Journal of Biological Chemistry 279*, 54494-54501

Rijnboutt, S., Jansen, G., Posthuma, G., Hynes, J.B., Schornagel, J.H. and Strous, G.J. (1996). Endocytosis of GPI-linked membrane folate receptor-alpha. *Journal of Cell Biology 132*, 35-47

Robays, J., Nyamowala, G., Sese, C., Betu Ku Mesu Kande, V., Lutumba, P., Van der Veken, W. and Boelaert, M. (2008). High failure rates of melarsoprol for sleeping sickness, Democratic Republic of Congo. *Emerging Infectious Diseases 14*, 966-967

Robello, C., Navarro, P., Castanys, S. and Gamarro, F. (1997). A pteridine reductase gene ptr1 contiguous to a P-glycoprotein confers resistance to antifolates in *Trypanosoma cruzi*. *Molecular and Biochemical Parasitology 90*, 525-535

Rock, F.L., Mao, W.M., Yaremchuk, A., Tukalo, M., Crepin, T., Zhou, H.C., Zhang, Y.K., Hernandez, V., Akama, T., Baker, S.J., Plattner, J.J., Shapiro, L., Martinis, S.A., Benkovic, S.J., Cusack, S. and Alley, M.R.K. (2007). An antifungal agent inhibits an aminoacyl-tRNA synthetase by trapping tRNA in the editing site. *Science 316*, 1759-1761

Roy, G. and Ouellette, M. (2015). Inactivation of the cytosolic and mitochondrial serine hydroxymethyl transferase genes in *Leishmania major*. *Molecular and Biochemical Parasitology 204*, 106-110

Schmitz, J.C., Grindey, G.B., Schultz, R.M. and Priest, D.G. (1994). Impact of dietary folic-acid on reduced folates in mouse plasma and tissues - relationship to dideazatetrahydrofolate sensitivity. *Biochemical Pharmacology 48*, 319-325

Schneider, A., Charriere, F., Pusnik, M. and Horn, E.K. (2007). Isolation of mitochondria from procyclic *Trypanosoma brucei*. *Methods Mol. Biol. 372*, 67-80

Schormann, N., Pal, B., Senkovich, O., Carson, M., Howard, A., Smith, C., Delucas, L. and Chattopadhyay, D. (2005). Crystal structure of *Trypanosoma cruzi* pteridine reductase 2 in complex with a substrate and an inhibitor. *Journal of Structural Biology 152*, 64-75

Schormann, N., Senkovich, O., Walker, K., Wright, D.L., Anderson, A.C., Rosowsky, A., Ananthan, S., Shinkre, B., Velu, S. and Chattopadhyay, D. (2008). Structure-based approach to pharmacophore identification, in silico screening, and three-dimensional quantitative structure-activity relationship studies for inhibitors of *Trypanosoma cruzi* dihydrofolate reductase function. *Proteins: Structure, Function and Genetics 73*, 889-901

Schumann-Burkard G., Jutzi, P. and Roditi, I. (2011). Genome-wide RNAi screens in bloodstream form trypanosomes identify drug transporters. *Molecular and Biochemical Parasitology 175*, 91-94

Scientific Working Group. (2004). Report on Leishmaniasis. *TDR/SWG/04*, 1-137

Scott, D.A., Hickerson, S.M., Vickers, T.J. and Beverley, S.M. (2008). The role of the mitochondrial glycine cleavage complex in the metabolism and virulence of the protozoan parasite *Leishmania major*. *Journal of Biological Chemistry 283*, 155-165

Senkovich, O., Pal, B., Schormann, N. and Chattopadhyay, D. (2003). *Trypanosoma cruzi* genome encodes a pteridine reductase 2 protein. *Molecular and Biochemical Parasitology 127*, 89-92

Senkovich, O., Schormann, N. and Chattopadhyay, D. (2009). Structures of dihydrofolate reductase-thymidylate synthase of *Trypanosoma cruzi* in the folate-free state and in complex with two antifolate drugs, trimetrexate and methotrexate. *Acta Crystallographica Section D, Biological Crystallography 65*, 704-716

Shahi, S.K., Krauth-Siegel, R.L. and Clayton, C.E. (2002). Overexpression of the putative thiol conjugate transporter *Tb*MRPA causes melarsoprol resistance in *Trypanosoma brucei*. *Molecular Microbiology 43*, 1129-1138

Shanks, E.J., Ong, H.B., Robinson, D.A., Thompson, S., Sienkiewicz, N., Fairlamb, A.H. and Frearson, J.A. (2010). Development and validation of a cytochrome *c*-coupled assay for pteridine reductase 1 and dihydrofolate reductase. *Analytical Biochemistry 396*, 194-203

Shapiro, T.A. and Englund, P.T. (1995). The structure and replication of kinetoplast DNA. *Annual Review of Microbiology 49*, 117-143

Shea, B., Swinden, M.V., Ghogomu, E.T., Ortiz, Z., Katchamart, W., Rader, T., Bombardier, C., Wells, G.A. and Tugwell, P. (2014). Folic acid and folinic acid for reducing side effects in patients receiving methotrexate for rheumatoid arthritis. *J. Rheumatol. 41*, 1049-1060

Shih, C., Chen, V.J., Gossett, L.S., Gates, S.B., MacKellar, W.C., Habeck, L.L., Shackelford, K.A., Mendelsohn, L.G., Soose, D.J., Patel, V.F., Andis, S.L., Bewley, J.R., Rayl, E.A., Moroson, B.A., Beardsley, G.P., Kohler, W., Ratnam, M. and Schultz, R.M. (1997). LY231514, a pyrrolo[2,3-d]pyrimidine-based antifolate that inhibits multiple folate-requiring enzymes. *Cancer Research 57*, 1116-1123

Shiroky, J.B., Neville, C., Esdaile, J.M., Choquette, D., Zummer, M., Hazeltine, M., Bykerk, V., Kanji, M., St-Pierre, A., Robidoux, L. and . (1993). Low-dose methotrexate with leucovorin (folinic acid) in the management of rheumatoid arthritis. Results of a multicenter randomized, double-blind, placebo-controlled trial. *Arthritis & Rheumatology 36*, 795-803

Sienkiewicz, N., Jaroslawski, S., Wyllie, S. and Fairlamb, A.H. (2008). Chemical and genetic validation of dihydrofolate reductase-thymidylate synthase as a drug target in African trypanosomes. *Molecular Microbiology 69*, 520-533

Sienkiewicz, N., Ong, H.B. and Fairlamb, A.H. (2010). *Trypanosoma brucei* pteridine reductase 1 is essential for survival *in vitro* and for virulence in mice. *Molecular Microbiology 77*, 658-671

Simarro, P.P., Cecchi, G., Franco, J.R., Paone, M., Diarra, A., Ruiz-Postigo, J.A., Fevre, E.M., Mattioli, R.C. and Jannin, J.G. (2012). Estimating and mapping the population at risk of sleeping sickness. *PLoS Neglected Tropical Diseases 6*, e1859

Sirotnak, F.M. (1985). Obligate genetic expression in tumor cells of a fetal membrane property mediating "folate" transport: biological significance and implications for improved therapy of human cancer. *Cancer Research 45*, 3992-4000

Sirotnak, F.M. and Tolner, B. (1999). Carrier-mediated membrane transport of folates in mammalian cells. *Annual Review of Nutrition 19*, 91-122

Sistrom, M., Evans, B., Benoit, J., Balmer, O., Aksoy, S. and Caccone A. (2016). De Novo Genome Assembly Shows Genome Wide Similarity between Trypanosoma brucei brucei and Trypanosoma brucei rhodesiense. *PLoS One 24*, 11 e0147660

Sobrero, A.F. and Bertino, J.R. (1986). Endogenous thymidine and hypoxanthine are a source of error in evaluating methotrexate cytotoxicity by clonogenic assays using undialyzed fetal bovine serum. *International Jornal of Cell Cloning 4*, 51-62

Sokolova, A.Y., Wyllie, S., Patterson, S., Oza, S.L., Read, K.D. and Fairlamb, A.H. (2010). Cross-resistance to nitro drugs and implications for treatment of human African trypanosomiasis. *Antimicrobial Agents and Chemotherapy 54*, 2893-2900

Song, J., Baker, N., Rothert, M., Henke, B., Jeacock, L., Horn, D. and Beitz, E. (2016). Pentamidine is not a permeant but a nanomolar inhibitor of the *Trypanosoma brucei* aquaglyceroporin-2. *PLoS Pathogens 12*, e1005436

Spinks, D., Ong, H.B., Mpamhanga, C.P., Shanks, E.J., Robinson, D.A., Collie, I.T., Read, K.D., Frearson, J.A., Wyatt, P.G., Brenk, R., Fairlamb, A.H. and Gilbert, I.H. (2011). Design, synthesis and biological evaluation of novel inhibitors of *Trypanosoma brucei* pteridine reductase 1. *ChemMedChem 6*, 302-308

Spinks, D., Torrie, L.S., Thompson, S., Harrison, J.R., Frearson, J.A., Read, K.D., Fairlamb, A.H., Wyatt, P.G. and Gilbert, I.H. (2012). Design, synthesis and biological evaluation of *Trypanosoma brucei* trypanothione synthetase inhibitors. *ChemMedChem 7*, 95-106

Sprehe, M., Fisk, J.C., McEvoy, S.M., Read, L.K. and Schumacher, M.A. (2010). Structure of the *Trypanosoma brucei* p22 protein, a cytochrome oxidase subunit II-specific RNA-editing accessory factor. *Journal of Biological Chemistry 285*, 18899-18908

Stevens, J.R., Noyes, H.A., Schofield, C.J. and Gibson, W. (2001). The molecular evolution of Trypanosomatidae. *Advances in Parasitology, Vol 48 48*, 1-56

Stewart, M.L., Burchmore, R.J., Clucas, C., Hertz-Fowler, C., Brooks, K., Tait, A., MacLeod, A., Turner, C.M., De Koning, H.P., Wong, P.E. and Barrett, M.P. (2010). Multiple genetic mechanisms lead to loss of functional TbAT1 expression in drug-resistant trypanosomes. *Eukaryotic Cell 9*, 336-343

Stover, P. and Schirch, V. (1990). Serine hydroxymethyltransferase catalyzes the hydrolysis of 5,10-methenyltetrahydrofolate to 5-formyltetrahydrofolate. *Journal of Biological Chemistry 265*, 14227-14233

Sykes, M.L., Baell, J.B., Kaiser, M., Chatelain, E., Moawad, S.R., Ganame, D., Ioset, J.R. and Avery, V.M. (2012). Identification of compounds with anti-proliferative activity against *Trypanosoma brucei brucei* strain 427 by a whole cell viability based HTS campaign. *PLoS Neglected Tropical Diseases 6*, e1896

Synold, T.W., Willits, E.M. and Barredo, J.C. (1996). Role of folylpolygutamate synthetase (FPGS) in antifolate chemotherapy; A biochemical and clinical update. *Leukemia & Lymphoma 21*, 9-15

Tan, T.H.P., Bochud-Allemann, N., Horn, E.K. and Schneider, A. (2002). Eukaryotic-type elongator tRNA(Met) of *Trypanosoma brucei* becomes formylated after import into mitochondria. *Proceedings of the National Academy of Sciences of the United States of America 99*, 1152-1157

Tarral, A., Blesson, S., Mordt, O.V., Torreele, E., Sassella, D., Bray, M.A., Hovsepian, L., Evene, E., Gualano, V., Felices, M. and Strub-Wourgaft, N. (2014). Determination of an optimal dosing regimen for fexinidazole, a novel oral drug for the treatment of Human African Trypanosomiasis: first-in-human studies. *Clinical Pharmacokinetics 53*, 565-580

Taylor, I.W. and Tattersall, M.H. (1981). Methotrexate cytotoxicity in cultured human leukemic cells studied by flow cytometry. *Cancer Research 41*, 1549-1558

Taylor, M.C., Kaur, H., Blessington, B., Kelly, J.M. and Wilkinson, S.R. (2008). Validation of spermidine synthase as a drug target in African trypanosomes. *Biochemical Journal 409*, 563-569

Thirion, P.,Michiels, S.,Pignon, J.P., Buyse, M., Bruad, A.C.,Crlson, R.W., O'Connell, M., Sargent, P. and Piadbois, P. (2004). Modulation of fluorouracil by leucovorin in patients with adnavced colorectal cancer. *Journal of Clinical Oncology 22*, 3766-2775

Tiberti, N., Lejon, V., Hainard, A., Courtioux, B., Robin, X., Turck, N., Kristensson, K., Matovu, E., Enyaru, J.C., Mumba, N.D., Krishna, S., Bisser, S., Ndung'u, J.M., Buscher, P. and Sanchez, J.C. (2013). Neopterin is a cerebrospinal fluid marker for treatment outcome evaluation in patients affected by *Trypanosoma brucei gambiense* sleeping sickness. *PLoS Neglected Tropical Diseases 7*, e2088

Torreele, E., Trunz, B.B., Tweats, D., Kaiser, M., Brun, R., Mazue, G., Bray, M.A. and Pecoul, B. (2010). Fexinidazole - a new oral nitroimidazole drug candidate entering clinical development for the treatment of sleeping sickness. *PLoS Neglected Tropical Diseases 4*, e923

Torrie, L.S., Wyllie, S., Spinks, D., Oza, S.L., Thompson, S., Harrison, J.R., Gilbert, I.H., Wyatt, P.G., Fairlamb, A.H. and Frearson, J.A. (2009). Chemical validation of trypanothione synthetase: a potential drug target for human trypanosomiasis. *Journal of Biological Chemistry 284*, 36137-36145

Treon, S.P. and Chabner, B.A. (1996). Concepts in use of high-dose methotrexate therapy. *Clinical Chemistry 42*, 1322-1329

Tsurusawa, M., Niwa, M., Katano, N. and Fujimoto, T. (1990). Methotrexate cytotoxicity as related to irreversible S phase arrest in mouse L1210 leukemia cells. *Japanese Journal of Cancer Research 81*, 85-90

Ulrich, C.M., Reed, M.C. and Nijhout, H.F. (2008). Modeling folate, one-carbon metabolism, and DNA methylation. *Nutrition Reviews 66 Suppl 1*, S27-S30

Urbaniak, M.D., Guther, M.L. and Ferguson, M.A. (2012). Comparative SILAC proteomic analysis of *Trypanosoma brucei* bloodstream and procyclic lifecycle stages. *Plos One 7*, e36619

Urbaniak, M.D., Martin, D.M. and Ferguson, M.A. (2013). Global quantitative SILAC phosphoproteomics reveals differential phosphorylation is widespread between the procyclic and bloodstream form lifecycle stages of *Trypanosoma brucei*. *Journal of Proteome Research 12*, 2233-2244

Van den Abbeele, J., Claes, Y., van, B.D., Le, R.D. and Coosemans, M. (1999). *Trypanosoma brucei spp*. development in the tsetse fly: characterization of the post-mesocyclic stages in the foregut and proboscis. *Parasitology 118 (Pt 5)*, 469-478

van den Hoff, M.J., Moorman, A.F. and Lamers, W.H. (1992). Electroporation in 'intracellular' buffer increases cell survival. *Nucleic Acids Research 20*, 2902

van der Heijden, J.W., Dijkmans, B.A., Scheper, R.J. and Jansen, G. (2007). Drug Insight: resistance to methotrexate and other disease-modifying antirheumatic drugs--from bench to bedside. *Nature Clinical Pracice. Rheumatology 3*, 26-34

van der Wilt, C.L., Backus, H.H.J., Smid, K., Comijn, L., Veerman, G., Wouters, D., Voorn, D.A., Priest, D.G., Bunni, M.A., Mitchell, F., Jackman, A.L., Jansen, G. and Peters, G.J. (2001). Modulation of both endogenous folates and thymidine enhance the therapeutic efficacy of thymidylate synthase inhibitors. *Cancer Research 61*, 3675-3681

Vanichtanankul, J., Taweechai, S., Yuvaniyama, J., Vilaivan, T., Chitnumsub, P., Kamchonwongpaisan, S. and Yuthavong, Y. (2011). Trypanosomal dihydrofolate reductase reveals natural antifolate resistance. *ACS Chemical Biology 6*, 905-911

Vickerman, K. (1976). The diversity of Kinetoplastid flagellates. In *Biology of the Kinetoplastida*, W.H. Lumsden and D.A. Evans, eds. (New York: Academic Press), pp. 1-34

Vickers, T.J. and Beverley, S.M. (2011). Folate metabolic pathways in Leishmania. *Essays Biochemisty 51*, 63-80

Vickers, T.J., Orsomando, G., de la Garza, R.D., Scott, D.A., Kang, S.O., Hanson, A.D. and Beverley, S.M. (2006). Biochemical and genetic analysis of methylenetetrahydrofolate reductase in *Leishmania* metabolism and virulence. *Journal of Biological Chemistry 281*, 38150-38158

Vincent, I.M., Creek, D., Watson, D.G., Kamleh, M.A., Woods, D.J., Wong, P.E., Burchmore, R.J.S. and Barrett, M.P. (2010). A molecular mechanism for eflornithine resistance in African trypanosomes. *PLoS Pathogens 6*, e1001204

Visentin, M., Diop-Bove, N., Zhao, R.B. and Goldman, I.D. (2014). The intestinal absorption of folates. *Annual Review of Physiology 76*, 251-274

Wahlin, A., Backman, L., Hultdin, J., Adolfsson, R. and Nilsson, L.G. (2002). Reference values for serum levels of vitamin B_{12} and folic acid in a population-based sample of adults between 35 and 80 years of age. *Public Health Nutrition 5*, 505-511

Walling, J. (2006). From methotrexate to pemetrexed and beyond. A review of the pharmacodynamic and clinical properties of antifolates. *Invest New Drugs 24*, 37-77

Wang, C.C. (1995). Molecular mechanisms and therapeutic approaches to the treatment of African trypanosomiasis. *Annual Review of Pharmacology and Toxicology 35*, 93-127

Wang, L., Cherian, C., Desmoulin, S.K., Polin, L., Deng, Y.J., Wu, J.M., Hou, Z.J., White, K., Kushner, J., Matherly, L.H. and Gangjee, A. (2010). Synthesis and antitumor activity of a novel series of 6-substituted pyrrolo[2,3-d]pyrimidine thienoyl antifolate inhibitors of purine biosynthesis with selectivity for high affinity folate receptors and the proton-coupled folate transporter over the reduced folate carrier for cellular entry. *Journal of Medicinal Chemistry 53*, 1306-1318

Wang, P., Wang, Q., Sims, P.F. and Hyde, J.E. (2007). Characterisation of exogenous folate transport in *Plasmodium falciparum*. *Molecular and Biochemical Parasitology 154*, 40-51

Wang, Y., Zhao, R. and Goldman, I.D. (2004). Characterization of a folate transporter in HeLa cells with a low pH optimum and high affinity for pemetrexed distinct from the reduced folate carrier. *Clinical Cancer Research 10*, 6256-6264

Watson, J.V., Chambers, S.H. and Smith, P.J. (1987). A pragmatic approach to the analysis of DNA histograms with a definable G1 peak. *Cytometry 8*, 1-8

Webber, S.E., Bleckman, T.M., Attard, J., Deal, J.G., Kathardekar, V., Welsh, K.M., Webber, S., Janson, C.A., Matthews, D.A., Smith, W.W., Freer, S.T., Jordan, S.R., Bacquet, R.J., Howland, E.F., Booth, C.L.J., Ward, R.W., Hermann, S.M., White, J., Morse, C.A., Hilliard, J.A. and Bartlett, C.A. (1993). Design of thymidylate synthase inhibitors using protein crystal structures: the synthesis and biological evaluation of a novel class of 5-substituted quinazolinones. *Journal of Medicinal Chemistry 36*, 733-746

Weiss, L.M., Harris, C., Berger, M., Tanowitz, H.B. and Wittner, M. (1988). Pyrimethamine concentrations in serum and cerebrospinal fluid during treatment of acute *Toxoplasma* encephalitis in patients with AIDS. *Jornal of Infectious Diseases 157*, 580-583

Welburn, S.C., Molyneux, D.H. and Maudlin, I. (2016). Beyond tsetse--implications for research and control of human African trypanosomiasis epidemics. *Trends in Parasitology 32*, 230-241

White, J.H. and Kilbey, B.J. (1996). DNA replication in the malaria parasite. *Parasitology Today 12*, 151-155

Wilson, P.M., Danenberg, P.V., Johnston, P.G., Lenz, H.J. and Ladner, R.D. (2014). Standing the test of time: targeting thymidylate biosynthesis in cancer therapy. *Nature Reviews Clinical Oncology 11*, 282-298

Winstanley, P.A., Mberu, E.K., Szwandt, I.S.F., Breckenridge, A.M. and Watkins, W.M. (1995). In vitro activities of novel antifolate drug combinations against *Plasmodium falciparum* and human granulocyte CFUs. *Antimicrobial Agents and Chemotherapy 39*, 948-952

Wirtz, E., Leal, S., Ochatt, C. and Cross, G.A.M. (1999). A tightly regulated inducible expression system for conditional gene knock-outs and dominant-negative genetics in *Trypanosoma brucei*. *Molecular and Biochemical Parasitology 99*, 89-101

World Health Organization. (2012a). Accelerating work to overcome the global impact of neglected tropical diseases - A roadmap for implementation. 1-37

World Health Organization. (2012b). Chagas disease (American trypanosomiasis) - fact sheet (revised in August 2012). *Weekly Epidemiological Record 87*, 519-522

Wright, D.L. and Anderson, A.C. (2011). Antifolate agents: a patent review (2006-2010). *Expert Opinion on Therapeutic Patients 21*, 1293-1308

Wyllie, S., Foth, B.J., Kelner, A., Sokolova, A.Y., Berriman, M. and Fairlamb, A.H. (2016). Nitroheterocyclic drug resistance mechanisms in *Trypanosoma brucei*. *Journal of Antimicrobial Chemotherapy 71*, 625-634

Xu, W.S., Parmigiani, R.B. and Marks, P.A. (2007). Histone deacetylase inhibitors: molecular mechanisms of action. *Oncogene 26*, 5541-5552

Yamey, G. (2002). The world's most neglected diseases - Ignored by the pharmaceutical industry and by public-private partnerships. *British Medical Journal 325*, 176-177

Young, H.D. (1962). Statistical treatement of experimental data. New York , McGraw-Hill Book Company.

Zeng, H., Chen, Z.S., Belinsky, M.G., Rea, P.A. and Kruh, G.D. (2001). Transport of methotrexate (MTX) and folates by multidrug resistance protein (MRP) 3 and MRP1: effect of polyglutamylation on MTX transport. *Cancer Research 61*, 7225-7232

Zhao, R., Babani, S., Gao, F., Liu, L. and Goldman, I.D. (2000). The mechanism of transport of the multitargeted antifolate (MTA) and its cross-resistance pattern in cells with markedly impaired transport of methotrexate. *Clinical Cancer Research 6*, 3687-3695

Zhao, R., Diop-Bove, N., Visentin, M. and Goldman, I.D. (2011). Mechanisms of membrane transport of folates into cells and across epithelia. *Annual Review of Nutrition 31*, 177-201

Zhao, R., Min, S.H., Qiu, A., Sakaris, A., Goldberg, G.L., Sandoval, C., Malatack, J.J., Rosenblatt, D.S. and Goldman, I.D. (2007). The spectrum of mutations in the PCFT gene, coding for an intestinal folate transporter, that are the basis for hereditary folate malabsorption. *Blood 110*, 1147-1152

Zhao, R., Qiu, A., Tsai, E., Jansen, M., Akabas, M.H. and Goldman, I.D. (2008). The proton-coupled folate transporter: impact on pemetrexed transport and on antifolates activities compared with the reduced folate carrier. *Molecular Pharmacology 74*, 854-862

Zhao, R., Unal, E.S., Shin, D.S. and Goldman, I.D. (2010). Membrane topological analysis of the proton-coupled folate transporter (PCFT-SLC46A1) by the substituted cysteine accessibility method. *Biochemistry 49*, 2925-2931

Zhou, S.F., Wang, L.L., Di, Y.M., Xue, C.C., Duan, W., Li, C.G. and Li, Y. (2008). Substrates and inhibitors of human multidrug resistance associated proteins and the implications in drug development. *Current Medicinal Chemistry 15*, 1981-2039

Zoltner, M., Leung, K.F., Alsford, S., Horn, D. and Field, M.C. (2015). Modulation of the surface proteome through multiple ubiquitylation pathways in African trypanosomes. *PLoS Pathogens 11*, e1005236

Xu, D., Brandan, C.P., Basombrio, M.A. and Tarleton R.L. (2009). Evaluation of high efficiency gene knockout strategies for *Trypanosoma cruzi*. *BMC Microbioliogy 9*, 90

Supplementary Tables

Table S1: MTX Low-RIT Data

Band	Primer	Hit	Score	Probability	Name
1	Fw	No sequence			
1	Rev	Tb927.10.1750	580	3 e-154	Hypothetical protein
2	Fw	Poor quality sequence			
2	Rev	No sequence			
3	Fw	Tb927.8.3650	345	7 e-94	Putative folate transporter
		Tb927.8.3630	102	1 e-20	Putative folate transporter
		Tb927.8.3620	84.2	4 e-15	Putative folate transporter
		Tb11.v5.0766	37.4	0.47	Orphan folate transporter
3	Rev	Tb927.8.3650	50	4 e-5	Putative folate transporter
4	Fw	No sequence			
4	Rev	Poor quality sequence			
5	Fw	Tb927.8.3620	188	4 e-47	Putative folate transporter
		Tb927.8.3630	188	4 e-47	Putative folate transporter
		Tb927.8.3650	179	2 e-44	Putative folate transporter
5	Rev	No sequence			

Table S2. RTX Low-RIT Data

Band	Primer	Hit	Score	Probability	Name
1	Fw	Tb927.10.1740	331	8 e-90	Hypothetical protein
1	Rev	Tb927.10.1750	554	6 e-157	Hypothetical protein
2	Fw	Tb927.10.2430	329	3 e-89	Receptor-type adenylate cyclase GRESAG 4, putative
2	Rev	No sequence			
3	Fw	Tb927.8.3630	210	1 e-53	Putative folate transporter
		Tb927.8.3620	188	5 e-47	Putative folate transporter
		Tb927.8.3650	188	5 e-47	Putative folate transporter
		Tb11.v5.0766	210	1 e-53	orphan folate transporter
3	Rev	Tb927.8.3630	95.1	8 e-19	Putative folate transporter
		Tb927.8.3650	95.1	8 e-19	Putative folate transporter
		Tb927.8.3620	87.8	1 e-16	Putative folate transporter
		Tb11.v5.0766	95.1	8 e-19	Orphan folate transporter
4	Fw	Tb927.8.3630	248	2 e-64	Putative folate transporter
		Tb927.8.3620	241	2 e-62	Putative folate transporter
		Tb927.8.3650	149	1 e-34	Putative folate transporter
		Tb11.v5.0766	149	1 e-34	Orphan folate transporter
4	Rev	Tb927.8.3620	338	6 e-92	Putative folate transporter
		Tb927.8.3630	324	1 e-87	Putative folate transporter
		Tb927.8.3650	324	1 e-87	Putative folate transporter
		Tb11.v5.0766	324	1 e-87	Orphan folate transporter
5	Fw	No sequence			
5	Rev	No sequence			

Supplementary Figures

Figure S1: A, B + C; DNA alignments of the folate transporters in MTX-resistant trypanosomes.

Highlighted in yellow: Base changes occurring in both MTX R1 and MTX R2 different to both WT and 927 reference
Highlighted in blue: Base changes occurring in both MTXR1 and MTXR2 different to WT but same as 927 reference.
Highlighted in green: Base changes in WT, MTXR1 and MTXR2 that are different than 927 reference.
Highlighted in purple: Base changes occurring in MTXR2 but not MTXR1.

Figure S1.A DNA alignments for FT1, comparing MTXR1, MTR2 to parental WT and reference *T.brucei* 927 strain.

```
FT1927          ATGACCACGTCACCGAACGCATGCCAGGACCAACCACCTCAACATTCCGCACCCCAAGCT
FT1WT           ATGACCACGTCACCGAACGCATGCCAGGACCAACCGCCTCAACATTCCGCACCCCAAGCT
FT1MTXR1        ------------------------------------------------------------
FT1MTXR2        ------------------------------------------------------------

FT1927          CACGAAGCTGAGTGTACAACTCACAAACTCTCTGCAGAGGAAACAATGGATGCTCGTCCT
FT1WT           CACGAAGCTGAGTGTACAACTCACAAACTCTCTGCAGAGGAAACAATGGATGCTCGTCCT
FT1MTXR1        ------------------------------------------------------------
FT1MTXR2        ------------------------------------------------------------

FT1927          GTACACCCTGACGCAAGGGCCTTGTTCCGAAAGCTGCCATGCGTGTGGAGCATTCCCGTA
FT1WT           GTACACCCTGACGCAAGGGCCTTGTTCCGAAAGCTGCCATGCGTGTGGAGCATTCCCGTA
FT1MTXR1        ------------------------------------------------------------
FT1MTXR2        ------------------------------------------------------------

FT1927          CTCGGCACTGCTGTGGAAGCGTTCGGACCGAAGTTTGTTTTCGCCCTTGGTTTCTGCGAG
FT1WT           CTCGGCACTGCTGTGGAAGCGTTCGGACCGAAGTTTGTTTTCGCCCTTGGTTTCTGCGAG
FT1MTXR1        ------------------------------------------------------------
FT1MTXR2        ------------------------------------------------------------

FT1927          CTCTTCGGCAAAGGAATTGCTGACAACATCATTCGATCCTCACTTTTTCCAATGTTTACC
FT1WT           CTCTTCGGCAAAGGAATTGCTGACAACATCATTCGATCCTCACTTTTTCCAATGTTTACC
FT1MTXR1        ------------------------------------------------------------
FT1MTXR2        ------------------------------------------------------------

FT1927          TACACCTTTGGTGCTGATGCAAAGCTTTACCAACTGATGGGTGGTATGTCGTCGTTGGGT
FT1WT           TACACCTTTGGTGCTGATGCAAAACTTTACCAACTGATGGGTGGTATGTCGTCGTTGGGT
FT1MTXR1        ------------------------------------------------------------
FT1MTXR2        ------------------------------------------------------------

FT1927          TACGCAGTGAAGCCGTTTGCAGCTATGTTCAGTGACCTCTTTGCGTTATTTGGGTACACG
FT1WT           TACGCAGTGAAACCGTTTGCAGCTATGTTCAGTGACCTCTTTGCGTTATTTGGGTACACC
FT1MTXR1        ------------------------------------------------------------
FT1MTXR2        ------------------------------------------------------------

FT1927          AAGCGATGGTACCTCGCTCTATCCTGTGTGGTGGGTTCCACCCTCGCTATTGTGTACGGT
FT1WT           AAGCGATGGTACCTCGCTCTATCCTGTGTGGTGGGTTCCACCCTCGCTATTGTGTACGGT
FT1MTXR1        ------------------------------------------------------------
FT1MTXR2        ------------------------------------------------------------

FT1927          TCACTGCCCGGAGAGTTGTCGTATGTACCGGTGGCTGGCTTCCTTGTTTTTGTCATTACC
FT1WT           TCACTGCCTGGAGAGTTGTCGTATGTACCGGTGGCTGGCTTCCTTGTTTTTGTCATTACC
FT1MTXR1        ------------------------------------------------------------
FT1MTXR2        ------------------------------------------------------------
```

```
FT1927          TTCACAGTTGCTAACCTTGATATCCTCACACAAGGGCATTACAGTCGCTTGATTCGCCGC
FT1WT           TTCACTGTTGCTAACCTTGATATCCTCACACAAGGGCATTACAGTCGCTTGATTCGCCGC
FT1MTXR1        ---------GCTAACCTTGATATCCTCACACAAGGGCATTACAGTCGCTTGATTCGCCGC
FT1MTXR2        ----------CTAACCTTGATATCCTCACACAAGGGCATTACAGTCGCTTGATTCGCCGC
                          **************************************************

FT1927          GTCCCATTGGCGGGCCCATCGCTTGTGAGTTGGGTTTGGTGGTGCCTTTTGGTTGGCTCC
FT1WT           GTCCCATTGGCGGGCCCATCGCTTGTGAGTTGGGTTTGGTGGTGCCTTTTGGTTGGCTCC
FT1MTXR1        GTCCCATTGGCGGGCCCATCGCTTGTGAGTTGGGTTTGGTGGTGCGTTCTAACTGGTTCC
FT1MTXR2        GTCCCATTGGCGGGCCCATCGCTTGTGAGTTGGGTTTGGTGGTGCGTTCTAACTGGTTCC
                ******************************************** ** *   *** ***

FT1927          CTTGTTGCGTCCTCCATTGTAGGACCACTTACCGATAAGAGGTTGCAGCGAGTGGCTGTG
FT1WT           CTTGTTGCGTCCTCCATTGTAGGGCCACTTACCGATAAGAGGTTGCAGCGAGTGGCTGTG
FT1MTXR1        CTTGTTGCGTCCTCCATTGTAGGGCCACTTACCGATAAGAGGTTGCAGCGAGTGGCTGTG
FT1MTXR2        CTTGTTGCGTCCTCCATTGTAGGGCCACTTACCGATAAGAGGTTGCAGCGAGTGGCTGTG
                ********************** ************************************

FT1927          TTTATCTCTGCTGGGATGCAGTTGGTGCCGACGATATTCTTCATACTGAATTGGTATGGT
FT1WT           TTTATCTCTGCTGGGATGCAGTTGGTGCCGACGATATTCTTCATACTGAATTGGTATGGT
FT1MTXR1        TTTATCTCTGCTGGGATGCAGTTGGTGCCGACGATATTCTTCATACTGAATTGGTATGGT
FT1MTXR2        TTTATCTCTGCTGGGATGCAGTTGGTGCCGACGATATTCTTCATACTGAATTGGTATGGT
                ************************************************************

FT1927          GAACGGAAGAACCGAGAGGAACGTGCGTACGACCTGAAGATTATTCGCGAAAAGAAGCTG
FT1WT           GAACGGAGGAACCGAGAGGAACGTGCGTACGACCTGAAGATTATTCGCGAAAAGCAGCTG
FT1MTXR1        GAACGGAGGAACCGAGAGGAACGTGCGTACGACCTGAAGATTATTCGCGAAAAGCAGCTG
FT1MTXR2        GAACGGAGGAACCGAGAGGAACGTGCGTACGACCTGAAGATTATTCGCGAAAAGCAGCTG
                ******* ********************************************* *****

FT1927          GAGCATGAAGCCGACGCCGTGAGGTTACAGGGGAGCGAAGCAACAAGTGGCTCACTGGAC
FT1WT           GAGCATGAAGCCGACGCCGTGAGGTTACAGGGGAGCGAAGCAACAAGTGGCTCACTGGAC
FT1MTXR1        GAGCATGAAGCCGACGCCGTGAGGTTACAGGGGAGCGAAGCAACAAGTGGCTCACTGGAC
FT1MTXR2        GAGCATGAAGCCGACGCCGTGAGGTTACAGGGGAGCGAAGCAACAAGTGGCTCACTGGAC
                ************************************************************

FT1927          AATCCATCGGATACCGAGGAAGTGGGTGAGGGCGGAGCACGGATACTACCTTGTTGCTGT
FT1WT           AATCCATCGGATACCGAGGAAGTGGGTGAGGGCGGGGCACGGATACTACCTTGTTGCTGT
FT1MTXR1        AATCCATCGGATACCGAGGAAGTGGGTGAGGGCGGGGCACGGATACTACCTTGTTGCTGT
FT1MTXR2        AATCCATCGGATACCGAGGAAGTGGGTGAGGGCGGGGCACGGATACTACCTTGTTGCTGT
                ********************************** ************************

FT1927          GGTGCCTTTGAAGTGAATCGAGAAGTGTTTGCTCGCAACAAGAAGGTTGTGTTTTACTGC
FT1WT           GGTGCCTTTGAAGTGAATCGAGAAGTGTTTGCTCGCAACAAGAAGGTTGTGTTTTACTGC
FT1MTXR1        GGTGCCTTTGAAGTGAATCGAGAAGTGTTTGCTCGCAACAAGAAGGTTGTGTTTTACTGC
FT1MTXR2        GGTGCCTTTGAAGTGAATCGAGAAGTGTTTGCTCGCAACAAGAAGGTTGTGTTTTACTGC
                ************************************************************

FT1927          ATGCTTCTCACACTTGGCGCCATCGGTATGGTTCTCGTGACAGTCCTTGGCACAAGGTTG
FT1WT           ATGCTTCTCACACTTGGCGCCATCGGTATGGTTCTCGTGACAGTCCTTGGCACAAGGTTG
FT1MTXR1        ATGCTTCTCACACTTGGCGCCATCGGTATGGTTCTCGTGACAGTCCTTGGCACAAGGTTG
FT1MTXR2        ATGCTTCTCACACTTGGCGCCATCGGTATGGTTCTCGTGACAGTCCTTGGCACAAGGTTG
                ************************************************************

FT1927          CAGCTGCTAATAACCAGTGTTGTGGCGTCATTTACACTCTGTGGACTCGGTTTCGTTGCC
FT1WT           CAGCTGCTAATAACCAGTGTTGTGGCGTCATTTACACTCTGTGGTCTCGGTTTCGTTGCT
FT1MTXR1        CAGCTGCTAATAACCAGTGTTGTGGCGTCATTTACACTCTGTGGTCTCGGTTTCGTTGCT
FT1MTXR2        CAGCTGCTAATAACCAGTGTTGTGGCGTCATTTACACTCTGTGGTCTCGGTTTCGTTGCT
                ******************************************* **************

FT1927          CTTCCACTTGTGATCGCGAAGGCAAATATGTTCACATTCATCTCGAGGGTCACGTACATC
FT1WT           CTTCCACTTGTGATCGCGAAGGCAAATATGTTCACATTCATCTCGAGGGTCGCGTACATC
FT1MTXR1        CTTCCACTTGTGATCGCGAAGGCAAATATGTTCACATTCATCTCGAGGGTCGCGTACATC
FT1MTXR2        CTTCCACTTGTGATCGCGAAGGCAAATATGTTCACATTCATCTCGAGGGTCGCGTACATC
                ************************************************** ********

FT1927          CAACTTCGTGGCGCAATGGACAATGTCTTCATGGCGACCCCCGATTGTTTCCCTGGTGGT
FT1WT           CAACTTCGTGGCGCAATGGACAATGTCTTCATGGCGACCCCCGATTGTTTCCCTGGTGGT
FT1MTXR1        CAACTTCGTGGCGCAATGGACAATGTCTTCATGGCGACCCCCGATTGTTTCCCTGGTGGT
FT1MTXR2        CAACTTCGTGGCGCAATGGACAATGTCTTCATGGCGACCCCCGATTGTTTCCCTGGTGGT
                ************************************************************

FT1927          CCTAACTTTTCATACTTTTACTACAACACTGTGGGTAACGTGATTGGGACTATGGGTGGT
FT1WT           CCTAACTTTTCATACTTTTACTACAACACTGTGGGTAACGTGATTGGGACTATGGGTGGT
FT1MTXR1        CCTAACTTTTCATACTTTTACTACAACACTGTGGGTAACGTGATTGGGACTATGGGTGGT
FT1MTXR2        CCTAACTTTTCATACTTTTACTACAACACTGTGGGTAACGTGATTGGGACTATGGGTGGT
                ************************************************************
```

```
FT1927          GTTATTGGTGTGACGTTATTCAGATACGTATTCTCAAAGCGCAGCTATCGCCTAACATTC
FT1WT           GTTATTGGTGTGACGTTATTCAGATACGTATTCTCAAAGCGCAGCTATCGCCTAACATTC
FT1MTXR1        GTTATTGGTGTGACGTTATTCAGATACGTATTCTCAAAGCGCAGCTATCGCCTAACATTC
FT1MTXR2        GTTATTGGTGTGACGTTATTCAGATACGTATTCTCAAAGCGCAGCTATCGCCTAACATTC
                ************************************************************

FT1927          ATCGTAACAACTTTGATTGAGATAGTTTCGAGTATCTTTGATATAATCATTGTGGAGCGA
FT1WT           ATCGTAACAACTTTGATTGAGATAGTTTCGAGTATCTTTGATATAATCATTGTGGAGCGA
FT1MTXR1        ATCGTAACAACTTTGATTGAGATAGTTTCGAGTATCTTTGATATAATCATTGTGGAGCGA
FT1MTXR2        ATCGTAACAACTTTGATTGAGATAGTTTCGAGTATCTTTGATATAATCATTGTGGAGCGA
                ************************************************************

FT1927          TGGAACCGTCCGTATGTTAGCGATCACGTTGTATTCGTTCTTGGTGACCAAATTATACAG
FT1WT           TGGAACCGTCCGTATGTTAGCGATCACGTTGTATTCGTTCTTGGTGACCAAATTATACAG
FT1MTXR1        TGGAACCGTCCGTATGTTAGCGATCACGTTGTATTCGTTCTTGGTGACCAAATTATACAG
FT1MTXR2        TGGAACCGTCCGTATGTTAGCGATCACGTTGTATTCGTTCTTGGTGACCAAATTATACAG
                ************************************************************

FT1927          CAGGTGTGCTACATGATGCACTTCATGCCAACTGTAATGCTCATTTCGAGGCTCTGTCCC
FT1WT           CAGGTGTGCTACATGATGCACTTCATGCCAACTGTAATGCTCATTTCGAGGCTCTGTCCC
FT1MTXR1        CAGGTGTGCTACATGATGCACTTCATGCCAACTGTAATGCTCATTTCGAGGCTCTGTCCC
FT1MTXR2        CAGGTGTGCTACATGATGCACTTCATGCCAACTGTAATGCTCATTTCGAGGCTCTGTCCC
                ************************************************************

FT1927          CGTGGGTCTGAAAGTATGGTGTATGCGGTACTTGCAGGATGTGCGCATTTTGGCCGTTCC
FT1WT           CGTGGGTCTGAAAGTATGGTGTATGCGGTACTTGCAGGATGTGCGCATTTTGGCCGTTCC
FT1MTXR1        CGTGGGTCTGAAAGTATGGTGTATGCGGTACTTGCAGGATGTGCGCATTTTGGCCGTTCC
FT1MTXR2        CGTGGGTCTGAAAGTATGGTGTATGCGGTACTTGCAGGATGTGCGCATTTTGGCCGTTCC
                ************************************************************

FT1927          GTTTCCAACACACTTGGATGGCTTTTGATGGAATACGTATGGAATGTGCAATCAGACATT
FT1WT           GTTTCCAACACACTTGGATGGCTTTTGATGGAATACGTATGGAATGTGCAATCAGACATT
FT1MTXR1        GTTTCCAACACACTTGGATGGCTTTTGATGGAATACGTATGGAATGTGCAATCAGACATT
FT1MTXR2        GTTTCCAACACACTTGGATGGCTTTTGATGGAATACGTATGGAATGTGCAATCAGACATT
                ************************************************************

FT1927          ACGGTGGGTCCATGCGACTTCAGTAATGTGAAGTGGCTTCTACTTCTTGGTCACTTTGGC
FT1WT           ACGGTGGGTCCATGCGACTTCAGTAATGTGAAGTGGCTTCTGCTTCTTGGTCACTTTGGC
FT1MTXR1        ACGGTGGGTCCATGCGACTTCAGTAATGTGAAGTGGCTTCTGCTTCTTGGTCACTTTGGC
FT1MTXR2        ACGGTGGGTCCATGCGACTTCAGTAATGTGAAGTGGCTTCTGCTTCTTGGTCACTTTGGC
                ****************************************** ******************

FT1927          ACTCCACTCATCAGCATTCCTCTTGTGTTTTTACTGATACCTGCGGCACGTATATGTGAT
FT1WT           ACTCCACTCATCAGCATTCCTCTTGTGTTTTTACTGATACCTGCGGCACGTATATGTGAC
FT1MTXR1        ACTCCACTCATCAGCATTCCTCTTGTGTTTTTACTGATACCTGCGGCACGTATATGTGAC
FT1MTXR2        ACTCCACTCATCAGCATTCCTCTTGTGTTTTTACTGATACCTGCGGCACGTATATGTGAC
                ************************************************************

FT1927          GTTCTTGACGAAAACGGCAAAGCTATTACAAAGAAGGCGGAGGATGTTCATGCCCCCTCT
FT1WT           GTTCTTGACGAAAACGGCAAAGCTATTACAAAGAAGGCGGAGGATGTTCATGCCCCCTCT
FT1MTXR1        GTTCTTGACGAAAACGGCAAAGCTATTACAAAGAAGGCGGAGGATGTTCATGCCCCCTCT
FT1MTXR2        GTTCTTGACGAAAACGGCAAAGCTATTACAAAGAAGGCGGAGGATGTTCATGCCCCCTCT
                ************************************************************

FT1927          AATGATTCTCCCAGACGGCGGGAACCCACAGCCAATTAG
FT1WT           AATGATTCTCCCAGACGGCGGGAACCCACAGCCAATTAG
FT1MTXR1        AATGATTCTCCCAGACGGCGGGAACCCACAGCCAATTAG
FT1MTXR2        AATGATTCTCCCAGACGGCGGGAACCCACAGCCAATTAG
                ****************************************
```

Figure S1.B DNA alignments for FT2, comparing MTXR1, MTR2 to parental WT and reference *T.brucei* 927 strain.

```
FT2927          ATGACCACGTCACCGAACGCATGCCAGGACCAACCACCTCAACATTCCGCACCCCAAGCT
FT2WT           ATGACCACGTCACCGAACGCATGCCAGGACCAACCGCCTCAACATTCCGCACCCCAAGCT
FT2MTXR1        ATGACCACGTCACCGAACGCATGCCAGGACCAGCCGCCTCAACATTCCGCACCCCAAGCT
FT2MTXR2        ATGACCACGTCACCGAACGCATGCCAGGACCAGCCGCCTCAACATTCCGCACCCCAAGCT
                ****************************** ** ************************

FT2927          CACGAAGCTGAGTGTACAACTCACAAACTCTCTGCAGAGGAAACAATGGATGCTCGTCCT
FT2WT           CACGAAGCTGAGTGTACAACTCACAAACTCTCTGCAGAGGAAACAATGGATGCTCGTCCT
FT2MTXR1        CACGAAGCTGAGTGTACAACTCACAAACTCTCTGCAGAGGAAACAATGGATGCTCGTCCT
FT2MTXR2        CACGAAGCTGAGTGTACAACTCACAAACTCTCTGCAGAGGAAACAATGGATGCTCGTCCT
                ************************************************************

FT2927          GTACACCCTGACGCAAGGGCCTTGTTCCGAAAGCTGCCATGCGTGTGGAGCATTCCCGTA
FT2WT           GTACACCCTGACGCAAGGGCCTTGTTCCGAAAGCTGCCATGCGTGTGGAGCATTCCCGTA
FT2MTXR1        GTACACCCTGACGCAAGGGCCTTGTTCCGAAAGCTGCCATGCGTGTGGAGCATTCCCGTA
FT2MTXR2        GTACACCCTGACGCAAGGGCCTTGTTCCGAAAGCTGCCATGCGTGTGGAGCATTCCCGTA
                ************************************************************

FT2927          TTCGGCACTGCTGTGGAAGCGTTCGGACCGAGATGTGTCCTCGCCCTTGGCCTCTCCGAG
FT2WT           TTCGGCACTGCTGTGGAAGCGTTCGGACCGAAATGTGTCCTCGCCCTTGGCCTCTCCGAG
FT2MTXR1        TTCGGCACTGCTGTGGAAGCGTTCGGACCGAAATGTGTCCTAGCCCTTGGCCTCTCCGAG
FT2MTXR2        TTCGGCACTGCTGTGGAAGCGTTCGGACCGAAATGTGTCCTAGCCCTTGGCCTCTCCGAG
                ****************************** ********* ******************

FT2927          CTCTTCGGCAAAGGAATTGCTGACAACATCATTCGAACCACACTTTTTCCAATGTTTACC
FT2WT           CTCTTCGGCAAAGGAATTGCTGACAACATCATTCGAACCACACTTTTTCCAATGTTTACC
FT2MTXR1        CTCTTCGGCAAAGGAATTGCTGACAACATCATTCGAACCACACTTTTTCCAATGTTTACC
FT2MTXR2        CTCTTCGGCAAAGGAATTGCTGACAACATCATTCGAACCACACTTTTTCCAATGTTTACC
                ************************************************************

FT2927          TACACCTTTGGTGCTGATGCAAAGCTTTACCAACGAATGAGTAGCTTGGTTACATTTGGT
FT2WT           TACACCTTTGGTGCTGATGCAAAGCTTTACCAACGAATGAGTAGCTTGGTTACATTTGGT
FT2MTXR1        TACACCTTTGGTGCTGATGCAAAGCTTTACCAACGAATGAGTAGCTTGGTTACATTTGGT
FT2MTXR2        TACACCTTTGGTGCTGATGCAAAGCTTTACCAACGAATGAGTAGCTTGGTTACATTTGGT
                ************************************************************

FT2927          TACGCAGTGAAGCCGTTTGCAGCTATGTTCAGTGACCTCTTTGCGTTATTTGGGTACACG
FT2WT           TACGCAGTGAAACCGTTTGCAGCTATGTTCAGTGACCTCTTTGCGTTATTTGGGTACACG
FT2MTXR1        TACGCAGTGAAACCGTTTGCAGCTATGTTCAGTGACCTCTTTGCGTTATTTGGGTACACG
FT2MTXR2        TACGCAGTGAAACCGTTTGCAGCTATGTTCAGTGACCTCTTTGCGTTATTTGGGTACACG
                *********** ************************************************

FT2927          AAGCGATGGTACCTCGCTCTATCCTGTGTGGTGGGTTCCACCCTCGCTATTGTGTACGGT
FT2WT           AAGCGATGGTACCTCGCTCTATCCTGTGTGGTGGGTTCCACCCTCGCTATTGTGTACGGT
FT2MTXR1        AAGCGATGGTACCTCGCTCTATCCTGTGTGGTGGGTTCCACCCTCGCTATTGTGTACGGT
FT2MTXR2        AAGCGATGGTACCTCGCTCTATCCTGTGTGGTGGGTTCCACCCTCGCTATTGTGTACGGT
                ************************************************************

FT2927          TCACTGCCCGGAGAGTTGTCGTATGTACCGGTGGCCGGAATACTGGTTTTTGTGACGTCG
FT2WT           TCACTGCCCGGAGAGTTGTCGTATGTACCGGTGGCCGGAATACTGGTTTTTGTGACGTCG
FT2MTXR1        TCACTGCCCGGAGAGTTGTCGTATGTACCGGTGGCCGGAATACTGGTTTTTGTGACGTCG
FT2MTXR2        TCACTGCCCGGAGAGTTGTCGTATGTACCGGTGGCCGGAATACTGGTTTTTGTGACGTCG
                ************************************************************

FT2927          TTTACCAAGGCTAACCTTGATATCCTCACACAAGGGCATTACAGTCGCTTGATTCGCCGC
FT2WT           TTTACCAAGGCTAACCTTGATATCCTCACACAAGGGCATTACAGTCGCTTGATTCGCCGC
FT2MTXR1        TTTAC-------------------------------------------------------
FT2MTXR2        TTTACCAAGGCTA-----------------------------------------------
                *****

FT2927          GTCCCATTGGCGGGCCCATCGCTTGTGAGTTGGGTTTGGTGGTGCGTTCTAACTGGTTCC
FT2WT           GTCCCATTGGCGGGCCCATCGCTTGTGAGTTGGGTTTGGTGGTGCGTTCTAACTGGTTCC
FT2MTXR1        ------------------------------------------------------------
FT2MTXR2        ------------------------------------------------------------


FT2927          CTTGTTGCGTCCTCCATTGTAGGACCACTTACCGATAAGAGGTTGCAGCGAGTGGCTGTG
FT2WT           CTTGTTGCGTCCTCCATTGTAGGGCCACTTACCGATAAGAGGTTGCAGCGAGTGGCTGTG
FT2MTXR1        ------------------------------------------------------------
FT2MTXR2        ------------------------------------------------------------
```

```
FT2927          TTTATCTCTGCTGGGATGCAGTTGGTGCCGACGATATTCTTCATGCTGAATTGGTATGGT
FT2WT           TTTATCTCTGCTGGGATGCAGTTGGTGCCGACGATATTCTTCATACTGAATTGGTATGGT
FT2MTXR1        ------------------------------------------------------------
FT2MTXR2        ------------------------------------------------------------

FT2927          GAACGGAAGAACCGAGAGGAACGTGCGTACGACCTGAAGATTATTCGGGAAGAGCAGCTG
FT2WT           GAACGGAGGAACCGAGAGGAACGTGCGTACGACCTGAAGATTATTCGGGAAGAGCAGCTG
FT2MTXR1        ------------------------------------------------------------
FT2MTXR2        ------------------------------------------------------------

FT2927          GAGCGTGAAGCCGACGCCGCGAGGTTACAGGGGAGCGAAGCAACAAGTGGCTCACTGGAC
FT2WT           GAGCGTGAAGCCGACGCCGTGAGGTTACAGGGGAGCGAAGCAACAAGTGGCTCACTGGAC
FT2MTXR1        ------------------------------------------------------------
FT2MTXR2        ------------------------------------------------------------

FT2927          AATCCATCGGATACCGAGGAAGTGGGTGAGGGCGGAGCACGGATACTACCTTGTTGCTGT
FT2WT           AATCCATCGGATACCGAGGAAGTGGGTGAGGGCGGCGCACGGATACTACCTTGTTGCTGT
FT2MTXR1        ------------------------------------------------------------
FT2MTXR2        ------------------------------------------------------------

FT2927          GGTGCCTTTGAAGTGAATCGAGAAGTGTTTGCTCGCAACAAGAAGGTTGTGTTTTACTGC
FT2WT           GGTGCCTTTGAAGTGAATCGAGAAGTGTTTGCTCGCAACAAGAAGGTTGTGTTTTACTGC
FT2MTXR1        ------------------------------------------------------------
FT2MTXR2        ------------------------------------------------------------

FT2927          ATGCTTCTCACACTTGGCGCCATCGGTATGGTTCTCGTGACAGTCCTTGGCACAAGGTTG
FT2WT           ATGCTTCTCACACTTGGCGCCATCGGTATGGTTCTCGTGACAGTCCTTGGCACAAGGTTG
FT2MTXR1        ------------------------------------------------------------
FT2MTXR2        ------------------------------------------------------------

FT2927          CAGCTGCTAATAACCAGTGTTGTGGCGTCATTTACACTCTGTGGACTCGGTTTCGTTGCT
FT2WT           CAGCTGCTAATAACCAGTGTTGTGGCGTCATTTACACTCTGTGGTCTCGGTTTCGTTGCT
FT2MTXR1        ------------------------------------------------------------
FT2MTXR2        ------------------------------------------------------------

FT2927          CTTCCACTTGTGATCGCGAAGGCAAATATGTTCACATTCATCTCGAGGGTCGCGTACATC
FT2WT           CTTCCACTTGTGATCGCGAAGGCAAATATGTTCACATTCATCTCGAGGGTCGCGTACATC
FT2MTXR1        ------------------------------------------------------------
FT2MTXR2        ------------------------------------------------------------

FT2927          CAACTTCCTGGCGCAATCGACAATGTCTTCATGGCGACCCCCGATTGTTTCCCTGGTGGT
FT2WT           CAACTTCCTGGCGCAATCGACAATGTCTTCATGGCGACCCCCGATTGTTTCCCTGGTGGT
FT2MTXR1        ------------------------------------------------------------
FT2MTXR2        ------------------------------------------------------------

FT2927          CCTAACTTTTCATACTTTTACTACAGCACTGTGGGTAATATGATTGGAGCTGTGGGTGGT
FT2WT           CCTAACTTTTCATACTTTTACTACAGCACTGTGGGTAATATGATTGGAGCTATGGGTGGT
FT2MTXR1        ------------------------------------------------------------
FT2MTXR2        ------------------------------------------------------------

FT2927          GTTATTGGTGTGACGTTATTCAGATACGTATTCTCAAAGCGCAGCTATCGCCTAACATTC
FT2WT           GTTATTGGTGTGACGTTATTCAGATACGTATTCTCAAAGCGCAGCTATCGCCTAACATTC
FT2MTXR1        ------------------------------------------------------------
FT2MTXR2        ------------------------------------------------------------

FT2927          ATCGTAACAACTTTGATTGAGATAGTTTCGAGTATCTTTGATATAATCATTGTGGAGCGA
FT2WT           ATCGTAACAACTTTGATTGAGATAGTTTCGAGTATCTTTGATATAATCATTGTGGAGCGA
FT2MTXR1        ------------------------------------------------------------
FT2MTXR2        ------------------------------------------------------------

FT2927          TGGAACCGTCCGTATGTTAGCGATCACGTTGTATTCGTTCTTGGTGACCAAATTATACAC
FT2WT           TGGAACCGTCCGTATGTTAGCGATCACGTTGTATTCGTTCTTGGTGACCAAATTATACAC
FT2MTXR1        ------------------------------------------------------------
FT2MTXR2        ------------------------------------------------------------
```

```
FT2927          CAGGTGTGCTACATGATGCACTTCATGCCAACTGTAATGCTCATTTCGAGGCTCTGTCCC
FT2WT           CAGGTGTGCTACATGATGCACTTCATGCCAACTGTAATGCTCATTTCGAGGCTCTGTCCC
FT2MTXR1        ------------------------------------------------------------
FT2MTXR2        ------------------------------------------------------------

FT2927          CGTGGGTCTGAAAGTATGGTGTATGCATTACTTGCAGGATTCGCTAATTTTGGCCGTTCT
FT2WT           CGTGGGTCTGAAAGTATGGTGTATGCATTACTTGCAGGATTCGCTAATTTTGGCCGTTCT
FT2MTXR1        ------------------------------------------------------------
FT2MTXR2        ------------------------------------------------------------

FT2927          CTTTCCAACACACTTGGATGGCTTTTGATGGAATACGTATGGAATGTGCAATCAGACATT
FT2WT           CTTTCCAACACACTTGGATGGCTTTTGATGGAATACGTATGGAATGTGCAATCAGACATT
FT2MTXR1        ------------------------------------------------------------
FT2MTXR2        ------------------------------------------------------------

FT2927          ACGGTGGGTCCATGCGACTTCAGTAATGTGAAGTGGCTTCTACTTCTTGGTCACTTTGGC
FT2WT           ACGGTGGGTCCATGCGACTTCAGTAATGTGAAGTGGCTTCTGCTTCTTGGTCACTTTGGC
FT2MTXR1        ------------------------------------------------------------
FT2MTXR2        ------------------------------------------------------------

FT2927          ACTCCACTCATCAACATTCCTCTTGTGTTTTTACTGATACCTGCGGCACGTATATGTGAT
FT2WT           ACTCCACTCATCAACATTCCTCTTGTGTTTTTACTGATACCTGCGGCACGTATATGTGAC
FT2MTXR1        ------------------------------------------------------------
FT2MTXR2        ------------------------------------------------------------

FT2927          GTTCTTGACGAAAACGGCAAAGCTATTACAAAGAAGGCGGAGGATGTTCATGCCCCCTCT
FT2WT           GTTCTTGACGAAAACGGCAAAGCTATTACAAAGAAGGCGGAGGATGTTCATGCCCCCTCT
FT2MTXR1        ------------------------------------------------------------
FT2MTXR2        ------------------------------------------------------------

FT2927          AATGATTCTCCCAGACGGCGGGAACCCACAGCCAATTAG
FT2WT           AATGATTCTCCCAGACGGCGGGAACCCACAGCCAATTAG
FT2MTXR1        ---------------------------------------
FT2MTXR2        ---------------------------------------
```

Figure S1.C DNA alignments for FT3, comparing MTXR1, MTR2 to parental WT and reference *T.brucei* 927 strain.

```
FT3MTXR1        ATGACCACGTCACCGAACGCATGCCAGGACCAGCCGCCTCAACATTCCGCACCCCAAGCT
FT3MTXR2        ATGACCACGTCACCGAACGCATGCCAGGACCAGCCGCCTCAACATTCCGCACCCCAAGCT
FT3927          ATGACCACGTCACCGAACGCATGCCAGGACCAGCCGCCTCAACATTCCGCACCCCAAGCT
FT3WT           ATGACCACGTCACCGAACGCATGCCAGGACCAGCCGCCTCAACATTCCGCACCCCAAGCT
                ************************************************************

FT3MTXR1        CACGAAGCTGAGTGTACAACTCACAAACTCTCTGCAGAGGAAACAATGGATGCTCGTCCT
FT3MTXR2        CACGAAGCTGAGTGTACAACTCACAAACTCTCTGCAGAGGAAACAATGGATGCTCGTCCT
FT3927          CACGAAGCTGAGTGTACAACTCACAAACTCTCTGCAGAGGAAACAATGGATGCTCGTCCT
FT3WT           CACGAAGCTGAGTGTACAACTCACAAACTCTCTGCAGAGGAAACAATGGATGCTCGTCCT
                ************************************************************

FT3MTXR1        GTACACCCTGACGCAAGGGCCTTGTTCCGAAAGCTGCCATGCGTGTGGAGCATTCCCGTA
FT3MTXR2        GTACACCCTGACGCAAGGGCCTTGTTCCGAAAGCTGCCATGCGTGTGGAGCATTCCCGTA
FT3927          GTACACCCTGACGCAAGGGCCTTGTTCCGAAAGCTGCCATGCGTGTGGAGCATTCCCGTA
FT3WT           GTACACCCTGACGCAAGGGCCTTGTTCCGAAAGCTGCCATGCGTGTGGAGCATTCCCGTA
                ************************************************************

FT3MTXR1        TTCGGCACTGCTGTGGAAGCGTTCGGACCGAAGTTTGTTTTCGCCCTTGGTTTCTGCGAG
FT3MTXR2        TTCGGCACTGCTGTGGAAGCGTTCGGACCGAAGTTTGTTTTCGCCCTTGGTTTCTGCGAG
FT3927          TTCGGCACTGCTGTGGAAGCGTTCGGACCGAAGTTTGTTTTCGCCCTTGGTTTCTGCGAG
FT3WT           TTCGGCACTGCTGTGGAAGCGTTCGGACCGAAGTTTGTTTTCGCCCTTGGTTTCTGCGAG
                ************************************************************

FT3MTXR1        CTCTTCGGCAAAGGAATTGCTGACAACATCATTCGATCCTCACTTTTTCCAATGTTTACC
FT3MTXR2        CTCTTCGGCAAAGGAATTGCTGACAACATCATTCGATCCTCACTTTTTCCAATGTTTACC
FT3927          CTCTTCGGCAAAGGAATTGCTGACAACATCATTCGATCCTCACTTTTTCCAATGTTTACC
FT3WT           CTCTTCGGCAAAGGAATTGCTGACAACATCATTCGATCCTCACTTTTTCCAATGTTTACC
                ************************************************************

FT3MTXR1        TACACCTTTGGTGCTGATGCAAAGCTTTACCAACGAATGAGTAGCTTGGTTACATTTGGT
FT3MTXR2        TACACCTTTGGTGCTGATGCAAAGCTTTACCAACGAATGAGTAGCTTGGTTACATTTGGT
FT3927          TACACCTTTGGTGCTGATGCAAAGCTTTACCAACGAATGAGTAGCTTGGTTACATTTGGT
FT3WT           TACACCTTTGGTGCTGATGCAAAGCTTTACCAACGAATGAGTAGCTTGGTTACATTTGGT
                ************************************************************

FT3MTXR1        TACGCAGTGAAACCGTTTGCAGCTATGTTCAGTGACCTCTTTGCGTTATTTGGGTACACG
FT3MTXR2        TACGCAGTGAAACCGTTTGCAGCTATGTTCAGTGACCTCTTTGCGTTATTTGGGTACACC
FT3927          TACGCAGTGAAACCGTTTGCAGCTATGTTCAGTGACCTCTTTGCGTTATTTGGGTACACG
FT3WT           TACGCAGTGAAACCGTTTGCAGCTATGTTCAGTGACCTCTTTGCGTTATTTGGGTACACG
                ************************************************************

FT3MTXR1        AAGCGATGGTACCTCGCTCTATCCTGTGTGGTGGGTTCCACCCTCGCTATTGTGTACGGT
FT3MTXR2        AAGCGATGGTACCTCGCTCTATCCTGTGTGGTGGGTTCCACCCTCGCTATTGTGTACGGT
FT3927          AGGCGATGGTACCTCGCTCTATCCTGTGTGGTGGGTTCCACCCTCGCTATTGTGTACGGT
FT3WT           AAGCGATGGTACCTCGCTCTATCCTGTGTGGTGGGTTCCACCCTCGCTATTGTGTACGGT
                * ************************************************************

FT3MTXR1        TCACTGCCCGGAGAGTTGTCGTATGTACCGGTGGCCGGAATACTGGTTTTTGTGACGTCG
FT3MTXR2        TCACTGCCCGGAGAGTTGTCGTATGTACCGGTGGCCGGAATACTGGTTTTTGTGACGTCG
FT3927          TCACTGCCTGGAGAGTTGTCGTATGTACCGGTGGCCGGAATACTGGTTTTTGTGACGTCG
FT3WT           TCACTGCCCGGAGAGTTGTCGTATGTACCGGTGGCCGGAATACTGGTTTTTGTGACGTCG
                ******** ************************************************

FT3MTXR1        TTTACCAAGGCTAACCTTGATATCCTCACACAAGGACATTACAGTCGCTTGATTCGCCGC
FT3MTXR2        TTTACCAAGGCTAACCTTGATATCCTCACACAAGGACATTACAGTCGCTTGATTCGCCGC
FT3927          TTTACCAAGGCTAACCTTGATATCCTCACACAAGGGCATTACAGTCGCTTGATTCGCCGC
FT3WT           TTTACCAAGGCTAACCTTGATATCCTCACACAAGGGCATTACAGTCGCTTGATTCGCCGC
                ********************************** ************************

FT3MTXR1        GTCCCATTGGCGGGCCCATCGCTTGTGAGTTGGGTTTGGTGGTGCCTTTTGGTTGGCTCT
FT3MTXR2        GTCCCATTGGCGGGCCCATCGCTTGTGAGTTGGGTTTGGTGGTGCCTTTTGGTTGGCTCT
FT3927          GTCCCATTGGCGGGCCCATCGCTTGTGAGTTGGGTTTGGTGGTGCCTTTTGGTTGGTTCC
FT3WT           GTCCCATTGGCGGGCCCATCGCTTGTGAGTTGGGTTTGGTGGTGCGTTCTAACTGGTTCC
                ******************************************** ** *   *** **

FT3MTXR1        CTTGTTGCGTCCTCCATTGTAGGACCACTTACCGATAAGAGGTTGCAGCGAGTGGCTGTG
FT3MTXR2        CTTGTTGCGTCCTCCATTGTAGGACCACTTACCGATAAGAGGTTGCAGCGAGTGGCTGTG
FT3927          CTTGTTGCGTCCTCCATTGTAGGACCACTTACCGATAAGAGGTTGCAGCGAGTGGCTGTG
FT3WT           CTTGTTGCGTCCTCCATTGTAGGACCACTTACCGATAAGAGGTTGCAGCGAGTGGCTGTG
                ************************************************************
```

```
FT3MTXR1        TTTATCTCTGCTGGGATGCAGTTGGTGCCGACGATATTCTTCATACTGAATTGGTATGGT
FT3MTXR2        TTTATCTCTGCTGGGATGCAGTTGGTGCCGACGATATTCTTCATACTGAATTGGTATGGT
FT3927          TTTATCTCTGCTGGGATGCAGTTGGTGCCGACGATATTCTTCATGCTGAATTGGTATGGT
FT3WT           TTTATCTCTGCTGGGATGCAGTTGGTGCCGACGATATTCTTCATACTGAATTGGTATGGT
                ******************************************** ***************

FT3MTXR1        GAACGGAGGAACCGAGAGGAACGTGCGTACGACCTGAAGATTATTCGGGAAGAGCAGCTG
FT3MTXR2        GAACGGAGGAACCGAGAGGAACGTGCGTACGACCTGAAGATTATTCGGGAAGAGCAGCTG
FT3927          GAACGGAAGAACCGAGAGGAACGTGCGTACGACCTGAAGATTATTCGCGAAAAGAAGCTG
FT3WT           GAACGGAGGAACCGAGAGGAACGTGCGTACGACCTGAAGATTATTCGCGAAAAGCAGCTG
                ******* ************************************** *** ** *****

FT3MTXR1        GAGCGTGAAGCCGACGCCGTGAGGTTACAGGGGAGCGAAGCAACAAGTGGCTCACTGGAC
FT3MTXR2        GAGCGTGAAGCCGACGCCGTGAGGTTACAGGGGAGCGAAGCAACAAGTGGCTCACTGGAC
FT3927          GAGCATGAAGCCGACGCCGTGAGGTTACAGGGGAGCGAAGCAACAAGTGGCTCACTGGAC
FT3WT           GAGCATGAAGCCGACGCCGTGAGGTTACAGGGGAGCGAAGCAACAAGTGGCTCACTGGAC
                **** ************************************************************

FT3MTXR1        AATCCATCGGATACCGAGGAAGTGGGTGAGGGCGGAGCACGGATACTACCTTGTTGCTGT
FT3MTXR2        AATCCATCGGATACCGAGGAAGTGGGTGAGGGCGGAGCACGGATACTACCTTGTTGCTGT
FT3927          AATCCATCGGATACCGAGGAAGTGGGTGAGGGCGGAGCACGGATACTACCTTGTTGCTGT
FT3WT           AATCCATCGGATACCGAGGAAGTGGGTGAGGGCGGAGCACGGATACTACCTTGTTGCTGT
                ************************************************************

FT3MTXR1        GGTGCCTTTGAAGTGAATCGAGAAGTGTTTGCTCGCAACAAGAAGGTTGTGTTTTACTGC
FT3MTXR2        GGTGCCTTTGAAGTGAATCGAGAAGTGTTTGCTCGCAACAAGAAGGTTGTGTTTTACTGC
FT3927          GGTGCCTTTGAAGTGAATCGAGAAGTGTTTGCTCGCAACAAGAAGGTTGTGTTTTACTGC
FT3WT           GGTGCCTTTGAAGTGAATCGAGAAGTGTTTGCTCGCAACAAGAAGGTTGTGTTTTACTGC
                ************************************************************

FT3MTXR1        ATGCTTCTCACACTTGGCGCCATCGGGATGGTTCTCGTGACAGTCCTTGGCACAAGGTTG
FT3MTXR2        ATGCTTCTCACACTTGGCGCCATCGGGATGGTTCTCGTGACAGTCCTTGGCACAAGGTTG
FT3927          ATGCTTCTCACACTTGGCGCCATCGGTATGGTTCTCGTGACAGTCCTTGGCACAAGGTTG
FT3WT           ATGCTTCTCACACTTGGCGCCATCGGTATGGTTCTCGTGACAGTCCTTGGCACAAGGTTG
                ************************** *********************************

FT3MTXR1        CAGCTGCTAATAACCAGTGTTGTGGCGTCATTTACACTCTGTGGTCTCGGTTTCGTTGCT
FT3MTXR2        CAGCTGCTAATAACCAGTGTTGTGGCGTCATTTACACTCTGTGGTCTCGGTTTCGTTGCT
FT3927          CAGCTGCTAATAACCAGTGTTGTGGCGTCATTTACACTCTGTGGACTCGGTTTCGTTGCC
FT3WT           CAGCTGCTAATAACCAGTGTTGTGGCGTCATTTACACTCTGTGGTCTCGGTTTCGTTGCT
                ******************************************** ***************

FT3MTXR1        CTTCCACTTGTGATCGCGAAGGCAAATATGTTCACATTCATCTCGAGGGTCGCGTACATC
FT3MTXR2        CTTCCACTTGTGATCGCGAAGGCAAATATGTTCACATTCATCTCGAGGGTCGCGTACATC
FT3927          CTTCCACTTGTGATCGCGAAGGCAAATATGTTCACATTCATCTCGAGGGTCGCGTACATC
FT3WT           CTTCCACTTGTGATCGCGAAGGCAAATATGTTCACATTCATCTCGAGGGTCGCGTACATC
                ************************************************************

FT3MTXR1        CAACTTCCAGGCGCAATTGACAATGTCTTCATGGCAACCCCCGATTGTTTCCCTGGTGGT
FT3MTXR2        CAACTTCCAGGCGCAATTGACAATGTCTTCATGGCAACCCCCGATTGTTTCCCTGGTGGT
FT3927          CAACTTCCTGGCGCAATCGACAATGTCTTCATGGCGACCCCCGATTGTTTCCCTGGTGGT
FT3WT           CAACTTCCTGGCGCAATCGACAATGTCTTCATGGCGACCCCCGATTGTTTCCCTGGTGGT
                ******** ******** ***************** ************************

FT3MTXR1        CCTAACTTTTCATACTTTTACTACAGCACTGTGGGTAATATGATTGGAGCTATGGGTGGT
FT3MTXR2        CCTAACTTTTCATACTTTTACTACAGCACTGTGGGTAATATGATTGGAGCTATGGGTGGT
FT3927          CCTAACTTTTCATACTTTTACTACAGCACTGTGGGTAATATGATTGGAGCTGTGGGTGGT
FT3WT           CCTAACTTTTCATACTTTTACTACAGCACTGTGGGTAATATGATTGGAGCTATGGGTGGT
                ************************************************** ********

FT3MTXR1        GTTATTGGTGTGACGTTATTCAGATACGTATTCTCAAAGCGCAGCTATCGCCTAACATTC
FT3MTXR2        GTTATTGGTGTGACGTTATTCAGATACGTATTCTCAAAGCGCAGCTATCGCCTAACATTC
FT3927          GTTATTGGTGTGACGTTATTCAGATACGTATTCTCAAAGCGCAGCTATCGCCTAACATTC
FT3WT           GTTATTGGTGTGACGTTATTCAGATACGTATTCTCAAAGCGCAGCTATCGCCTAACATTC
                ************************************************************

FT3MTXR1        ATCGTAACAACTTTGATTGAGATAGTTTCGAGTATCTTTGATATAATCATTGTGGAGCGA
FT3MTXR2        ATCGTAACAACTTTGATTGAGATAGTTTCGAGTATCTTTGATATAATCATTGTGGAGCGA
FT3927          ATCGTAACAACTTTGATTGAGATAGTTTCGAGTATCTTTGATATAATCATTGTGGAGCGA
FT3WT           ATCGTAACAACTTTGATTGAGATAGTTTCGAGTATCTTTGATATAATCATTGTGGAGCGA
                ************************************************************

FT3MTXR1        TGGAACCGTCCGTATGTTAGCGATCACGTTGTATTCGTTCTTGGTGACCAAATTATACAC
FT3MTXR2        TGGAACCGTCCGTATGTTAGCGATCACGTTGTATTCGTTCTTGGTGACCAAATTATACAC
FT3927          TGGAACCGTCCGTATGTTAGCGATCACGTTGTATTCGTTCTTGGTGACCAAATTATACAC
FT3WT           TGGAACCGTCCGTATGTTAGCGATCACGTTGTATTCGTTCTTGGTGACCAAATTATACAC
                ************************************************************
```

```
FT3MTXR1        CAGGTGTGCTACATGATGCACTTCATGCCAACTGTAATGCTCATTTCGAGGCTCTGTCCC
FT3MTXR2        CAGGTGTGCTACATGATGCACTTCATGCCAACTGTAATGCTCATTTCGAGGCTCTGTCCC
FT3927          CAGGTGTGCTACATGATGCACTTCATGCCAACTGTAATGCTCATTTCGAGGCTCTGTCCC
FT3WT           CAGGTGTGCTACATGATGCACTTCATGCCAACTGTAATGCTCATTTCGAGGCTCTGTCCC
                ************************************************************

FT3MTXR1        CGTGGGTATGAAAGTGCGGTGTATGCGGTACTTGCGGGATGTGCCCATTTTGGCCGTTCT
FT3MTXR2        CGTGGGTATGAAAGTGCGGTGTATGCGGTACTTGCGGGATGTGCCCATTTTGGCCGTTCT
FT3927          CGTGGGTCTGAAAGTATGGTGTATGCATTACTTGCAGGATTCGCTAATTTTGGCCGTTCT
FT3WT           CGTGGGTCTGAAAGTATGGTGTATGCATTACTTGCAGGATGCGCTAATTTTGGCCGTTCT
                ******* *******  *********  ******* ****  **  **************

FT3MTXR1        CTTTCCAACACACTTGGATGGCTTTTGATGGAATACGTATGGAATGTGCAATCAGACATT
FT3MTXR2        CTTTCCAACACACTTGGATGGCTTTTGATGGAATACGTATGGAATGTGCAATCAGACATT
FT3927          CTTTCCAACACACTTGGATGGCTTTTGATGGAATACGTATGGAATGTGCAATCAGACATT
FT3WT           CTTTCCAACACACTTGGATGGCTTTTGATGGAATACGTATGGAATGTGCAATCAGACATT
                ************************************************************

FT3MTXR1        ACGGTGGGTCCATGCGACTTCAGTAATGTGAAGTGGCTTCTGCTTCTTGGTCACTTTGGC
FT3MTXR2        ACGGTGGGTCCATGCGACTTCAGTAATGTGAAGTGGCTTCTGCTTCTTGGTCACTTTGGC
FT3927          ACGGTGGGTCCATGCGACTTCAGTAATGTGAAGTGGCTTCTACTTCTTGGTCACTTTGGC
FT3WT           ACGGTGGGTCCATGCGACTTCAGTAATGTGAAGTGGCTTCTGCTTCTTGGTCACTTTGGC
                ****************************************** ******************

FT3MTXR1        ACTCCACTCATCAACATTCCTCTTGTGTTTTTACTGATACCTGCGGCACGTATATGTGAC
FT3MTXR2        ACTCCACTCATCAACATTCCTCTTGTGTTTTTACTGATACCTGCGGCACGTATATGTGAC
FT3927          ACTCCACTCATCAACATTCCTCTTGTGTTTTTACTGATACCTGCGGCACGTATATGTGAT
FT3WT           ACTCCACTCATCAACATTCCTCTTGTGTTTTTACTGATACCTGCGGCACGTATATGTGAC
                ************************************************************

FT3MTXR1        GTTCTTGACGAAAACGGCAAAGCTATTACAAAGAAGGCGGAGGATGTTCATGCCCCCTCT
FT3MTXR2        GTTCTTGACGAAAACGGCAAAGCTATTACAAAGAAGGCGGAGGATGTTCATGCCCCCTCT
FT3927          GTTCTTGACGAAAACGGCAAAGCTATTACAAAGAAGGCGGAGGATGTTCATGCCCCCTCT
FT3WT           GTTCTTGACGAAAACGGCAAAGCTATTACAAAGAAGGCGGAGGATGTTCATGCCCCCTCT
                ************************************************************

FT3MTXR1        AATGATTCTCCCAGACGGCGGGAACCCACAGCCAATTAG
FT3MTXR2        AATGATTCTCCCAGACGGCGGGAACCCACAGCCAATTAG
FT3927          AATGATTCTCCCAGACGGCGGGAACCCACAGCCAATTAG
FT3WT           AATGATTCTCCCAGACGGCGGGAACCCACAGCCAATTAG
                ***************************************
```

Figures S2: A, B + C; Protein alignments of the folate transporters in MTX-resistant trypanosomes.

Highlighted in yellow: Base changes occurring in both MTXR1 and MTXR2 different to both WT and 927 reference
Highlighted in blue: Base changes occurring in both MTXR1 and MTXR2 different to WT but same as 927 reference.
Highlighted in green: Base changes in WT, MTXR1 and MTXR2 that are different than 927 reference.

Figure S2.A Protein alignments for FT1, comparing MTXR1, MTR2 to parental WT and reference *T.brucei* 927 strain.

```
FT1927          MTTSPNACQDQPPQHSAPQAHEAECTTHKLSAEETMDARPVHPDARALFRKLPCVWSIPV
FT1WT           MTTSPNACQDQPPQHSAPQAHEAECTTHKLSAEETMDARPVHPDARALFRKLPCVWSIPV
FT1MTXR1        ------------------------------------------------------------
FT1MTXR2        ------------------------------------------------------------

FT1927          LGTAVEAFGPKFVFALGFCELFGKGIADNIIRSSLFPMFTYTFGADAKLYQLMGGMSSLG
FT1WT           LGTAVEAFGPKFVFALGFCELFGKGIADNIIRSSLFPMFTYTFGADAKLYQLMGGMSSLG
FT1MTXR1        ------------------------------------------------------------
FT1MTXR2        ------------------------------------------------------------

FT1927          YAVKPFAAMFSDLFALFGYTKRWYLALSCVVGSTLAIVYGSLPGELSYVPVAGFLVFVIT
FT1WT           YAVKPFAAMFSDLFALFGYTKRWYLALSCVVGSTLAIVYGSLPGELSYVPVAGFLVFVIT
FT1MTXR1        ------------------------------------------------------------
FT1MTXR2        ------------------------------------------------------------

FT1927          FTVANLDILTQGHYSRLIRRVPLAGPSLVSWVWWCLLVGSLVASSIVGPLTDKRLQRVAV
FT1WT           FTVANLDILTQGHYSRLIRRVPLAGPSLVSWVWWCLLVGSLVASSIVGPLTDKRLQRVAV
FT1MTXR1        ---ANLDILTQGHYSRLIRRVPLAGPSLVSWVWWCVLTGSLVASSIVGPLTDKRLQRVAV
FT1MTXR2        ---ANLDILTQGHYSRLIRRVPLAGPSLVSWVWWCVLTGSLVASSIVGPLTDKRLQRVAV
                   ********************************:*.**********************

FT1927          FISAGMQLVPTIFFILNWYGERKNREERAYDLKIIREKKLEHEADAVRLQGSEATSGSLD
FT1WT           FISAGMQLVPTIFFILNWYGERRNREERAYDLKIIREKQLEHEADAVRLQGSEATSGSLD
FT1MTXR1        FISAGMQLVPTIFFILNWYGERRNREERAYDLKIIREKQLEHEADAVRLQGSEATSGSLD
FT1MTXR2        FISAGMQLVPTIFFILNWYGERKNREERAYDLKIIREKQLEHEADAVRLQGSEATSGSLD
                ********************:***************:**********************

FT1927          NPSDTEEVGEGGARILPCCCGAFEVNREVFARNKKVVFYCMLLTLGAIGMVLVTVLGTRL
FT1WT           NPSDTEEVGEGGARILPCCCGAFEVNREVFARNKKVVFYCMLLTLGAIGMVLVTVLGTRL
FT1MTXR1        NPSDTEEVGEGGARILPCCCGAFEVNREVFARNKKVVFYCMLLTLGAIGMVLVTVLGTRL
FT1MTXR2        NPSDTEEVGEGGARILPCCCGAFEVNREVFARNKKVVFYCMLLTLGAIGMVLVTVLGTRL
                ************************************************************

FT1927          QLLITSVVASFTLCGLGFVALPLVIAKANMFTFISRVTYIQLRGAMDNVFMATPDCFPGG
FT1WT           QLLITSVVASFTLCGLGFVALPLVIAKANMFTFISRVAYIQLRGAMDNVFMATPDCFPGG
FT1MTXR1        QLLITSVVASFTLCGLGFVALPLVIAKANMFTFISRVAYIQLRGAMDNVFMATPDCFPGG
FT1MTXR2        QLLITSVVASFTLCGLGFVALPLVIAKANMFTFISRVAYIQLRGAMDNVFMATPDCFPGG
                ************************************:***********************

FT1927          PNFSYFYYNTVGNVIGTMGGVIGVTLFRYVFSKRSYRLTFIVTTLIEIVSSIFDIIIVER
FT1WT           PNFSYFYYNTVGNVIGTMGGVIGVTLFRYVFSKRSYRLTFIVTTLIEIVSSIFDIIIVER
FT1MTXR1        PNFSYFYYNTVGNVIGTMGGVIGVTLFRYVFSKRSYRLTFIVTTLIEIVSSIFDIIIVER
FT1MTXR2        PNFSYFYYNTVGNVIGTMGGVIGVTLFRYVFSKRSYRLTFIVTTLIEIVSSIFDIIIVER
                ************************************************************

FT1927          WNRPYVSDHVVFVLGDQIIQQVCYMMHFMPTVMLISRLCPRGSESMVYAVLAGCAHFGRS
FT1WT           WNRPYVSDHVVFVLGDQIIQQVCYMMHFMPTVMLISRLCPRGSESMVYAVLAGCAHFGRS
FT1MTXR1        WNRPYVSDHVVFVLGDQIIQQVCYMMHFMPTVMLISRLCPRGSESMVYAVLAGCAHFGRS
FT1MTXR2        WNRPYVSDHVVFVLGDQIIQQVCYMMHFMPTVMLISRLCPRGSESMVYAVLAGCAHFGRS
                ************************************************************
```

```
FT1927          VSNTLGWLLMEYVWNVQSDITVGPCDFSNVKWLLLLGHFGTPLISIPLVFLLIPAARICD
FT1WT           VSNTLGWLLMEYVWNVQSDITVGPCDFSNVKWLLLLGHFGTPLISIPLVFLLIPAARICD
FT1MTXR1        VSNTLGWLLMEYVWNVQSDITVGPCDFSNVKWLLLLGHFGTPLISIPLVFLLIPAARICD
FT1MTXR2        VSNTLGWLLMEYVWNVQSDITVGPCDFSNVKWLLLLGHFGTPLISIPLVFLLIPAARICD
                ************************************************************

FT1927          VLDENGKAITKKAEDVHAPSNDSPRRREPTAN*
FT1WT           VLDENGKAITKKAEDVHAPSNDSPRRREPTAN*
FT1MTXR1        VLDENGKAITKKAEDVHAPSNDSPRRREPTAN*
FT1MTXR2        VLDENGKAITKKAEDVHAPSNDSPRRREPTAN*
                *********************************
```

Figure S1.B Protein alignments for FT2, comparing MTXR1, MTR2 to parental WT and reference *T.brucei* 927 strain.

```
FT2927          MTTSPNACQDQPPQHSAPQAHEAECTTHKLSAEETMDARPVHPDARALFRKLPCVWSIPV
FT2WT           MTTSPNACQDQPPQHSAPQAHEAECTTHKLSAEETMDARPVHPDARALFRKLPCVWSIPV
FT2MTXR2        MTTSPNACQDQPPQHSAPQAHEAECTTHKLSAEETMDARPVHPDARALFRKLPCVWSIPV
FT2MTXR1        MTTSPNACQDQPPQHSAPQAHEAECTTHKLSAEETMDARPVHPDARALFRKLPCVWSIPV
                ************************************************************

FT2927          FGTAVEAFGPRCVLALGLSELFGKGIADNIIRTTLFPMFTYTFGADAKLYQRMSSLVTFG
FT2WT           FGTAVEAFGPKCVLALGLSELFGKGIADNIIRTTLFPMFTYTFGADAKLYQRMSSLVTFG
FT2MTXR2        FGTAVEAFGPKCVLALGLSELFGKGIADNIIRTTLFPMFTYTFGADAKLYQRMSSLVTFG
FT2MTXR1        FGTAVEAFGPKCVLALGLSELFGKGIADNIIRTTLFPMFTYTFGADAKLYQRMSSLVTFG
                **********:*************************************************

FT2927          YAVKPFAAMFSDLFALFGYTKRWYLALSCVVGSTLAIVYGSLPGELSYVPVAGILVFVTS
FT2WT           YAVKPFAAMFSDLFALFGYTKRWYLALSCVVGSTLAIVYGSLPGELSYVPVAGILVFVTS
FT2MTXR2        YAVKPFAAMFSDLFALFGYTKRWYLALSCVVGSTLAIVYGSLPGELSYVPVAGILVFVTS
FT2MTXR1        YAVKPFAAMFSDLFALFGYTKRWYLALSCVVGSTLAIVYGSLPGELSYVPVAGILVFVTS
                ************************************************************

FT2927          FTKANLDILTQGHYSRLIRRVPLAGPSLVSWVWWCVLTGSLVASSIVGPLTDKRLQRVAV
FT2WT           FTKANLDILTQGHYSRLIRRVPLAGPSLVSWVWWCVLTGSLVASSIVGPLTDKRLQRVAV
FT2MTXR2        FTKA*-------------------------------------------------------
FT2MTXR1        F*----------------------------------------------------------
                *

FT2927          FISAGMQLVPTIFFMLNWYGERKNREERAYDLKIIREEQLEREADAARLQGSEATSGSLD
FT2WT           FISAGMQLVPTIFFILNWYGERRNREERAYDLKIIREEQLEREADAVRLQGSEATSGSLD
FT2MTXR2        ------------------------------------------------------------
FT2MTXR1        ------------------------------------------------------------

FT2927          NPSDTEEVGEGGARILPCCCGAFEVNREVFARNKKVVFYCMLLTLGAIGMVLVTVLGTRL
FT2WT           NPSDTEEVGEGGARILPCCCGAFEVNREVFARNKKVVFYCMLLTLGAIGMVLVTVLGTRL
FT2MTXR2        ------------------------------------------------------------
FT2MTXR1        ------------------------------------------------------------

FT2927          QLLITSVVASFTLCGLGFVALPLVIAKANMFTFISRVAYIQLPGAIDNVFMATPDCFPGG
FT2WT           QLLITSVVASFTLCGLGFVALPLVIAKANMFTFISRVAYIQLPGAIDNVFMATPDCFPGG
FT2MTXR2        ------------------------------------------------------------
FT2MTXR1        ------------------------------------------------------------

FT2927          PNFSYFYYSTVGNMIGAVGGVIGVTLFRYVFSKRSYRLTFIVTTLIEIVSSIFDIIIVER
FT2WT           PNFSYFYYSTVGNMIGAMGGVIGVTLFRYVFSKRSYRLTFIVTTLIEIVSSIFDIIIVER
FT2MTXR2        ------------------------------------------------------------
FT2MTXR1        ------------------------------------------------------------

FT2927          WNRPYVSDHVVFVLGDQIIHQVCYMMHFMPTVMLISRLCPRGSESMVYALLAGFANFGRS
FT2WT           WNRPYVSDHVVFVLGDQIIHQVCYMMHFMPTVMLISRLCPRGSESMVYALLAGFANFGRS
FT2MTXR2        ------------------------------------------------------------
FT2MTXR1        ------------------------------------------------------------

FT2927          LSNTLGWLLMEYVWNVQSDITVGPCDFSNVKWLLLLGHFGTPLINIPLVFLLIPAARICD
FT2WT           LSNTLGWLLMEYVWNVQSDITVGPCDFSNVKWLLLLGHFGTPLINIPLVFLLIPAARICD
FT2MTXR2        ------------------------------------------------------------
FT2MTXR1        ------------------------------------------------------------
```

```
FT2927          VLDENGKAITKKAEDVHAPSNDSPRRREPTAN*
FT2WT           VLDENGKAITKKAEDVHAPSNDSPRRREPTAN*
FT2MTXR2        ---------------------------------
FT2MTXR1        ---------------------------------
```

Figure S2.C Protein alignments for FT3, comparing MTXR1, MTR2 to parental WT and reference *T.brucei* 927 strain.

```
FT3MTXR1        MTTSPNACQDQPPQHSAPQAHEAECTTHKLSAEETMDARPVHPDARALFRKLPCVWSIPV
FT3MTXR2        MTTSPNACQDQPPQHSAPQAHEAECTTHKLSAEETMDARPVHPDARALFRKLPCVWSIPV
FT3927          MTTSPNACQDQPPQHSAPQAHEAECTTHKLSAEETMDARPVHPDARALFRKLPCVWSIPV
FT3WT           MTTSPNACQDQPPQHSAPQAHEAECTTHKLSAEETMDARPVHPDARALFRKLPCVWSIPV
                ************************************************************

FT3MTXR1        FGTAVEAFGPKFVFALGFCELFGKGIADNIIRSSLFPMFTYTFGADAKLYQRMSSLVTFG
FT3MTXR2        FGTAVEAFGPKFVFALGFCELFGKGIADNIIRSSLFPMFTYTFGADAKLYQRMSSLVTFG
FT3927          FGTAVEAFGPKFVFALGFCELFGKGIADNIIRSSLFPMFTYTFGADAKLYQRMSSLVTFG
FT3WT           FGTAVEAFGPKFVFALGFCELFGKGIADNIIRSSLFPMFTYTFGADAKLYQRMSSLVTFG
                ************************************************************

FT3MTXR1        YAVKPFAAMFSDLFALFGYTKRWYLALSCVVGSTLAIVYGSLPGELSYVPVAGILVFVTS
FT3MTXR2        YAVKPFAAMFSDLFALFGYTKRWYLALSCVVGSTLAIVYGSLPGELSYVPVAGILVFVTS
FT3927          YAVKPFAAMFSDLFALFGYTRRWYLALSCVVGSTLAIVYGSLPGELSYVPVAGILVFVTS
FT3WT           YAVKPFAAMFSDLFALFGYTKRWYLALSCVVGSTLAIVYGSLPGELSYVPVAGILVFVTS
                ********************:***************************************

FT3MTXR1        FTKANLDILTQGHYSRLIRRVPLAGPSLVSWVWWCLLVGSLVASSIVGPLTDKRLQRVAV
FT3MTXR2        FTKANLDILTQGHYSRLIRRVPLAGPSLVSWVWWCLLVGSLVASSIVGPLTDKRLQRVAV
FT3927          FTKANLDILTQGHYSRLIRRVPLAGPSLVSWVWWCLLVGSLVASSIVGPLTDKRLQRVAV
FT3WT           FTKANLDILTQGHYSRLIRRVPLAGPSLVSWVWWCVLTGSLVASSIVGPLTDKRLQRVAV
                ************************************:*.**********************

FT3MTXR1        FISAGMQLVPTIFFILNWYGERRNREERAYDLKIIREEQLEREADAVRLQGSEATSGSLD
FT3MTXR2        FISAGMQLVPTIFFILNWYGERRNREERAYDLKIIREEQLEREADAVRLQGSEATSGSLD
FT3927          FISAGMQLVPTIFFMLNWYGERKNREERAYDLKIIREKKLEHEADAVRLQGSEATSGSLD
FT3WT           FISAGMQLVPTIFFILNWYGERRNREERAYDLKIIREKQLEHEADAVRLQGSEATSGSLD
                **************:*******:**************::**:******************

FT3MTXR1        NPSDTEEVGEGGARILPCCCGAFEVNREVFARNKKVVFYCMLLTLGAIGMVLVTVLGTRL
FT3MTXR2        NPSDTEEVGEGGARILPCCCGAFEVNREVFARNKKVVFYCMLLTLGAIGMVLVTVLGTRL
FT3927          NPSDTEEVGEGGARILPCCCGAFEVNREVFARNKKVVFYCMLLTLGAIGMVLVTVLGTRL
FT3WT           NPSDTEEVGEGGARILPCCCGAFEVNREVFARNKKVVFYCMLLTLGAIGMVLVTVLGTRL
                ************************************************************

FT3MTXR1        QLLITSVVASFTLCGLGFVALPLVIAKANMFTFISRVAYIQLPGAIDNVFMATPDCFPGG
FT3MTXR2        QLLITSVVASFTLCGLGFVALPLVIAKANMFTFISRVAYIQLPGAIDNVFMATPDCFPGG
FT3927          QLLITSVVASFTLCGLGFVALPLVIAKANMFTFISRVAYIQLPGAIDNVFMATPDCFPGG
FT3WT           QLLITSVVASFTLCGLGFVALPLVIAKANMFTFISRVAYIQLPGAIDNVFMATPDCFPGG
                ************************************************************

FT3MTXR1        PNFSYFYYSTVGNMIGAMGGVIGVTLFRYVFSKRSYRLTFIVTTLIEIVSSIFDIIIVER
FT3MTXR2        PNFSYFYYSTVGNMIGAMGGVIGVTLFRYVFSKRSYRLTFIVTTLIEIVSSIFDIIIVER
FT3927          PNFSYFYYSTVGNMIGAVGGVIGVTLFRYVFSKRSYRLTFIVTTLIEIVSSIFDIIIVER
FT3WT           PNFSYFYYSTVGNMIGAMGGVIGVTLFRYVFSKRSYRLTFIVTTLIEIVSSIFDIIIVER
                *****************:******************************************

FT3MTXR1        WNRPYVSDHVVFVLGDQIIHQVCYMMHFMPTVMLISRLCPRGYESAVYAVLAGCAHFGRS
FT3MTXR2        WNRPYVSDHVVFVLGDQIIHQVCYMMHFMPTVMLISRLCPRGYESAVYAVLAGCAHFGRS
FT3927          WNRPYVSDHVVFVLGDQIIHQVCYMMHFMPTVMLISRLCPRGSESMVYALLAGFANFGRS
FT3WT           WNRPYVSDHVVFVLGDQIIHQVCYMMHFMPTVMLISRLCPRGSESMVYALLAGCANFGRS
                ****************************************** ** ***:*** *.****

FT3MTXR1        LSNTLGWLLMEYVWNVQSDITVGPCDFSNVKWLLLLGHFGTPLINIPLVFLLIPAARICD
FT3MTXR2        LSNTLGWLLMEYVWNVQSDITVGPCDFSNVKWLLLLGHFGTPLINIPLVFLLIPAARICD
FT3927          LSNTLGWLLMEYVWNVQSDITVGPCDFSNVKWLLLLGHFGTPLINIPLVFLLIPAARICD
FT3WT           LSNTLGWLLMEYVWNVQSDITVGPCDFSNVKWLLLLGHFGTPLINIPLVFLLIPAARICD
                ************************************************************

FT3MTXR1        VLDENGKAITKKAEDVHAPSNDSPRRREPTAN*
FT3MTXR2        VLDENGKAITKKAEDVHAPSNDSPRRREPTAN*
FT3927          VLDENGKAITKKAEDVHAPSNDSPRRREPTAN*
FT3WT           VLDENGKAITKKAEDVHAPSNDSPRRREPTAN*
                ********************************
```

Appendix

Gibson, M.W., **Dewar, S.,** Ong, H.B., Sienkiewicz, N. and Fairlamb, A.H. (2016). *Trypanosoma brucei* DHFR-TS revisited: characterisation of a bifunctional and highly unstable recombinant dihydrofolate reductase-thymidylate synthase. ***PLoS Neglected Tropical Diseases*** *10*, e0004714